NASA CONTRACTOR
REPORT

NASA CR-61366

TEST AND EVALUATION OF APOLLO 14 COMPOSITE CASTING DEMONSTRATION SPECIMENS AND FLIGHT AND CONTROL SAMPLES

By Richard C. Fabiniak and Thaddeus J. Fabiniak
Cornell Aeronautical Laboratory
4455 Genesee St.
Buffalo, N. Y. 14221

September 1971

Final Report

Prepared for

NASA-GEORGE C. MARSHALL SPACE FLIGHT CENTER
Marshall Space Flight Center, Alabama 35812

TECHNICAL REPORT STANDARD TITLE PAGE

1. REPORT NO.	2. GOVERNMENT ACCESSION NO.	3. RECIPIENT'S CATALOG NO.
NASA CR-61366		

4. TITLE AND SUBTITLE	5. REPORT DATE
TEST AND EVALUATION OF APOLLO 14 COMPOSITE CASTING DEMONSTRATION SPECIMENS AND FLIGHT AND CONTROL SAMPLES	September 1971
	6. PERFORMING ORGANIZATION CODE

7. AUTHOR(S)	8. PERFORMING ORGANIZATION REPORT #
Richard C. Fabiniak and Thaddeus J. Fabiniak	KE-3101-D-1

9. PERFORMING ORGANIZATION NAME AND ADDRESS	10. WORK UNIT NO.
Cornell Aeronautical Laboratory 4455 Genesee St. Buffalo, N. Y. 14221	11. CONTRACT OR GRANT NO. NAS 8-27106
	13. TYPE OF REPORT & PERIOD COVERED

12. SPONSORING AGENCY NAME AND ADDRESS	Contractor Report 12-28-70 Final 8-31-71
National Aeronautics and Space Administration Washington, D. C. 20546	14. SPONSORING AGENCY CODE

15. SUPPLEMENTARY NOTES

Contract Monitor: Iva C. Yates, Jr., PT Laboratory,
George C. Marshall Space Flight Center

16. ABSTRACT

Discussed in this report are the results of experiments 1, 2, and 10 of the Apollo 14 composite casting demonstration. The purpose of the demonstration, with regard to samples 1 and 2, was to obtain preliminary understanding of the liquid phase sintering process in a weightless environment. With regard to sample 10, the purpose was to obtain preliminary information on how to achieve uniform dispersion of dense particles on a metal matrix by employing shaking modes or forces in the system when the metal matrix is molten.

Results of the demonstrations have been interpreted in a quantitative and qualitative manner. For experiment 1 it is found that the tungsten particles redistributed more uniformly in the Flight Sample than in the Control Sample. Experiment 2 results indicate that complete melting may not have occured and thus a high degree of significance cannot be associated with the qualitative results relating to particle redistribution data. Since the particle-matrix system of experiment 10 was found to be non-wetting, results are difficult to interpret.

17. KEY WORDS	18. DISTRIBUTION STATEMENT
	Iva C. Yates, Jr. Unclassified-unlimited

19. SECURITY CLASSIF. (of this report)	20. SECURITY CLASSIF. (of this page)	21. NO. OF PAGES	22. PRICE
U	U	196	$3.00

MSFC - Form 3292 (May 1969)

TABLE OF CONTENTS

TABLE OF CONTENTS (Cont.)

TABLE OF CONTENTS (Cont.)

LIST OF ILLUSTRATIONS

LIST OF ILLUSTRATIONS (Cont.)

LIST OF ILLUSTRATIONS (Cont.)

LIST OF ILLUSTRATIONS (Cont.)

LIST OF ILLUSTRATIONS (Cont.)

I. INTRODUCTION AND SUMMARY

This report describes Cornell Aeronautical Laboratory (CAL) efforts during the period 12/28/70 through 31 August 1971 under NASA Contract No. NAS8-27106 and discusses the results of experiment 1, 2, and 10 of Apollo 14 composite casting demonstration. CAL was a contributor to the selection and fabrication of samples 1 and 2, with particular emphasis on liquid phase sintering of precompressed powder compacts, containing dispersed particles. The basic materials used as a matrix for the compacts were Indium-Bismuth eutectic powder alloy which melts at 72°C. The dispersed particles were copper-coated tungsten and copper-coated boron carbide. The tungsten particles were chosen because their density was approximately twice that of the eutectic alloy; the boron carbide particles were chosen because their density is approximately half that of the alloy.

The dispersion of Tungsten and Boron Carbide spheres in the In-Bi eutectic alloy for samples 1 and 2 was investigated in each of three samples. These included:

(a) A Developmental Sample in the "as-pressed" condition.

(b) A Control Sample - having undergone melting under the same conditions as the Flight Sample but in an earth gravity environment.

(c) The Flight Sample - having undergone melting under a negligible gravity condition.

The three samples were identical in composition and shape, namely 30 volume percent copper-coated Tungsten or Boron Carbide particles in Indium-Bismuth eutectic alloy powder.

The dispersion of Tungsten spheres in the In-Bi eutectic alloy for sample 10 was investigated in two samples. These included a ground control and a flight sample. The samples were identical in composition, namely 30 volume percent copper-coated Tungsten particles in In-Bi eutectic alloy.

The purpose of the demonstration, with regard to samples 1 and 2, was to obtain preliminary understanding of the liquid phase sintering process in a weightless environment. The primary objective was to evaluate the hypothesis that in a weightless environment mixtures of solids, liquids and gases of different densities will not segregate during solidification and consequently unique composite materials may be formed.

The purpose of the demonstration with regard to sample 10 was to obtain preliminary information on how to achieve a uniform dispersion of dense particles on a metal matrix by employing shaking modes or forces to the system when the metal matrix is molten.

Results of the demonstrations have been interpreted in a quantitative and qualitative manner. The qualitative interpretations include surface distortion observations and an association between the Tungsten and/or Boron Carbide particles and voids. It is found that these phenomena are reflected differently in the Control and Flight samples for experiment #1 and thus must certainly be strong indications of more subtle zero gravity effects. Inasmuch as such observations lack the advantage of extensive or repeated documentation from more than one Apollo demonstration, it is concluded that verification in future flight experiments is necessary before strong emphasis on their zero gravity dependence is made. For this reason a strong emphasis has been placed on the documentation of results or effects and little emphasis on interpretation of results or effects.

The quantitative interpretations are concerned with the determination of tungsten particle redistribution as a function of the zero gravity condition. For experiment #1 it is found that the tungsten particles redistributed more uniformly in the Flight Sample than in the Control Sample. Inasmuch as the redistribution data is obtained by point intercept counting of tungsten particle volume fractions, high reliability is associated with this result. The conclusion is therefore reached that the absence of a gravity force can be used to advantage in liquid phase sintering or composite casting processes.

For experiment 2 the results indicate that complete melting may not have occurred and thus a high degree of significance cannot be associated with the quantitative results relating to particle redistribution data. However, from a qualitative point of view the conclusion is reached that a positive redistribution of the B_4C in the flight sample had occurred, i.e. that a trend to a more uniform distribution seems to have been initiated in that portion of the flight sample which had undergone some degree of melting.

The results of experiment 10 are difficult to interpret inasmuch as the particle-matrix system was found to be non-wetting. However, qualitative observations have been made which indicate that the matrix material (In-Bi alloy) was able to accept more of the non-wetted tungsten particles in the flight sample than in the ground control sample.

2. SAMPLE PREPARATION

2.1 General Description

The preparation methods employed for samples 1 and 2 involved standard powder metallurgical techniques. Sample 1 contained a mixture of 30 volume percent copper-coated tungsten particles and 70 volume percent Indium-Bismuth eutectic alloy powder. Sample 2 contained 30 volume percent copper-coated Boran Carbide (B_4C) particles and 70 volume percent Indium-Bismuth eutectic alloy powder. All the alloy powders and particles were restricted to a -325 mesh (less than 44 micronium dimension) size. Both the tungsten and B_4C particles were copper coated by an electroless plating process to promote wetting. The eutectic alloy powder was leached to remove any excessive oxide film as a precaution for promoting wetting and obtaining improved melting properties.

2.2 Materials

2.2.1 Indium-Bismuth Powder

A 66 weight percent Indium - 34 weight percent Bismuth eutectic alloy was obtained in powder form from the Indium Corporation of America. Only one evaluation procedure was applied to the powder and that was concerned with a determination of the powders melting properties. It was found that the lose powder could not visibly liquify at temperature 100°F above the eutectic melting temperature. In addition, it was noted that when the heated powder ($\approx$100°F above melting point) was pressed a separation of liquid could be achieved. These observations strongly indicated that the powder may have had an oxide layer of sufficient thickness to retain shape on melting of the powder alloy.

In an attempt to remove the oxide layer a procedure was established for leaching the eutectic alloy powder. This procedure involved using a 3%

hydrochloric acid solution in 200 ml. volumes with 60-70 gms of the powder. The powder and solution were mixed and stirred continuously until all the powder aglomerated. This aglomeration was viewed as an indication that clean or oxide free surfaces were produced and that such clean surfaces adhered to each other. The leaching procedure was followed by a minimum of three distilled water rinses. The aglomerated powder was then placed on filter paper to air dry after which it was subjected to a sieve series on a shaker to provide the required -325 mesh size. The powder are then used for sample preparation.

2.2.2 Boron Carbide (B_4C) Powder

The Boron Carbide powder was obtained from the Carborundum Co. in a -325 mesh size. The powder was designated as "reactor grade" indicating its high quality with regard to composition, density, and shape. Although this material is referred to as a powder, the individual Boron Carbide particles have a nearly spherical shape. No evaluation of these particles was undertaken in this study.

In order to improve wetting between the eutectic alloy and the Boron Carbide particles the particles were copper plated by an electroless process. The procedure involved the commercially available Cuposit process and the various solutions were obtained from the Shiply Company. The recommended procedures for coating non-conducting materials under this process were closely followed. Briefly this included 1) cleaning the particles in acetone and alcohol, 2) treating the particles with the Cuposit Catalyst 9F, 3) subjecting the particles to the action of Cuposit Accelerator 19, and 4) copper depositing with Cuposit Copper Mix 328. After the disposition step the particles were rinsed in distilled water and air dryed. In all instances the copper deposits

showed the characteristic copper color but appeared somewhat dull. For this reason a hydrogen reduction of the deposits was undertaken by heating the coated particles at 240°C under a continuous hydrogen gas flow of three cubic feet per minute for approximately 30 minutes. In all instances this was a sufficient treatment to cause significant improvement in the color and brightness of the copper coatings. The particles were then stored in air-tight containers.

2.2.3 Tungsten Powders

Tungsten micro-spheres consisting of -325 mesh and finer size were obtained from the Nuclear Materials & Equipment Corporation. No evaluation of the particles was undertaken in this study. The tungsten particles were copper plated by an electroless process identical to that used for the plating of the Boron Carbide particles. Since tungsten is conducting it was not necessary to use the Cuposit Catalyst 9F in the deposition process, all other procedures were identical to those outlined above (2.2.2) for the Boron Carbide particles. After copper deposition a hydrogen reduction step was employed identical to that described above for the Boron Carbide.

2.3 Compaction Procedure

The particles were weighed, placed in a sealed container and mixed for 4 hr to obtain a random distribution after which they were compressed in a double-action die to form a powder compact 1.74 cm (0.685 in) in diameter and 7.62 cm (3 in) long with a theoretical density of 96%. The compact was placed in an aluminum capsule that was hermetically sealed by NASA personnel using electron beam welding techniques. Three identical powder compacts of Sample 1 were fabricated: one labled Developmental Sample 1, another labled Control Sample 1 and the last was labled Flight Sample 1.

3. TECHNICAL DISCUSSION

3.1 General Objectives

This section contains a description of the capsule contents of experiments one and two, the evaluation procedures that were followed, and the results of those procedures. In addition, statements referring to the objectives and expected observations from each of the samples are included. In order to insure uniformity in sample description and proper control during evaluation, a specific sectioning and identidication procedure was established by NASA personnel. This procedure is also described below.

The evaluation procedures employed included: optical microscopy of surface features; optical microscopy of the sample bulk as reflected in longitudinal and transverse planes through the samples; a statistical determination of the dispersed phase (Tungsten or Boron Carbide) volume fraction from photomicrographs of selected areas in the longitudinal and transverse planes; and a determination of subsection or sample densities. A brief description of the procedure followed in determining the volume fraction of dispersed phase particles is also presented.

3.2 Experiment 1

3.2.1 Capsule Contents

70% Indium Bismuth - 30% Tungsten Powder Compact

3.2.2 Sample Composition and Preparation

Details relating to material preparation and sample compaction methods are provided in Section 2 and thus only a brief outline will be presented here.

A mixture of 30 volume percent spherical Copper-coated Tungsten particles and 70 volume percent Indium Bismuth eutectic powders were compressed.

to form a powder compact. The Tungsten particles and Indium Bismuth eutectic powders were of the same size, -325 mesh (less than 44 microns in diameter). The Tungsten particles were Copper-coated by the electroless plating process to promote wetting and were heated in a hydrogen atmosphere to reduce the oxides. The Indium Bismuth powders were leached in a three percent solution of hydrochloric acid to remove oxides. The two powders were weighed out, placed in a sealed container, and mixed for four hours to obtain a random distribution. The mixed powders were then compressed in a double acting die to form a powder compact 1.74 cm in diameter and 7.6 cm long with a theoretical density of 96 percent. The compact was subsequently placed in an Aluminum capsule which was hermetically sealed by electron beam welding.

3.2.3 Objectives and Expected Observations

The sample was designed to observe the differences in distribution of higher density particles in a lower density matrix melted and solidified in reduced gravity compared to a similar sample processed on earth. The density of the Tungsten particles (19.3 g/cm^3) is significantly greater than the density of Indium Bismuth (8.2 g/cm^3). Significant segregation of particles was expected when the matrix was melted under gravity. In the flight sample, g-induced segregation was not expected and a more homogeneous distribution of particles was expected since the molten metal would tend to flow around the particles separating those in contact after the compaction process.

3.2.4 Results

3.2.4.1 General

Experiment 1 results consist of data obtained from the Developmental (as-pressed) Sample, Control (earth-melted) Sample and Flight (0 G-melted)

Sample. The data includes (1) results of a microscopic examination of sample surface characteristics, and (2) results of the determination of Tungsten particle distribution.

A system was used to mark each sample with a numerical-alphabetical code to facilitate identification after removal from the capsules and subsequent sectioning. Although the procedure is covered in detail elsewhere [1], a brief explanation follows because the codes will appear in the data presentation.

Typical code: IF-A-001

This identifies Specimen 1 of the A half of Flight Sample 1. The translation is as follows:

1F - Sample 1, Flight Sample

A - "A" half of sample

001 - A specific segment (specimen) cut from the sample (see Figure 3-1).

The code 1F-A-00 indicates the A half of Flight Sample 1 is intact, i.e., no specimens have been cut (see Figure 3-2). To further demonstrate this identification procedure it is pointed out that Tungsten particle distributions were investigated in each of three samples half sections identified as:

a. 1D-A-00 - Developmental Sample 1 in the as-pressed condition.

b. 1C-A-00 - Control Sample 1 - melted under the same conditions as Flight Sample 1 but under earth gravity conditions.

c. 1F-A-00 - Flight Sample 1 - melted under a negligible gravity condition.

---

(1) Yates, I. C. Jr., Report on Results of Apollo 14 Composite Casting Demonstrations. July 13, 1971, S&E-PI-IN-71-1.

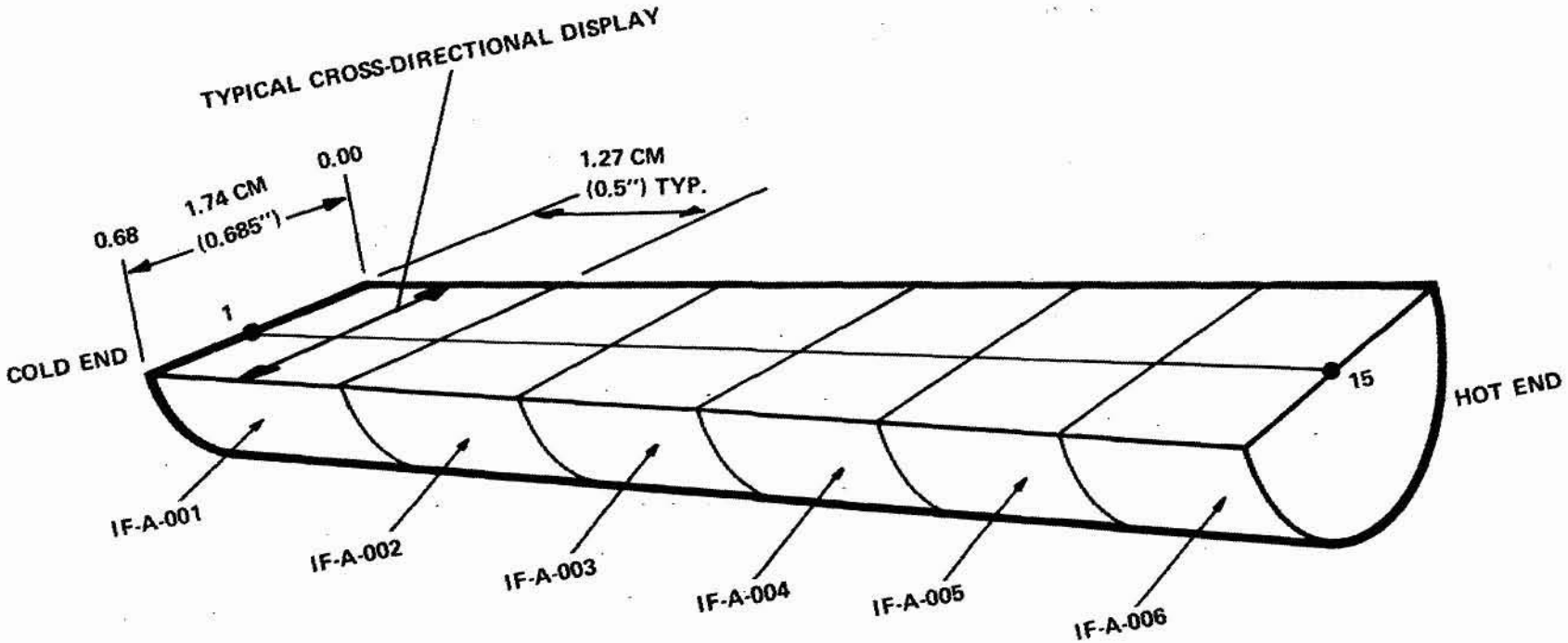

Figure 3-1 FLIGHT SAMPLE 1 SPECIMEN LOCATIONS

ID-A-00

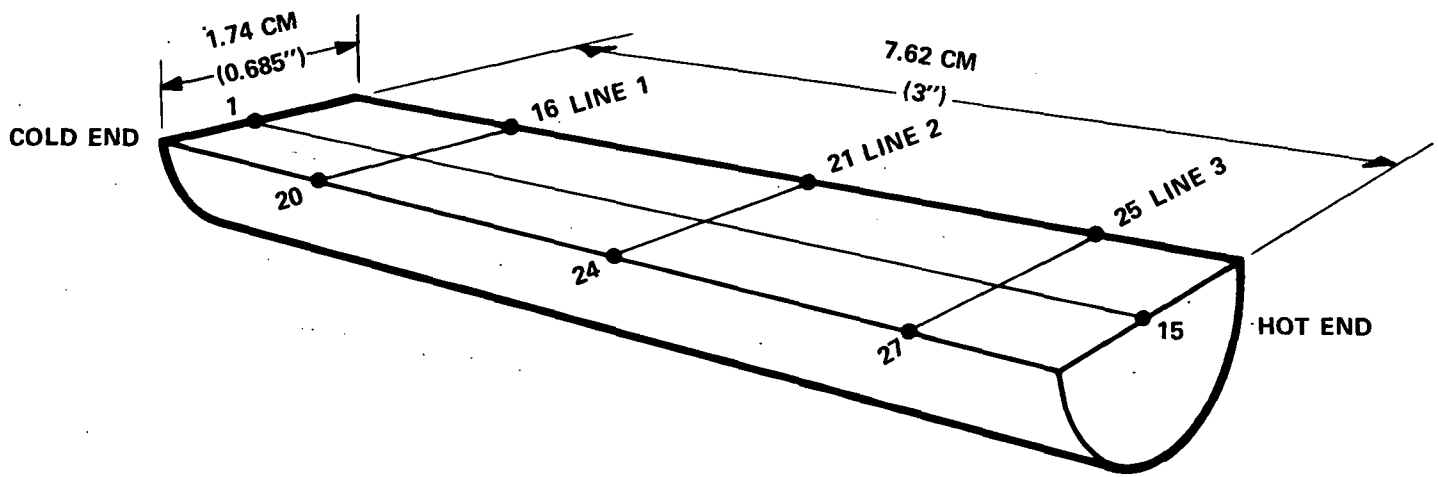

Figure 3-2 SCHEMATIC OF PHOTOGRAPHIC DOCUMENTATION

3.2.4.2 Developmental Sample 1 (1D-A-00)

Developmental Sample 1 was retained at CAL after compaction. The procedures employed to produce longitudinal half sections were identical to those employed by NASA and are reported elsewhere[1]. Of the two halves, analysis was performed on the one labeled "A" with the "B" half held in reserve. The section to be analyzed, labeled 1D-A-00, consists of a longitudinal plane (see Figure 3-2).

3.2.4.2.1 Surface Condition of Developmental Sample 1 (1D-A-00)

A microscopic examination was performed on the surface. Representative features of the surface at a magnification of 25X are shown in Figure 3-3. Particularly noteworthy were the presence of scoring marks in a longitudinal direction (as a result of rubbing against the die surface) and a trace of fine structure superimposed on the scoring marks. Figure 3-4 shows views of approximately the same areas taken at 500X. Figure 3-4(A) shows the area near the sample end and the presence of tungsten particles in the surface. Figure 3-4(B) represents an area near the sample center and shows the presence of tungsten particles in the surface together with longitudinal and randomly oriented score marks.

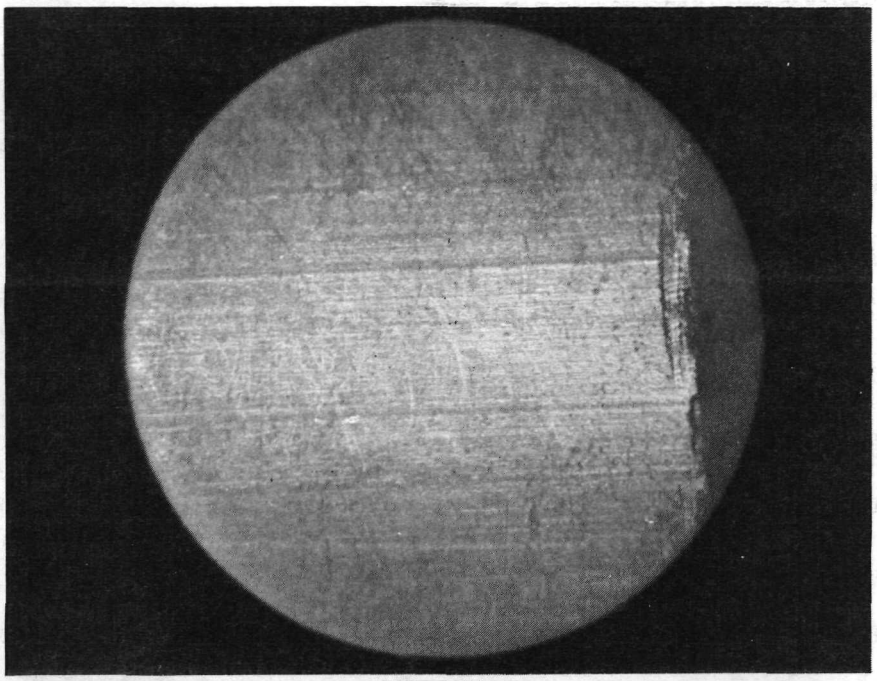

NEAR END
(A)

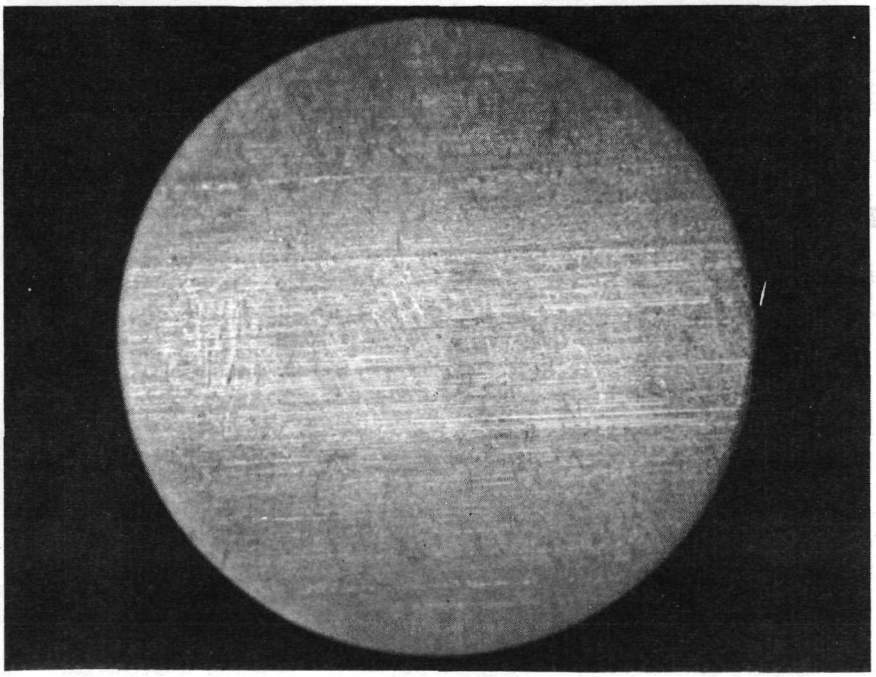

NEAR CENTER
(B)

Figure 3-3 DEVELOPMENTAL SAMPLE 1 (1D-A-00) SURFACE SCORING AT 25X

NEAR END
(A)

NEAR CENTER
(B)

Figure 3-4 DEVELOPMENTAL SAMPLE 1 (1D-A-00) SURFACE SCORING AT 500X

The surface features shown in Figures 3-3 and 3-4 will be used for comparison with those of Control Sample 1 (1C-A-00) and Flight Sample 1 (1F-A-00). Such comparisons will be used to determine if melting has occurred and if such melting caused any change in the complexion of the tungsten particles in the surface.

3.2.4.2.2 Tungsten Particle Distribution Determination Procedure

The distribution of tungsten particles was determined by the following procedure:

(1) The exposed planes were mechanically polished to produce a surface of particles and matrix.

(2) Microscopy (at 100X) was performed of the prepared surfaces in both the directional (axial) and cross-directional (radial) directions. Referring to Figure 3-2 for a definition of these directions, the line labeled 1 at its starting point and 15 at its end is the line along which photomicrographs 1 through 15 were taken. These were analyzed for directional display particle distribution data. Also, three series of photomicrographs were taken in a cross-directional mode and are designated as Line 1 (photomicrographs 16 through 20) Line 2 (photomicrographs 21 through 24) and Line 3 (photomicrographs 25 through 27). This data is the cross-directional display. The sample is labeled as having a cold end and a hot end which refers to the position in which the Control and Flight Samples were solidified.

(3) The 100X photographs were enlarged 2.5 times to produce large (8.75 x 11.25 in.) negatives. Particle distribution was determined from these negatives. The procedure involved the following:

(i) Each negative was placed on a view (light) table.

(ii) A thin sheet of paper with 1 cm ruled grid was used as an overlay.

(iii) Each grid point (intersection) which was occupied by a particle was checked.

(iv) The number of checked points on the overlay were counted and the particle volume fraction calculated.

The exact procedure and rationale for the determination of particle distribution is given in a series of memoranda written by H.T. McAdams of CAL and previously forwarded to NASA Personnel.

3.2.4.2.3 Tungsten Particle Distribution, Developmental Sample 1 (1D-A-00) Directional Display

Figure 3-2 shows the samples' dimensions, shape and areas used in the study of tungsten particle distribution. Fifteen photomicrographs were taken to determine the directional display. In the interest of efficiency, in this and subsequent instances, all photomicrographs will not be presented; instead, that number of photomicrographs necessary to represent the composite result in question will be presented.

Representative views for the directional display of Developmental Sample 1 (1D-A-00) are shown in Figures 3-5 through 3-8. The data from photomicrographs 1 and 15 shown in Figures 3-5(A) and 3-8(B) were not used in determining tungsten particle distribution because metallographic preparation was difficult and when a representative photomicrograph was finally obtained, enough alloy had been removed to effectively produce a new plane. The data obtained from such planes (both ends) cannot be plotted with that obtained from the plane (representative of photomicrographs 2 through 14). However, the representative views for the ends are included to show that the matrix had a decrease in particle density or contains a smaller volume of tungsten particles.

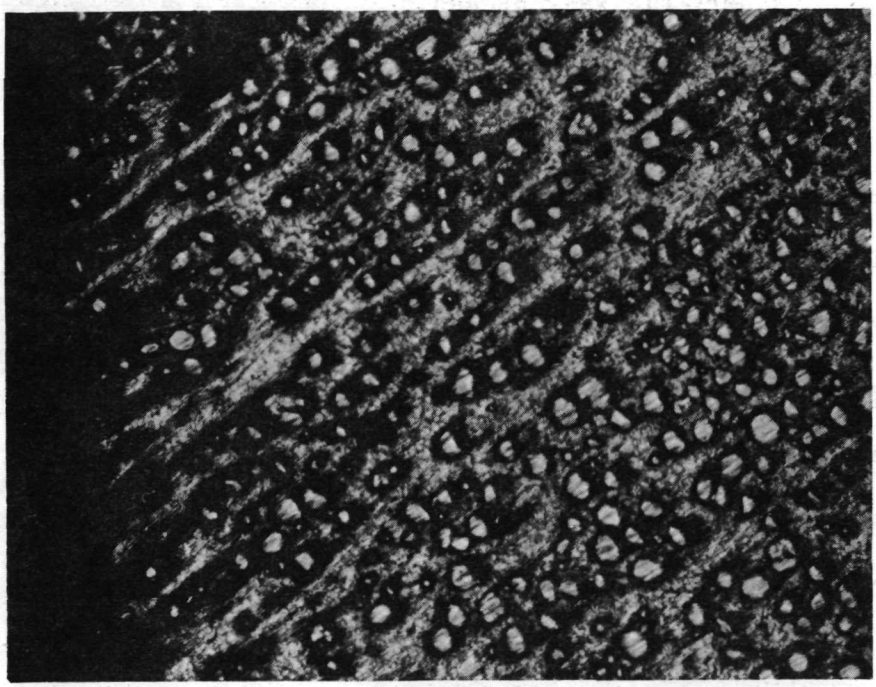

1
(A)

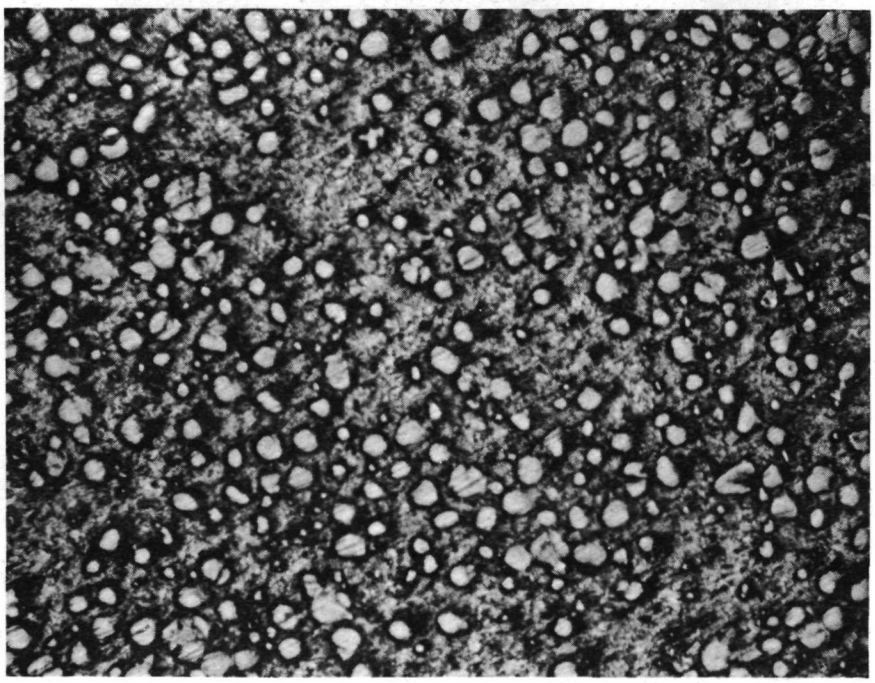

3
(B)

Figure 3-5 DEVELOPMENTAL SAMPLE 1 (1D-A-00) DIRECTIONAL DISPLAY AT 100X, PHOTOMICROGRAPHS 1 AND 3

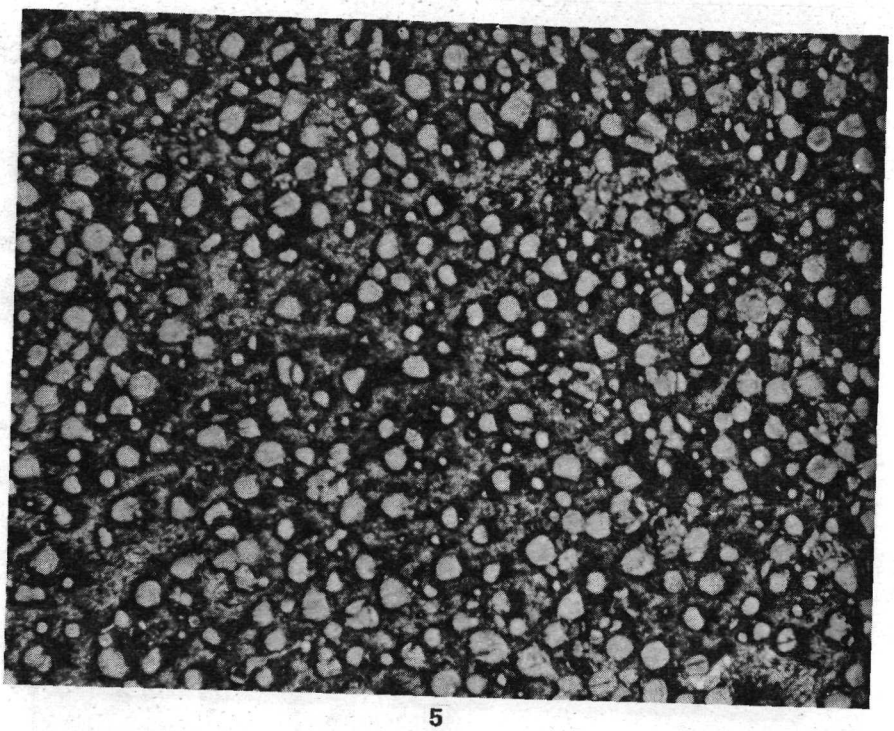

5
(A)

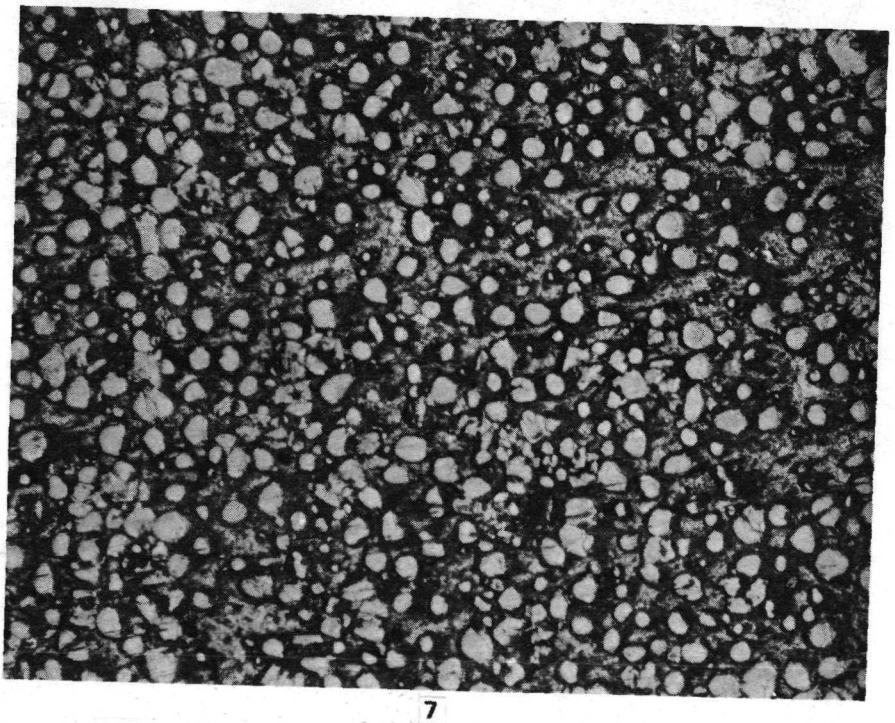

7
(B)

Figure 3-6 DEVELOPMENTAL SAMPLE 1 (1D-A-00) DIRECTIONAL DISPLAY AT 100X, PHOTOMICROGRAPHS 5 AND 7

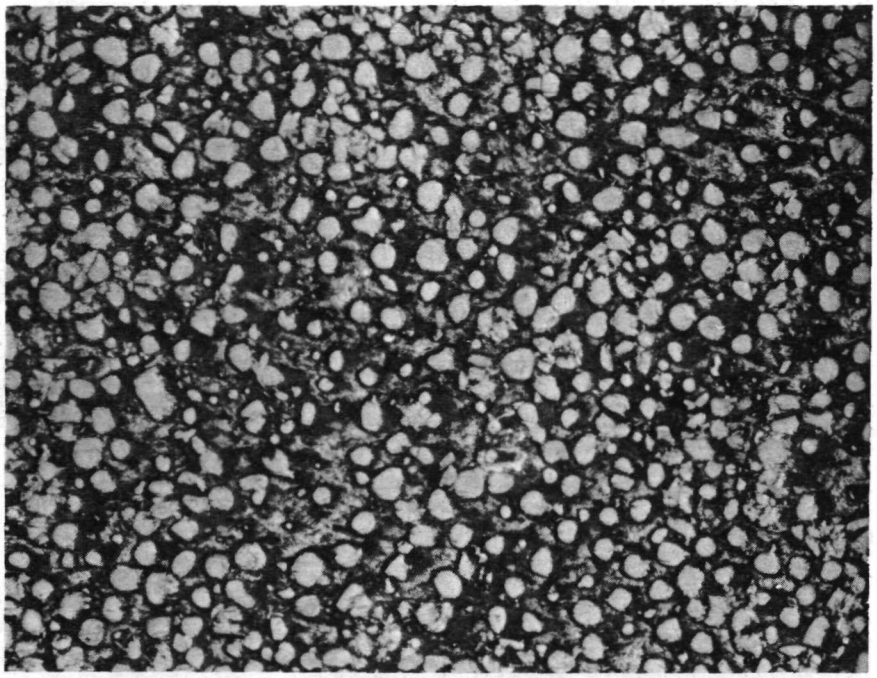

9
(A)

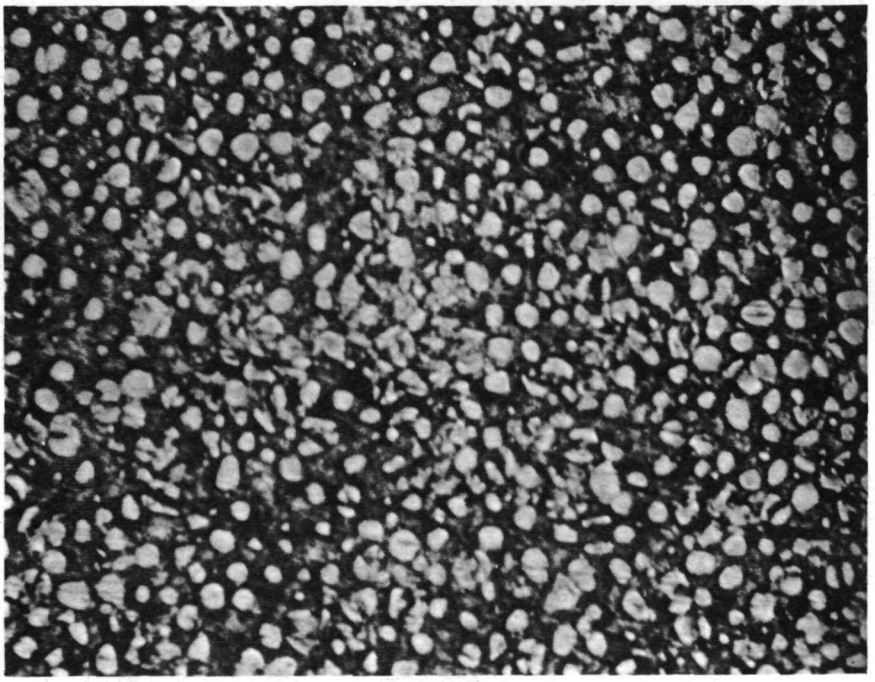

11
(B)

Figure 3-7 DEVELOPMENTAL SAMPLE 1 (1D-A-00) DIRECTIONAL DISPLAY AT 100X, PHOTOMICROGRAPHS 9 AND 11

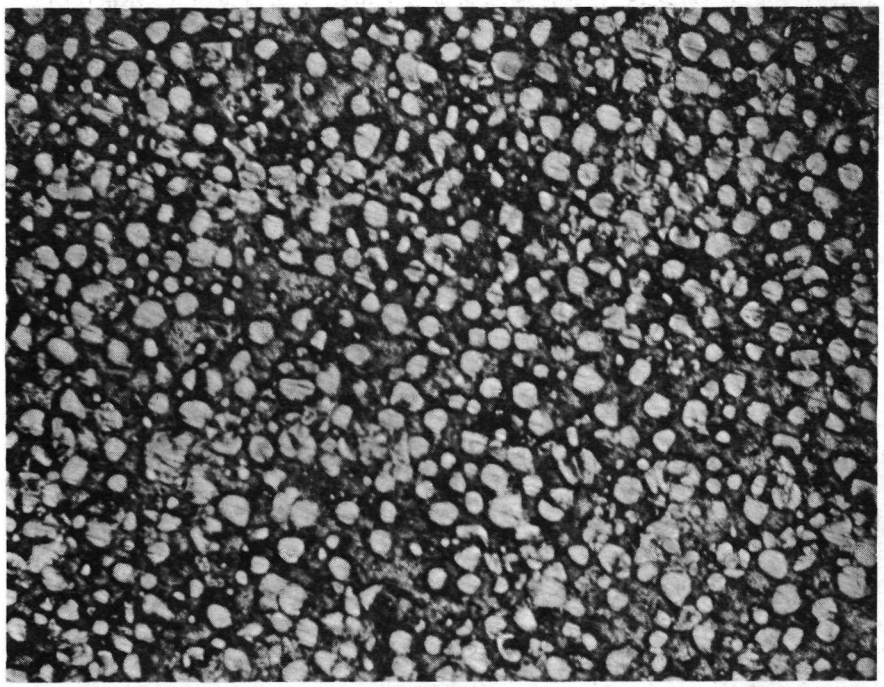

13
(A)

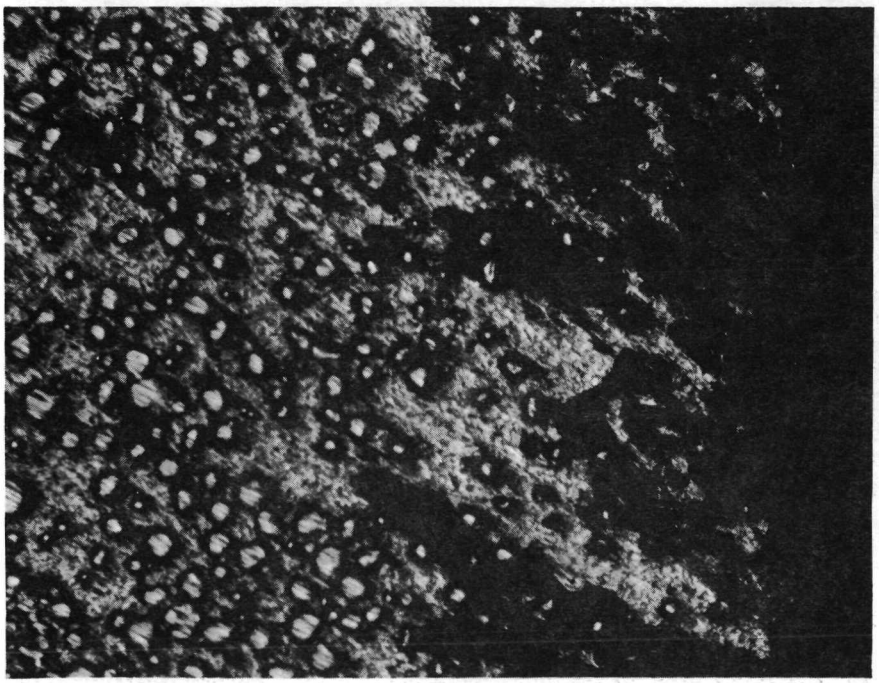

15
(B)

Figure 3-8 DEVELOPMENTAL SAMPLE 1 (1D-A-00) DIRECTIONAL DISPLAY AT 100X, PHOTOMICROGRAPHS 13 AND 15

Figure 3-9 is a plot of volume % tungsten versus location along the sample's axis. The tungsten particle distribution in Developmental Sample 1 (1D-A-00) is inhomogeneous. The range of tungsten volume % is from 36 at 1.27 cm (0.5 in) from End 1 to approximately 16 volume % (the extrapolated value at each end of the curve). The extrapolated values at either End 1 or End 2 cannot be considered as reliable data for plotting purposes because in a number of points along the curve abrupt directional changes occur and this could be the case for the end data. However, the density of tungsten particles does decrease at the sample ends as shown in Figure 3-5(A) and 3-8(B).

Cross-directional Display

Three cross-directional displays were taken along Line 1, Line 2 and Line 3 of Figure 3-2. The photomicrographs obtained from Line 1 are shown in Figures 3-10 and 3-11. These are also representative of those obtained from Line 2 and Line 3.

The volume % tungsten versus distance along location line for lines 1, 2 and 3 cross-directional displays is given in Figure 3-12. The volume % of tungsten particles changes radically with position. This is true even when allowance is made for surface effects by ignoring the data near surfaces and considering only that between 0.25 and 1.50 cm (0.1 and 0.6 in) on the location axis. This inhomogeneity in particle volume distribution is typical for Developmental Samples. An interesting aspect is the intersection of the curves with a line drawn at 0.85 cm (0.34 in) on the location axis to represent the center axis of the sample. The intersections indicate values of 34.5; 28.2 and 26.0 volume percents. These values represent new points (obtained by interpolation) for the Directional Display and appear as shown in Figure 3-13. The correlation is good in all locations except between 6.35 and 7.62 cm (2.5 and 3.0 in).

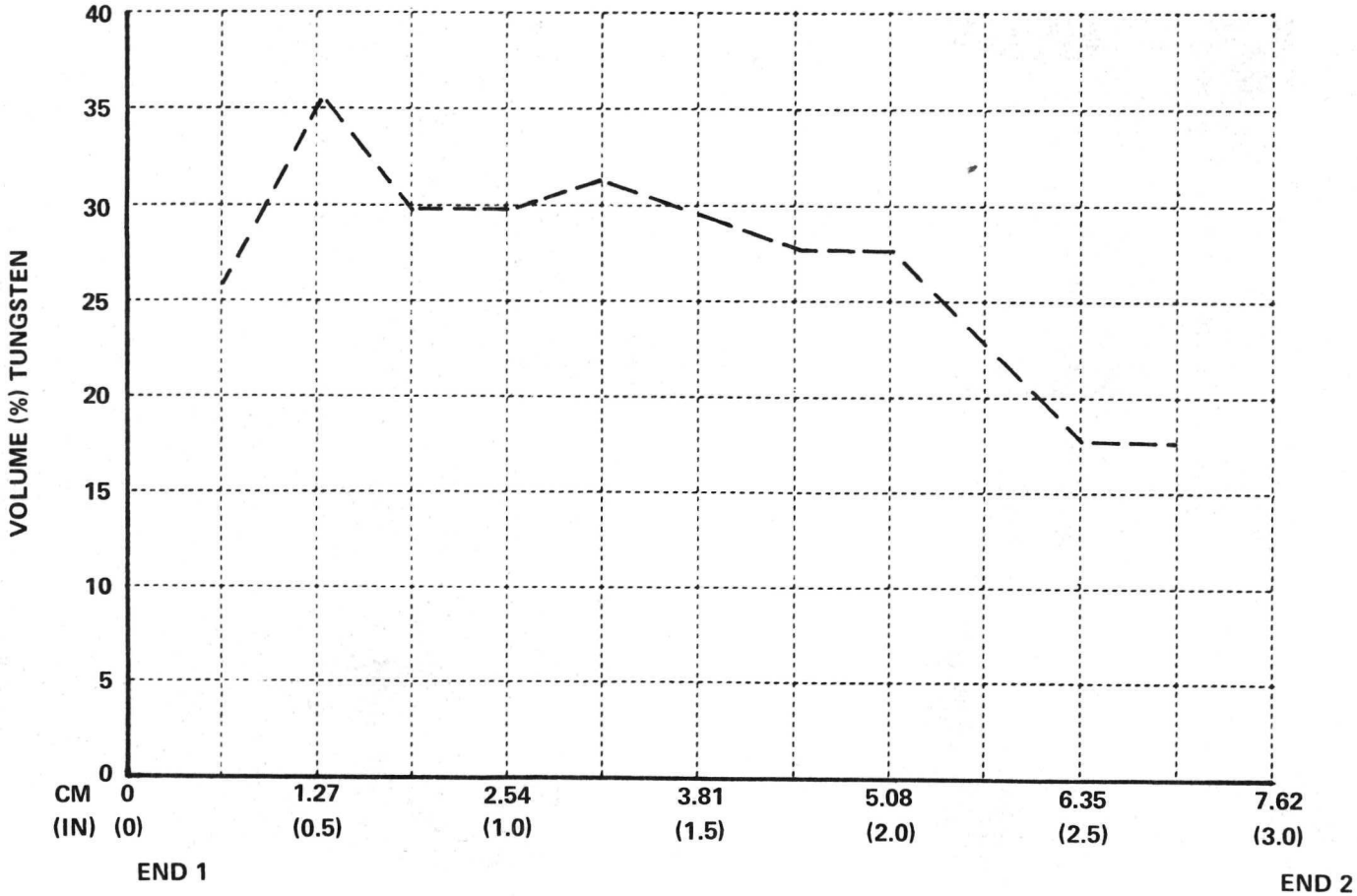

Figure 3-9 DATA PLOT, VOLUME % TUNGSTEN, DIRECTIONAL DISPLAY, DEVELOPMENTAL SAMPLE 1 (1D-A-00)

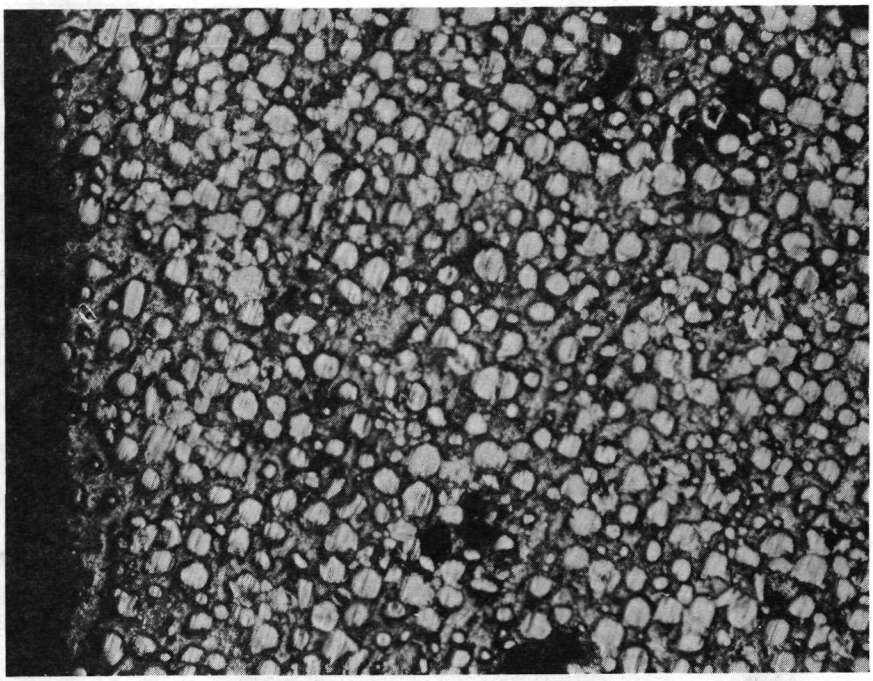

16
(A)

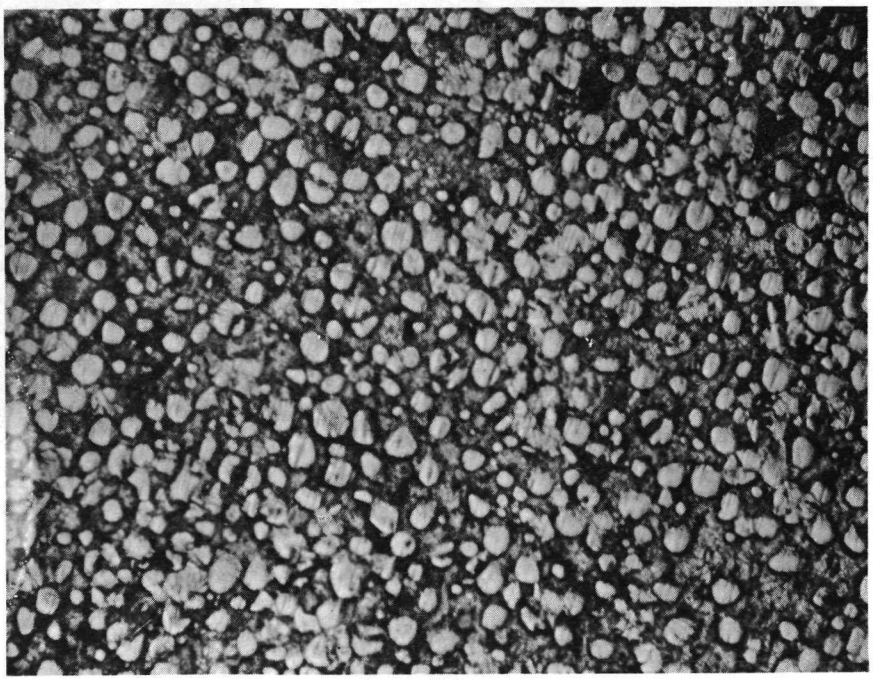

17
(B)

Figure 3-10 DEVELOPMENTAL SAMPLE 1 (1D-A-00) CROSS-DIRECTIONAL DISPLAY AT 100X, LINE 1 PHOTOMICROGRAPHS 16 AND 17

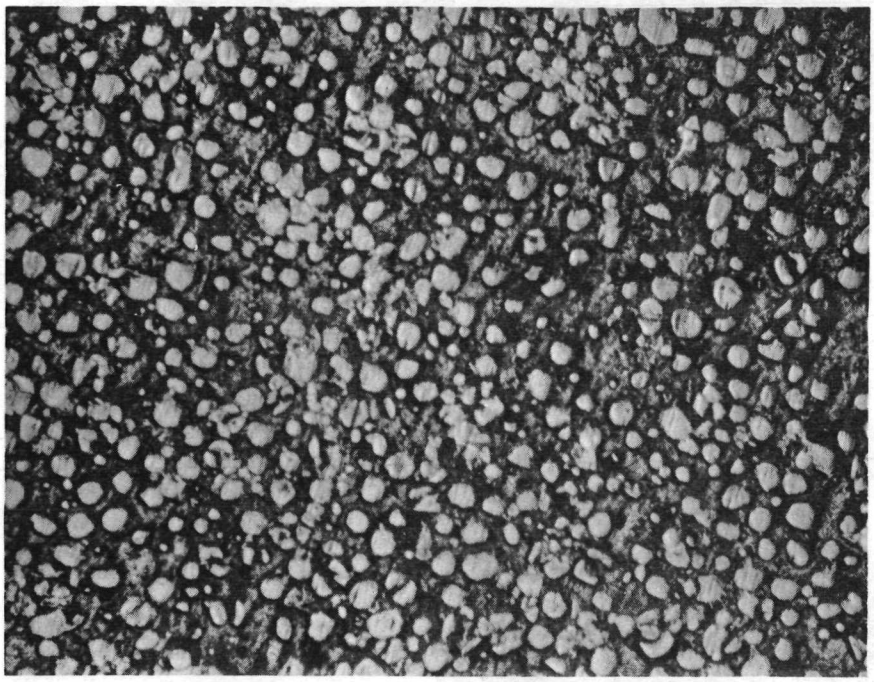

19
(A)

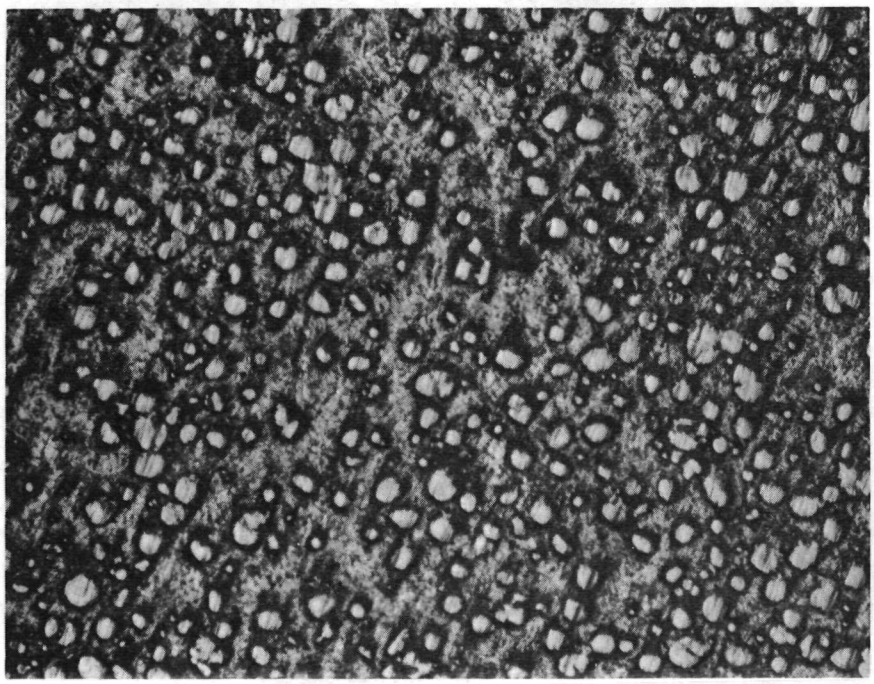

20
(B)

Figure 3-11 DEVELOPMENTAL SAMPLE 1 (1D-A-00) CROSS-DIRECTIONAL DISPLAY AT 100X, LINE 1 PHOTOMICROGRAPHS 19 AND 20

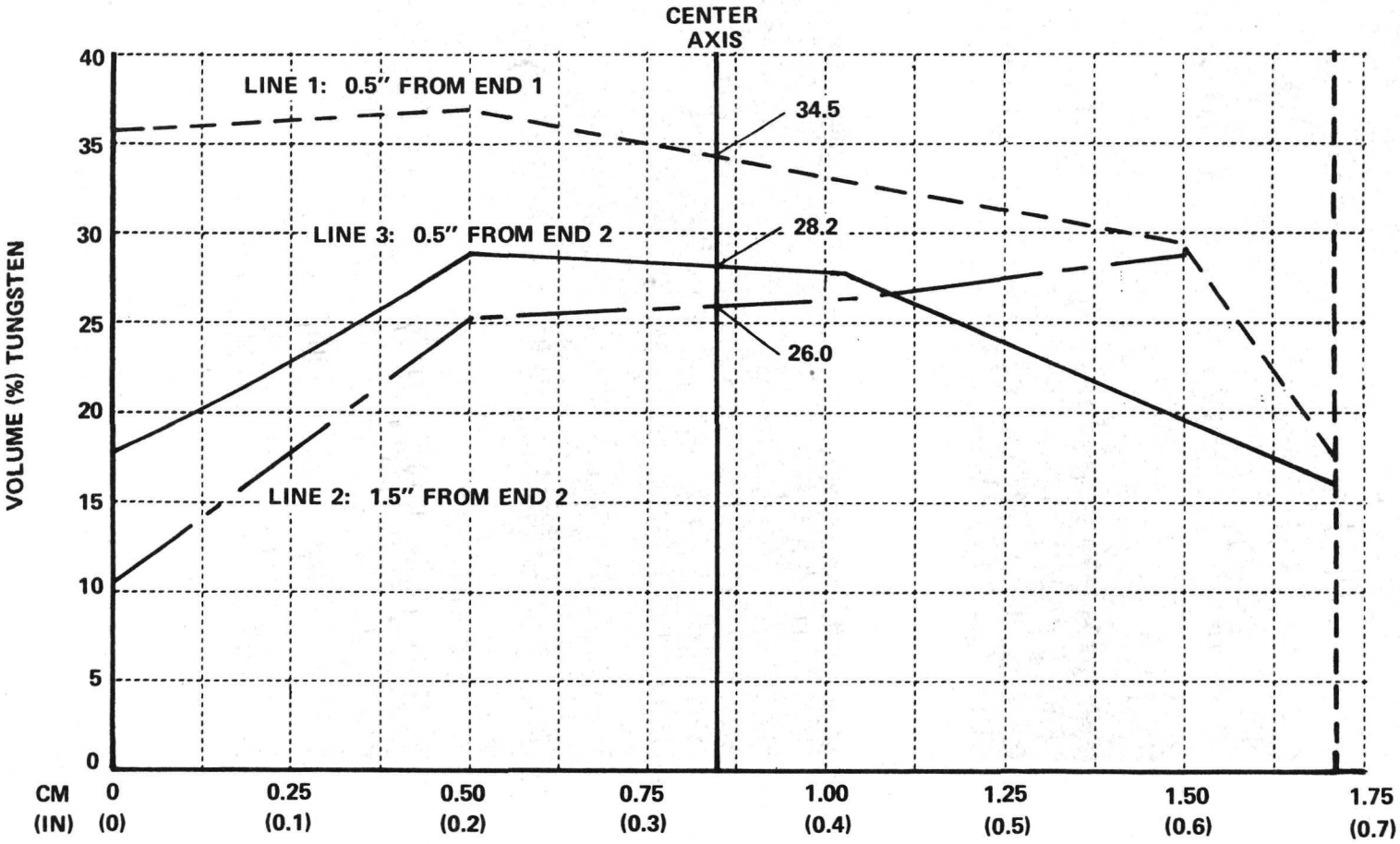

Figure 3-12 DATA PLOT, VOLUME % TUNGSTEN, CROSS-DIRECTIONAL DISPLAY, DEVELOPMENTAL MODEL 1 (1D-A-00)

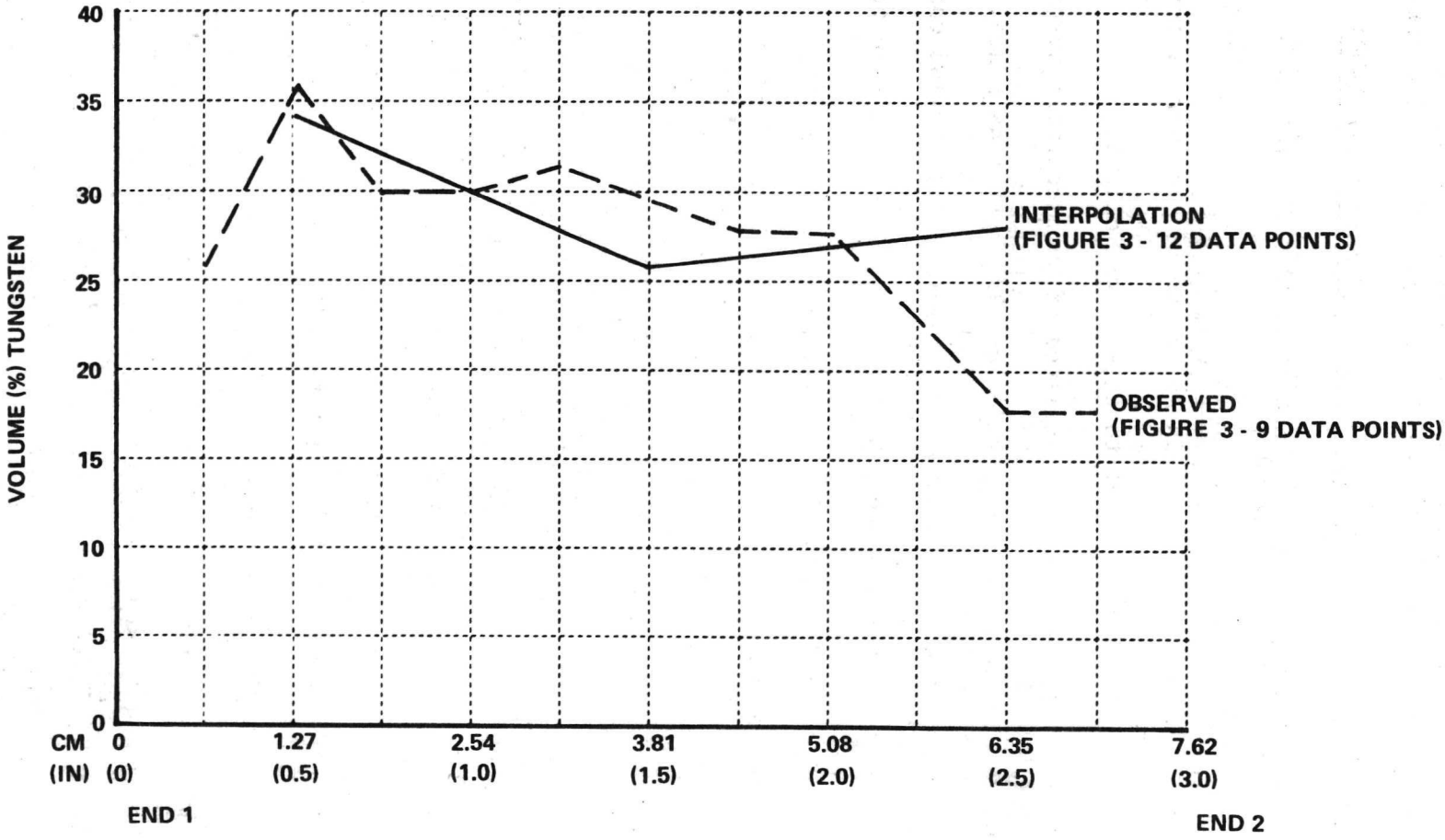

Figure 3-13 DATA PLOT, VOLUME % TUNGSTEN, COMPOSITE DIRECTIONAL DISPLAY, DEVELOPMENTAL SAMPLE 1 (1D-A-00)

The data of Figures 3-12 and 3-13 (representing the tungsten particle distribution in Developmental Sample 1) will be used as a basis for comparison with results for the Control Sample 1 and Flight Sample 1 experiments.

3.2.4.3 Control Sample 1 (1C-A-00) and Flight Sample 1 (1F-A-00)

3.2.4.3.1 Heater Characteristics and Compact Processing Procedure

A detailed description of the heater and procedure followed for melting the powder compacts is given in Reference 1. However, a brief abstract of Reference 1 information pertinent to this study follows.

The experimental apparatus consisted of an electrical heater and a storage box for the heater; the storage box also served as a heat sink for cooling. The compacts were contained in hermetically sealed capsules which were inserted into the heater, heated for a prescribed time to melt the compacts, and cooled by placing the heater and capsule into the heat sink. The heater operated on 27.5 vdc from the Command Module bus using the Data Acquisition Camera Power Cable. Nominal power consumption was 34 w. Redundant thermal switches were used to ensure that the outside surface of the heater did not exceed 105°F during the heating cycle. Maximum temperatures reached in the top of the capsules after 10 min were approximately 235°F. Cooling times of not less than 30 min in the heat sink reduced the temperature of the capsules to less than 100°F.

Melting of each powder compact was accomplished by placing the capsule containing the compact into the heater, heating for 10 min to melt the indium bismuth matrix, and then cooling on the heat sink for 30 min. In the case of Control Sample 1, the heater and sample were horizontal during the heating cycle and vertical during the cooling cycle.

Figure 3-14 shows data taken during processing of Control Sample 1 which indicates that the matrix material was molten after about 6 min and solidified after about 20 min. (This curve is also considered typical for Flight Sample 1.) Care was taken to minimize accelerations while the matrix was molten.

Sample Removal From Capsule

Removal of all samples from their capsules was performed in identical manner and included the following steps:

(1) The sealed capsule was mounted into a lathe chuck and made to run true.

(2) The capsule wall was turned to a thickness of approximately 0.10 cm (0.040 in).

(3) A thread was cut into the wall with thread depth of 0.05 cm (0.020 in).

(4) The remaining wall was then peeled off in a spiral and the sample was removed.

Sample Marking

After removal from its capsule, each sample was arbitrarily marked near its heat-sink end to establish a reference point. This point was used to determine the eventual cutting plane that resulted in the "A" and "B" halves. Also, the point was designated as the 0° position and rotation clockwise of the point for 180°, etc., was used to reference the sample "view" in subsequent photomicrography.

Results

The processing of Control Sample 1 (1C-A-00) was performed at the MSFC Huntsville, Alabama. A series of preliminary examiniations was performed at MSFC on the sample before it was bisected. After bisecting, one half was

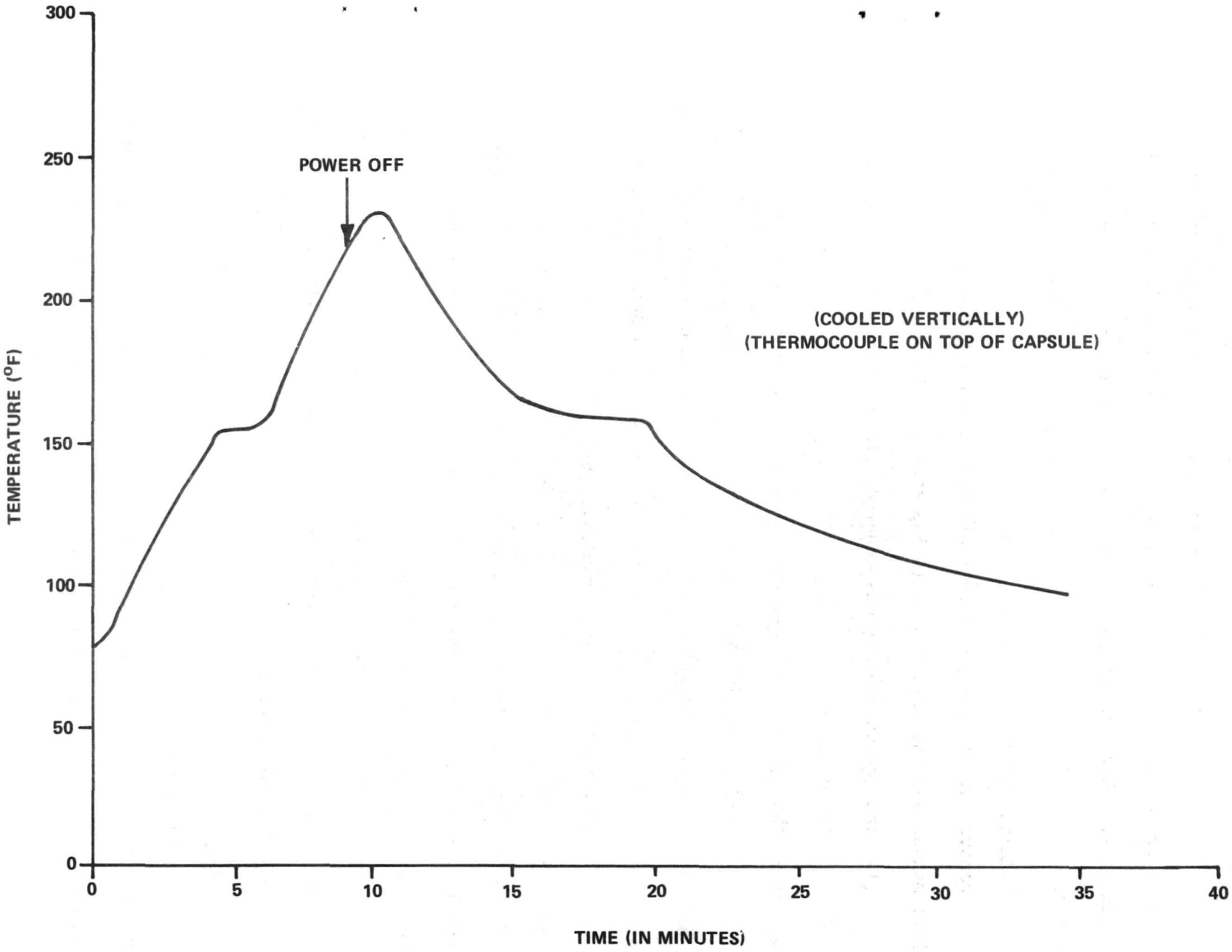

Figure 3-14 HEAT TEST ON SPECIMEN #1C IN QUAL HEATER

released to CAL personnel. A series of preliminary examinations were performed at CAL before mechanical polishing and cutting. The data from these examinations is of a purely documentary nature which can be used for comparison purposes with that obtained on other samples of this kind in the future.

Because the photographic documentations of the samples released to CAL were treated by MSFC personnel as a group, most photographs contain samples 1C-00 and 1F-00 as a "pair." Such documentation will therefore be presented as obtained; i.e., for both 1C-00 and 1F-00.

Figures 3-15 and 3-16 show the 1C-00 sample removed from its capsule. Two views are shown: 0° and 180°; thereby showing the entire surface. Also shown is an expansion slug produced during the melting of this sample. Slug formation is considered to have occurred as a result of solidification from both ends of the sample. A possible sequence of events would include the following:

(1) The compact (in its capsule) is heated until the matrix is molten.

(2) The compact is placed on the cooling pin and begins to solidify directionally.

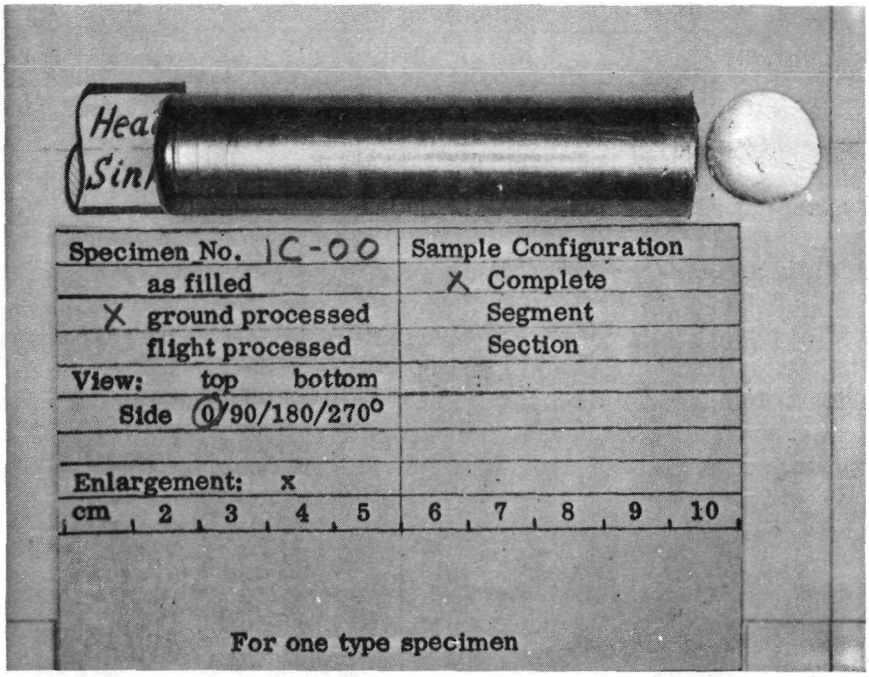

Figure 3-15 CONTROL SAMPLE 1 (1C-00) WITHOUT CAPSULE, 0° VIEW

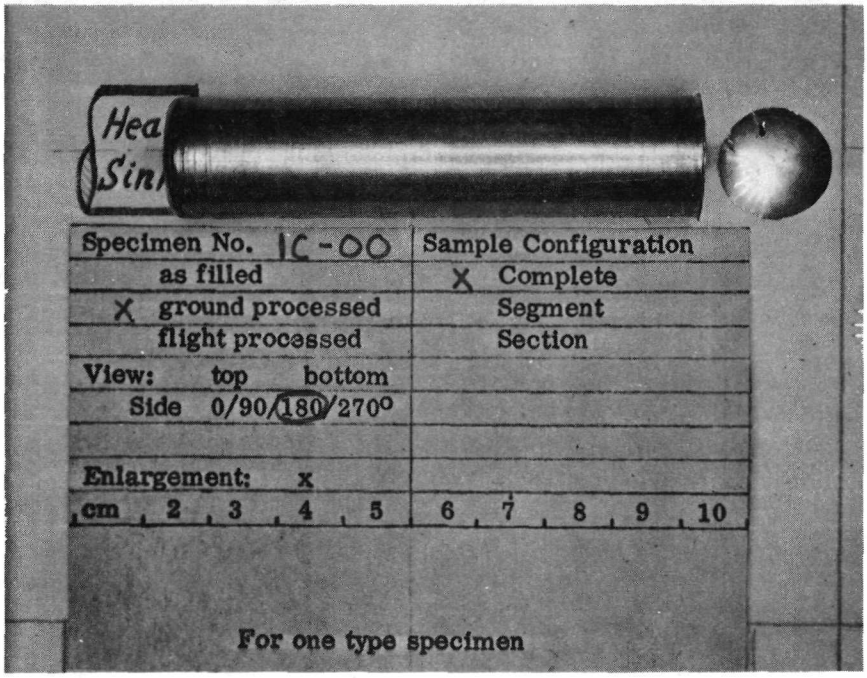

Figure 3-16 CONTROL SAMPLE 1 (1C-00) WITHOUT CAPSULE, 180° VIEW

(3) Because of the cooling assembly (Reference 1), heat extraction from the capsule was not unidirectional and eventually the end furthest from the heat sink reached a temperature low enough to initiate solidification at a time when most of the compact was in a solid state.

(4) Solidification of the compact proceeded in two directions (toward each other) until a point was reached where the remaining liquid was separated due to the stress set up between the advancing solid interfaces.

(5) This separation resulted in the formation of the expansion slug.

Figures 3-17 and 3-18 show the 1F-00 sample removed from its capsule. Shown are the 0° and 180° views. Two features are of interest in this case: first, an expansion slug was formed upon solidification of this sample as in the case of sample 1C-00 but the shape of this expansion slug is not round as in the former case (the possible reasons for this particular shape will be discussed later); second, the sample surface has two unusual features: a periodic grooving and the presence of a surface distortion for approximately 65-70% of the surface.

The periodic grooving can be attributed to the lathe work performed on the capsule. After melting, the sample probably was in contact with the capsule wall and, during machining of the thread grooves in the thin wall pressure of the cutting tool embossed the groove onto the sample surface.

The surface distortion may have occurred in many ways including the stripping off of matrix material (which had adhered to the capsule wall) during the sample removal process. However, this is not thought to be the case in that the distortion was not present near the heat sink end but the

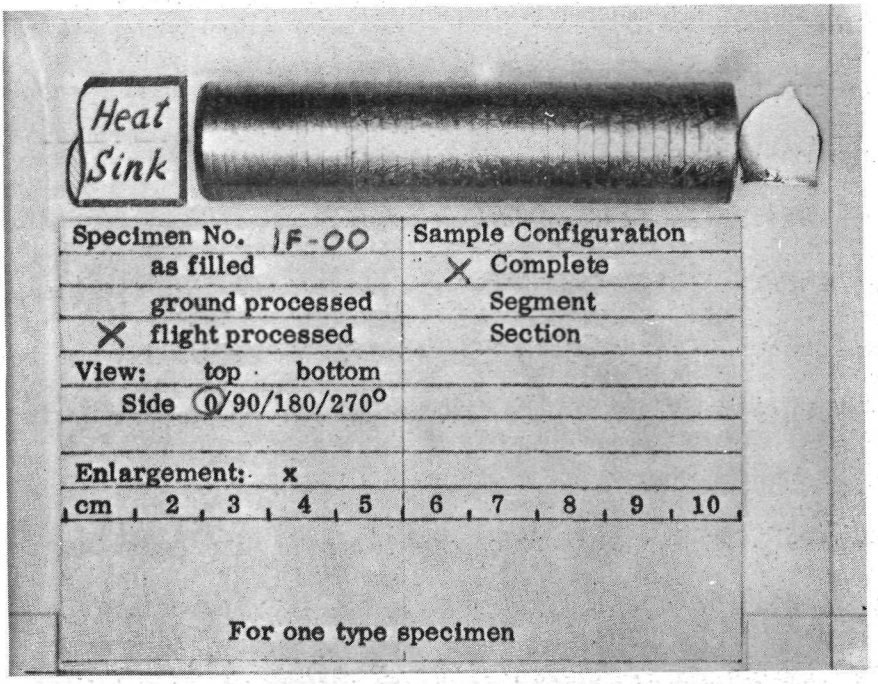

Figure 3-17 FLIGHT SAMPLE 1 (1F-00) WITHOUT CAPSULE. 0° VIEW

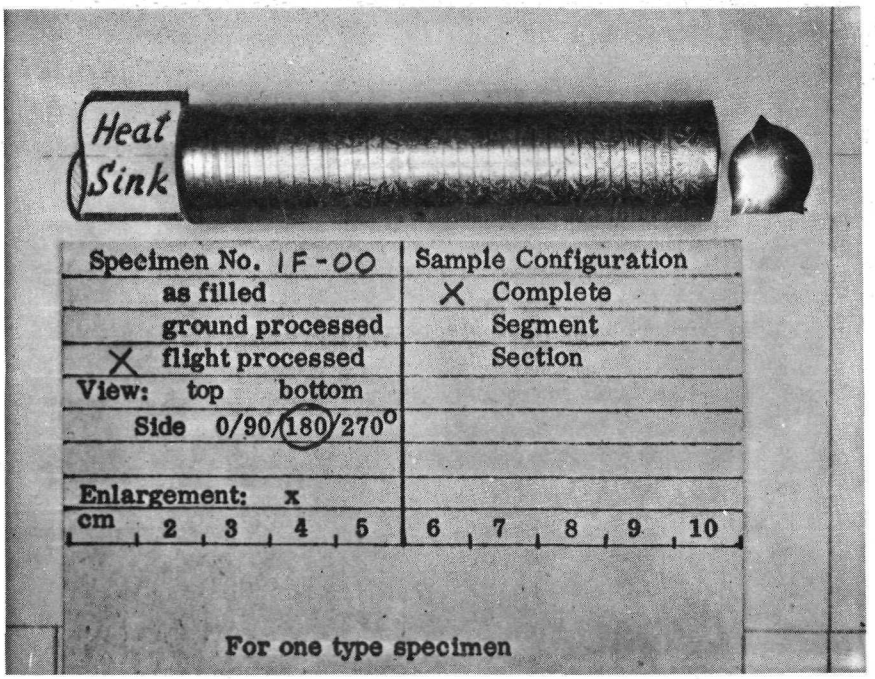

Figure 3-18 FLIGHT SAMPLE 1 (1F-00) WITHOUT CAPSULE, 180° VIEW

grooves were. The continuity of grooves indicates that all sections of the sample were in contact with the capsule wall under identical conditions. Therefore, if the surface distortion was due to stripping, such distortion would have occurred over the entire surface. This was not the case.

An explanation for the surface distortion could be the bursting of bubbles at the capsule-sample interface during solidification. It has been reported* that under a 0 G environment bubble motion will (in a liquid) be toward the container surface. The attachment of a bubble to a wall is accompanied by a decrease in total surface energy and this decrease is the driving force for such migration. Also, it has been reported[2] that in a directionally solidified metal, the motion of bubbles (in the melt) will be away from the advancing interface. The coupling of these two mechanisms could explain the observed phenomena in that bubble motion would be in a direction away from the advancing interface during initial solidification. After a given distance (volume) of solid formation the concentration of bubbles ahead of the solid-liquid interface would have increased sufficiently to cause a significant number of bubbles to contact the capsule wall. The accompanying decrease in total system energy and creation of a bubble concentration gradient drives this migration. Subsequently, the advancing solid freezes in the bubbles attached to the surface which, because of surface tension effects, have burst and result in the observed distortion.

The foregoing series of mechanisms require, as a basic condition, an incubation time (time for bubble-surface attachments). This is compatible with the smooth surface near the heat sink end. Also, it predicts that the sample end farthest from the heat sink (i.e., the hot end) will have the most surface distortion. (The end near the heat sink is the cold end.)

(2) Reynolds, W. C., Saad, M. A.; and Satterlee, H. M. Capillary Hydrostatics and Hydrodynamics at low g. Michigan Engineering Department, Stamford University. Technical Report Number LG-3, September 1, 1964.

Figure 3-19 shows a 5.5X magnification of the cold end of Flight Sample 1 (1F-A-00). The dendritic type of surface feature starts after approximately 2 cm of solidification had occurred. Figure 3-20 shows a 5.5X magnification of the remainder of Flight Sample 1 (1F-A-00) including the hot end. Apparently the degree of surface distortion increases along the length of the sample. However, a quantitative determination of this effect has not been made since (1) a satisfactory method to measure this distortion has not been found and (2) this effect is a unique event. Therefore, at this time precise documentation of the phenomenon is warranted but extensive theoretical consideration is not. If on subsequent flights similar casting demonstrations are performed, and supporting data obtained, a strict quantitative analysis of all (present and future) data will be appropriate.

Control Sample 1 (1C-A-00) did not have this surface distortion. Figures 3-21 and 3-22 are similar to Figures 3-19 and 3-20 but show Control Sample 1 (1C-A-00). At this magnification (5.5X) grooving resembling that of Flight Sample 1 (1F-00) is discernible. However, the surface distortion shown in Figures 3-19 and 3-20 is not apparent. This supports the preliminary contention that the surface distortion of Flight Sample 1 (1F-00) may be associated with the 0 G environment.

The contention that the 0 G environment is manifest in surface effects via bubble (or void) interaction with the container wall is also suggested when consideration is given to the surface features of the hot and cold ends of Control Sample 1 (1C-00) and Flight Sample 1 (1F-00). Figures 3-23 and 3-24 show comparison profile views of these ends.

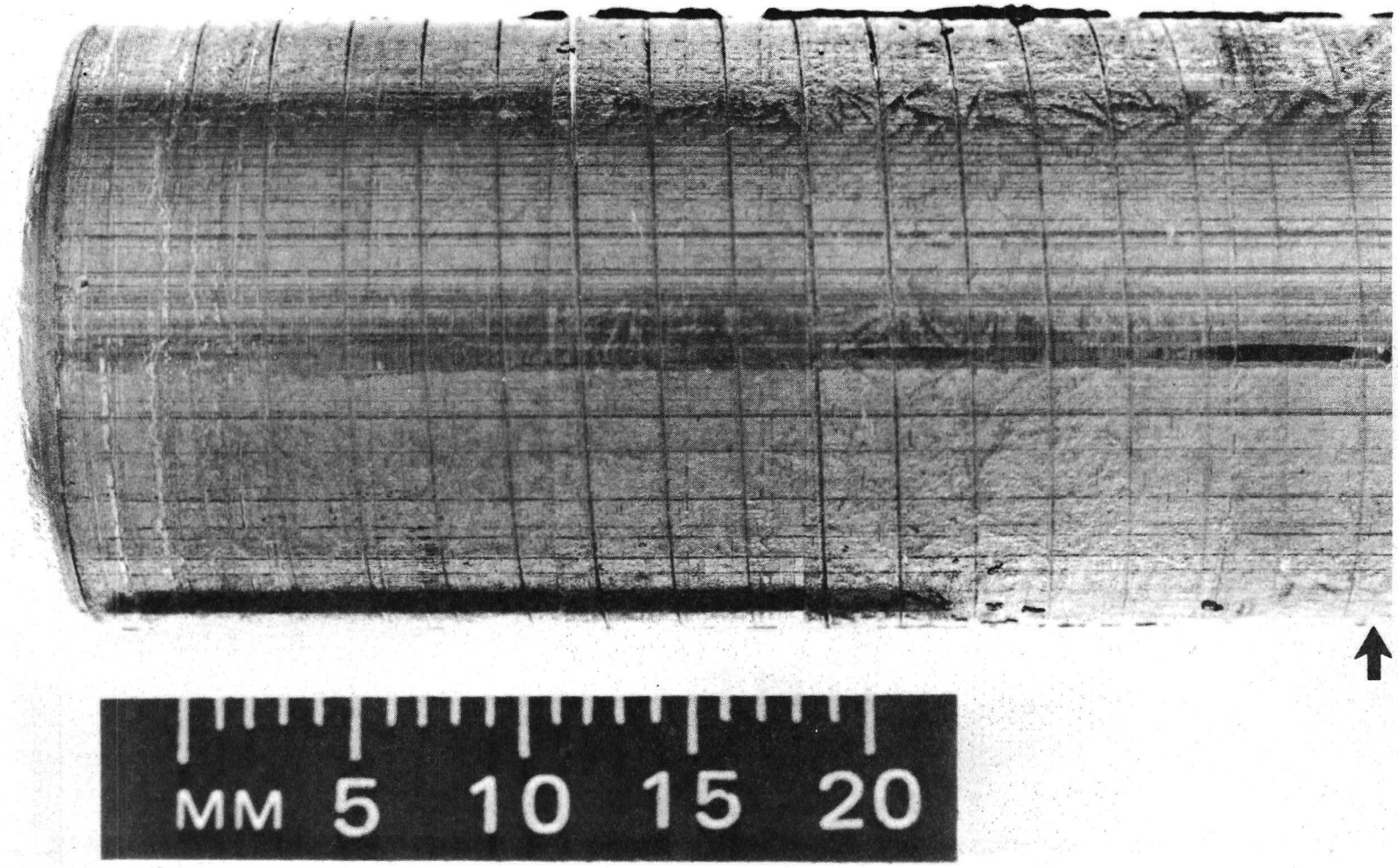

Figure 3-19 COLD END, FLIGHT SAMPLE 1 (1F-A-00) AT 5.5X

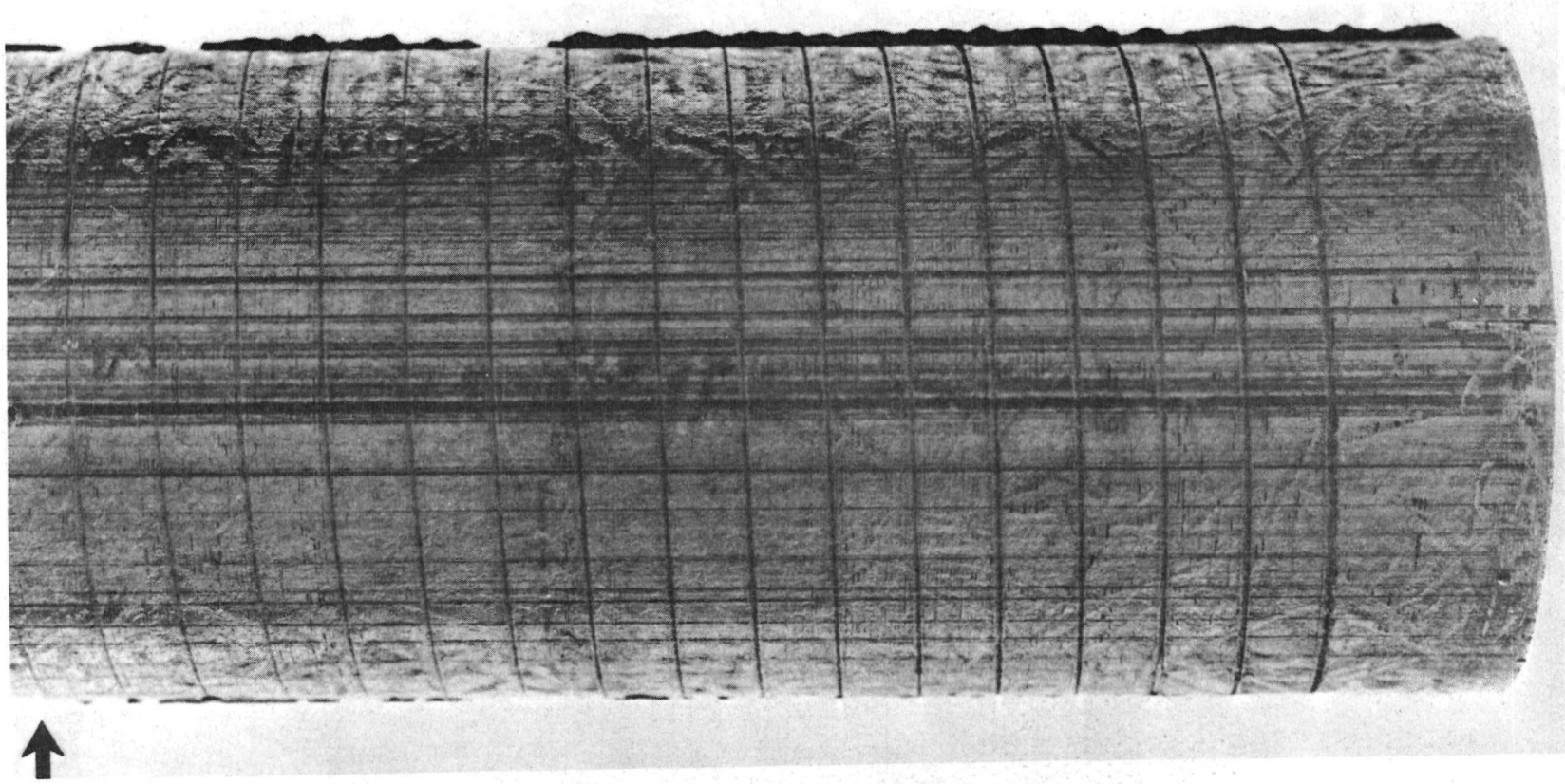

Figure 3-20 REMAINDER OF FLIGHT SAMPLE 1 (1F-A-00), INCLUDING HOT END, AT 5.5X

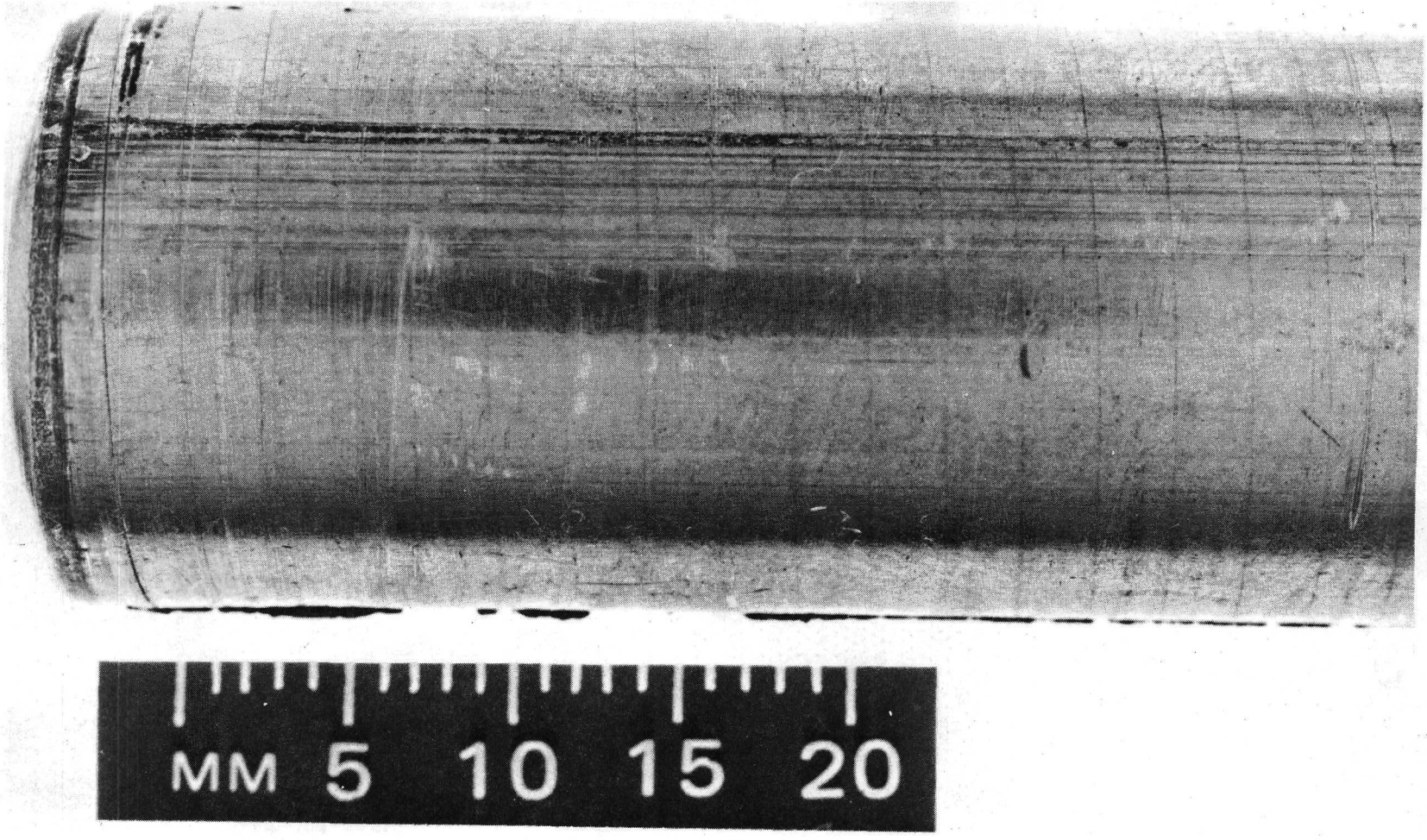

Figure 3-21 COLD END, CONTROL SAMPLE 1 (1C-A-00) AT 5.5X

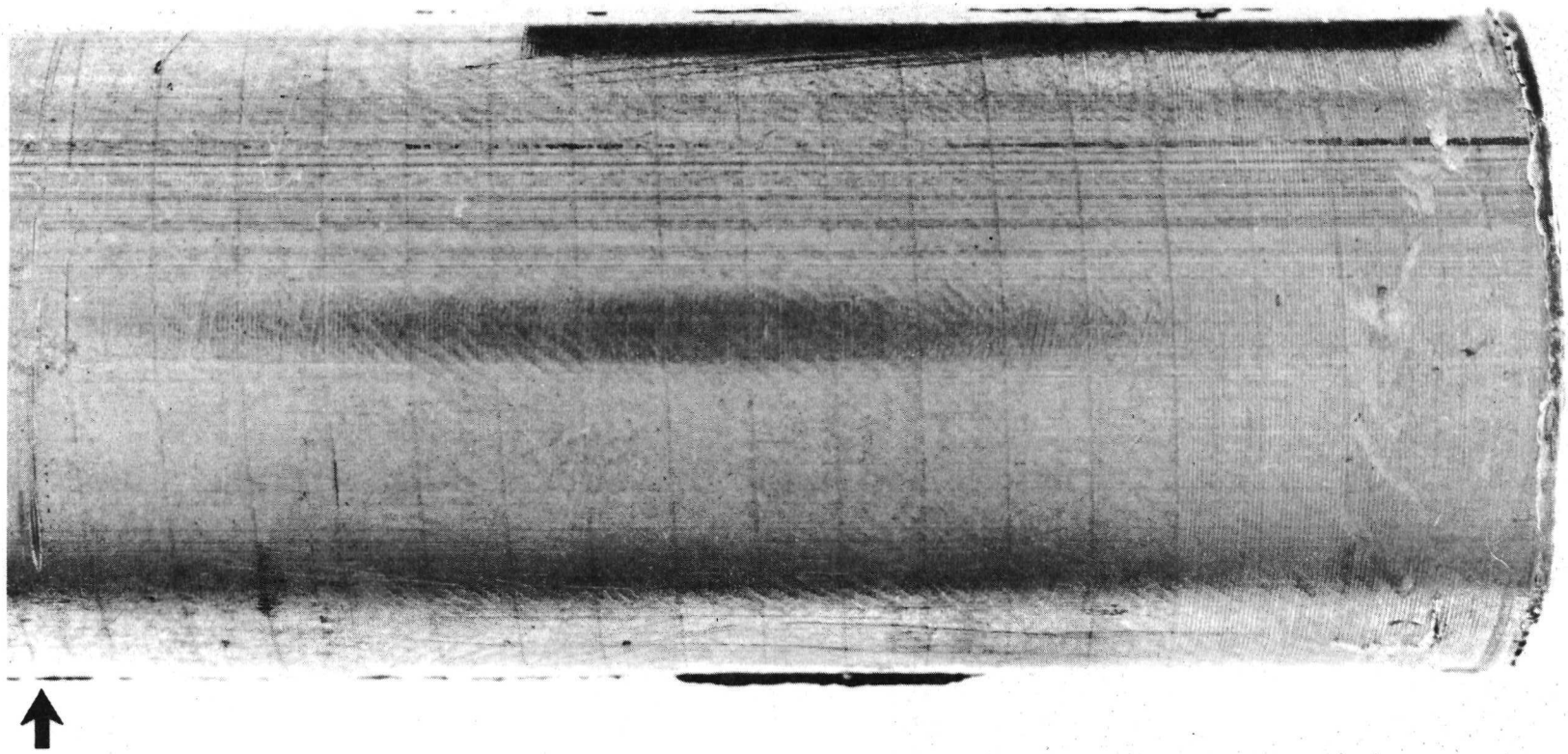

Figure 3-22 REMAINDER OF CONTROL SAMPLE 1 (1C-A-00), INCLUDING HOT END, AT 5.5X

The cold end (heat sink end) of Control Sample 1 (1C-00) exhibits a continuous surface condition showing the tool markings present in the capsule internal surface while that of Flight Sample 1 (1F-00) does not have such markings but does have a surface depression. This depression may have been formed by the coalescence of internal bubbles and/or voids which were near the surface when the heat sink was contacted and before solidification started. The appearance of this depression is not identical to those along the surface (discussed earlier) however, this may be related to the size and/or number of bubbles involved as well as to the severe thermal conditions occurring upon the initial contact of the sample with the heat sink. Nevertheless, an identical condition did not occur in Control Sample 1.

The hot ends of Control Sample 1 and Flight Sample 1 were not in contact with the capsule surface at any time. Both were formed by the last liquid to solidify between the sample and its individual expansion slug. The conditions resulting in pits on this surface of Control Sample 1 can be defined by considering that the sample was solidified in a vertical position. The high density of the matrix and particle components, each of which tends to settle, force any internal bubbles and/or voids to rise to the top. The mechanisms involved in the formation of surface pits as observed in Flight Sample 1 would be similarly based. However, the one most important, non-contradictory observation in this case, as in the others, is that a larger number of surface pits exists (or have occurred) on Flight Sample 1 than on Control Sample 1. This observation is consistent in every surface region observed.

Flight Sample 1 and Control Sample 1 were identical in their size, theoretical density and fabrication process. Assuming that the thermal profiles were also identical, as shown in Figure 3-14, the inescapable conclusion

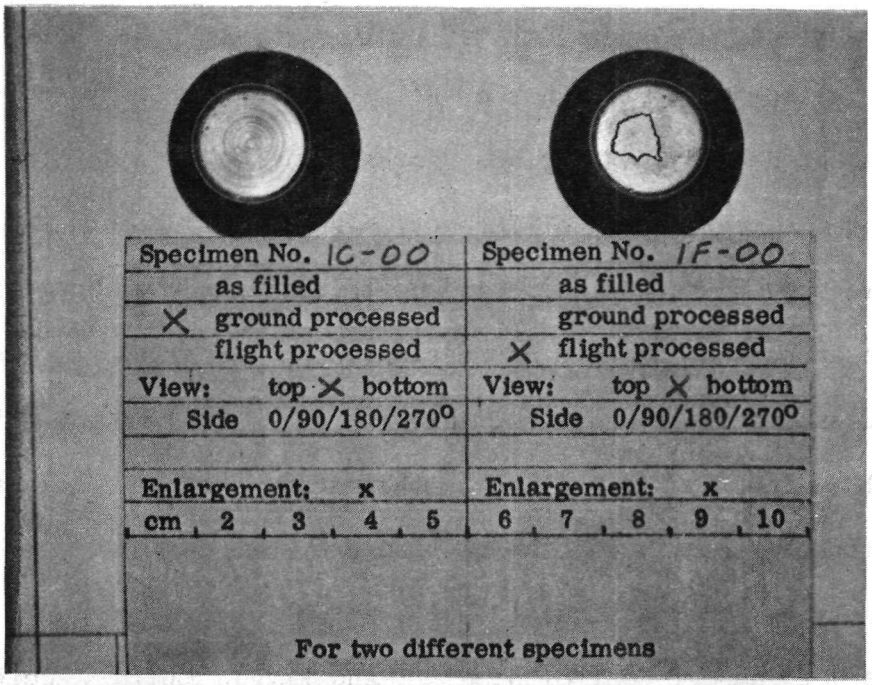

Figure 3-23 END VIEW, CONTROL SAMPLE 1 (1C-00) AND FLIGHT SAMPLE 1 (1F-00) COLD ENDS

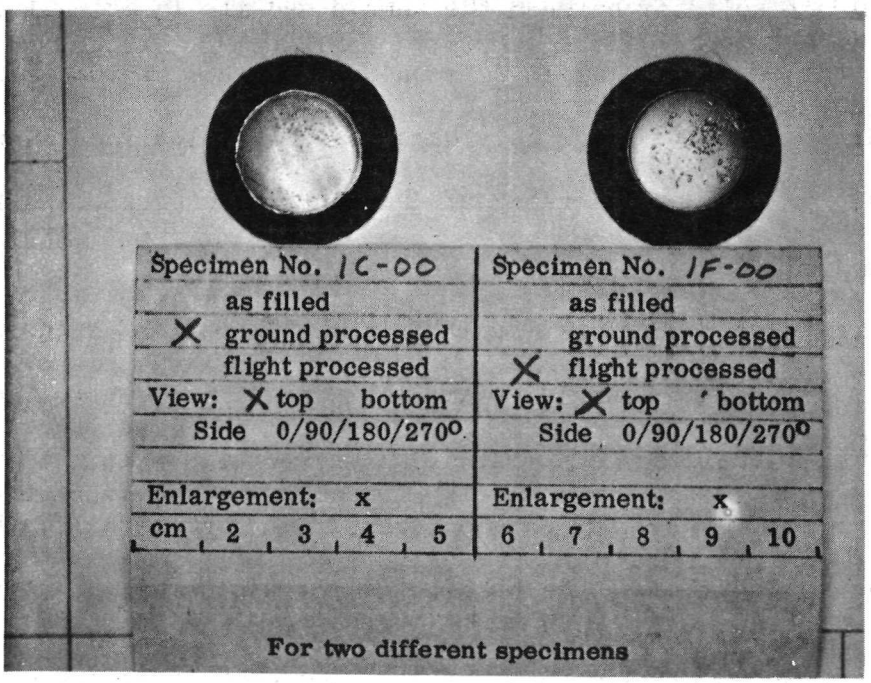

Figure 3-24 END VIEW, CONTROL SAMPLE 1 (1C-00) AND FLIGHT SAMPLE 1 (1F-00) HOT ENDS

is that regardless of the mechanisms involved (and based only on the fact that a significantly greater amount of surface distortion was present in Flight Sample 1) the migration (mobility) of bubbles and/or voids is enhanced in the 0-G environment.

Flight Sample 1 and Control Sample 1 were bisected longitudinally and the A half was released to CAL personnel for further analysis. Figure 3-25 shows both halves of Control Sample 1; Flight Sample 1 was similar.

The preliminary examinations at MSFC included a determination of sample weight, length, diameter and center of gravity for samples 1, 2 and 10. The data is given in Table 3-I including that of the expansion slugs of samples 1 and 2.

3.2.4.3.2 Control Sample 1 (1C-A-00) Metallographic Examination

Metallographic examination of Control Sample 1 (1C-A-00) consisted of a series of observations at 25X, 100X and 500X magnification to (1) gather "surface" data which would be useful in the interpretation of tungsten particle dispersion studies and (2) precisely document surface conditions so that data from future composite casting experiments could be correlated.

General Appearance - Low Magnification (25X)

Figures 3-26, 3-27 and 3-28 show the Control Sample 1 (1C-A-00) surface at low (25X)magnification. The cold end (heat sink) is shown in Figure 3-26 ;the central area in 3-27; and the hot end (last to solidfy) in 3-28. The areas shown represent most of the sample surface. The photographs were taken so that the long edge of the photomicrograph corresponds "directionally" with the longitudinal specimen direction. Note that, except for a small area of Figure 3-27, the typical longitudinal "die marks" (see Figure 3-3) have been removed during melting.

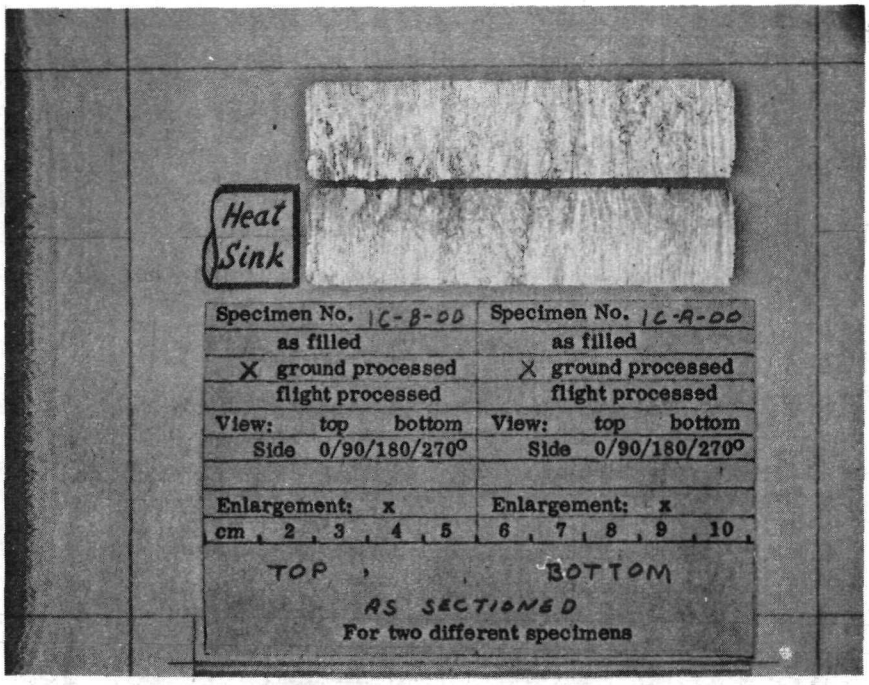

Figure 3-25 BISECTED CONTROL SAMPLE 1 (1C-A-00 AND 1C-B-00)

Table 3-1
DATA SHEET FOR PROCESSED COMPOSITE CASTING SAMPLES 1, 2 AND 10

PHYS. PROPERTIES \ SAMPLE NO.	1C-00	1F-00	2C-00	2F-00	10C-00	10F-00
WEIGHT OF SAMPLE (gram)	197.8	196.6	101.9	103.5	94.2	145.1
LENGTH OF SAMPLE (cm)	7.724	7.760	7.582	7.595	7.422	7.722
DIAMETER OF SAMPLE (cm)	1.755	1.758	1.737	1.742	1.745	1.722
CENTER OF GRAVITY FROM BOTTOM (cm)	3.820	3.785	–	–	–	–
HEIGHT OF EXPANSION SLUG (cm)	0.165	0.020	–	–	–	–
WEIGHT OF EXPANSION SLUG (gram)	1.11	1.11	–	–	–	–

4/9/71

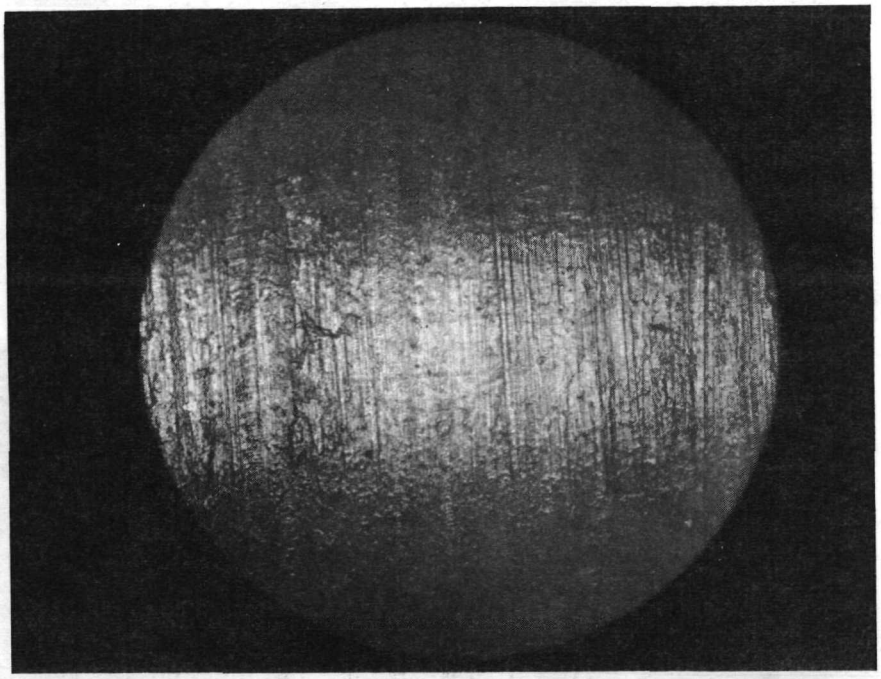

Figure 3-26 CONTROL SAMPLE 1 (1C-A-00) SURFACE AT COLD END (25X)

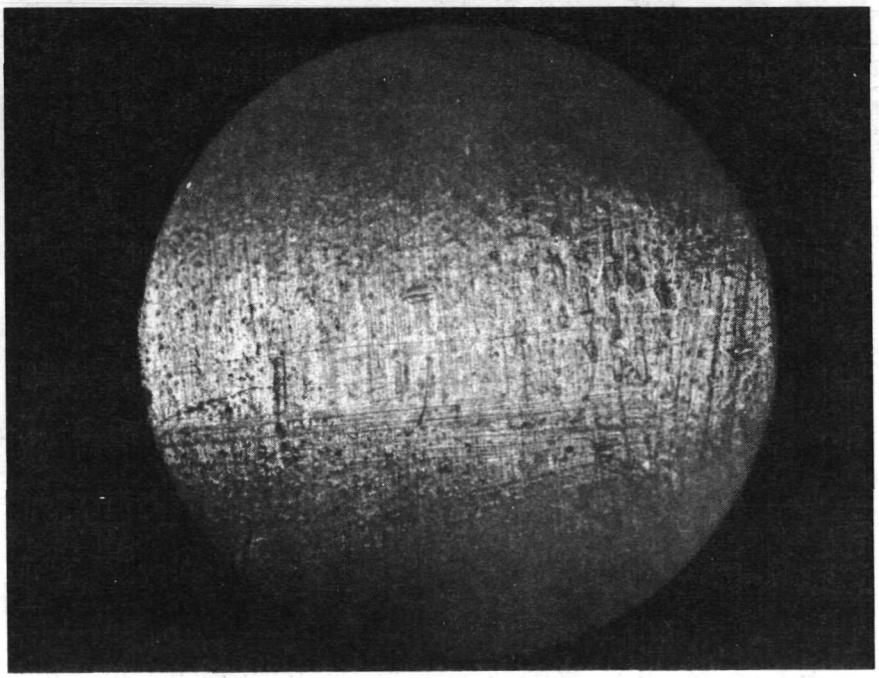

Figure 3-27 CONTROL SAMPLE 1 (1C-A-00) SURFACE AT CENTRAL AREA (25X)

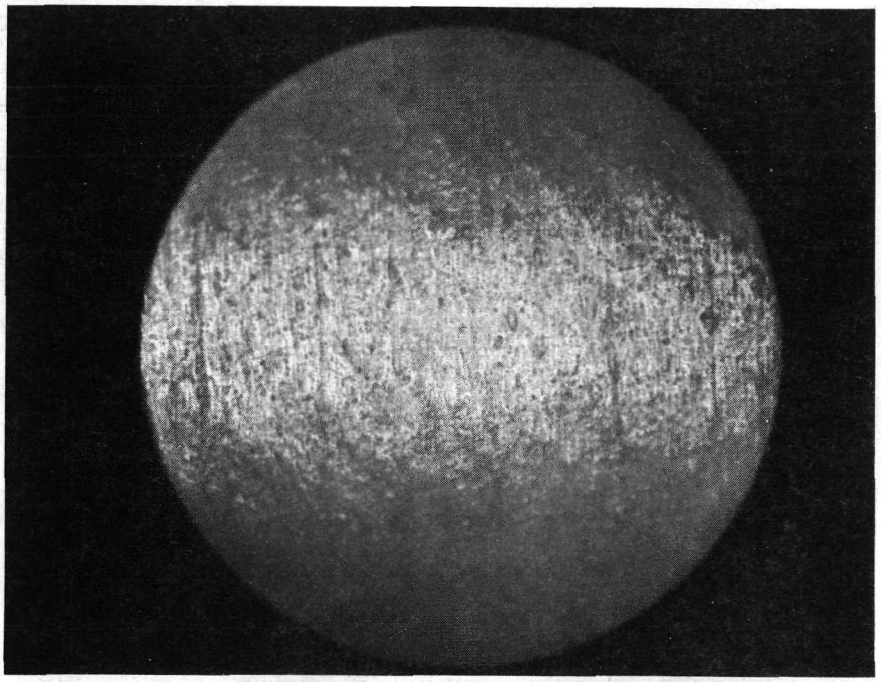

Figure 3-28 CONTROL SAMPLE 1 (1C-A-00) SURFACE AT HOT END (25X)

Figure 3-29 shows representative surface features which were not "generally" observed but were present. These include a cluster of tungsten particles exposed on the surface plus some tooling marks (Figure 3-29A) and a region exhibiting a high density of tooling marks (Figure 3-29B).

General Appearance - Intermediate (100X) and High (500X) Magnification

Control Sample 1 (1C-A-00) surface conditions at an intermediate magnification of 100X are shown in Figures 3-30 and 3-31 and 3-32 which are representative of the general surface characteristics observed at the cold end (Figure 3-30), the center (Figure 3-31), and the hot end (Figure 3-32) of the sample. The areas exhibiting tool markings and tungsten particle clustering are shown in Figures 3-33 and 3-34.

High magnification (500X) views of these features are shown in Figures 3-35 through 3-39. The general appearance at the cold end, center and hot end is shown in Figure 3-35, 3-36 and 3-37, respectively. These high-magnification views show surface features such as depressions and/or scratches probably caused by the capsule wall. Since the features are radically different from the longitudinal die markings on the Developmental Sample, they can be considered as evidence that melting, at least on the sample surface, had occurred.

Figure 3-38 shows a cluster of tungsten particles at 500X magnification. There is an area around some particles which has the appearance of a different phase. This "reaction zone" is also shown in Figure 3-39 which was specifically focused to accent the difference between the metal matrix (In-Bi) and the zone. MSFC personnel reported that in those samples where tungsten particles have been copper coated and melting had occurred, the formation is a Cu-In intermetallic phase. Optical comparison of MSFC views with Figure 3-39 indicates a similarity which is further evidence of sample melting in this case.

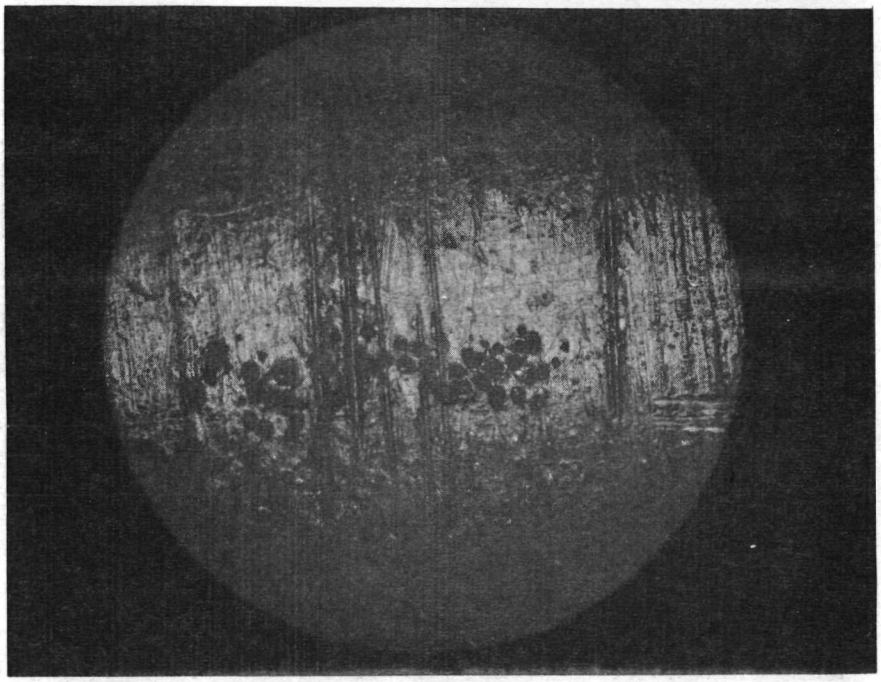

(A)

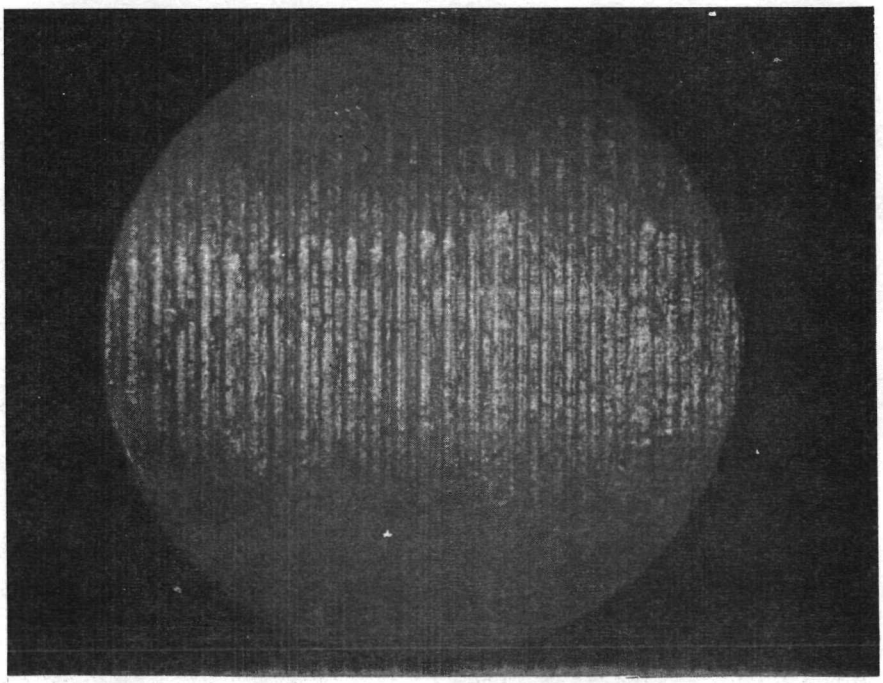

(B)

Figure 3-29 CONTROL SAMPLE 1 (1C-A-00) (25X) SURFACE TOOLING MARKS AND TUNGSTEN PARTICLE CLUSTER

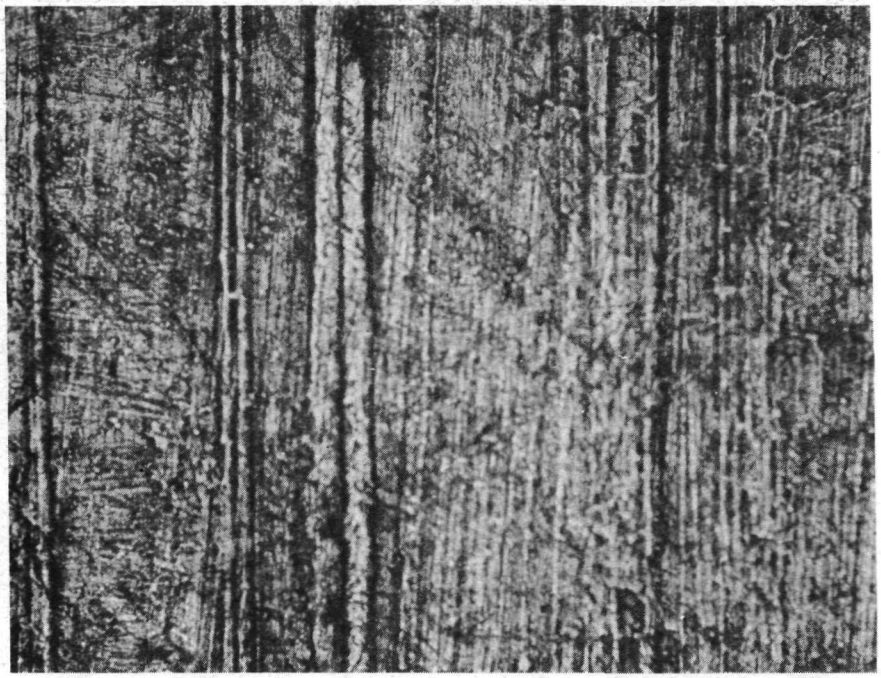

Figure 3-30 CONTROL SAMPLE 1 (1C-A-00) SURFACE AT COLD END (100X)

Figure 3-31 CONTROL SAMPLE 1 (1C-A-00) SURFACE AT CENTER (100X)

Figure 3-32 CONTROL SAMPLE 1 (1C-A-00) SURFACE AT HOT END (100X)

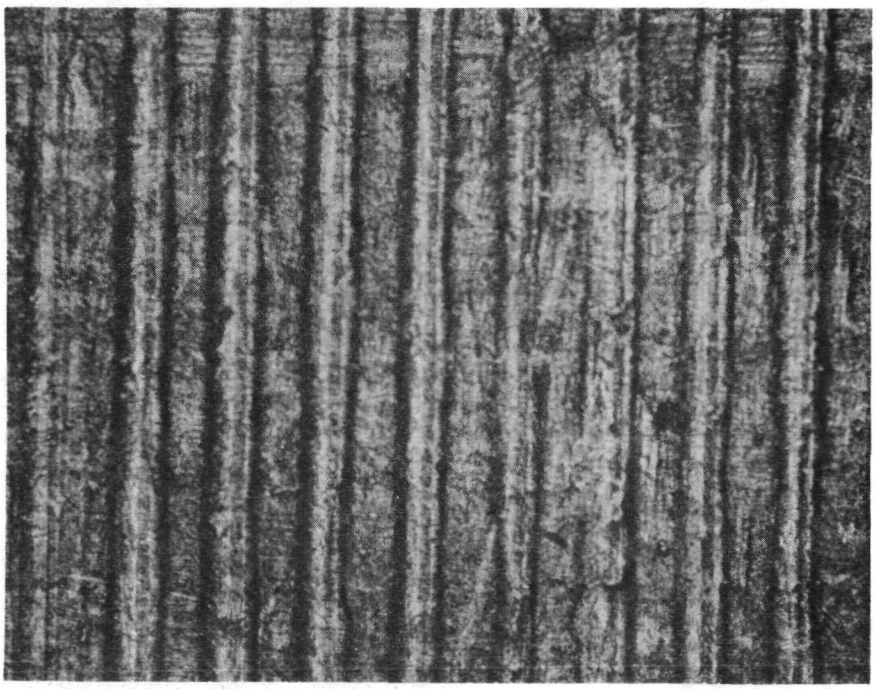

Figure 3-33 CONTROL SAMPLE 1 (1C-A-00) SURFACE TOOL MARKINGS (100X)

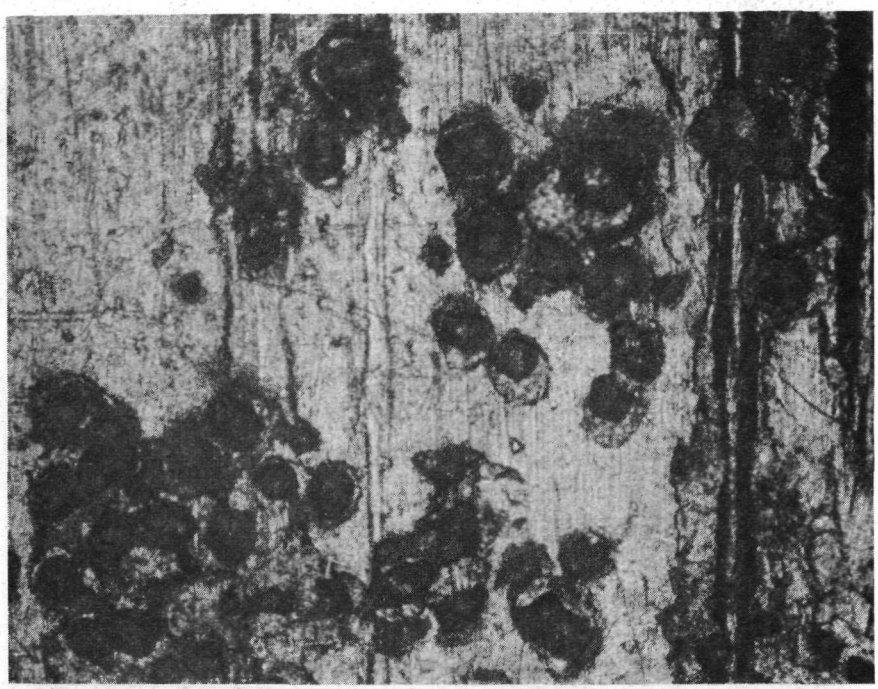

Figure 3-34 CONTROL SAMPLE 1 (1C-A-00) SURFACE TUNGSTEN PARTICLE CLUSTER (100X)

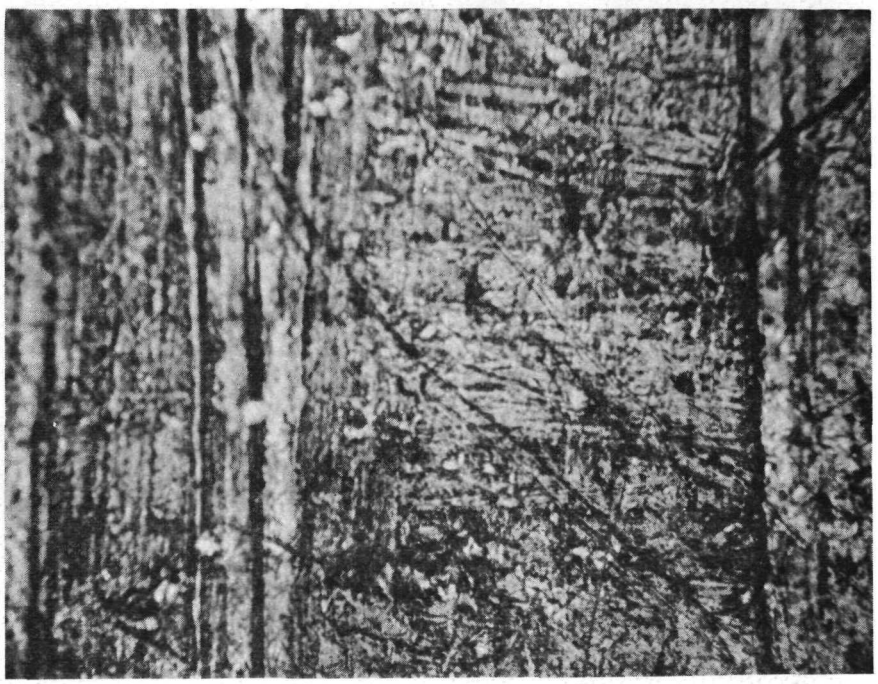

Figure 3-35 CONTROL SAMPLE 1 (1C-A-00) SURFACE AT COLD END (500X)

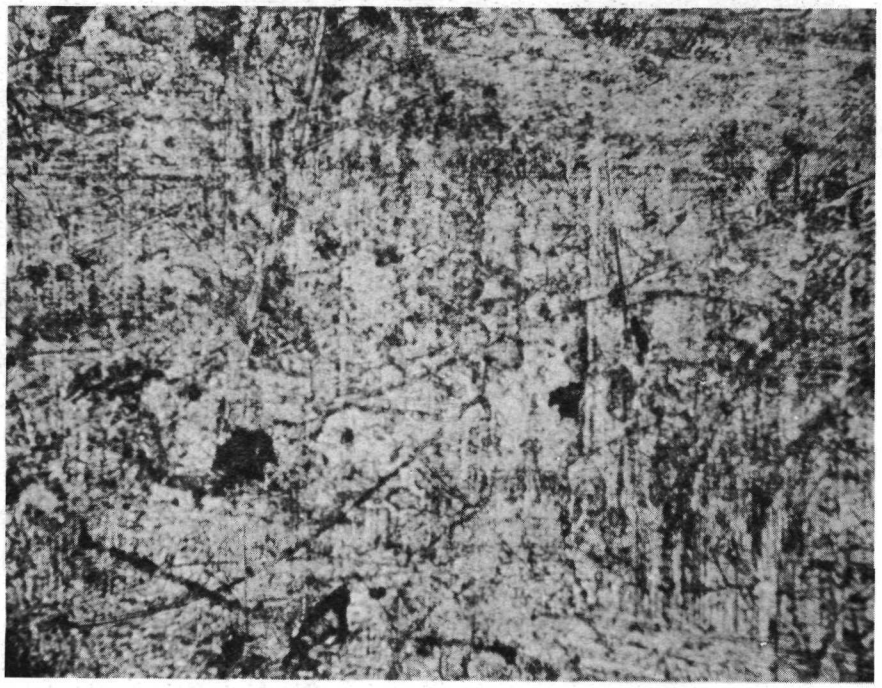

Figure 3-36 CONTROL SAMPLE 1 (1C-A-00) SURFACE AT CENTER (500X)

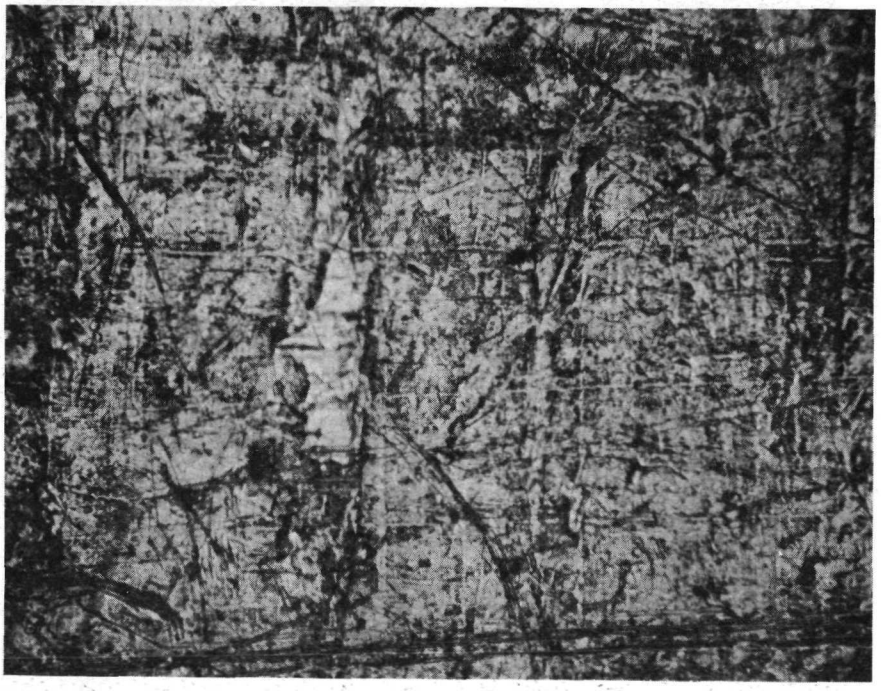

Figure 3-37 CONTROL SAMPLE 1 (1C-A-00) SURFACE AT HOT END (500X)

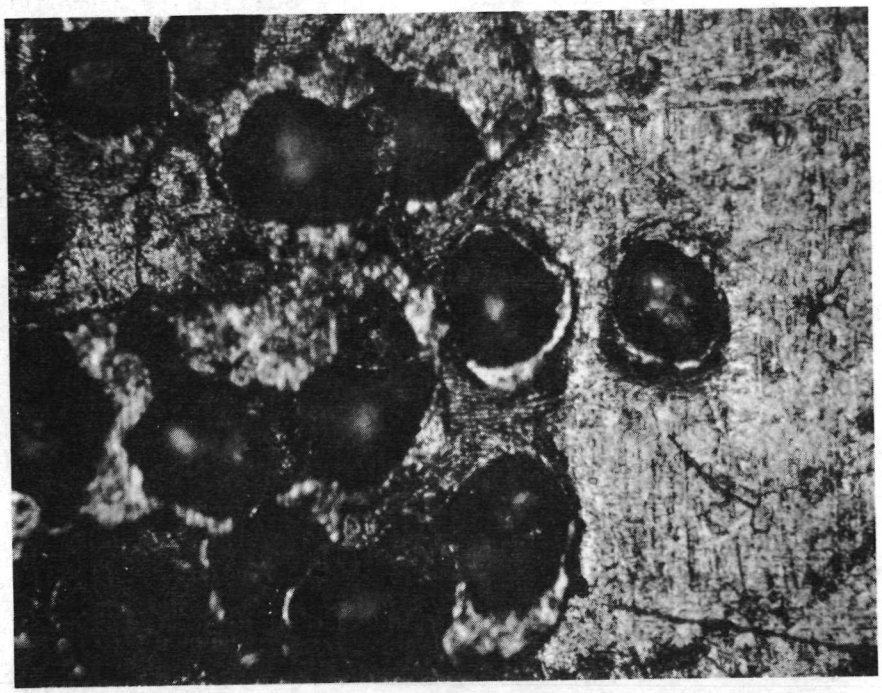

Figure 3-38 CONTROL SAMPLE 1 (1C-A-00) SURFACE TUNGSTEN PARTICLE CLUSTER (500X)

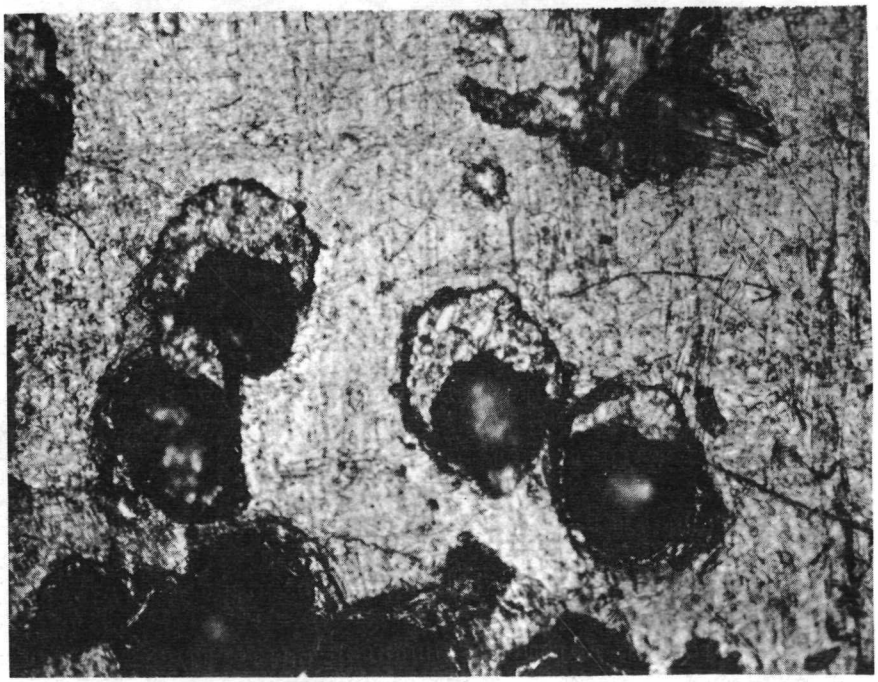

Figure 3-39 CONTROL SAMPLE 1 (1C-A-00) SURFACE TUNGSTEN PARTICLE CLUSTER REACTION ZONE (500X)

3.2.4.3.3 Summary of Control Sample 1 (1C-A-00) Surface Feature Observations

The surface features of Control Sample 1 (1C-A-00) have significance mainly in confirmation that melting occurred when the sample was subjected to the heating profile shown in Figure 3-14. This confirmation is substantiated by:

(1) lack of surface "die" markings similar to those observed on Developmental Sample 1 (1D-A-00), and

(2) occurrence of "reaction zones" near tungsten particles clustered at the sample surface.

Considering the presence of the sample expansion slug as further evidence of melting on a gross (bulk) scale, the performance of the melting sequence for Control Sample 1 (1C-A-00) was successful and the subsequent tungsten particle distribution study reflects this condition.

3.2.4.3.4 Tungsten Particle Distribution, Control Sample 1 (1C-A-00)

Figure 3-40 shows the Control Sample 1 (1C-A-00) surface area that was examined. Twenty-six photomicrographs were taken but not all are included in this report; only those necessary to represent the composite result in question are presented.

Directional Display

Representative views of the directional display of Control Sample 1 (1C-A-00) are shown in Figures 3-41 through 3-43. The directional display in this, and every case, was made along the sample axis in the plane shown in Figure 3-40. No attempt was made to select specific areas. The procedure included a determination of sample axis position via measurement on the microscope stage and subsequent photomicrography starting at the Cold End and traversing 0.63 cm (0.25 in) for each successive area. Photomicrograph 2 shows the area 0.63 cm (0.25 in) from the Cold End. The dark spots are pits formed during mechanical

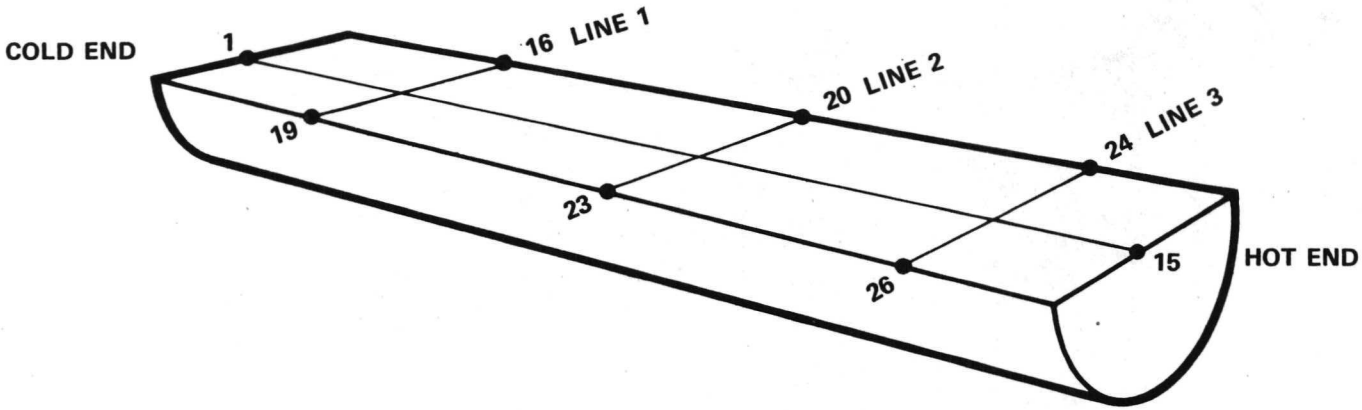

Figure 3-40 SCHEMATIC OF CONTROL SAMPLE 1(1C-A-00) PHOTOGRAPHIC DOCUMENTATION

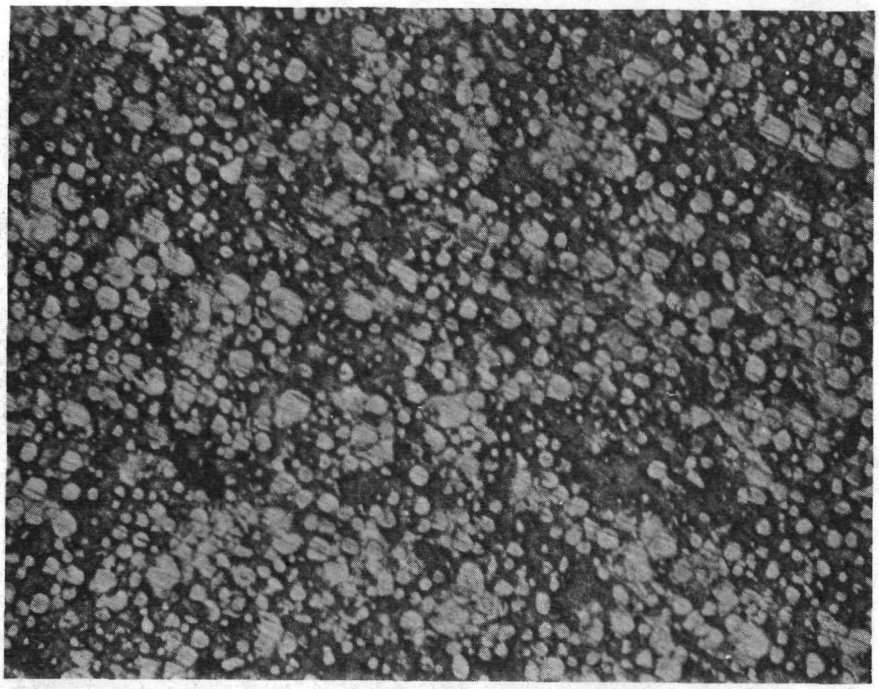

2
(A)

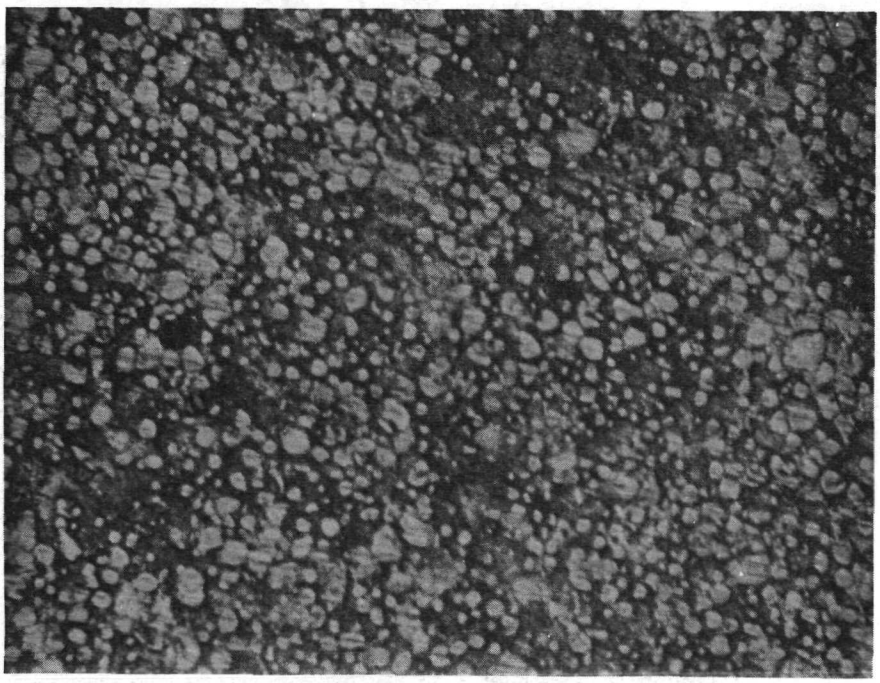

4
(B)

Figure 3-41 CONTROL SAMPLE 1 (1C-A-00) DIRECTIONAL DISPLAY AT 100X, PHOTOMICROGRAPHS 2 AND 4

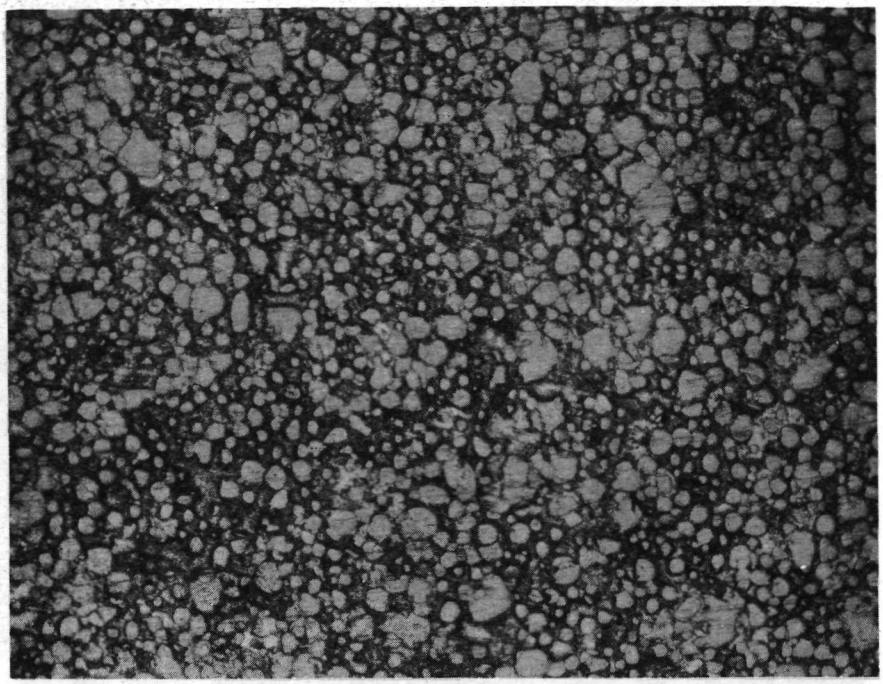

6
(A)

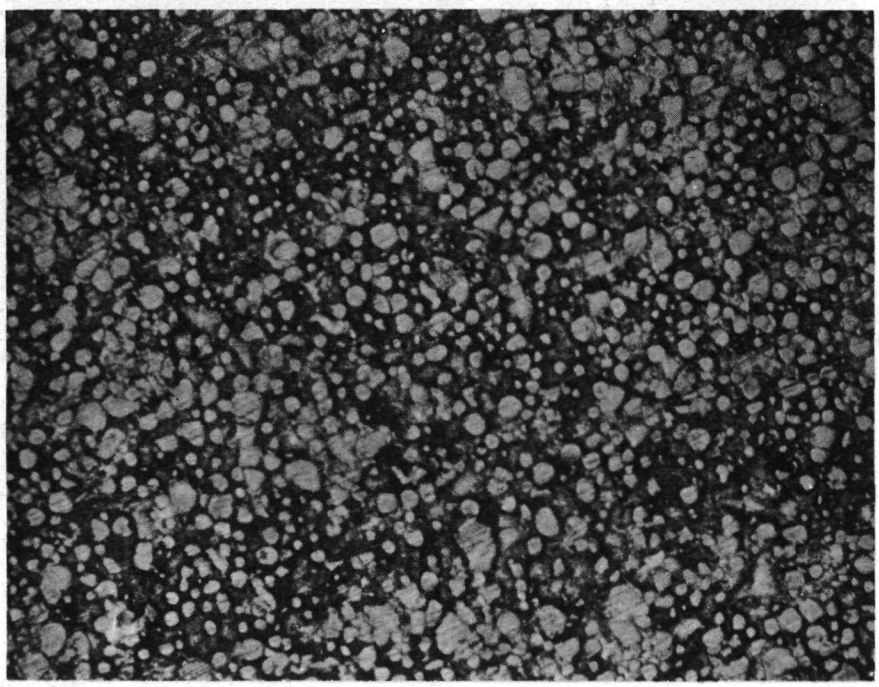

9
(B)

Figure 3-42 CONTROL SAMPLE 1 (1C-A-00) DIRECTIONAL DISPLAY AT 100X, PHOTOMICROGRAPHS 6 AND 9

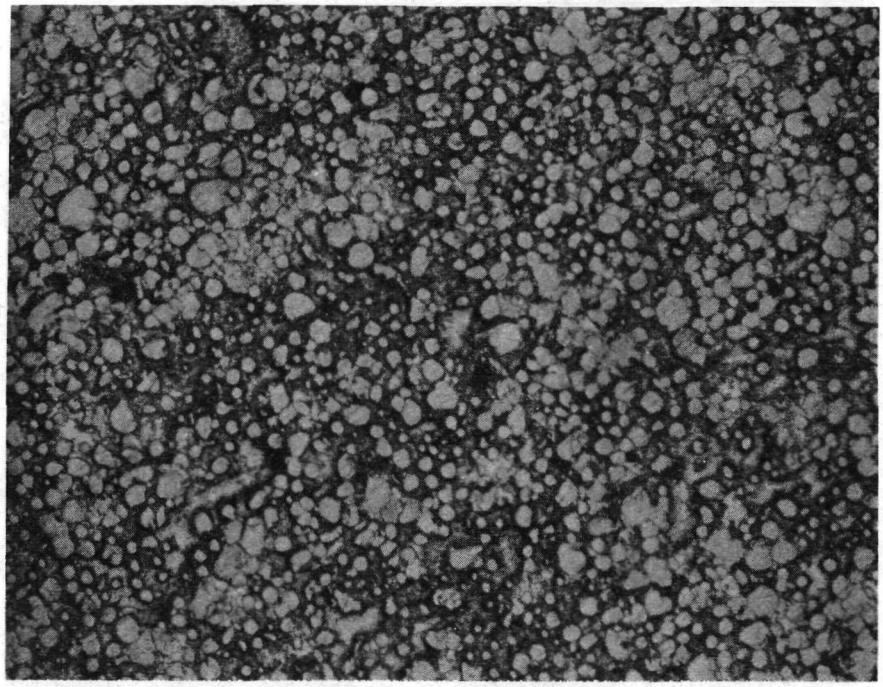

(A)

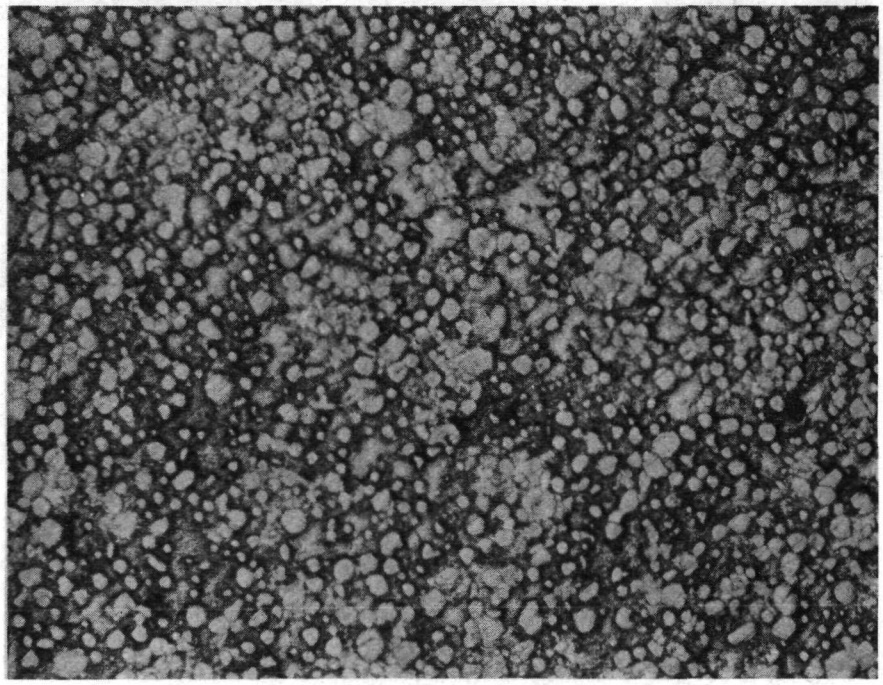

(B)

Figure 3-43 CONTROL SAMPLE 1 (1C-A-00) DIRECTIONAL DISPLAY AT 100X, PHOTOMICROGRAPHS 12 AND 14

polishing which was very difficult especially in the end and edge area. Cold End and Hot End tungsten particle distribution data are not presented because the amount of material that was removed by polishing before a representative surface was obtained was extensive and the resultant surface was on a plane below that shown in Figure 3-40. However, the ends of the sample were polished and will be discussed later.

Figures 3-42 and 3-43(A) show the tungsten particle distribution found in the sample bulk along the directional display line. Figure 3-43(B) shows the area 0.63 cm (0.25 in) from the Hot End and represents the last of the directional display data.

The determination of volume % tungsten was made as described in 3.2.4.2.2. Figure 3-44 shows the volume % tungsten as a function of location for the directional display. The increase in volume % tungsten throughout the sample's length indicates that upon melting and subsequent solification, particle redistribution was such as to cause preferential segregation toward both the center of the sample and toward the Cold End, i.e., the heat sink end. The rather abrupt and large changes in volume % tungsten at the Cold End indicate that particle settling started; however, due to the limited time at a temperature above melting while in a vertical position, total equilibrium or segregation did not occur.

As described in 3.2.4.3.1, the sample was held in a horizontal position during the heating cycle which lasted 10 min. The actual time at a molten condition during the heat up was approximately 3.5 min (obtained from the time versus temperature plot of Figure 3-14). During this initial liquid-state interval,tungsten particle motion and redistribution presumably was toward the sample's bottom surface along its entire length resulting in a motion that inhibits segregation toward any one end of the sample.

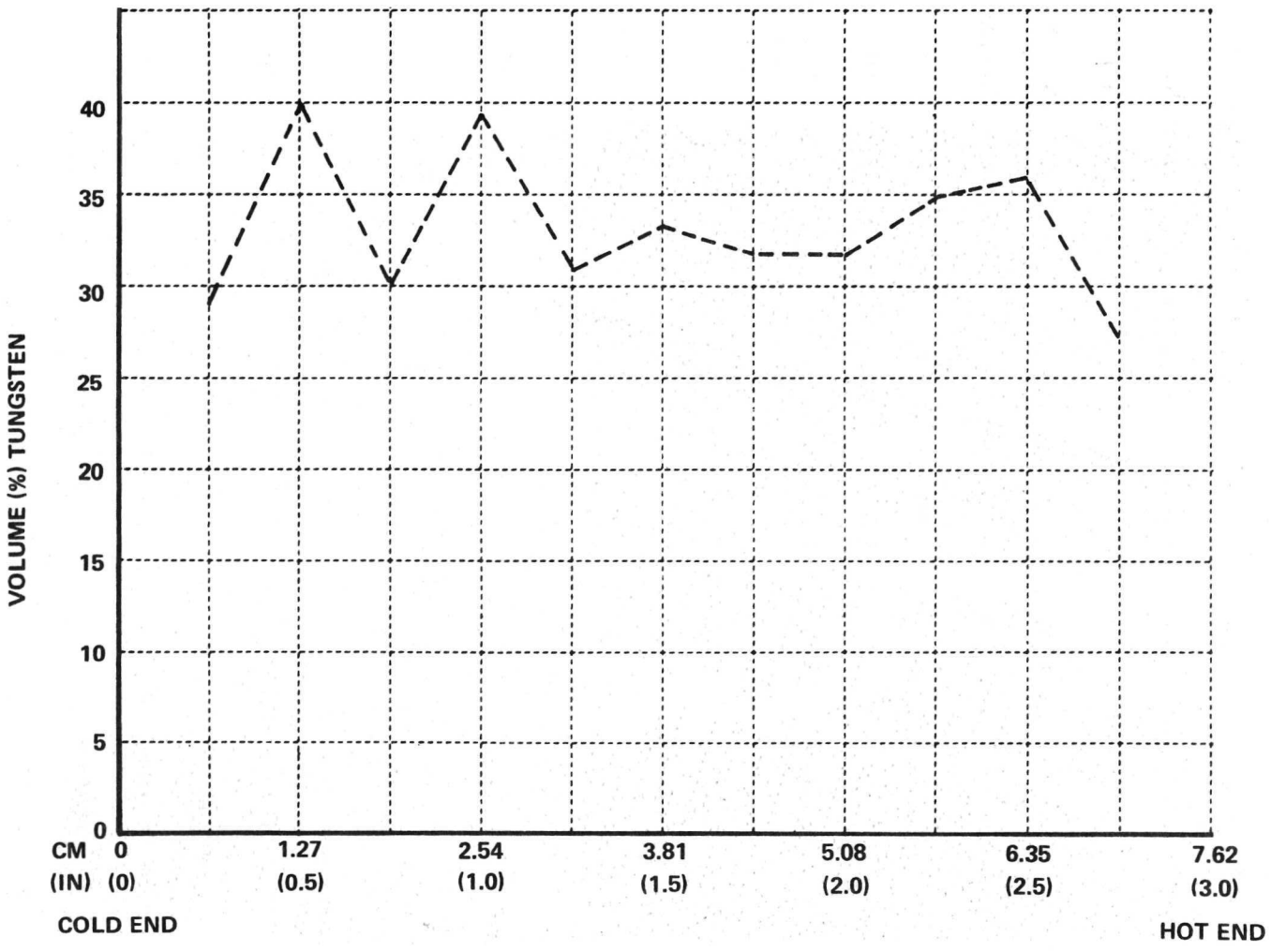

Figure 3-44 DATA PLOT, VOLUME % TUNGSTEN, DIRECTIONAL DISPLAY, CONTROL SAMPLE 1 (1C-A-00)

During the cooling cycle the sample was in a vertical position in the heat sink. Referring to Figure 3-14, the time available for tungsten particle redistribution in the entire sample volume is approximately 5 min. At this time the equilibrium condition is lost and directional solidification occurs. The approximately 5 min during which unperturbed redistribution occurs is itself a dynamic condition because of the continuous temperature drop. Also, the redistribution process with the sample in the upright position does not have as its region (or initial state) the tungsten particle distribution of Developmental Sample 1 (1D-A-00) shown in Figure 3-9. Rather the initial state for the start of vertical redistribution is some intermediate distribution which occurred because of melting with the sample in the horizontal position. This state is not known. Therefore, it seems appropriate to consider the tungsten particle distribution in the Control Sample as the result of a complicated, undefined series of events. In this context, it is appropriate to consider the trend of the tungsten particle distribution. This, of course, is the segregation of tungsten particles toward the Cold End with the achievement of approximately 40-48 volume % tungsten (depending on the packing mode and amount of wetting, etc.). Figure 3-44 shows that this is the trend in the control sample.

It is interesting to consider the following sequence of events that have occurred during melting, solidification and sample sectioning.

(1) A redistribution of tungsten particles started during the heat-up cycle with the sample in the horizontal position.

(2) The redistribution trend was toward one-half of the sample when considered in the context of the applied sectioning procedure.

(3) A second redistribution trend started toward the Cold End upon cooling with the sample in the vertical position as shown in Figure 3-45.

(4) The sectioning plane was randomly selected.

Thus any tungsten particle redistribution will be (and is) highly dependent on the randomly selected sectioning plane. Consequently, a plane could have been selected which passed through that half of the sample where tungsten particle settling occurred during the initial redistribution. This would result in a very unsymmetrical plot from the cross-directional display data. It will be shown however, that this was not the case for the sectioning plane chosen in the control sample.

It must also be remembered that during sectioning a thin slab of material was unavoidably cut from the geometric center of the sample; therefore, the plane of Control Sample 1 (1C-A-00) was not actually at the geometric center of the intact sample. However, it is possible that the plane studied was representative, in large measure, of that volume of the sample which experienced the initial redistribution thus explaining the high values of volume % tungsten shown in Figure 3-44.

The final conclusion regarding the redistribution of tungsten particles for Control Sample 1 (1C-A-00) as plotted in Figure 3-44 is that a redistribution occurred as the result of an incompletely understood series of events. However, the tungsten particle distribution plotted in Figure 3-44 is representative of that existing in the particular plane investigated. Also, since the sectioning procedure was identical for all samples, similar planes were used and, therefore, trends in redistribution can be ascertained.

On this basis, it can be concluded that for Control Sample 1 (1C-A-00) the redistribution of tungsten particles was toward the cold end because of vertical placement and toward the center of the plane investigated because of the initial and final distribution trends.

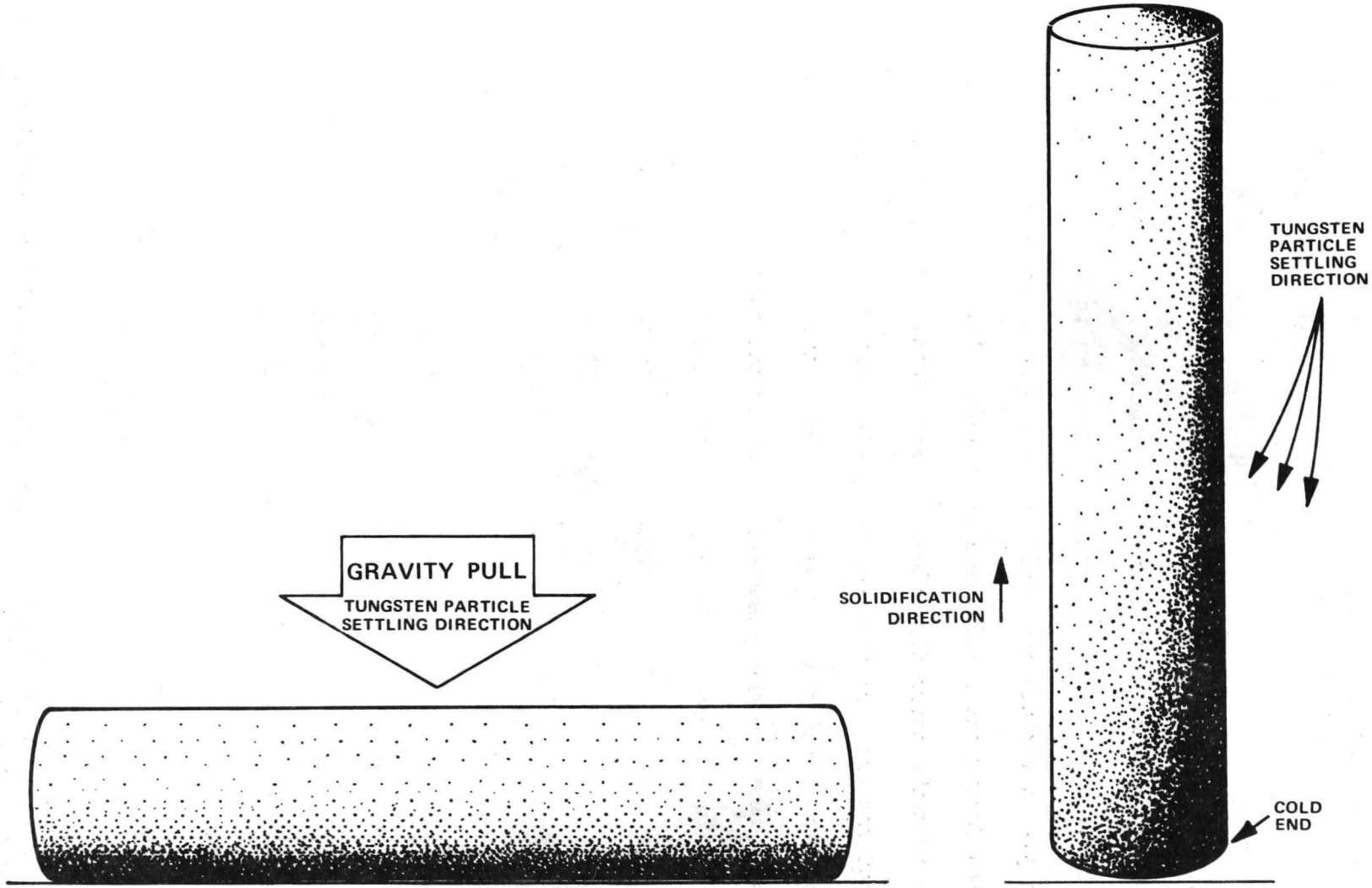

NOTE: TUNGSTEN PARTICLES REPRESENTED BY BLACK STIPPLING

Figure 3-45 PROBABLE TUNGSTEN PARTICLE REDISTRIBUTION DURING PROCESSING OF CONTROL SAMPLE (1C-00)

Cross-Directional Display

As shown in Figure 3-40, three cross-directional display lines were made on Control Sample 1 (1C-A-00). Line 1 was located 1.27 cm (0.5 in) from the Cold End; Line 2 the geometric center line of the surface, was located 3.81 cm (1.5 in) from the Cold End; and Line 3 was located 1.27 cm (0.5 in) from the Hot End. Line 2 photomicrographs 20-23 are shown in Figures 3-46 and 3-47.

Figure 3-48 is a plot of the volume % tungsten as a function of location for the cross-directional display lines as well as at the intersection of these lines with the center axis (directional display line). Line 1 exhibits the highest volume % tungsten on average, substantiating the postulation that gravity-induced settling had started in the sample. Line 2 and 3 data is complicated indicating that the sample was far from an equilibrium state. Line 2 had the lowest volume % tungsten while Line 3 had a higher volume % tungsten, on average, than Line 2. A postulated explanation for the complication is associated with the fact that the expansion slug, formed (during melting) at the top (hot end) of the sample, does not contain tungsten particles in its matrix. This could happen if the expansion slug was formed by the extrusion of the In-Bi matrix liquid. The volume % tungsten in the remaining top portion of the sample would automatically be increased and, because equilibrium was not reached for the system, resulting in the higher volume percents.

The intersection of curves from the cross-directional displays and the line drawn to represent the center axis, results in values of 41.4, 33.7 and 32.3 volume % tungsten. These values, representing new points for the directional display, plotted with the observed directional display as shown in Figure 3-49 indicate that the interpolated and observed tungsten particle distribution exhibit good reproducibility.

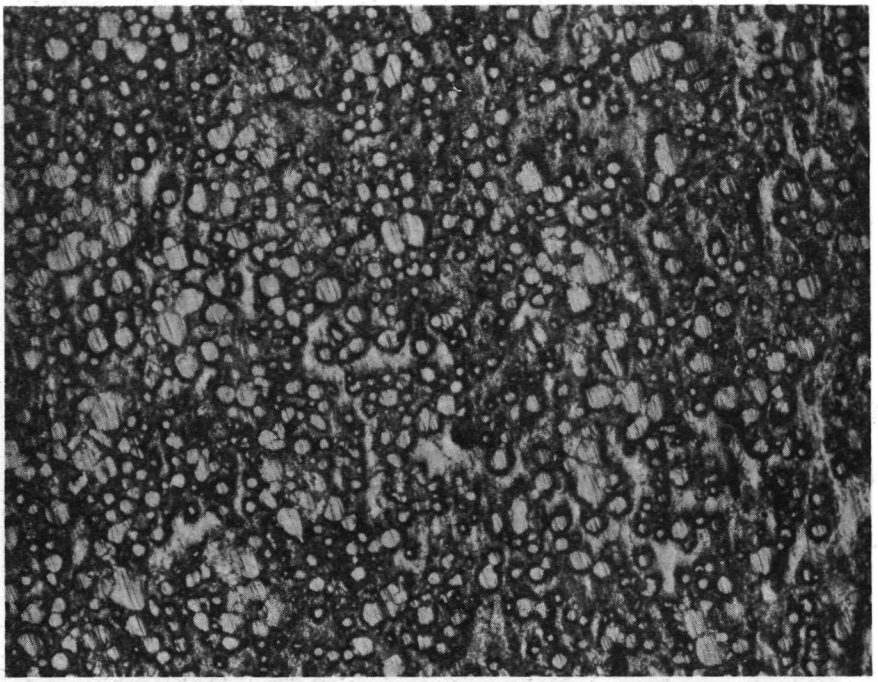

20
(A)

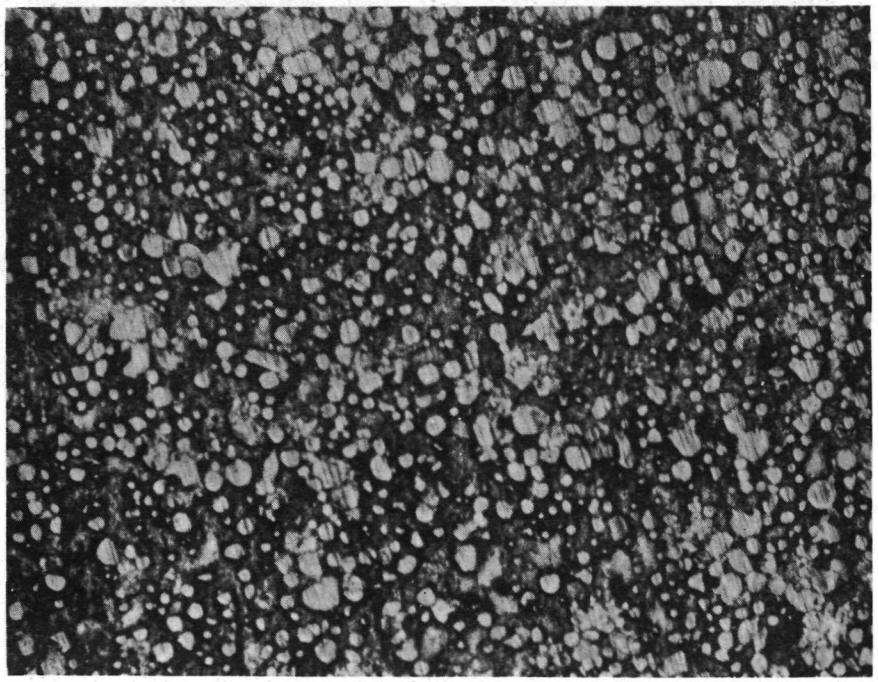

21
(B)

Figure 3-46 CONTROL SAMPLE 1 (1C-A-00) CROSS-DIRECTIONAL DISPLAY AT 100X, PHOTOMICROGRAPHS 20 AND 21 OF LINE 2

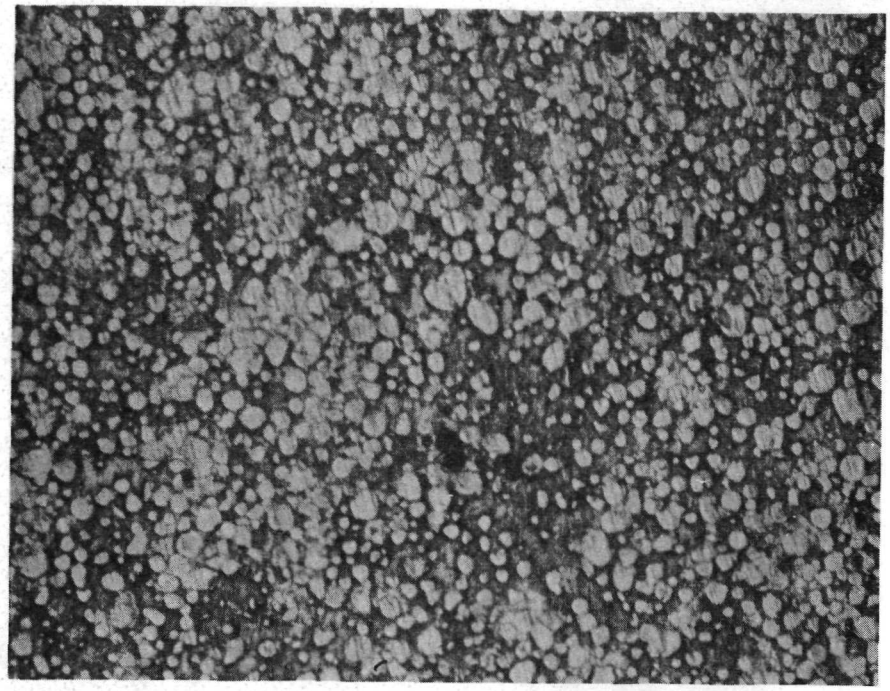

22
(A)

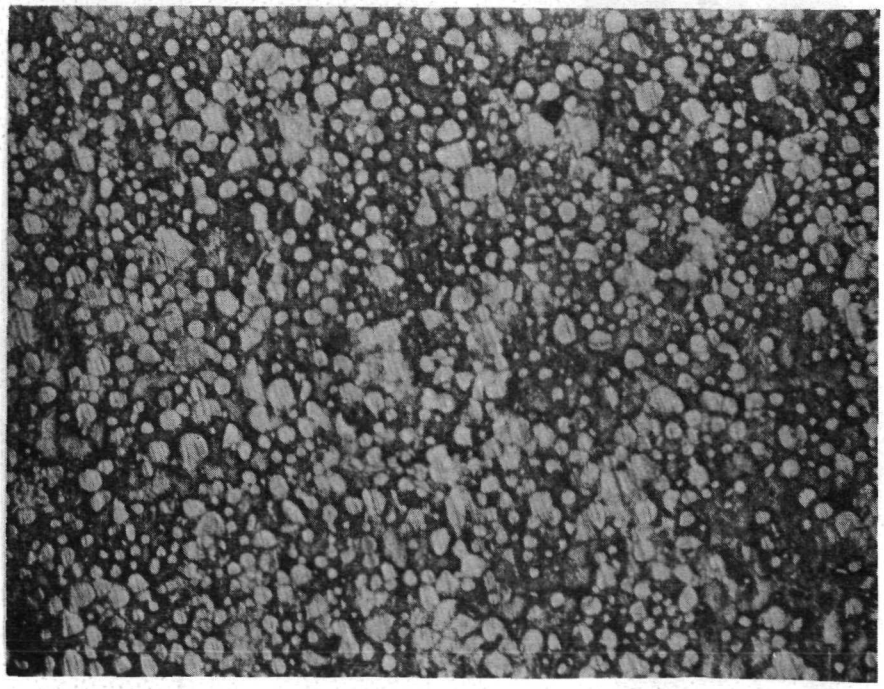

23
(B)

Figure 3-47 CONTROL SAMPLE 1 (1C-A-00) CROSS-DIRECTIONAL DISPLAY AT 100X. PHOTOMICROGRAPHS 22 AND 23 OF LINE 2

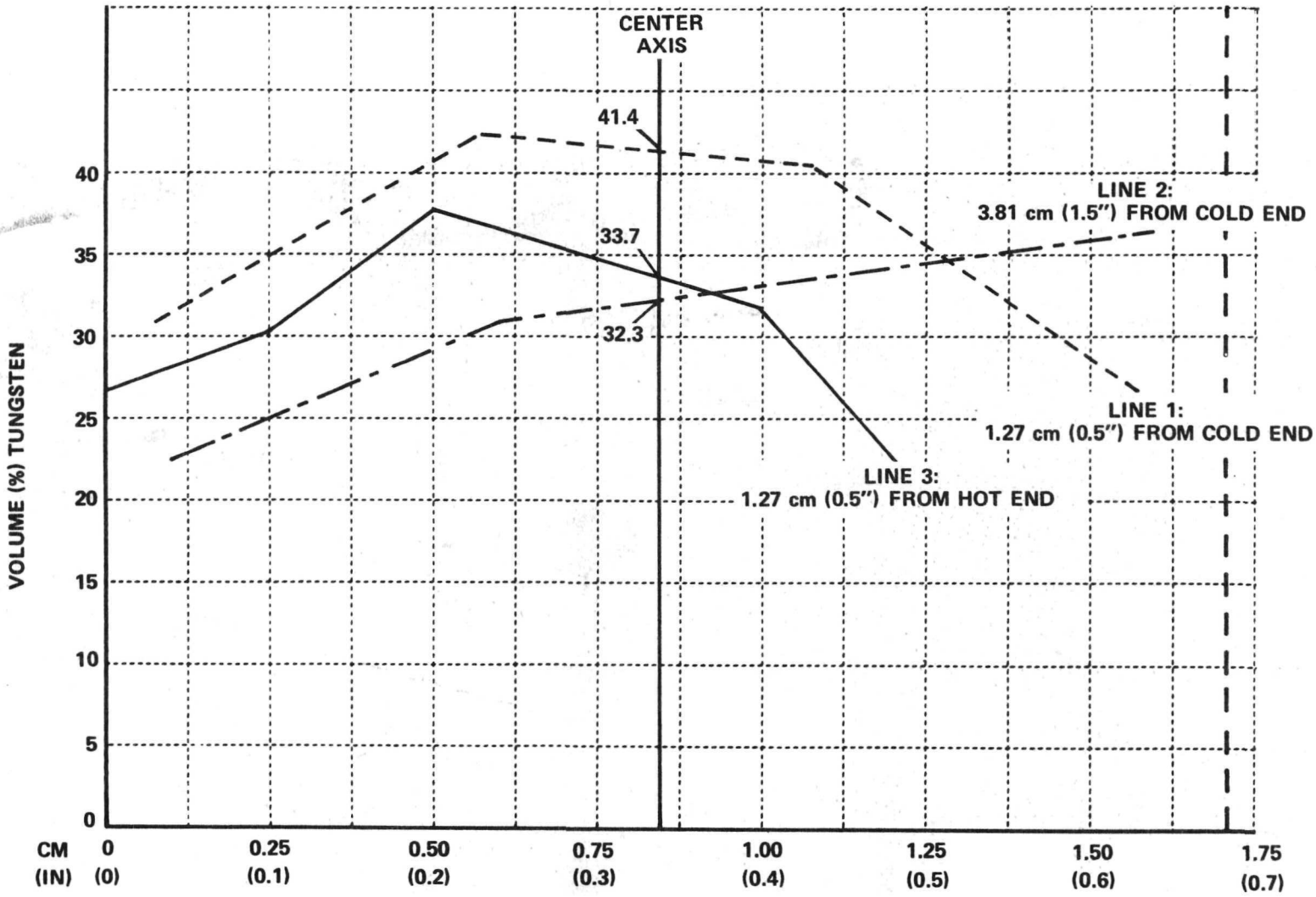

Figure 3-48 DATA PLOT, VOLUME % TUNGSTEN, CROSS-DIRECTIONAL DISPLAY, CONTROL SAMPLE 1 (1C-A-00)

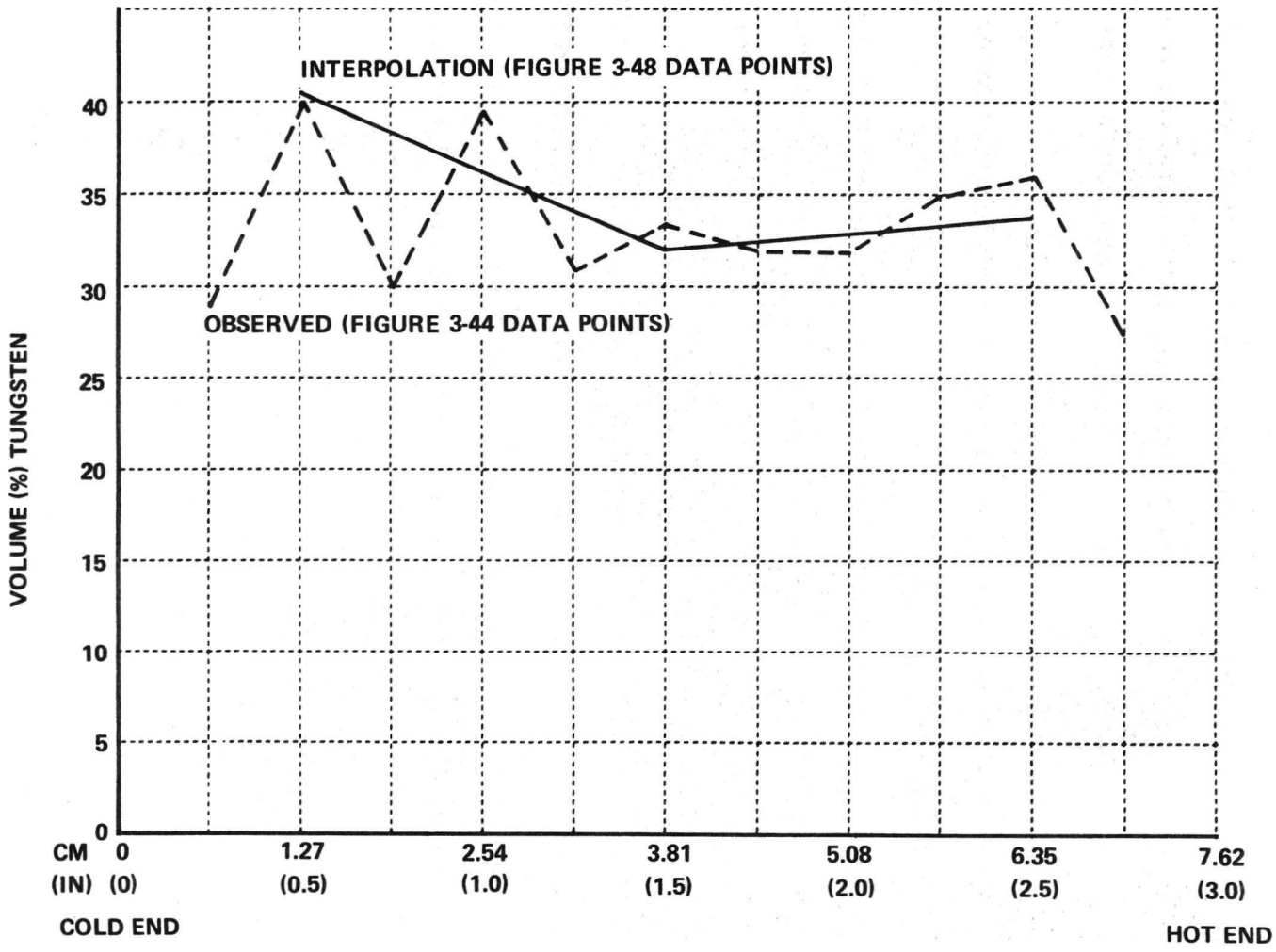

Figure 3-49 DATA PLOT, VOLUME % TUNGSTEN, COMPOSITE DIRECTIONAL DISPLAY, CONTROL SAMPLE 1 (1C-A-00)

3.2.4.3.4.1 Summary, Control Sample 1 (1C-A-00) Tungsten Particle Distribution

The observed distribution of tungsten particles results from a series of events which included an initial redistribution trend due to melting with the sample in a horizontal position and a final redistribution trend due to cooling with the sample in an upright position. Any conclusions pertaining to the mechanisms of tungsten particle motion must be intuitive at best. No attempt will be made to describe the mechanisms involved because the required experimental evidence does not exist at this time. The conclusions that can be drawn with certainty include the following:

(1) A change in tungsten particle distribution occurred after melting.

(2) The change in tungsten particle distribution is represented by the difference in the directional and cross directional displays for Developmental Sample 1 (1D-A-00) and Control Sample 1 (1C-A-00).

(3) The procedures instituted for determining particle distribution are sufficient to yield good reproducibility as indicated by the plotting of observed and interpolated (from cross-directional displays) tungsten particle distributions (see Figure 3-49).

3.2.4.4 Metallographic Examination Sample 1F-A-00

The procedure for handling the flight sample was identical to that discussed for Control Sample 1 (1C-A-00). Figures 3-16, 3-17, 3-18 and 3-19 show the flight sample after removal from its capsule. The presence of tooling marks extended along the entire length of the sample. Examinations were made at 25X followed by 100X and 500X recording of pertinent features.

3.2.4.4.1 General Appearance, Low Magnification (25X)

Twenty-three photomicrographs were taken of the flight sample surface at 25X magnification. The procedure involved overlapping fields of view so that a composite of the sample surface could be made if required. Representative photos of the cold end surface are given in Figure 3-50. Figure 3-51 is representative of the middle portion of the sample and Figure 3-52 of the Hot End.

The surface features observed at 25X magnification and shown in Figures 3-50 through 3-52 are: (1) distortions due to capsule wall impression and (2) distortion due to some unconfirmed mechanism suspected to be bubble bursting and which was not observed on the control sample. Of particular interest is the increase in surface distortion with distance along the specimen. As seen in Figure 3-50 the Cold End of the sample surface is characterized by surface distortion which is primarily an impression of the capsule wall (disregarding the tool markings). In that area of the sample surface which represents the mid-section (Figure 3-51) the distortions due to capsule wall impression have decreased in density and a distortion which is similar to surface bubble bursting effects has increased in density. The same trend is observable in Figure 3-52 where a further increase in the density of surface bubble is present. The conclusion

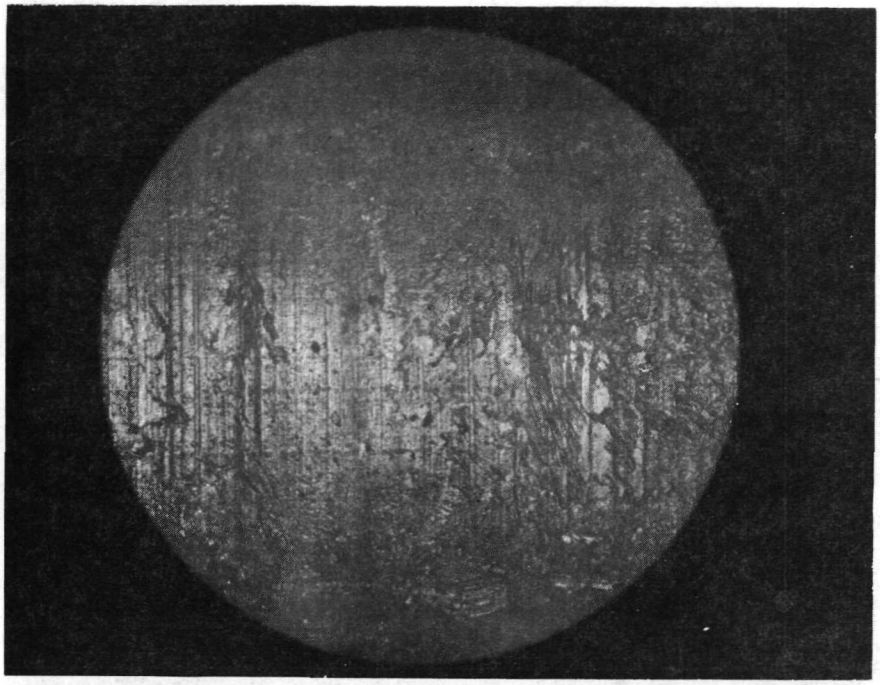

1
(A)

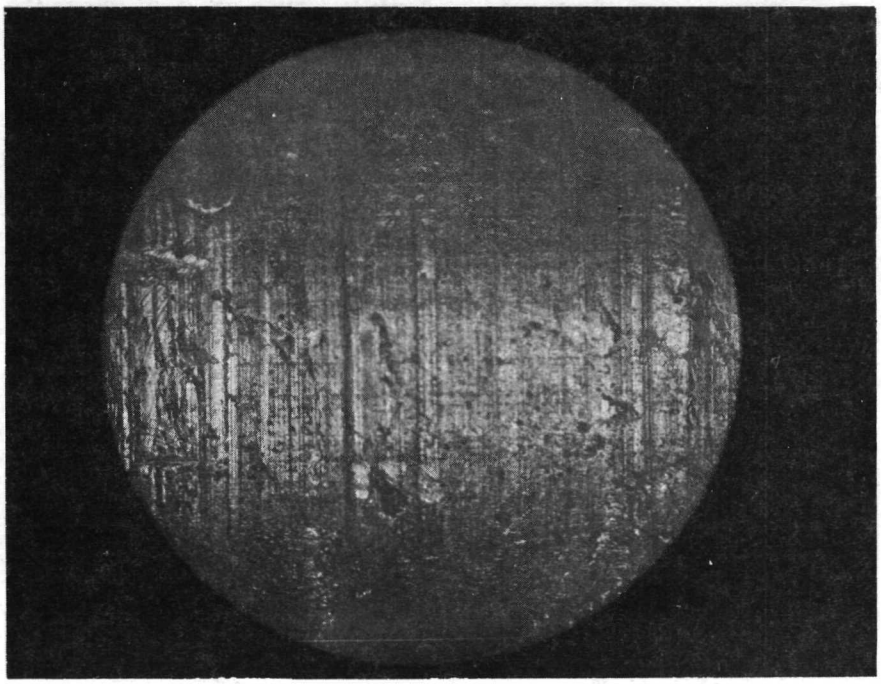

2
(B)

Figure 3-50 FLIGHT SAMPLE 1 (1F-A-00) SURFACE AT COLD END (25X) PHOTOMICROGRAPHS 1 AND 2

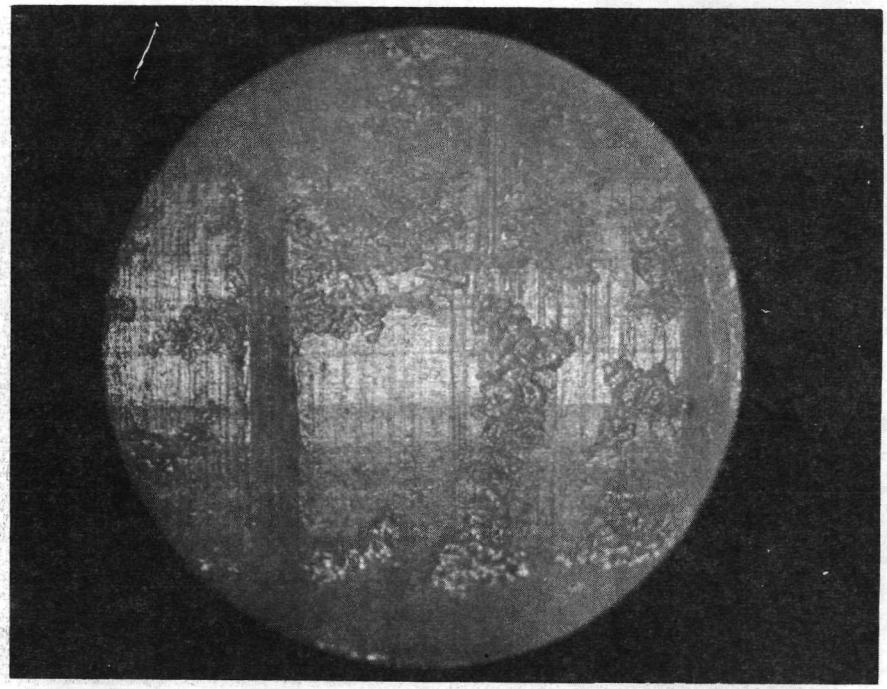

12
(A)

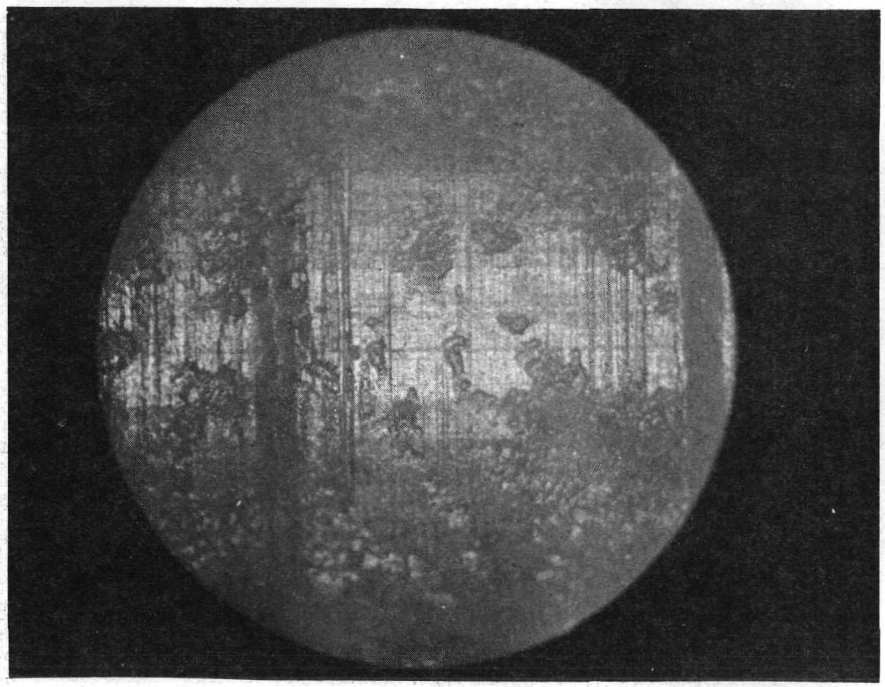

13
(B)

Figure 3-51 FLIGHT SAMPLE 1 (1F-A-00) SURFACE AT CENTER (25X) PHOTOMICROGRAPHS 12 AND 13

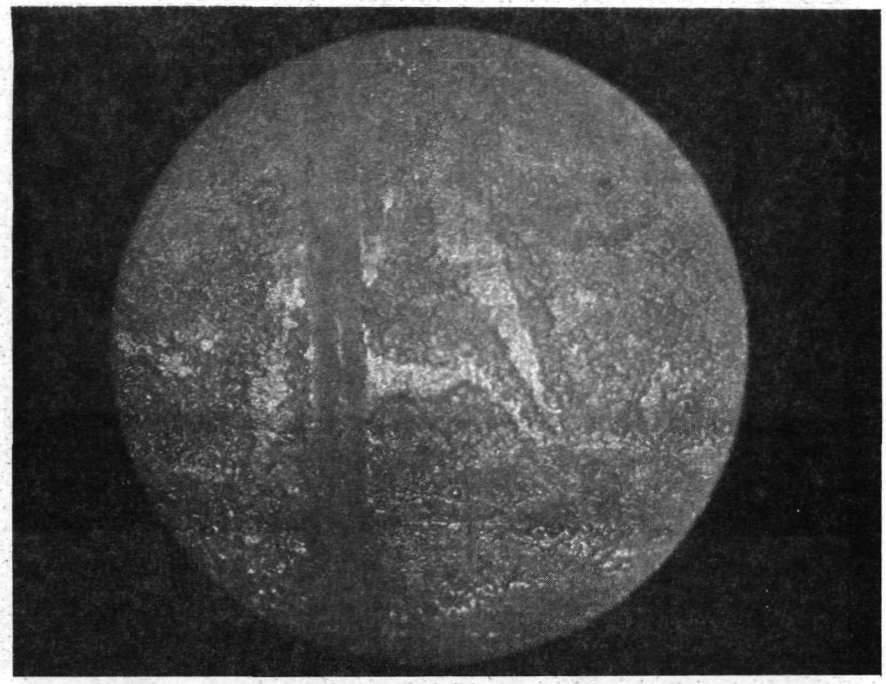

21
(A)

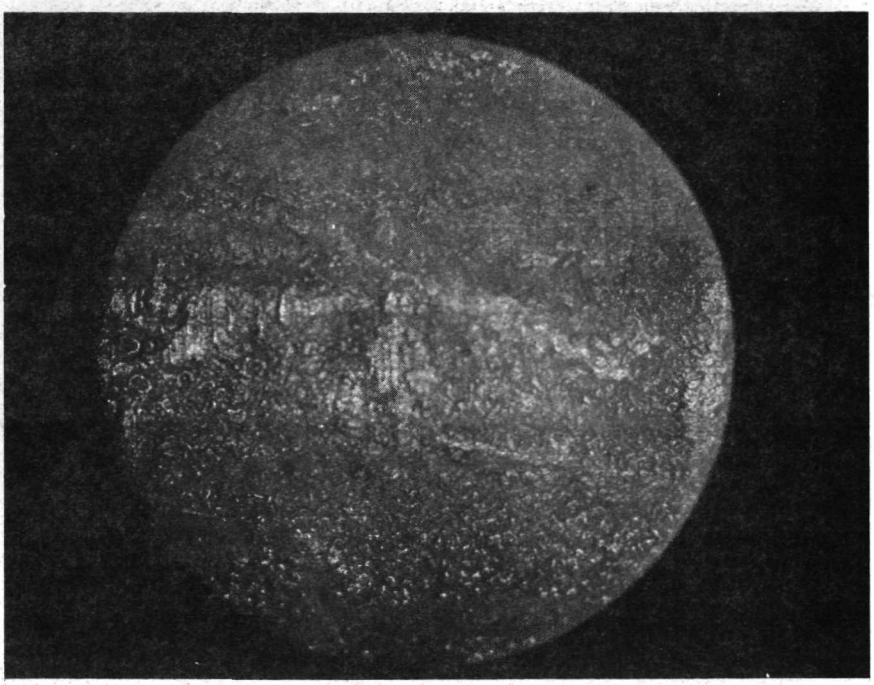

22
(B)

Figure 3-52 FLIGHT SAMPLE 1 (1F-A-00) SURFACE AT HOT END (25X) PHOTOMICROGRAPHS 21 AND 22

that the density of this surface distortion increases when observed toward the hot end of the sample has been discussed previously and these photos confirm the conclusions.

3.2.4.4.2 General Appearance, Intermediate (100X) and High (500X) Magnification

Intermediate magnification photomicrographs were taken along the sample surface starting just inside the Cold End and every 0.63 cm (0.25 in) toward the Hot End of the sample. In all, 14 photomicrographs were taken. Representative photomicrographs taken at the two ends and the center of the sample are given in Figure 3-53 through 3-55.

Figure 3-53 represents the sample surface conditions near the Cold End of the sample. As seen the surface distortion is primarily that due to capsule wall impression; this is the accicular shaped feature. Also note that two kinds of tool markings are shown. The dark (wider) is due to that imposed during sample removal from its capsule, while the light (narrow) is due to impression from the capsule wall. Some small round distortions are seen in Figure 3-53 and those are suspected to be due to surface bubble bursting.

Figure 3-54 represents the sample surface conditions near the center of the sample. As shown, the surface distortion has changed character as well as degree.

Figure 3-55 represents the sample surface conditions near the Hot End of the sample.

It should be noted that the density of surface distortion is approximately the same in the control areas previously shown and at the hot end. This is not the case for the areas between the Cold End and the central areas. Figure 3-56 represents an area taken 1.89 cm (0.75 in)

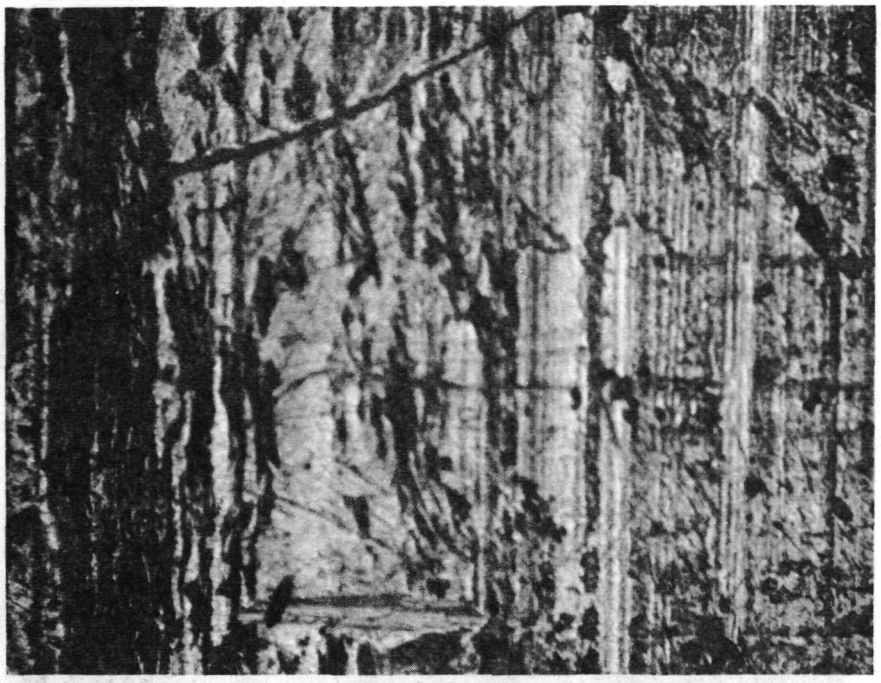

1
(A)

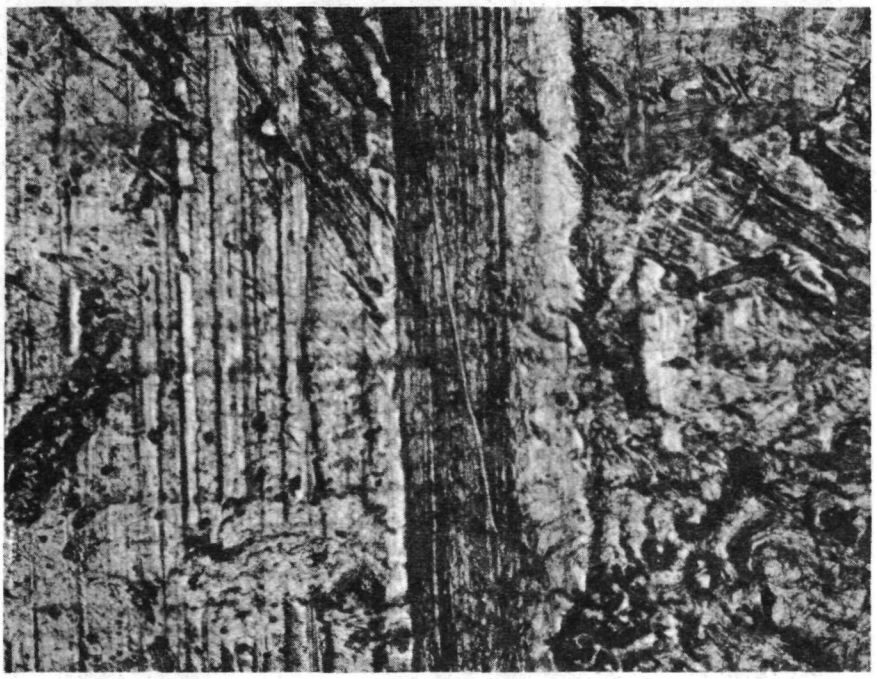

2
(B)

Figure 3-53 FLIGHT SAMPLE 1 (1F-A-00) SURFACE AT COLD END (100X) PHOTOMICROGRAPHS 1 AND 2

6
(A)

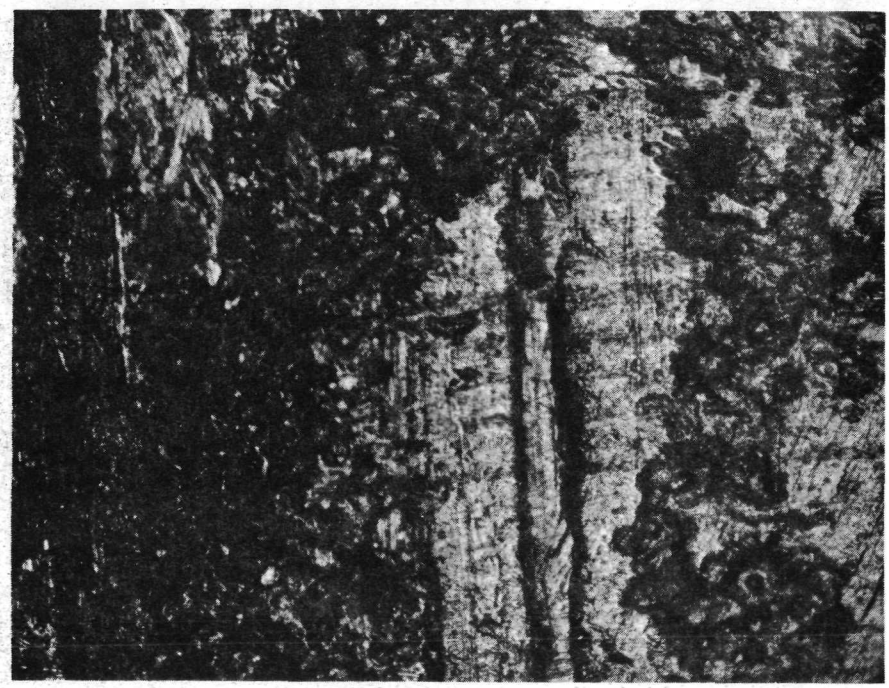

7
(B)

Figure 3-54 FLIGHT SAMPLE 1 (1F-A-00) SURFACE AT CENTER (100X) PHOTOMICROGRAPHS 6 AND 7

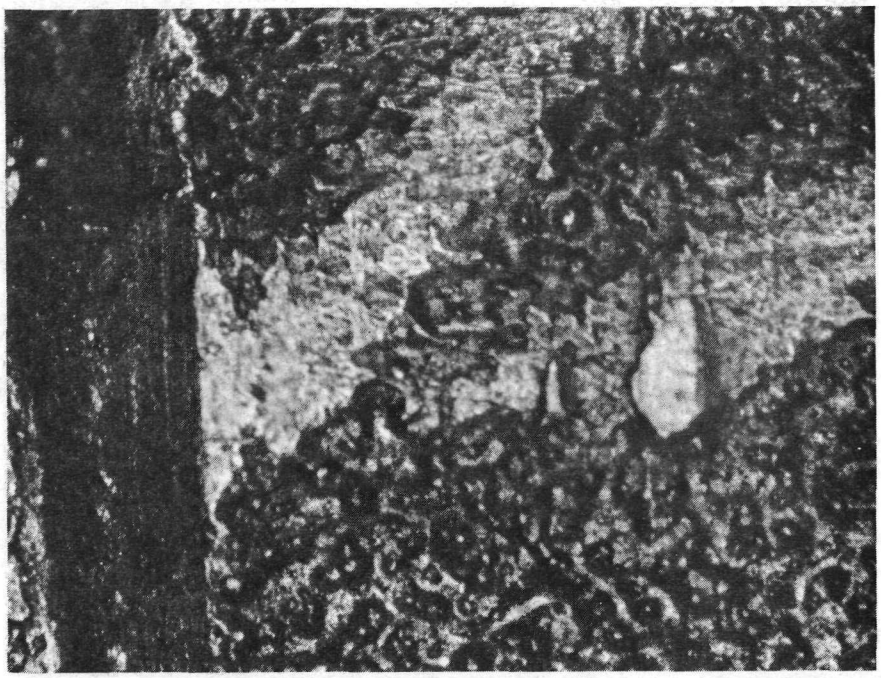

13
(A)

14
(B)

Figure 3-55 FLIGHT SAMPLE 1 (1F-A-00) SURFACE AT HOT END (100X) PHOTOMICROGRAPHS 13 AND 14

from the Cold End and shows that the surface distortion being discussed is present but of low density; note also the presence of distortion due the capsule wall. Of particular interest in Figure 3-56 is the presence of individual distortions, which are round in shape and varied in size.

A region of Flight Sample 1 (1F-A-00) surface showing a very high density of surface distortion is shown in Figure 3-56. The edge separating the distorted and undistorted region is shown in Figure 3-57. Note that on the undisturbed portion of the surface a line distortion is seen. This is the effect of impression from capsule wall tool marks and indicates that the major distortions shown are in fact depressions into the sample surface as well as individual high spots.

Figure 3-57 shows the individual high spot regions of the distorted area. The surface of the sample is not in focus. The high spots are tungsten particles at the sample surface. Note that the individual tungsten particles are surrounded by an irregular shaped matrix which is depressed into the sample surface. The result is that a matrix-tungsten particle interface is not present over the total surface area of the particle. This is shown again in Figure 3-58 where at the same magnification we have focused in the valleys; that is the matrix material which is in a plane below the particle tops and below the plane of sample surface in undistorted regions.

Figure 3-58 shows the pots or holes observed in the distorted regions of the sample. In this case the focus is on the sample surface plane. Note that the hole in this case is hemispherical in shape, however, its surface outline is irregular. In Figure 3-59 we show the surface hole bottom by focusing on a plane below the sample surface.

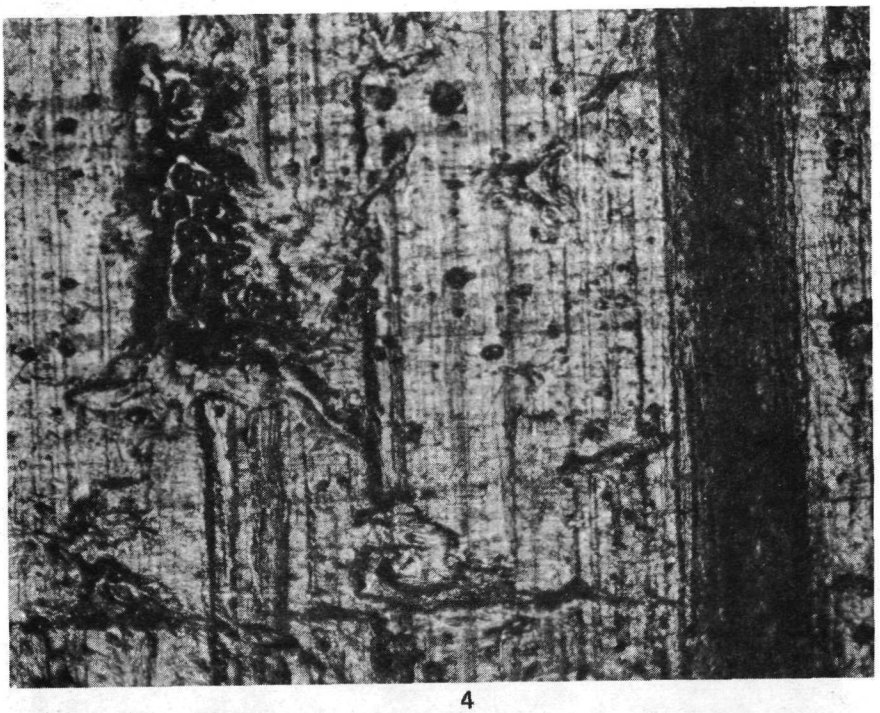

4
(A)

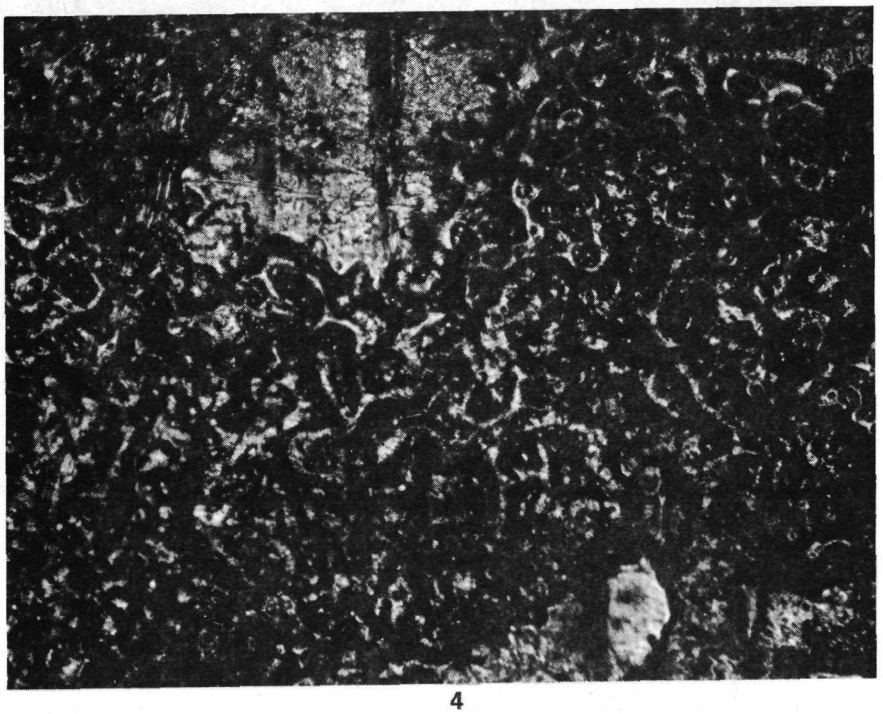

4
(B)

Figure 3-56 FLIGHT SAMPLE 1 (1F-A-00) SURFACE DISTORTION (100X) PHOTOMICROGRAPHS

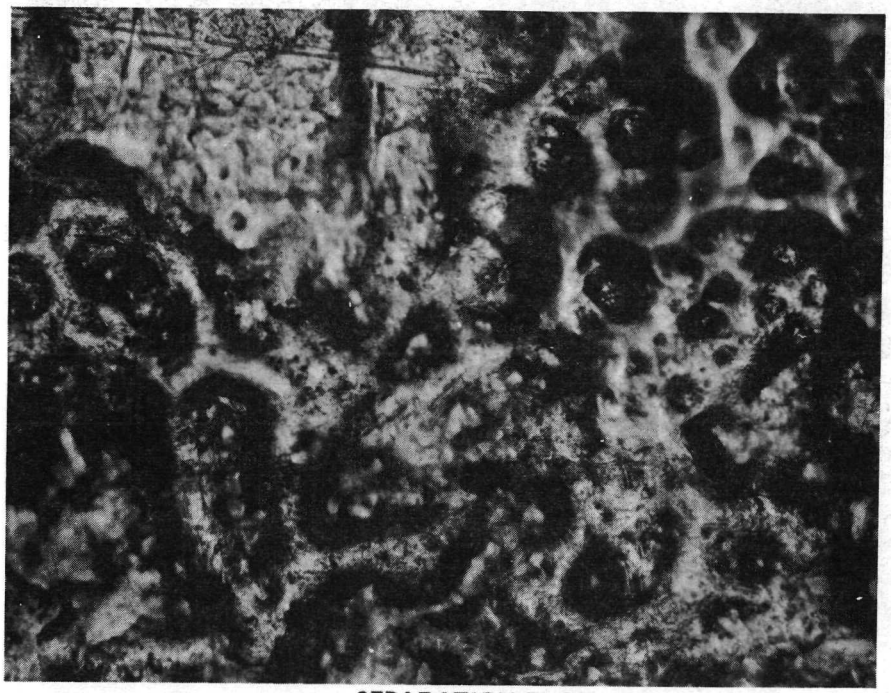

SEPARATION EDGE
(A)

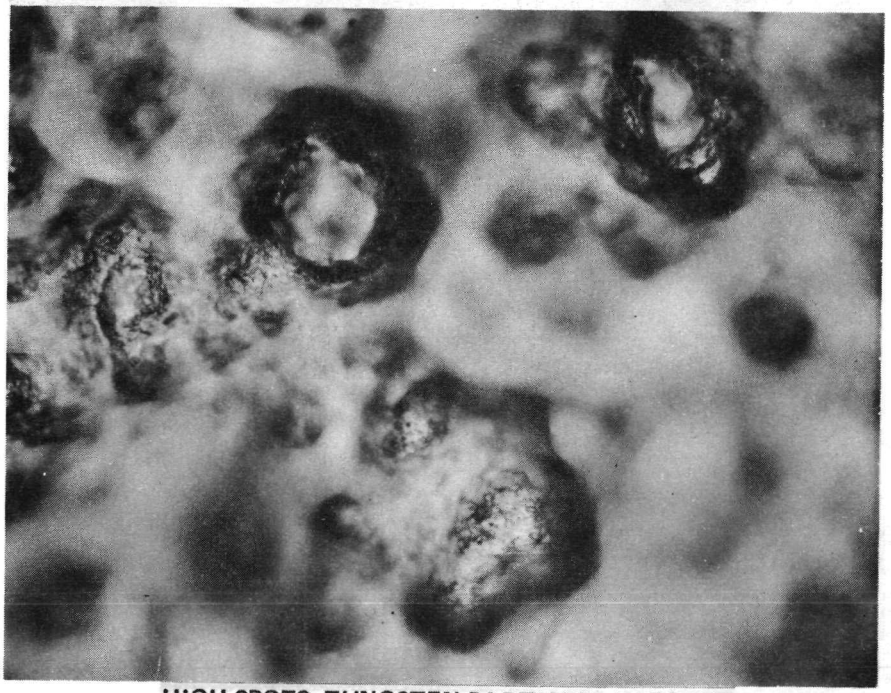

HIGH SPOTS, TUNGSTEN PARTICLES IN FOCUS
(B)

Figure 3-57 FLIGHT SAMPLE 1 (1F-A-00) SURFACE DISTORTION (250X) PHOTOMICROGRAPHS

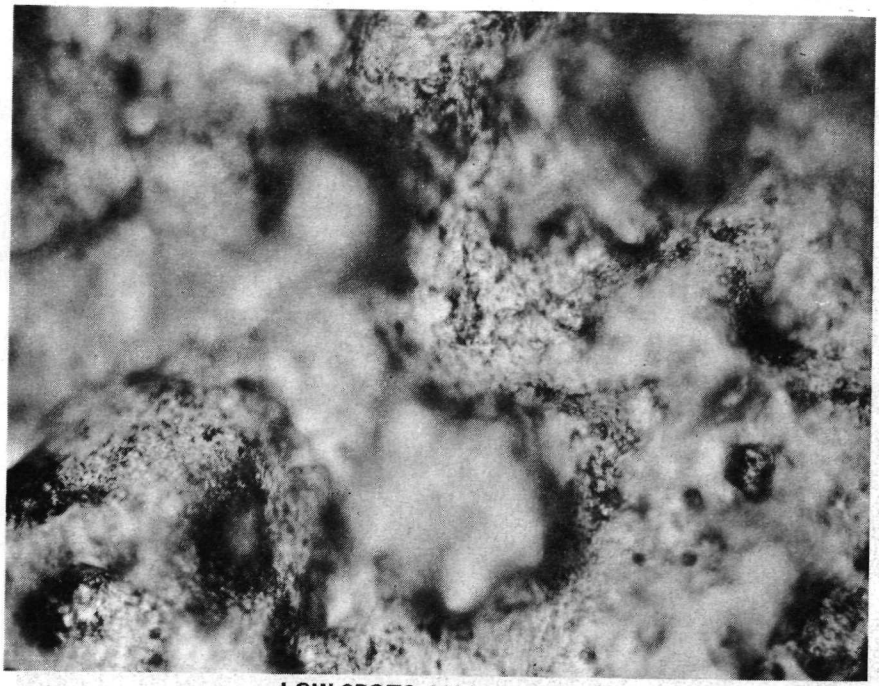

LOW SPOTS, VALLEYS IN FOCUS
(A)

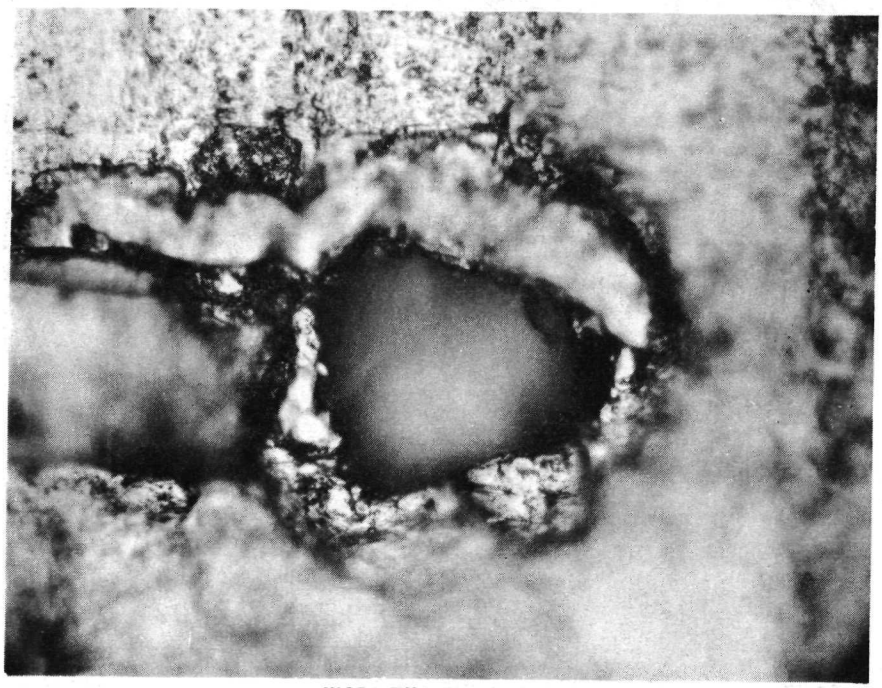

"HOLE" AT SURFACE
(B)

Figure 3-58 FLIGHT SAMPLE 1 (1F-A-00) SURFACE DISTORTION (500X) PHOTOMICROGRAPHS

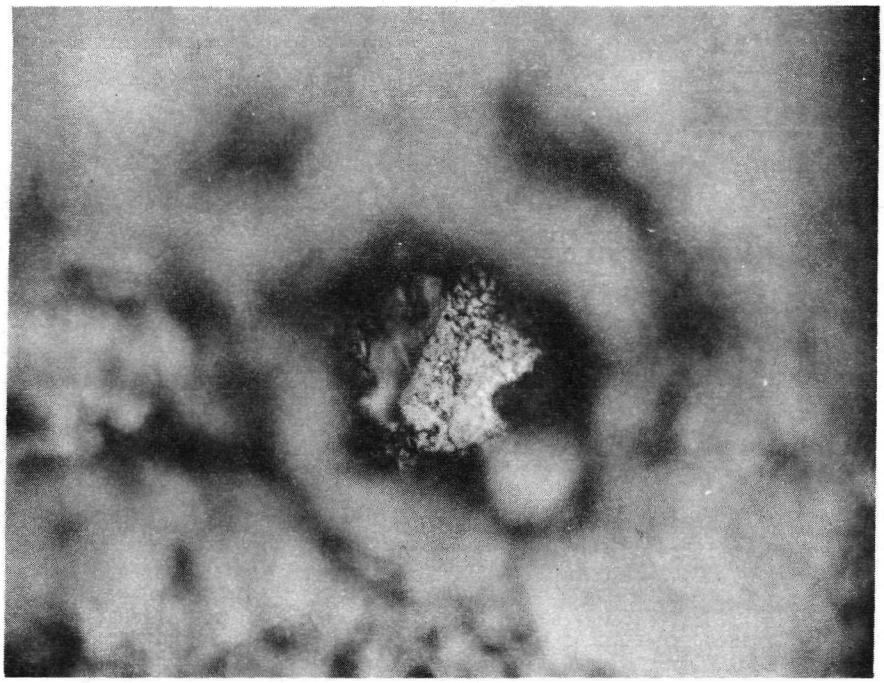

"HOLE" INTO MATRIX

Figure 3-59 FLIGHT SAMPLE 1 (1F-A-00) SURFACE DISTORTION (500X) PHOTOMICROGRAPH

3.2.4.4.3 Summary of Observed Surface Features, Flight Sample 1 (1F-A-00)

The features observed on Flight Sample 1 (1F-A-00) are:

(1) Tool markings as a consequence of removal from the sample capsule.

(2) Tool markings as a consequence of impression from capsule surface.

(3) Surface distortions in the form of "depressed" regions - these were present in increasing density as a function of position (location) on the sample. On areas near to the heat sink very few were present. These increased in number up to the sample center and then remained constant.

A comparison between the features observed on Flight Sample 1 (1F-A-00) and those observed on Control Sample 1 (1C-A-00) is interesting. The surface features observed at 100X magnification of the control sample are shown in Figures 3-30 through 3-34 from which we note that for those tungsten particles which are not in close proximity a zone of depressed matrix is observable. Also, it is apparent that the tungsten particles are situated (reside) in one corner (part) of this zone. It is postulated that upon melting, the particles near the sample surface had an effective volume composed of the individual particle volume plus a volume represented by the observed zone. This second volume is postulated to be due to void (bubble) attachment to the particle. The condition of particle position at one end of the void effected volume can be due to one of two mechanisms:

(1) The void-particle "system" would form upon sample melting and because of the difference in their effective bouyancy in the liquid metal a separation was occurring. The possibility of one component (tungsten) dragging the

second component (voids) is high with the result that particle-void attachment could (in some favorable cases) last until solidification has occurred.

(2) The void-particle system would form upon melting and would remain as such during any and all motion throughout the melt. The geometry of this system pair would be the lowest energy configuration and consist of a particle surrounded by attached bubbles. Upon solidification the solid-liquid interface would (upon moving) cause the voids (bubbles) to "run ahead" thus leaving the particle trapped. However, the binding energy between particles and voids is high and total detachment might not be made. The result would be a displaced void space which was pointing in the direction of solidification.

Of the above possibilities the former must be considered as operative in this case. This is so, since it is apparent from Figure 3-34 that the dark heavy surface deformation line (on the right hand side) is the result of tooling marks imposed to the sample during removal from its capsule. This mark lies in a direction perpendicular to the sample axis. Also, it must be remembered that solidification occurred in the vertical position and therefore along the sample axis. Consequently, the void region associated with the observed particles could not have been "running ahead" of the solid liquid interface. From Figure 3-34 it can also be concluded that the observed relative positions of the tool mark, the particle, and the void volume indicate that particle settling was in a direction perpendicular to the sample axis. This

could only occur when the sample was in a horizontal position; i.e., during the heat up cycle of the melting procedure. This conclusion further substantiates that postulated in Section 3.2.4.3.4.1.

It should also be noted that in the case of Control Sample 1 (1C-A-00) the surface features did not include holes (see Figures 3-34 and 3-38). All of the observable features as a result of void action are seen to be associated with tungsten particles.

One more observation of interest concerns the particle-void relationship occurring in Figure 3-38. Notice first that at this 500X magnification we can observe the presence of some void volume around most particles. Again, for those particles which are not in contact with other particles, the void volume is appreciably larger. Also note that in this case the particle position within any surrounding void volume is not symmetrical. It is not possible to determine the geometric relationships between particle-void volume, cooling direction, etc., in the case of Figure 3-38.

A view of surface distortion in Flight Sample 1 (1F-A-00) at 100X magnification is given in Figure 3-56. Comparison of these photos with Figure 3-34 of Control Sample 1 (1C-A-00) also at 100X shows that the surface distortions on the Flight Sample are both more numerous and are smaller. It should remembered that the distortion shown in Figure 3-34 is not a typical feature; however, it is a distortion which is "like" that observed as typical on the flight sample. Therefore, this comparison is being made here in an attempt to ascertain if melting under negligible gravity conditions is reflected by differences in all sample surface features. The principal difference in sample surface features can be summarized as follows:

(1) The Control Sample exhibits very little surface distortion attributable to other than tooling marks or capsule wall impression.

(2) The surface distortions observed on the Control Sample indicate that some particle-void interaction had occurred. This is evidenced by the void-volume associated observed at individual particle sites.

(3) The particle-void volume association was not symmetric suggesting that particle settling was proceeding during the molten state.

(4) The particle motion at the surface of the Control Sample left a direction trace which was in a direction perpendicular to that of the solid-liquid interface during solidification.

(5) The Flight Sample exhibited a large amount of surface distortion attributable to other than tooling marks of capsule wall impressions.

(6) Surface distortions on the Flight Sample indicated that much particle-void interaction had occurred as evidenced by the void-volume-particle association observed.

(7) The particle-void-volume association was, in most cases observed, symmetrical suggesting that particle settling did not occur at any time during the heating/cooling cycles.

(8) The particle-void volume motion on the surface of the Flight Sample was not such that a direction trace could be determined.

(9) The fact that particle redistribution did occur in the Flight Sample (see below) indicates that void-particle motion at the surface was in the same direction and at the same rate.

(10) The presence of void volume distribution as well as particle distribution on the Flight Sample was not uniformly observed. Instead very little surface distortion is observable at the Cold End of the sample. This distortion increases with distances along the sample till at a location approximately one half the sample length the distortion reaches a level from which it increases only slightly with position towards the Hot End.

The difference in surface features summarized above and previously discussed can be rationalized if we consider the following four main mechanisms as being operative.

(1) From the evidence (points 3 and 4 above), it is postulated that gravity induced settling of tungsten particles has occurred in the Control Sample. Also from the evidence of points 7 and 8 above it is concluded that gravity induced settling of tungsten particles has not occurred in the Flight Sample.

(2) From the evidence of points 1, 5, 6, above it is concluded that under negligible gravity condition the motion of voids and/or bubbles will be toward the container walls in that the total free energy of the system will be reduced by a reduction in bubble surface energy.

(3) During directional solidification the motion of bubbles is away from the solid liquid interface; i.e., into the liquid. This is evidenced in points 9 and 10 above.

(4) The adhesion of bubbles to particles can occur if surface energy relationships and concentrations permit and a total free energy decrease in the system results. Further, this adhesion (association) will allow for particle-void volume motion on a cooperative basis. This is evidenced by points 2, 3, 7, 8, 9, and 10 above.

The above mechanisms are apparent from a consideration of the observed surface features in samples 1C-A-00 and 1F-A-00 as listed above. Of some interest is the observation that in the Flight Sample, surface distortion did not occur homogeneously along the surface as a function of sample length. This can be explained if one considers that motion of bubbles to the capsule wall will require some driving force and that this driving force has two components. The first being a reduction in total system energy equal to the surface energy loss upon bubble attachment. The second (and of importance here) is a concentration gradient and a supersaturation of bubbles. This is brought about by the action of the advancing solid-liquid interface.

If we consider the conditions existing at a time when the complete sample is molten we postulate that a homogeneous distribution of bubbles exists and that only a slight concentration gradient occurs as the result of those bubbles near the capsule wall randomly walking to the wall and adhering. This creates a deficiency of complete bubbles in that part of the melt just away from the wall and a concentrate gradient with the interior is established. This gradient "drives" toward the capsule wall. The action here is random and therefore slow; consequently, very little surface distortion due to bubble bursting results.

When the melt is beginning to cool and solidify directionally two mechanisms occur simultaneously. First the heat-sink end of the sample loses heat very rapidly and effectively quenches in any void or bubble concentrates present. This of course does not allow motion to the surface or into the melt. Therefore, a volume of sample near the heat sink (cold end) should not have a distorted surface due to bubble bursting or adherence to the capsule wall. As the solid liquid interface is established and begins to advance the cooling rate is less than the initial rate at contact and bubble motion ahead of the interface is occuring and results in an increase in concentration. Also, since there is a decrease in temperature of the liquid ahead of the solid liquid interface the equilibrium bubble (void, vacancy, etc.) concentration which was present at the maximum temperature is now an excess concentration or super-saturation. This adds to the concentration at the liquid temperature just above melting and drives bubbles etc to the walls of the container resulting in the surface distortion (effect) observed. The incubation distance on the Flight Sample is,of course, the result of other complex variables such as temperature of the melt when placed on the heat sink, temperature of the heat sink, degree of contact of capsule to heat sink, conductivity, etc. However, mechanism postulated above is believed to be sound and is expected to change only in degree with a change in these variables.

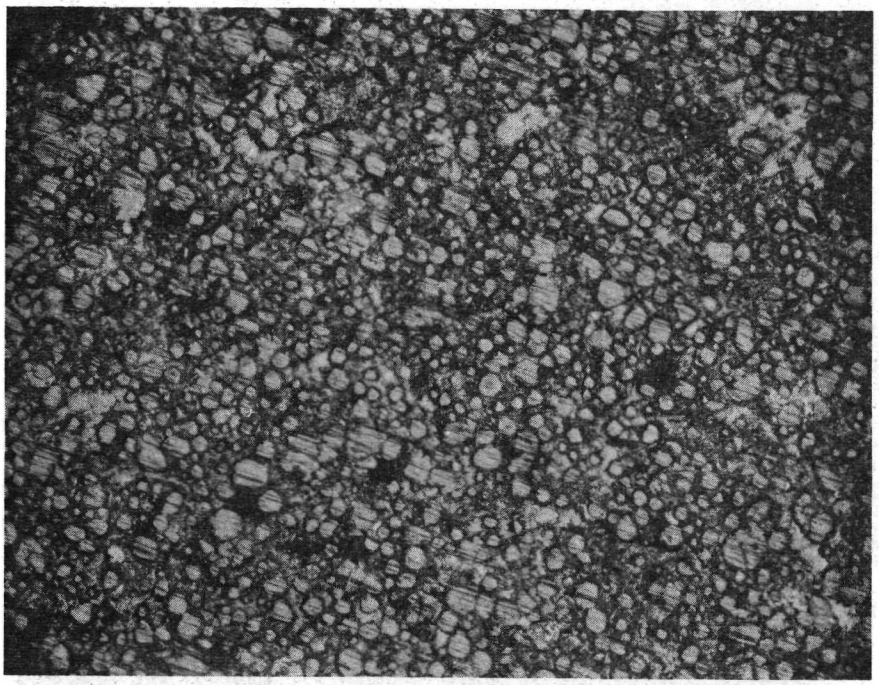

2
(A)

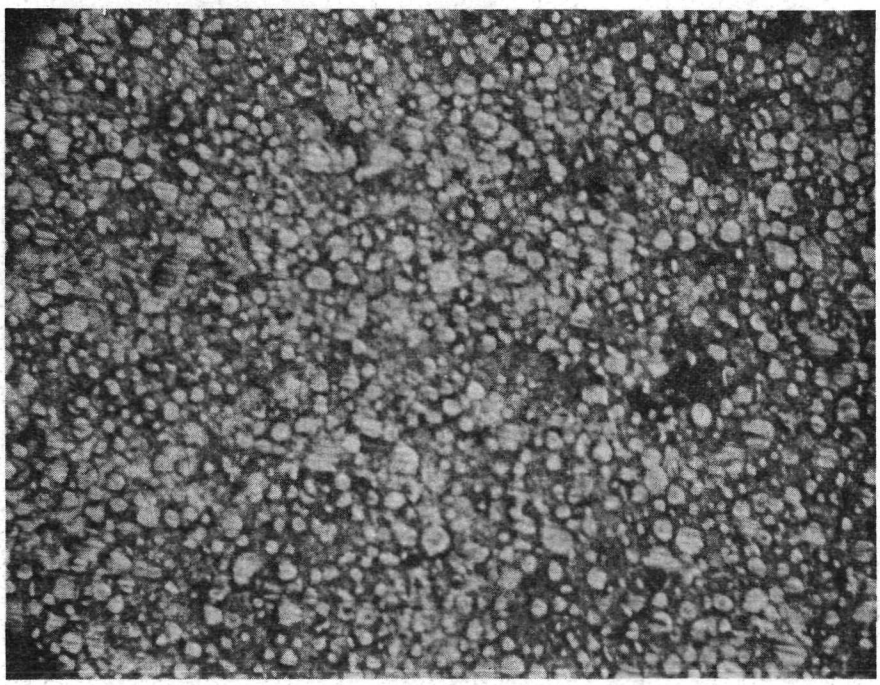

4
(B)

Figure 3-60 FLIGHT SAMPLE 1 (1F-A-00) DIRECTIONAL DISPLAY AT 100X PHOTOMICROGRAPHS 2 AND 4

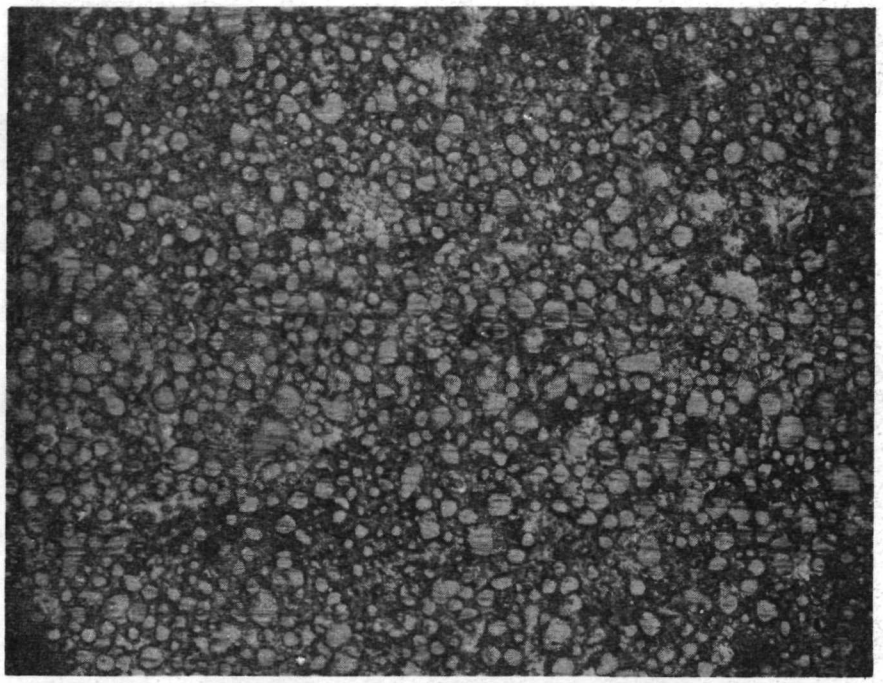

6
(A)

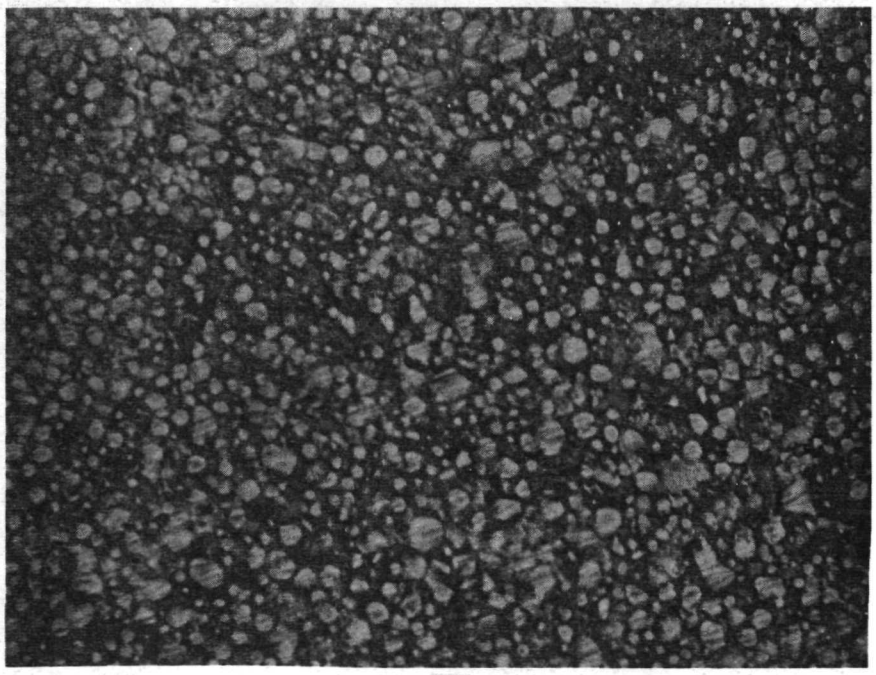

10
(B)

Figure 3-61 FLIGHT SAMPLE 1 (1F-A-00) DIRECTIONAL DISPLAY AT 100X PHOTOMICROGRAPHS 6 AND 10

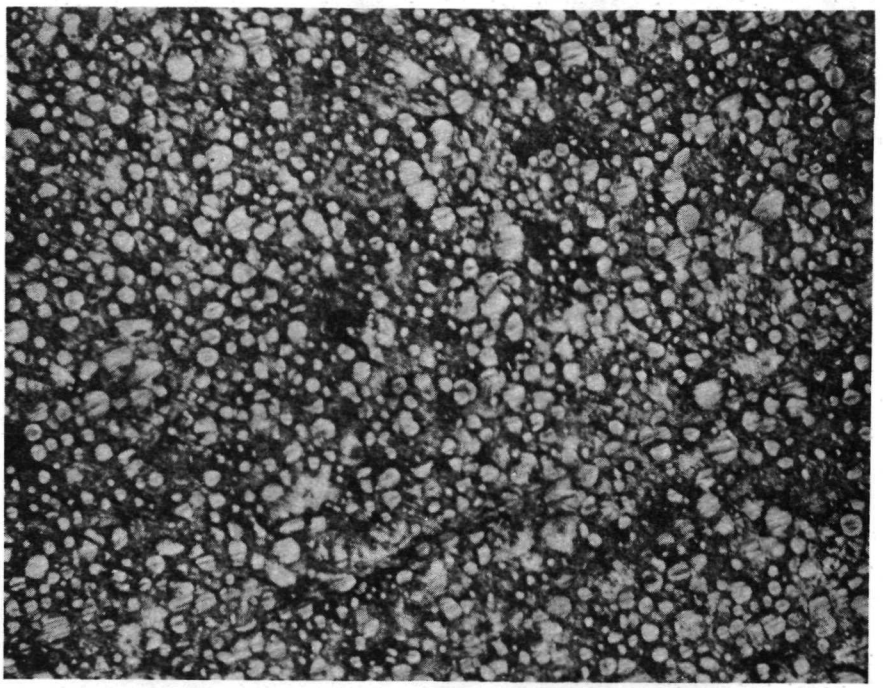

12
(A)

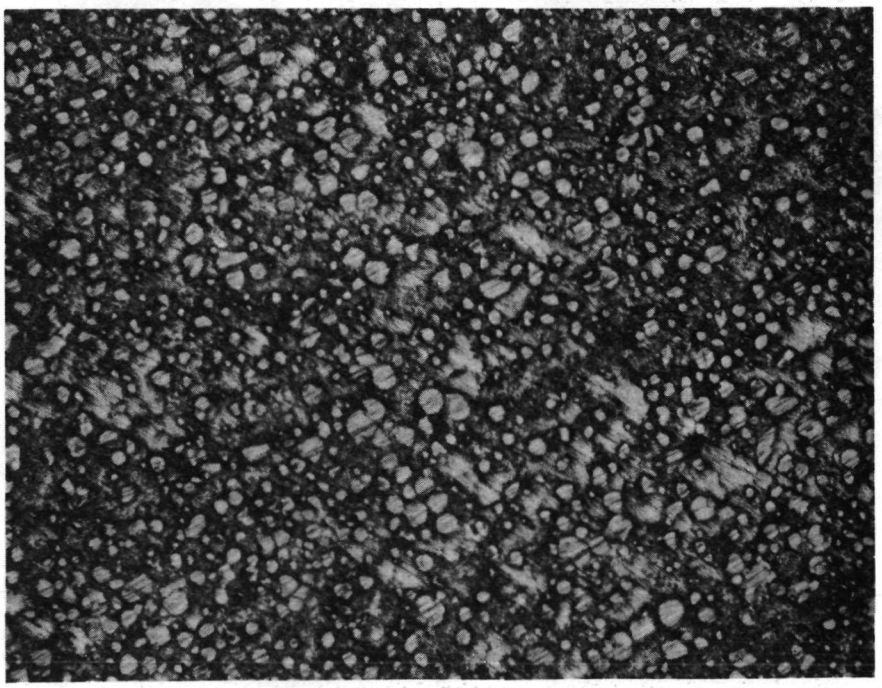

14
(B)

Figure 3-62 FLIGHT SAMPLE 1 (1F-A-00) DIRECTIONAL DISPLAY AT 100X PHOTOMICROGRAPHS 12 AND 14

This page intentionally left blank.

This page intentionally left blank.

3.2.4.4.4 Tungsten Particle Dispersion, Flight Sample 1 (1F-A-00)

A sketch of Flight Sample 1 (1F-A-00) is given in Figure 3-1 presenting the surface studied and outlining the directional and cross directional display paths investigated. The nomenclature utilized for this sample is identical to that discussed for sample 1D-A-00 (Section 3.2.4.2).

Directional Display

As seen in sketch 3-1 the directional display for sample 1F-A-00 was made by determining the volume percent tungsten in 15 separate areas of the surface. The line along the axis of the plane, shown in Figure 3-1, represents the path followed with point 1 representing the starting position. Figure 3-60 through 3-62 are representative of the photos taken for this display. Photomicrograph 1 was taken such that the sample was visible; succeeding photomicrographs were then taken every 0.635 cm (0.25 in).

Figure 3-63 represents the volume percent tungsten as a function of position for the directional display as obtained by actual count. As seen the concentration of tungsten particles is very nearly constant at 30 volume percent which was the initial compact concentration in each case.

Cross-Directional Display

Cross-directional displays were obtained after sample sectioning using an MR spark cutter. Cuts were made every 1.27 cm (0.5 in) resulting in six relatively equal sections, see Figure 3-1. Each section was labeled as follows:

Section	Label	Position on Sample
1	1F-A-001	Cold end of compact - 1.27 cm long
2	1F-A-002	Next to Section 1 - 1.27 cm long
3	1F-A-003	Next to Section 2 - 1.27 cm long
4	1F-A-004	Next to Section 3 - 1.27 cm long
5	1F-A-005	Next to Section 4 - 1.27 cm long
6	1F-A-006	Hot end of Compact - 1.27 cm long

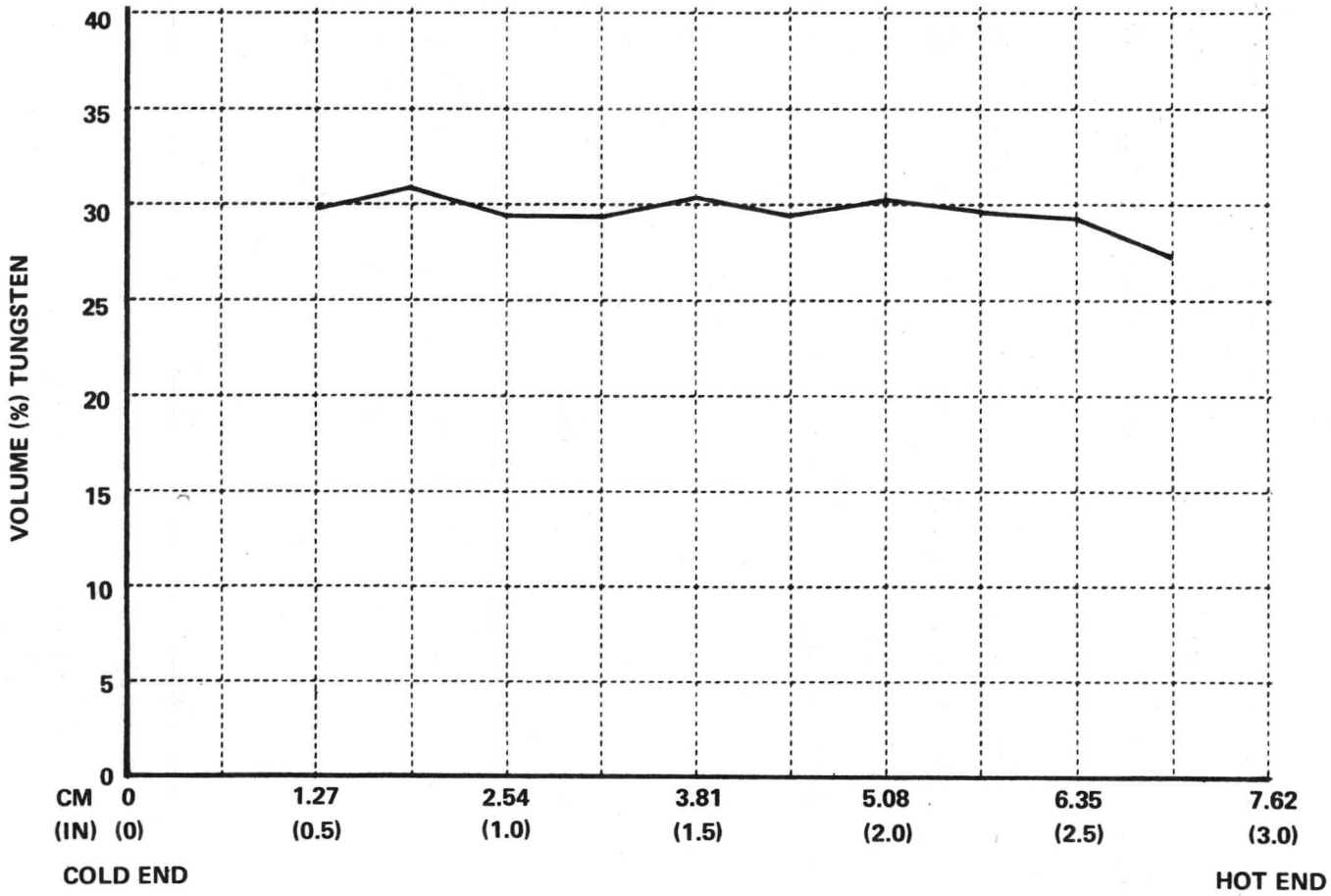

Figure 3-63 DATA PLOT, VOLUME % TUNGSTEN, DIRECTIONAL DISPLAY, FLIGHT SAMPLE 1 (1F-A-00)

The above sections were mechanically polished and etched using a solution consisting of 100 ml methyl alcohol, 0.5 grams picric acid and 2 ml hydrochloric acid. This etchant preferentially attacked the eutectic matrix. Cross directional particle concentration counts were then made at the center of each section (see Figure 3-1). In polishing the first section (1F-A-00), a rather large amount of material was removed before an acceptable surface was produced. This resulted in a surface which was "out of line" with that of the other sections, therefore, the cross-directional display for this section is not presented.

Figures 3-64 through 3-66 are photomicrographs used in the determination of the cross-directional display for Section 1F-A-002. Figures 3-67 through 3-69 are those obtained for Section 1F-A-005. The procedure for these (and the other sections) included taking an initial photo at the specimen edge (visible in each case) and then traversing 0.518 cm (0.2 in) into the bulk. The last photomicrograph in each display was taken with the opposite edge also visible. Figures 3-64(A), 3-66, 3-67(A) and 3-69 show that difficulty in polishing the edge portions of the specimens was encountered. This was typical in all cases. To compensate for this, the total area represented in these figures was not used in the determination of volume percent tungsten, rather, only that portion of the photo having little surface distortion was utilized. In all cases the percent of observable area utilized was in excess of 75 percent.

Figure 3-70 is a plot of volume percent tungsten versus position into the bulk of the sections for sections 1F-A-00 and -003. Figure 3-71 is the same kind of plot for sections -004; -005 and -006. The cross-directional displays present two characteristics: (1) the deviation from 30 volume percent tungsten is greatest near the edges (surface) of each section, and (2) the deviation from 30 volume percent in the bulk of the sections; i.e., for 0.25

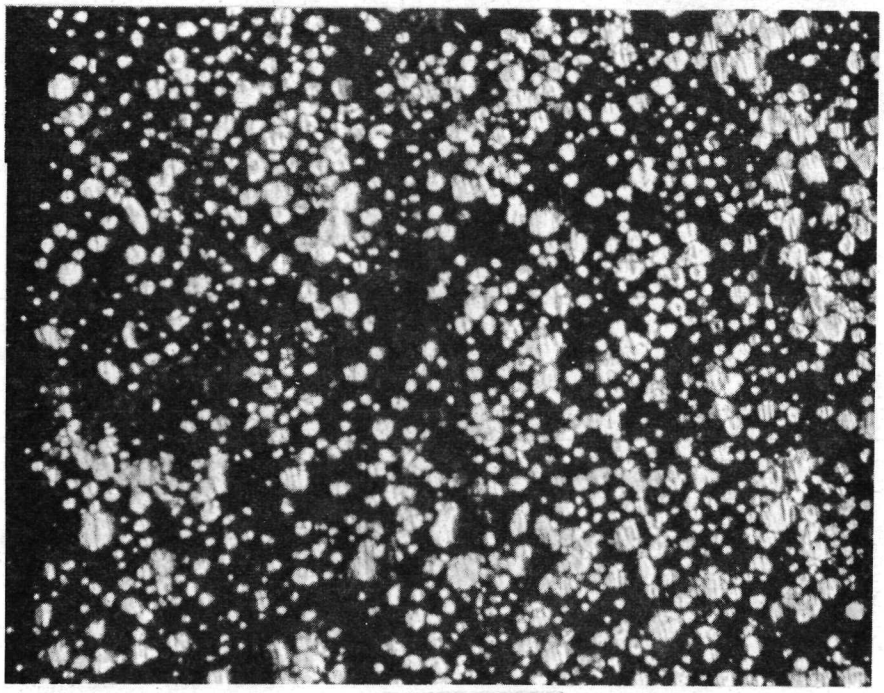

1 (NOTE EDGE)
(A)

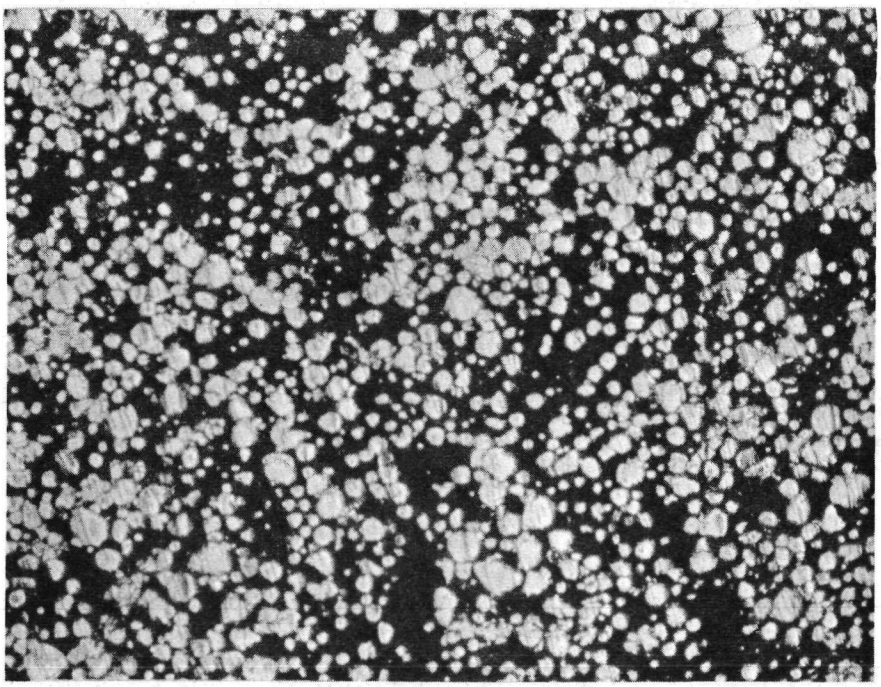

2 (0.51 cm FROM NO. 1)
(B)

Figure 3-64 FLIGHT SAMPLE 1 (IF-A-00) CROSS-DIRECTIONAL DISPLAY AT 100X, SPECIMEN 1F-A-002. ETCHED, PHOTOMICROGRAPHS 1 AND 2

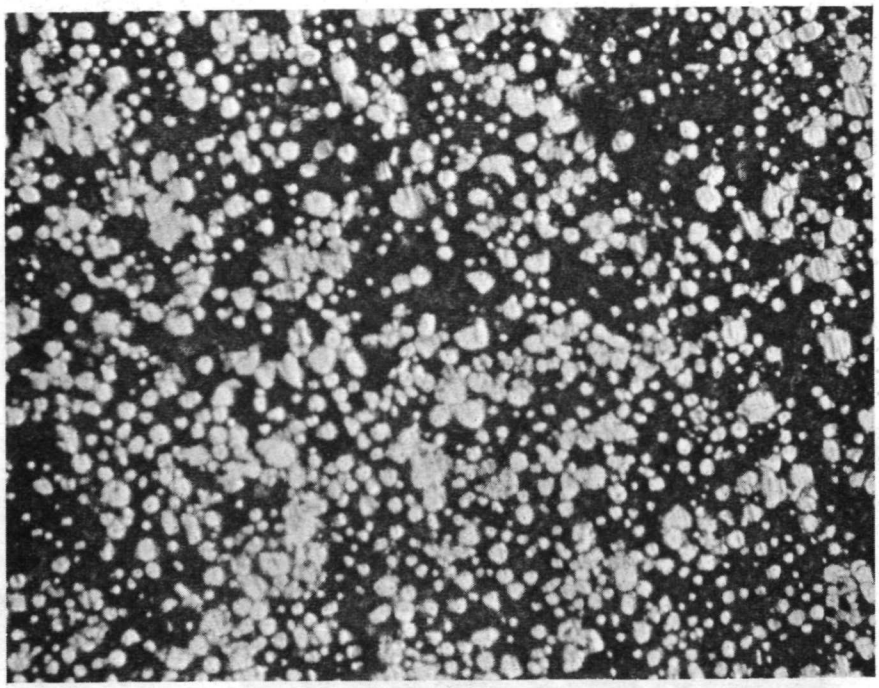

3 (0.51 cm FROM B OF FIGURE 3 - 64)

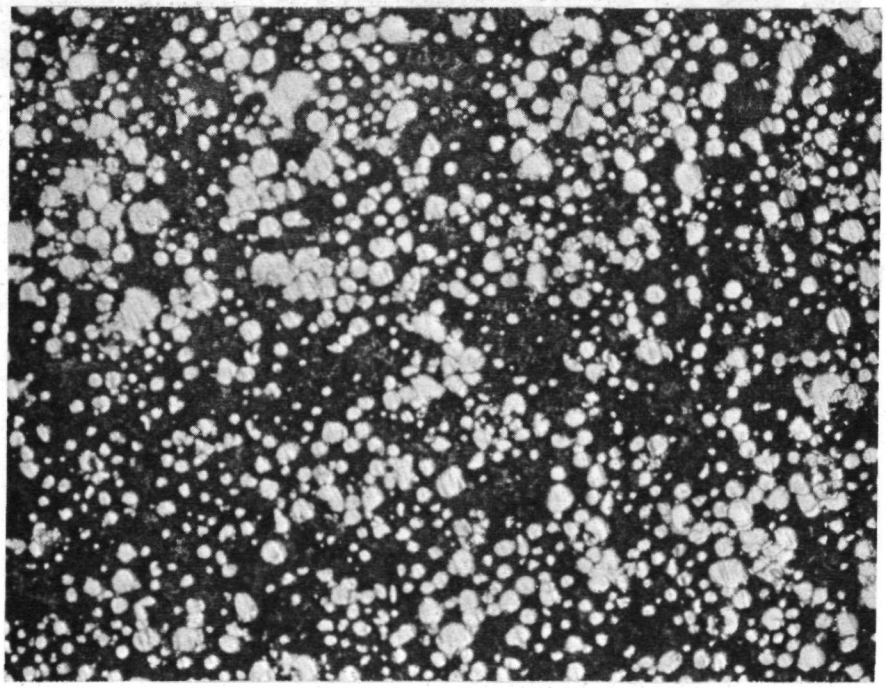

Figure 3-65 FLIGHT SAMPLE 1 (1F-A-00) CROSS-DIRECTIONAL DISPLAY AT 100X, SPECIMEN 1F-A-002, ETCHED, PHOTOMICROGRAPHS 3 AND 4

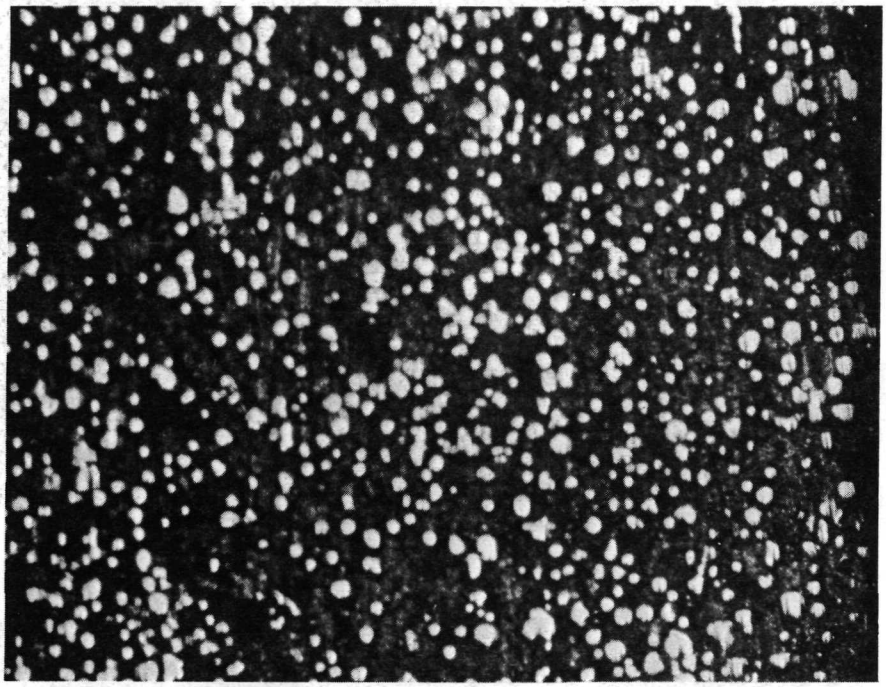

(NOTE EDGE)

Figure 3-66 FLIGHT SAMPLE 1 (1F-A-00) CROSS-DIRECTIONAL DISPLAY AT 100X, SPECIMEN 1F-A-002, PHOTOMICROGRAPH 5

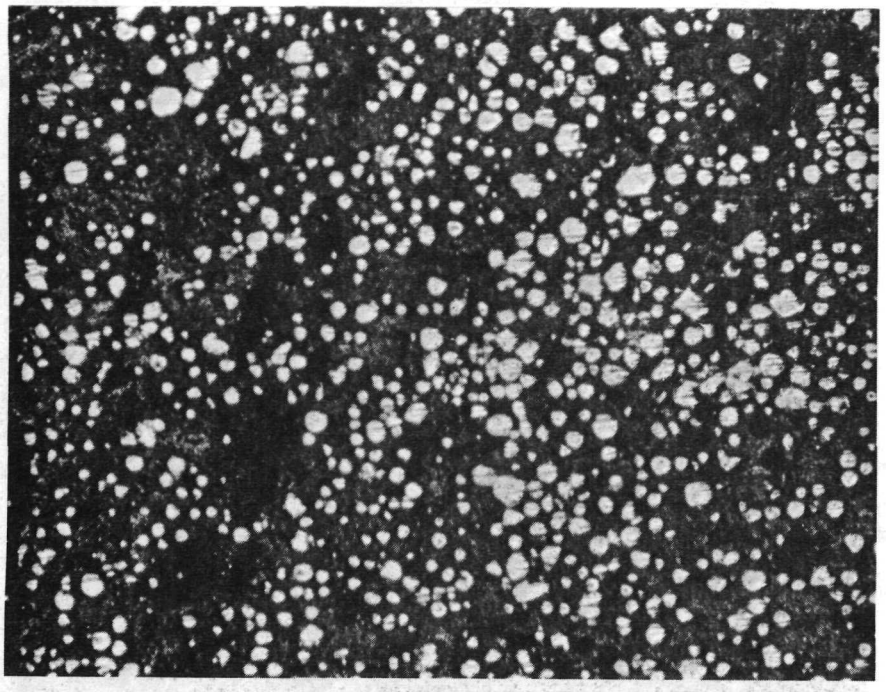

1 (NOTE EDGE)
(A)

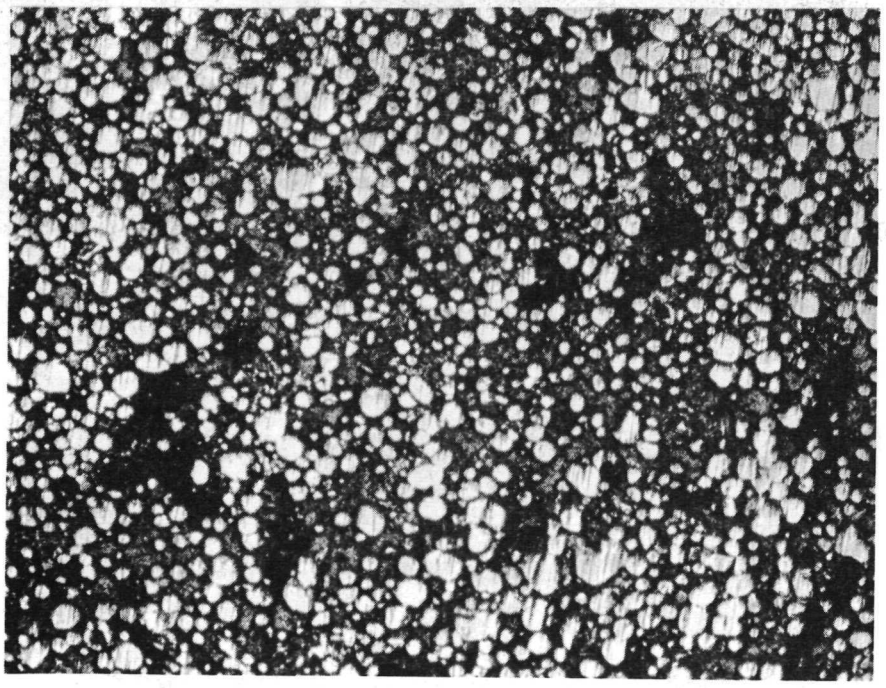

2 (0.51 cm FROM NO. 1)
(B)

Figure 3-67 FLIGHT SAMPLE 1 (1F-A-00) CROSS-DIRECTIONAL DISPLAY AT 100X, SPECIMEN 1F-A-005, ETCHED, PHOTOMICROGRAPHS 1 AND 2

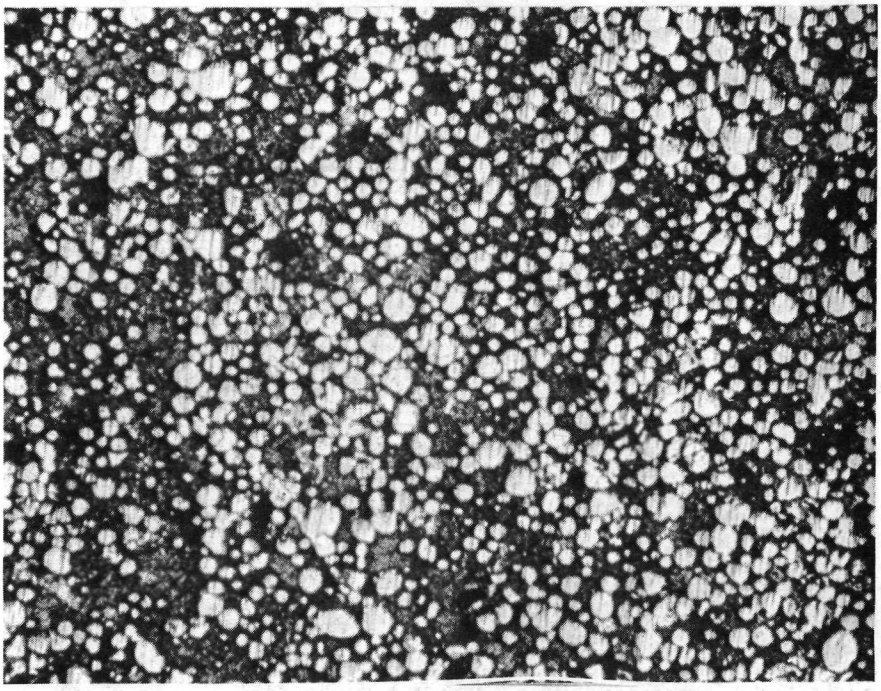

3 (0.51 cm FROM B OF FIGURE 3-67)
(A)

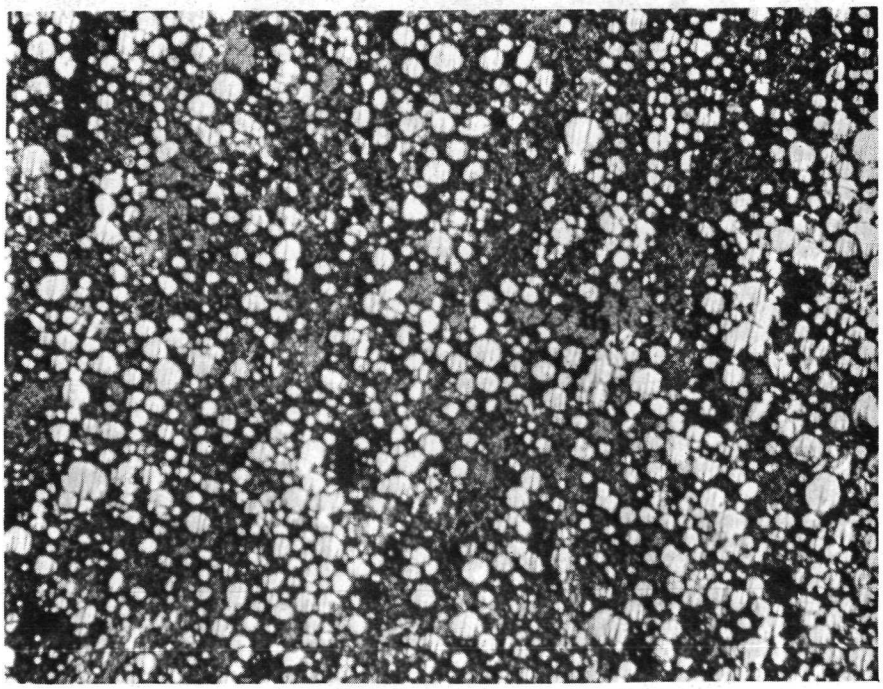

4 (0.51 cm FROM FIGURE 3-69)
(B)

Figure 3-68 FLIGHT SAMPLE 1 (1F-A-00) CROSS-DIRECTIONAL DISPLAY AT 100X, SPECIMEN 1F-A-005, ETCHED, PHOTOMICROGRAPHS 3 AND 4

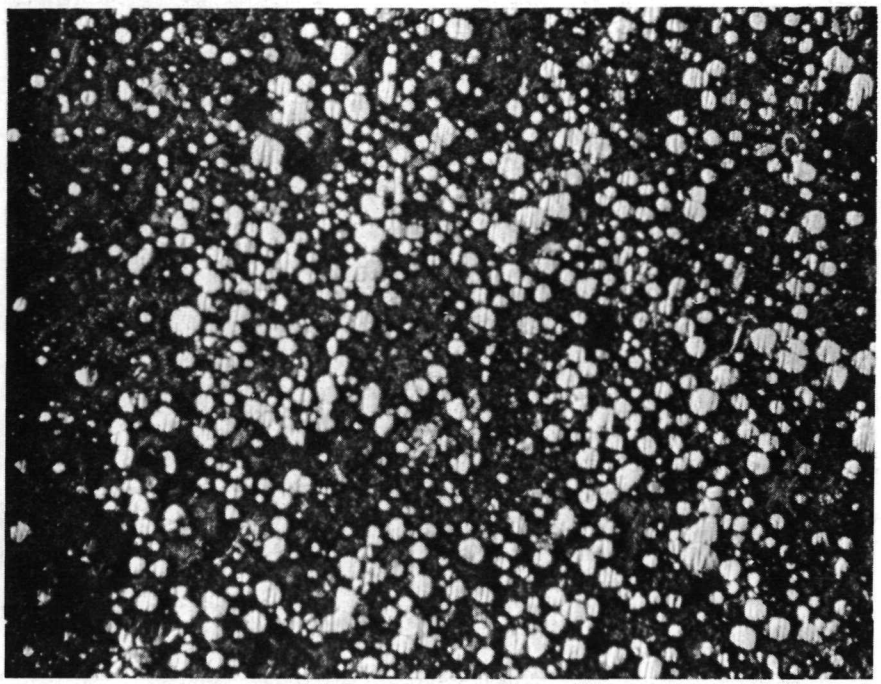

(NOTE EDGE)

Figure 3-69 FLIGHT SAMPLE 1 (1F-A-00) CROSS-DIRECTIONAL DISPLAY AT 100X, SPECIMEN 1F-A-005, ETCHED, PHOTOMICROGRAPH 5

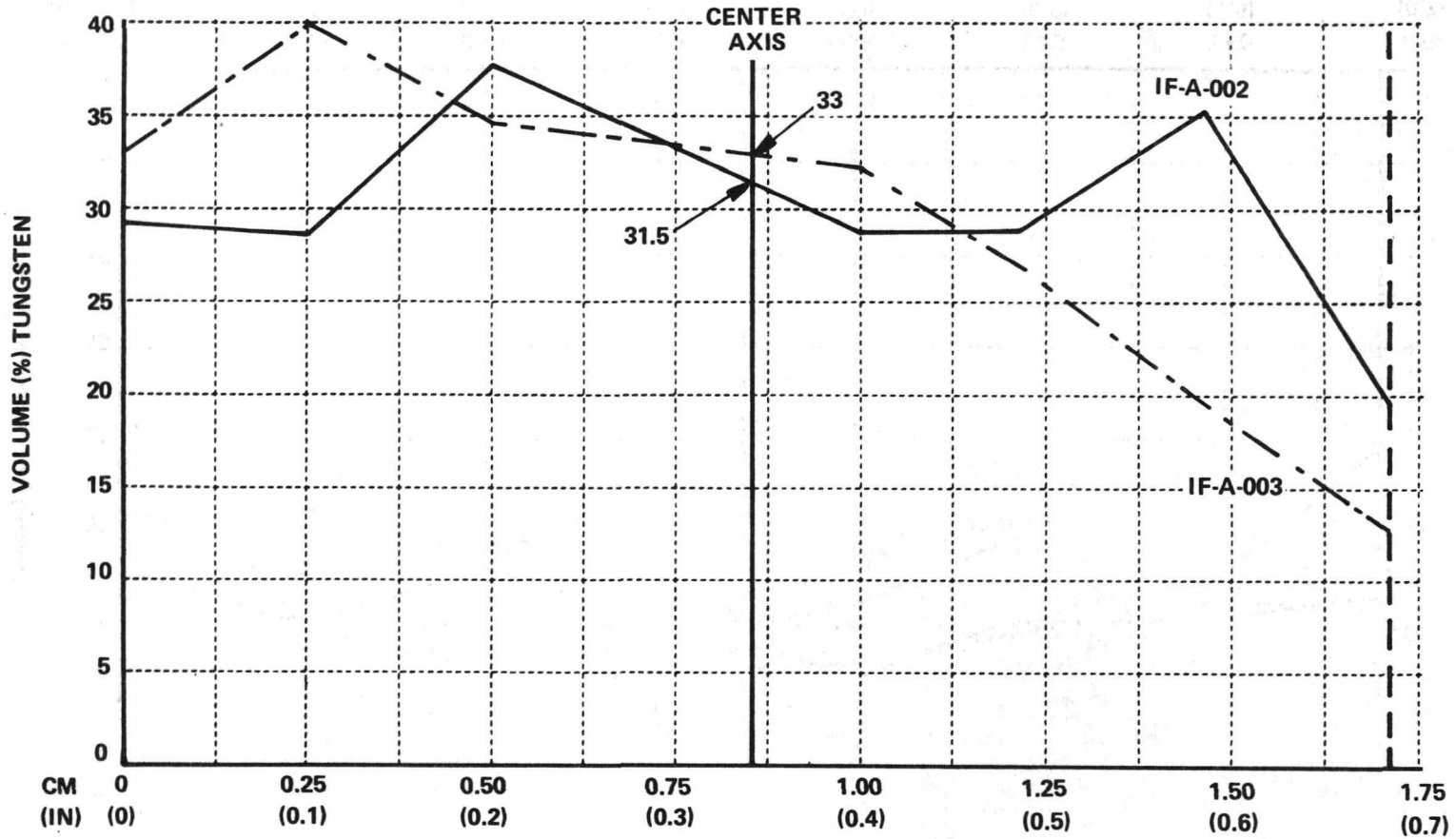

Figure 3-70 DATA PLOT, VOLUME % TUNGSTEN, CROSS-DIRECTIONAL DISPLAY, FLIGHT SAMPLE 1 (1F-A-00)

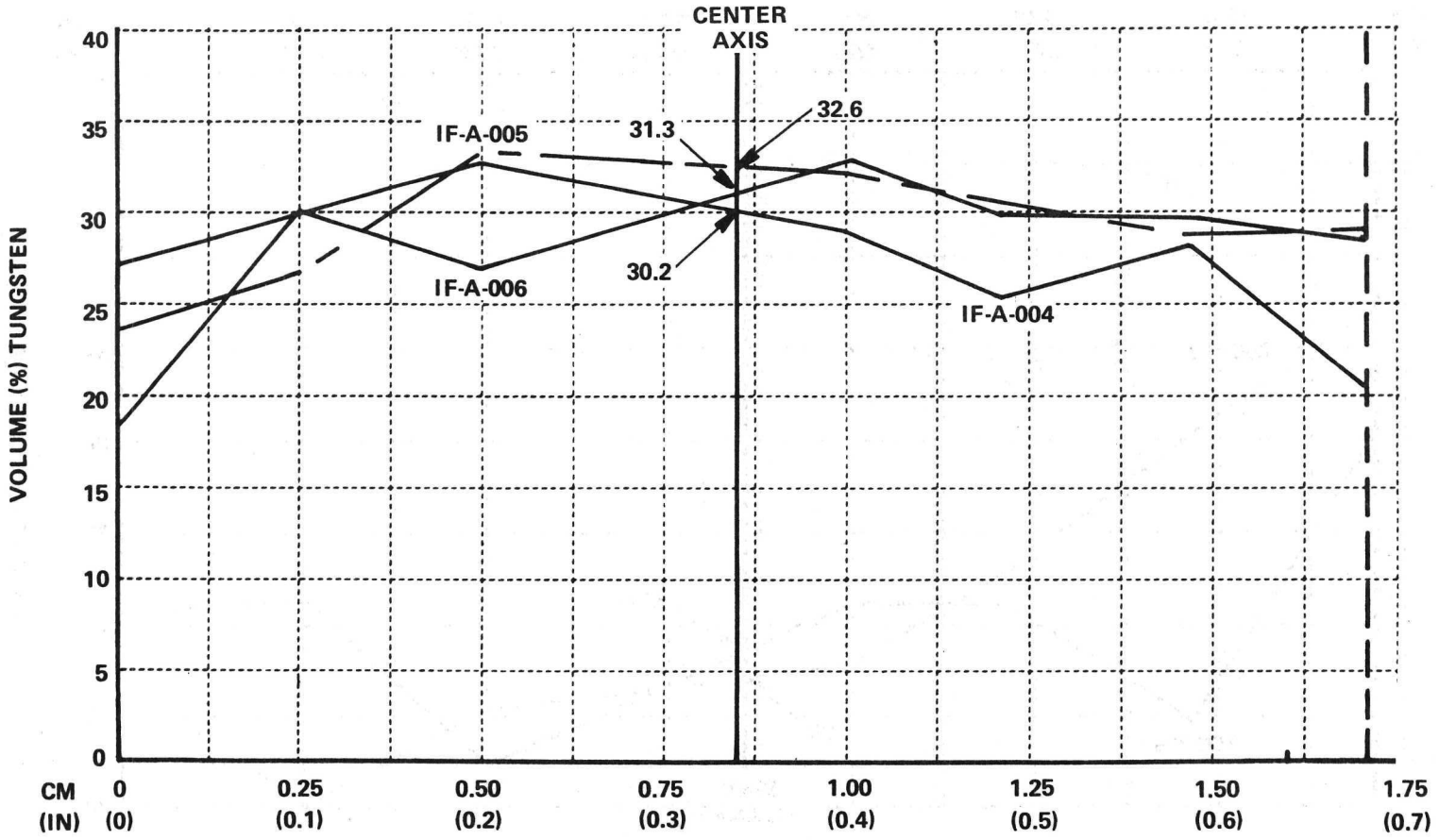

Figure 3-71 DATA PLOT, VOLUME % TUNGSTEN, CROSS-DIRECTIONAL DISPLAY, FLIGHT SAMPLE 1 (1F-A-00)

to 1.5 cm (0.1 to 0.6 in) is reduced as a function of distance from the Cold End. That is, the plots for sections -006 and -005 when compared to the plots for sections -002 and -003, in the position range 0.25 to 1.5 cm, exhibit a more uniform distribution as well as tending toward the 30 volume percent tungsten line.

The above characteristics can be considered as evidence that the tendency of the system toward equilibrium (equilibrium in this case is considered a totally uniform distribution of particles at 30 volume percent) is such that the central portion of the system (sample) is first to attain this condition. Also, the tendency toward equilibrium is dependent on time at temperature in that the sections which were first to cool (i.e., -002 and -003) exhibited the greatest deviation. However, this deviation could also be affected by the advance of the solid-liquid interface during the directional solidification. This would certainly be the case if a void (bubble) - particle interaction had occurred.

The concept that the central portion of the system is first to reach equilibrium is further substantiated by the data (volume percent tungsten) obtained from the intersection of the cross-directional display curves and the line representing specimen center axis in Figures 3-70 and 3-71. These values are replotted in Figure 3-72 as interpolated along with the original curve for the observed directional display. As seen in Figure 3-72, the interpolated and observed curves are identical within approximately two percent. Also notice that the interpolated curve is consistently higher in volume percent. It is felt that this is due to the fact that cross directional data was gathered from etched surfaces whereas the original observed directional display data was gathered from an as polished surface. The etching procedure obviously will expose tungsten particles which are just below the polished surface resulting in high counts. The reproducibility of the curves in Figure 3-72 is good and indicates again that procedure and data reliability is high.

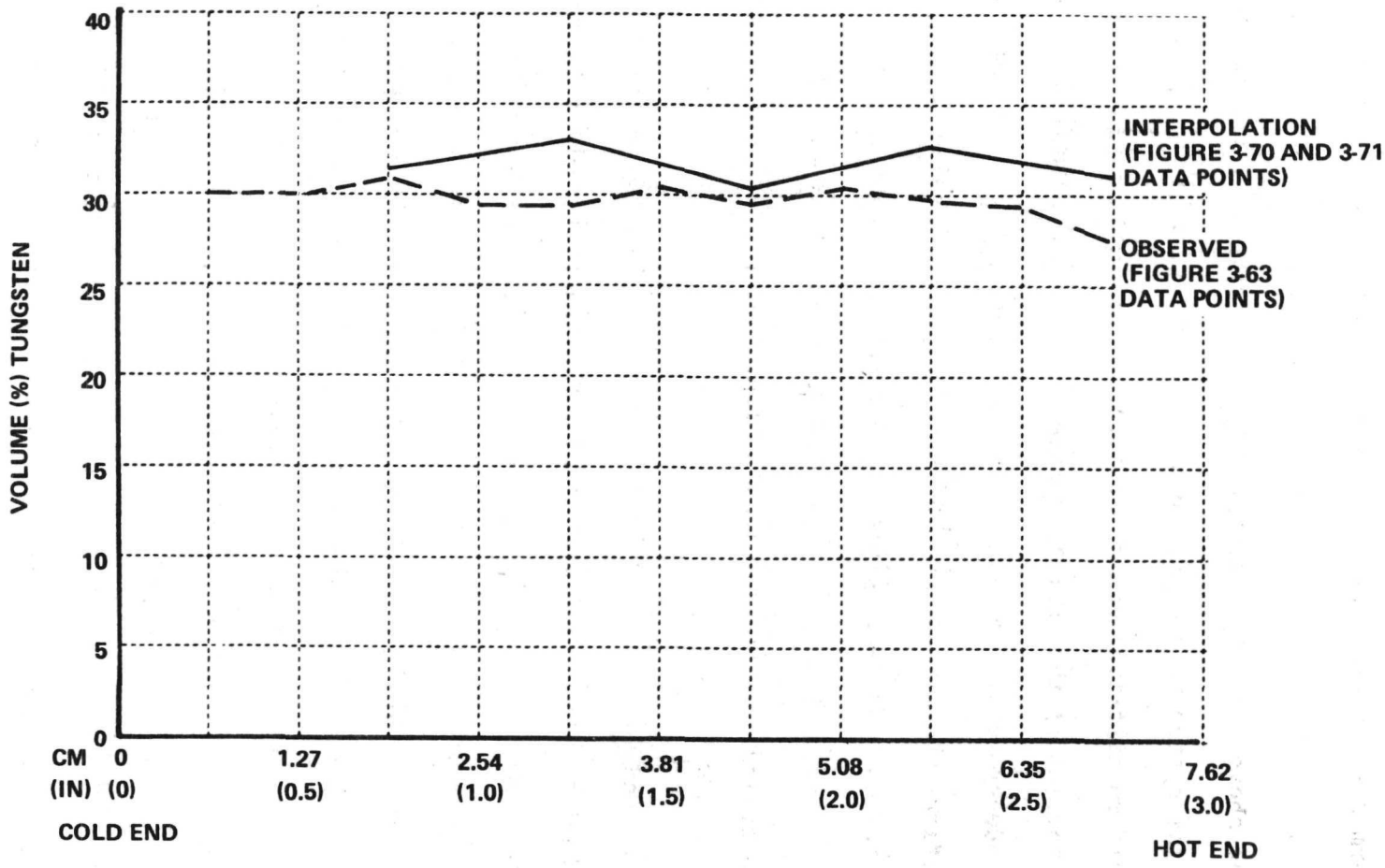

Figure 3-72 DATA PLOT, VOLUME % TUNGSTEN, COMPOSITE DIRECTIONAL DISPLAY, FLIGHT SAMPLE 1 (1F-A-00)

This page intentionally left blank.

3.2.5 Conclusions, Experiment 1

The conclusions drawn from the data obtained, and reported here, are summarized in two categories below: the first category is the result of qualitative data interpretation and must be considered as postulations needing eventual verifications via data analysis from future flights; the second category results from interpretation of quantitative data on the redistribution of tungsten particles -- the conclusions in this category have a firm experimental basis and, therefore,are of significant and immediate scientific value.

3.2.5.1 Qualitative Aspects

From the surface studies made of Developmental Sample 1 (1D-A-00), Control Sample 1 (1C-A-00) and Flight Sample 1 (1F-A-00) the following observations have importance:

(1) The degree of sample surface distortion observed increases from the Developmental to the Control and the Flight Samples.

(2) There is a distinct difference in the kind of surface distortion observed in Control Sample 1 (1C-A-00) and Flight Sample 1 (1F-A-00). This difference includes the size and density of distortion, the relationship between tungsten particle and associated void volumes, and the homogeneity of distortion through the sample surface area.

The above observations fit a rational sequence of events if one considers a series of mechanisms as operative during the cooling cycle (previously discussed in this section). This series of mechanisms must include the following:

(1) Formation and stabilization of bubbles during melting.

(2) Motion of bubbles in a direction away from the solid-liquid interface during directional solidification.

(3) An increase in the concentration of bubbles in the melt ahead of the solid-liquid interface.

(4) Attachment of bubbles to the capsule wall resulting in a total energy loss for the system.

The observations made in the surface of Control Sample 1 (1C-A-00) and Flight Sample 1 (1F-A-00) are still one-of-a-kind and therefore these observations must be verified in future flight experiments.

3.2.5.2 Quantitative Aspects

The distribution of tungsten particles in each of the samples has been determined quantitatively using a point-intercept method. Specifically, a plane produced by sectioning each sample into two halves was used to perform directional and cross-directional redistribution studies. The results obtained indicate the following:

(1) A redistribution of tungsten particles occurred after melting and solidification and both the Control and Flight samples as compared to the Developmental Sample.

Again it is recognized that this conclusion is based on specimens which are "one-of-a-kind". Also, that (precise) particle distribution for the flight and control samples was not known but was assumed to be equivalent to that obtained from distribution studies on one developmental (as-pressed) sample.

As previously stated this result (and all others presented here) must be verified in future flight experiments.

(2) The distribution obtained for Flight Sample 1 was more uniform than that obtained for Control Sample 2. This indicates that the absence of a gravity force can be used to advantage in liquid-phase sintering or composite casting processes.

3.3 Experiment 2

3.3.1. Capsule Contents

70 volume percent Indium Bismuth - 30 volume percent Boron Carbide (B_4C) compact.

3.3.2 Sample Composition and Preparation

Details relating to material preparation and sample compaction methods are provided in Section 2 and thus only a brief outline will be presented here.

A mixture of 30 volume percent spherical copper-coated Boron Carbide particles and 70 volume percent Indium Bismuth eutectic powders were compressed to form a powder compact. The Boron Carbide particles and Indium Bismuth eutectic powders were of the same size, -325 mesh (less than 44 microns in diameter). The Boron Carbide particles were copper-coated by the electroless plating process to promote wetting and were heated in a hydrogen atmosphere to reduce the oxides. The Indium Bismuth powders were leached in a three percent solution of hydrochloric acid to remove oxides. The two powders were weighed out, placed in a sealed container, and mixed for four (4) hours to obtain a random distribution. The mixed powders were then compressed in a double action die to form a powder compact 1.74 cm in diameter and 2.53 cm long with a theoretical density of 89-90 percent. Three such compacts were subsequently placed in an aluminum capsule which was hermetically sealed by election beam welding.

3.3.4 Objectives and Expected Observations

The sample was designed to observe the differences in distribution of lower density particles in a higher density matrix melted and solidified in reduced gravity compared to a similar sample processed on earth. The density

of the Boron Carbide particles (2.5 g/cm^3) is significantly lower than the density of Indium Bismuth (8.2 g/cm^3). Significant segregation of particles was expected when the matrix was melted under gravity. In the flight sample, g-induced segregation was not expected and a more homogeneous distribution of particles was expected since the molten metal would tend to flow around the particles separating those in contact after the compaction process. Also, the effect of bubble motion on particle distribution was expected to be significant in this experiment due to the lower theoretical density.

3.3.5 Results

3.3.5.1 General

Experiment 2 results consist of data obtained from the Developmental (as-pressed) Sample, Control (earth-melted) Sample and Flight (OG-melted) Sample. The results consist of two main sections (i) documentation of samples after removal from their capsules and (ii) Boron Carbide particle dispersion studies.

3.3.5.2 Developmental Sample 2 (2D-A-00)

3.3.5.2.1 Surface Conditions

As stated in Section 3.3.2 the developmental sample 2D-A-00 had dimensions of 1.74 cm diameter and 2.53 cm length, after pressing. The surface features of the sample were identical to those discussed for the developmental sample 1 (1D-A-00) Section 3.2.4.2.1.

3.3.5.2.2 Boron Carbide Particle Distribution Developmental Sample 2 (2D-A-00)

The distribution of B_4C particles in the developmental sample (2D-A-00) was performed utilizing the procedure described in Section 3.2.4.2.2. The directional display photographs were taken along the sample axis as in the case for the sample of experiment #1. Figure 3-73 is a sketch of the developmental sample.

2D-A-00

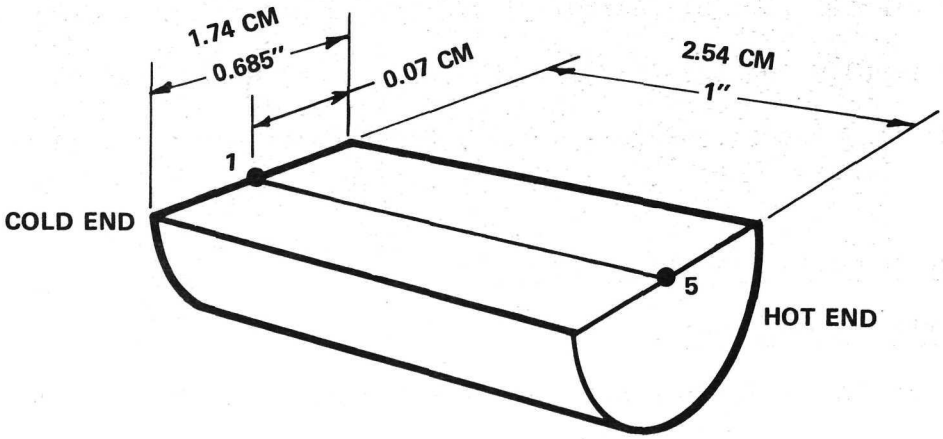

Figure 3-73 SCHEMATIC OF PHOTOGRAPHIC DOCUMENTATION

In Figure 3-73 the directional display line is represented by that line joining points one (1) and five (5). This indicates the position of the traverse made in determining the directional display and also that five (5) areas were photographed. The first photograph was taken such that the edge of the sample was observable, then photos were taken every .64 cm (.25 inch).

Figures 3-74, 3-75, 3-76, and 3-77 are representative photos of the Boron Carbide distribution as obtained after mechanical polishing of the surface shown in Figure 3-73. The determination of volume percent Boron Carbide was made as previously discussed. Figure 3-78 is a plot of volume percent B_4C versus position along the directional display line. As seen, the distribution of B_4C is not uniform. Also note that the ends have been labeled as cold and hot; this designates the position in which each developmental sample had been removed from the capsule.

3.3.5.3 Control Sample 2 (2C-00)

The control sample 2 (2C-00) had been processed (melted) as previously discussed. As stated above, this sample consisted of three (3) individual samples placed concurrently into the capsule. After melting, removal from the capsule was performed in a manner identical to that discussed for sample 1C-00.

Figures 3-79 and 3-80 are photographs of sample 2C-00 after removal from its capsule. Note that the three individual segments remained as individuals; that is, fusion did not occur. This would indicate that melting had not occurred; however, notice in Figure 3-80 that a small metal extrusion did form on the heat sink (cold end) indicating that melting did occur here, at least to a partial extent.

This sample, 2C-00, was sectioned in a manner identical to that previously discussed and the resulting halves were labeled A and B. Figure 3-81

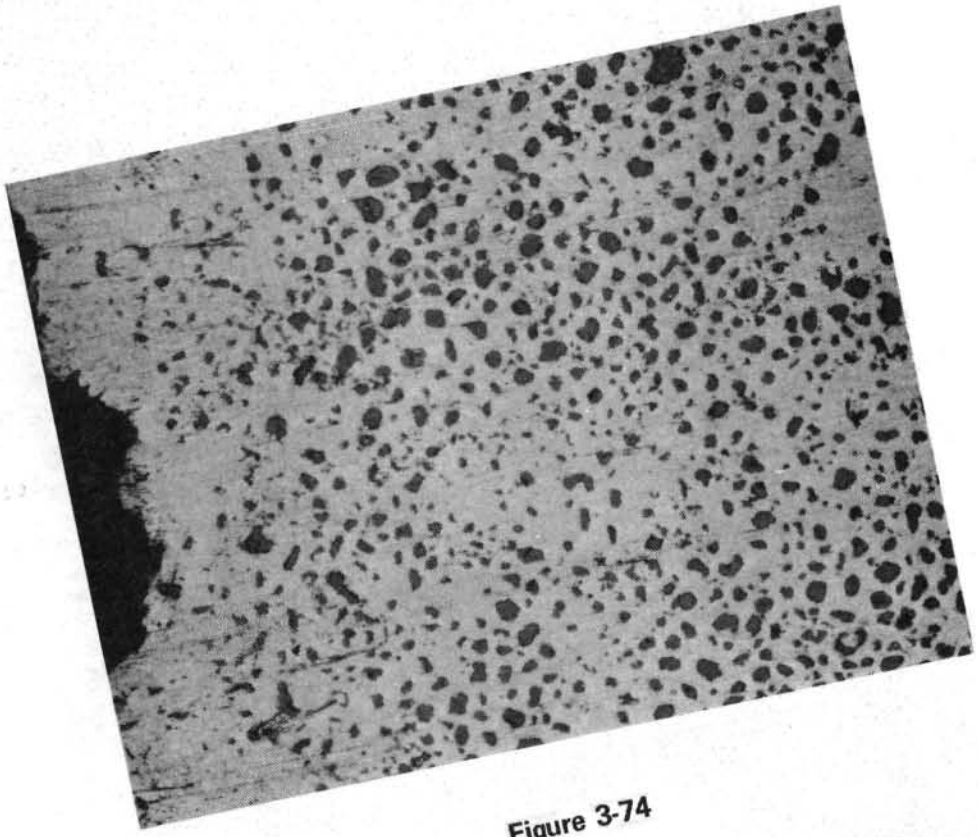

Figure 3-74

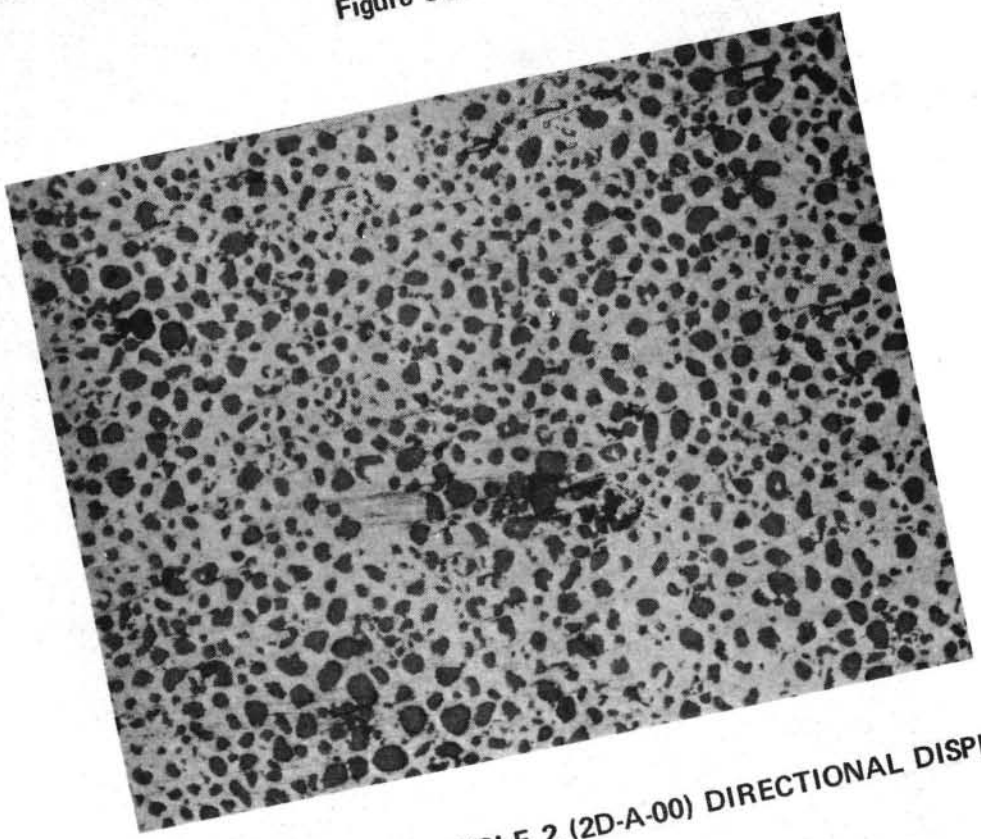

Figure 3-75 DEVELOPMENTAL SAMPLE 2 (2D-A-00) DIRECTIONAL DISPLAY AT 100X, PHOTOMICROGRAPHS 1 AND 3

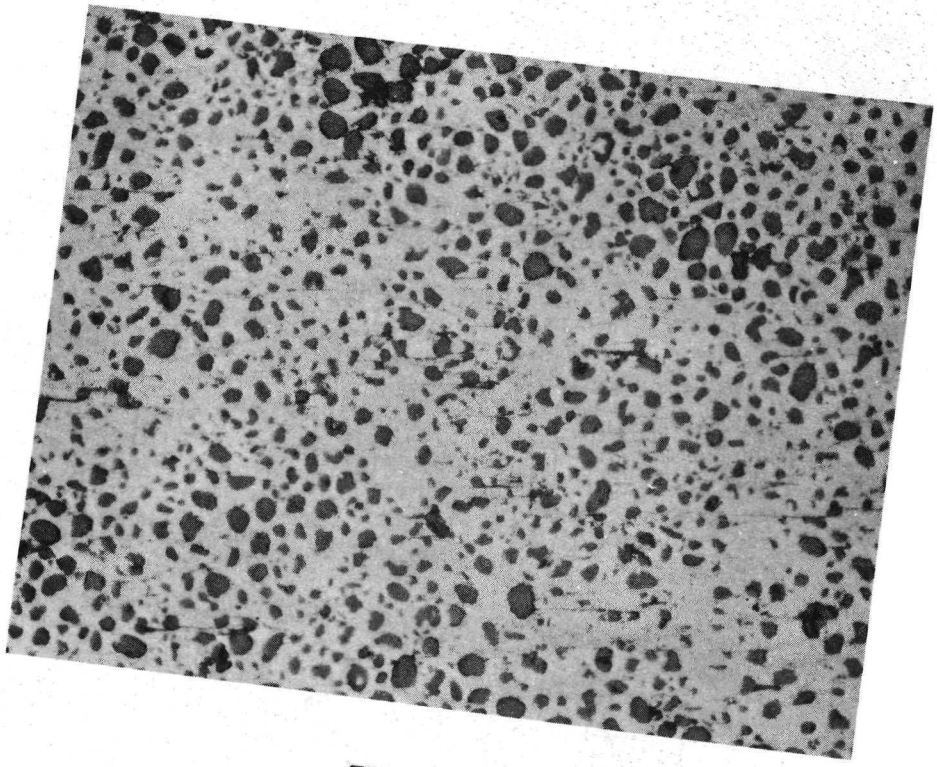

Figure 3-76

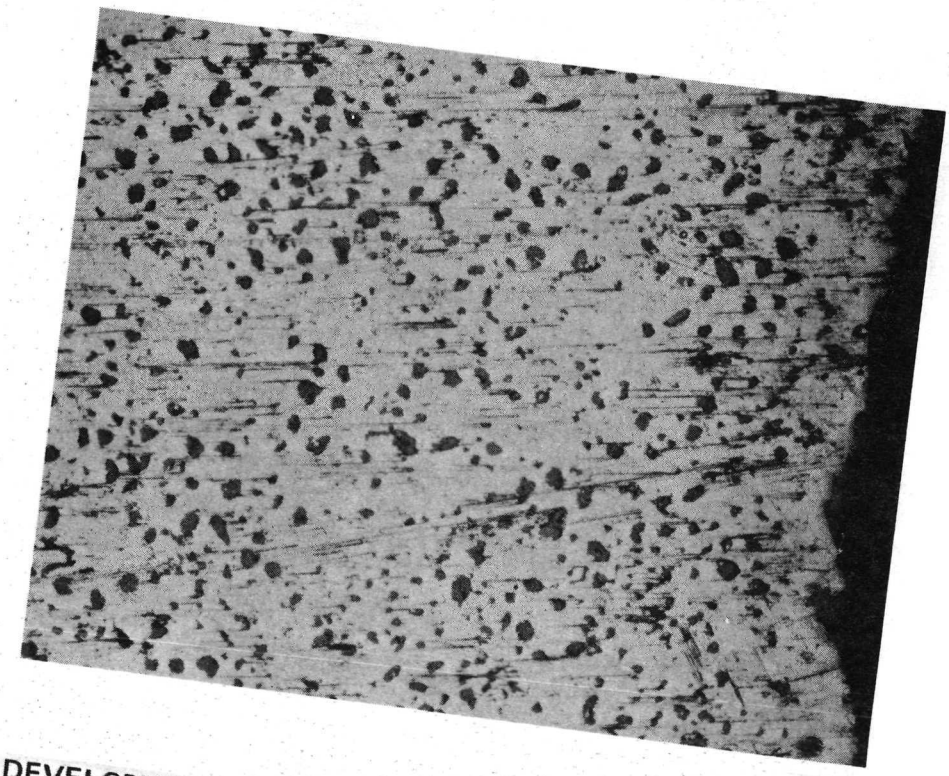

Figure 3-77 DEVELOPMENTAL SAMPLE 2 (2D-A-00) DIRECTIONAL DISPLAY AT 100X, PHOTOMICROGRAPHS 4 AND 5

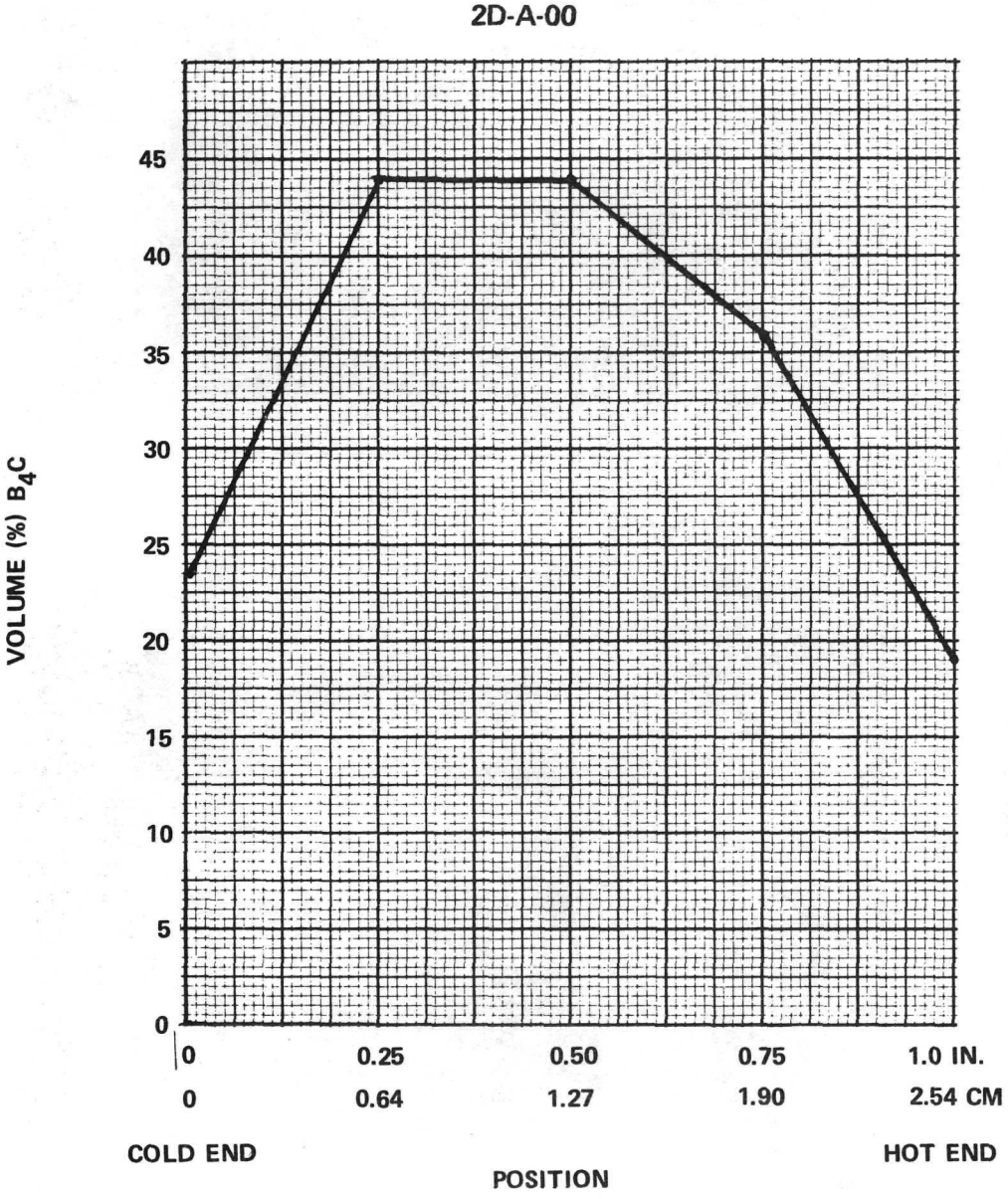

Figure 3-78 DIRECTIONAL DISPLAY

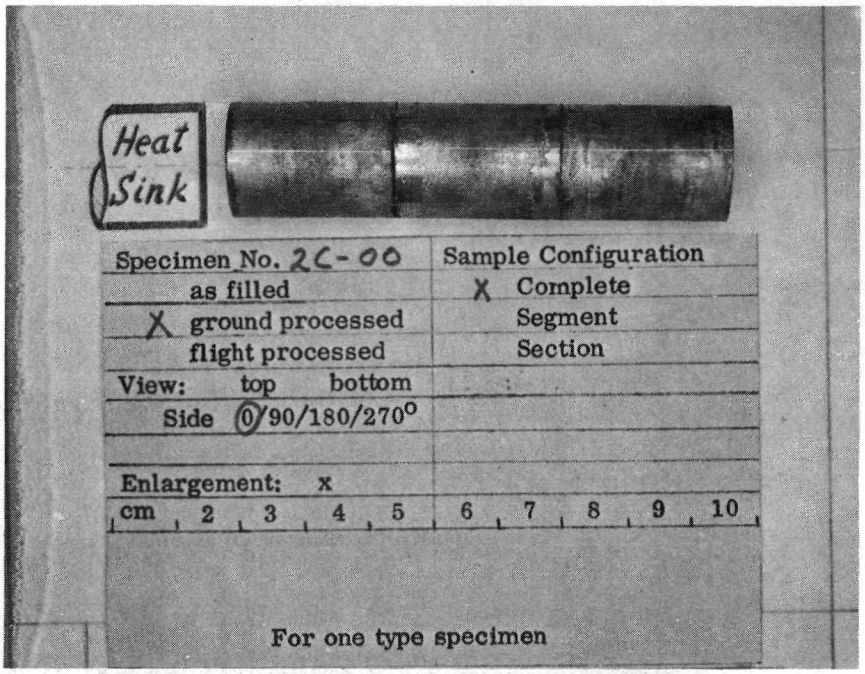

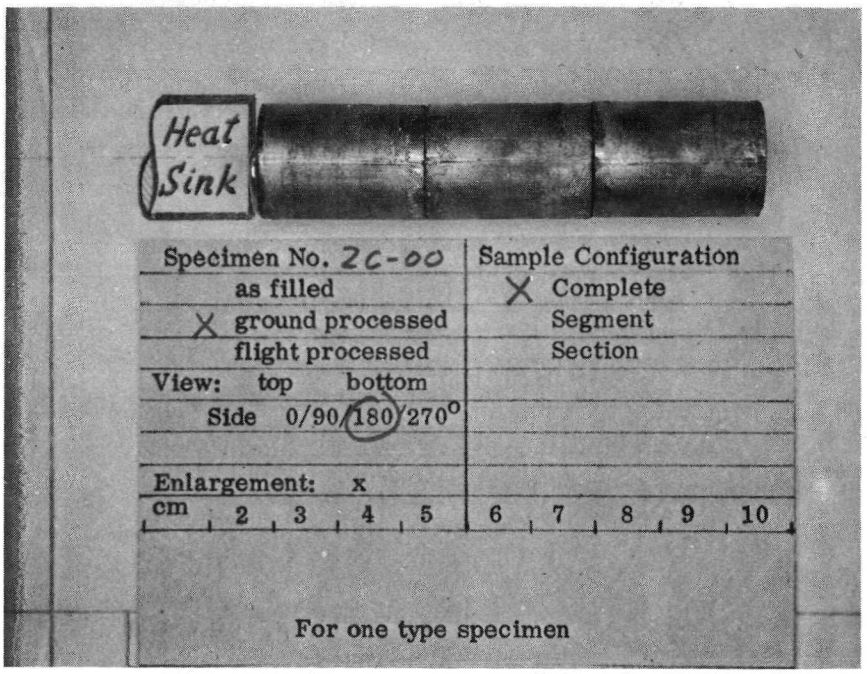

Figure 3-80 CONTROL SAMPLE 2 (2C-00) AFTER REMOVAL FROM CAPSULE

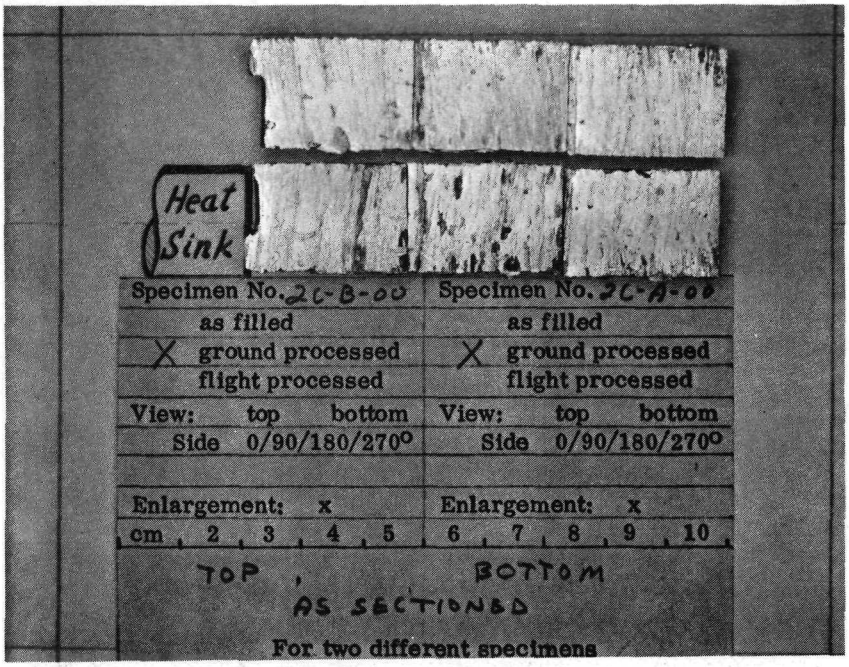

Figure 3-81 CONTROL SAMPLE 2C-00 AFTER SECTIONING

is a photograph of the "as-sectioned" sample, note the metal extrusion discussed above.

3.3.5.3.1 Boron Carbide Distribution Control Sample 2 (2C-A-00)

The control sample 2 was subjected to a particle (B_4C) distribution study utilizing the technique previously discussed. Since this sample was obtained in three individual sections, each section was individually labeled as follows:

Sample 2C-A-00-A - sample segment nearest the heat sink (cold end)

Sample 2C-A-00-B - sample segment second in line

Sample 2C-A-00-C - sample segment furthest from the heat sink (hot end)

Figure 3-82 is a sketch of the three (3) sample segments given above. Also shown on this sketch are the directional display paths and cross directional display paths utilized in the determination of boron carbide dispersion. Figures 3-83 and 3-84 are representative of the directional display path obtained from sample 2C-A-00-A, Figures 3-85 and 3-86 are representative of the directional display path obtained from sample 2C-A-00-B and Figures 3-87 and 3-88 are those from the directional display path of sample 2C-A-00-C. The directional display data obtained is given in the composite plot of Figure 3-99 and will be discussed below.

3.3.5.4 Flight Sample 2 (2F-00)

The flight sample 2 (2F-00) consisted of these individual segments identical to those used in the control samples and the developmental sample. The melting and cooling cycles were identical to that previously discussed as was the procedure for sample removal from its capsule. Figures 3-89 and 3-90

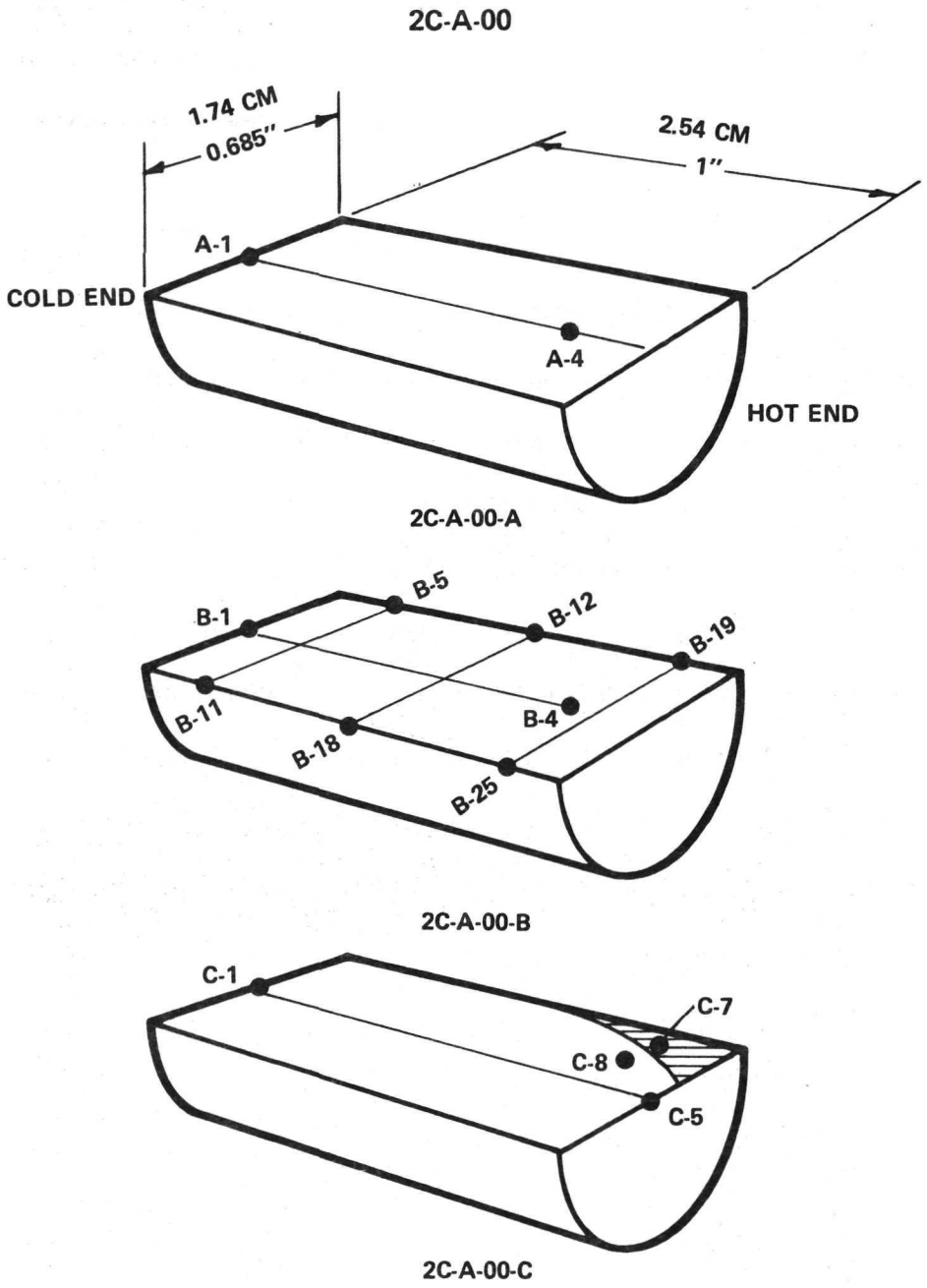

Figure 3-82 SCHEMATIC OF PHOTOGRAPHIC DOCUMENTATION

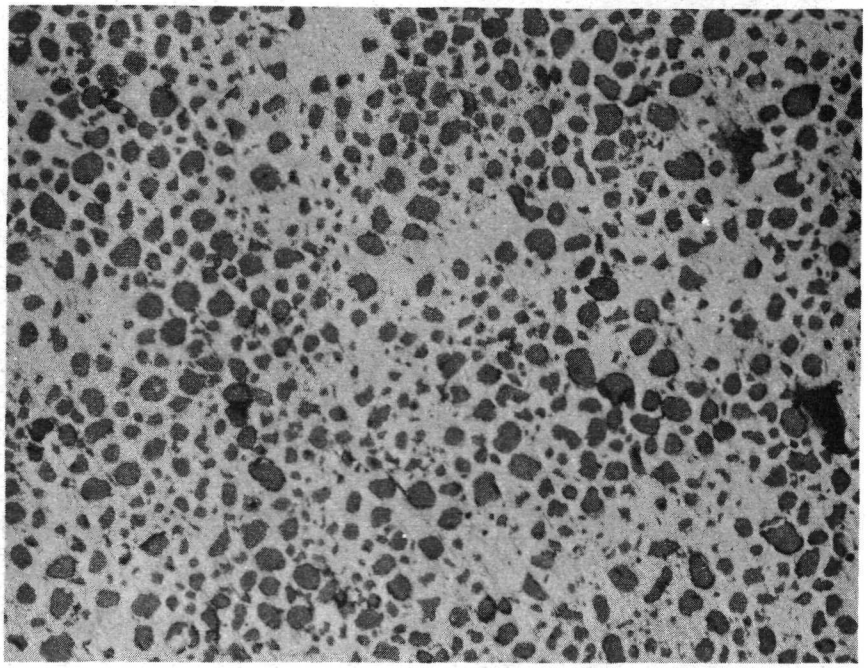

Figure 3-83

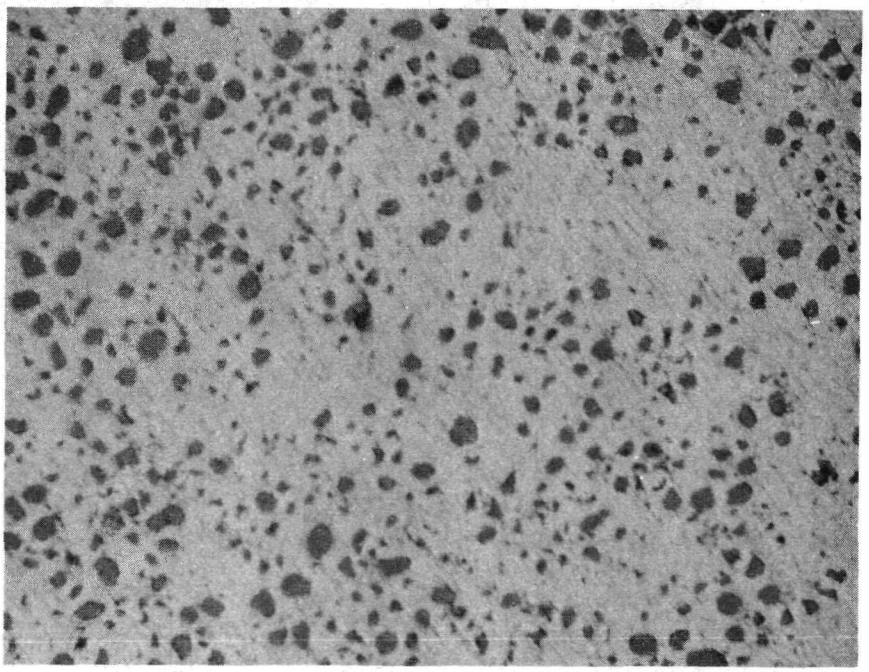

Figure 3-84 CONTROL SAMPLE (2C-A-00-A) DIRECTIONAL DISPLAY AT 100X, PHOTOMICROGRAPHS A-2 AND A-3

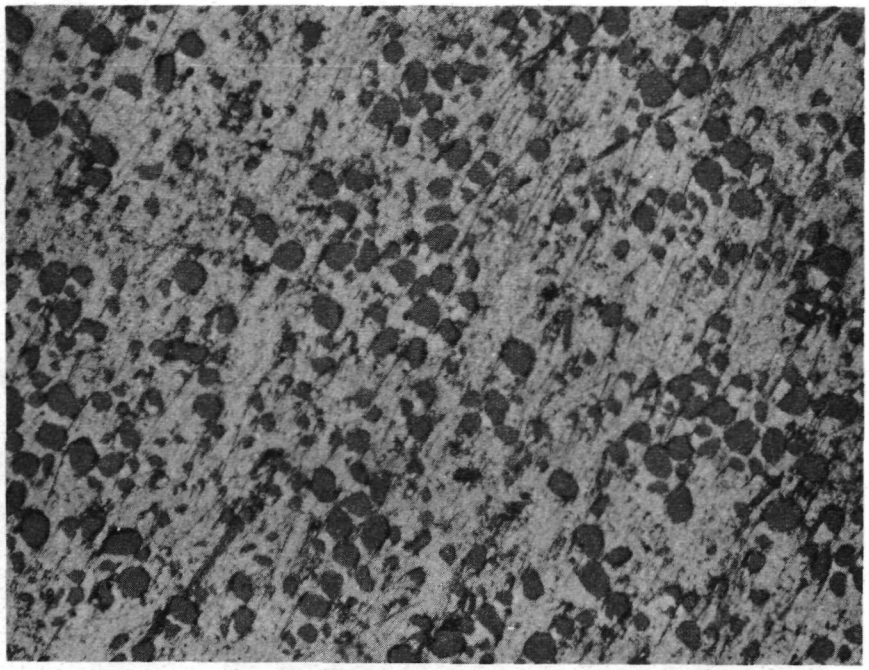

Figure 3-85

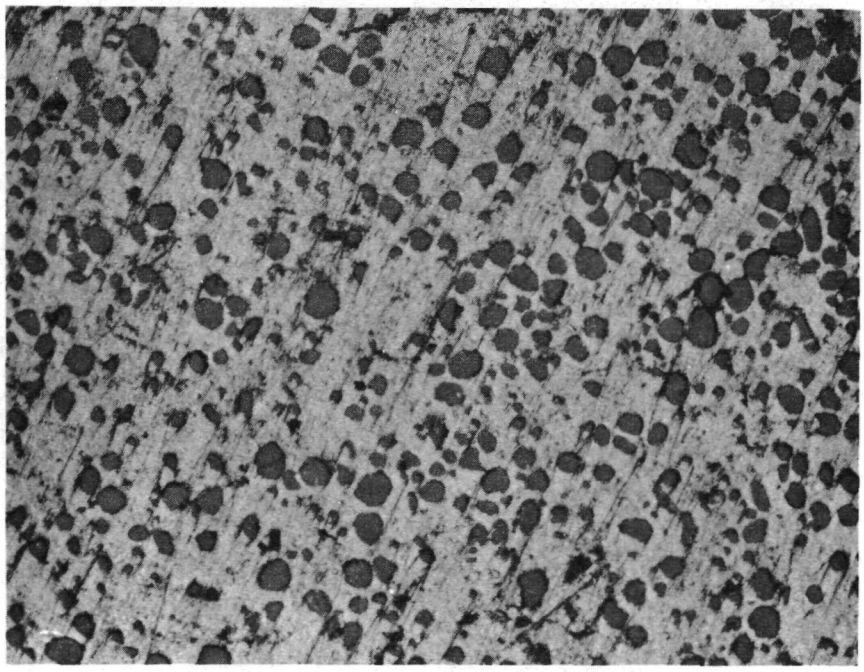

Figure 3-86 CONTROL SAMPLE (2C-A-00-B) DIRECTIONAL DISPLAY AT 100X, PHOTOMICROGRAPHS B-2 AND B-3

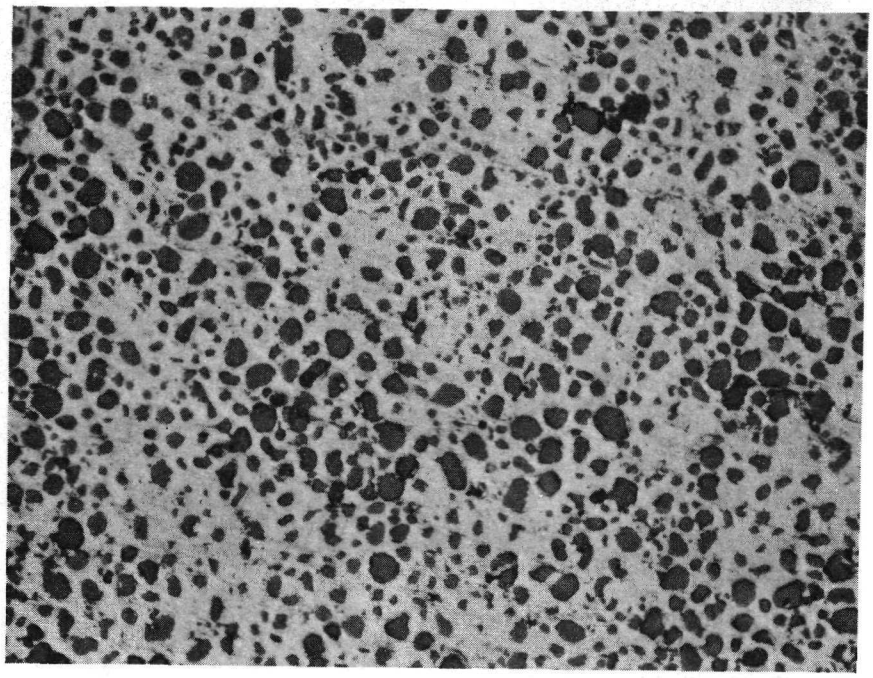

Figure 3-87

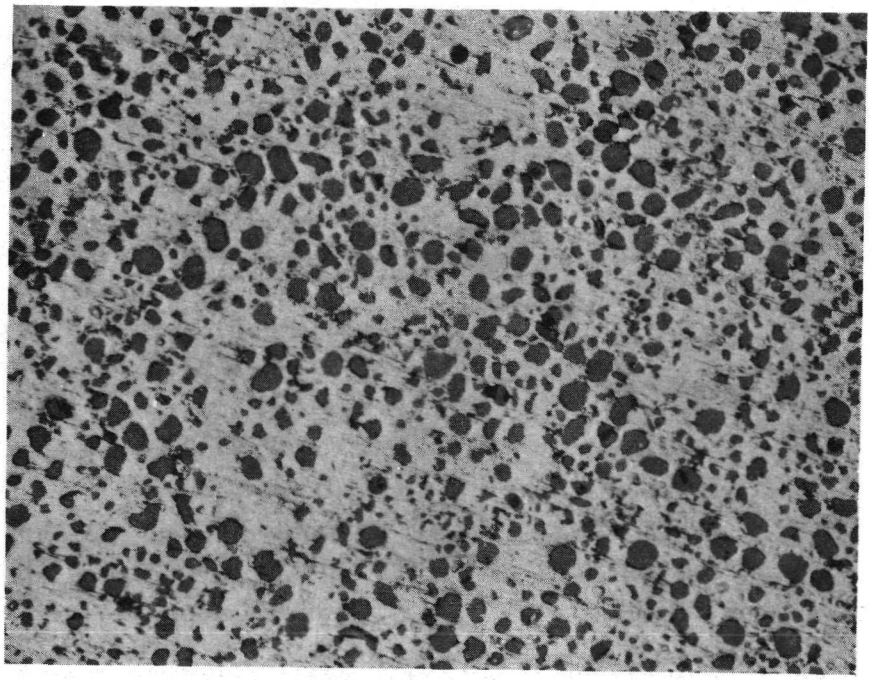

Figure 3-88 CONTROL SAMPLE (2C-A-00-C) DIRECTIONAL DISPLAY AT 100X, PHOTOMICROGRAPHS C-3 AND C-4

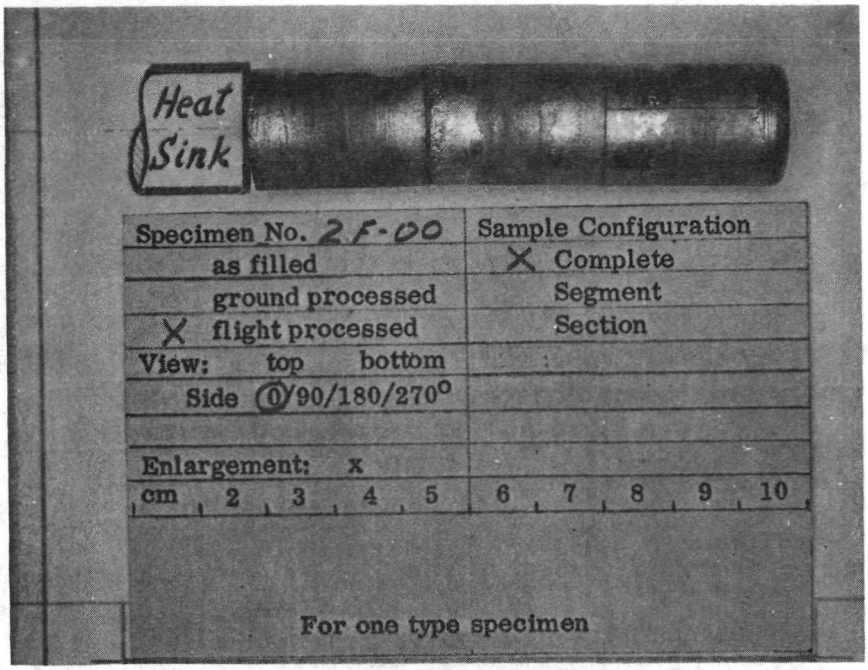

Figure 3-89

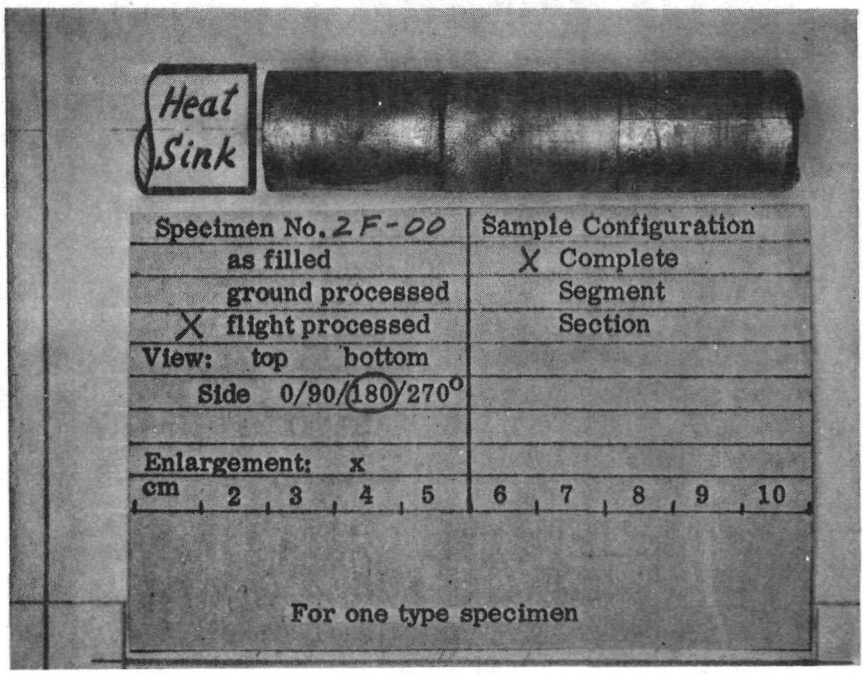

Figure 3-90 FLIGHT SAMPLE 2 (2F-00) AFTER REMOVAL FROM CAPSULE HEAT SINK MARKED IMPROPERLY

show the flight sample after removal from its capsule. In these photographs the heat sink end is improperly marked and should be to the left of the sample. Figure 3-91 shows the flight sample after sectioning and in this case, the heat sink end is properly marked. The "A" half was used for particle dispersion analysis. Note that of the three separate segments two (2) have fused together as a consequence of melting.

3.3.5.4.1 Boron Carbide Distribution Flight Sample 2 (2F-A-00)

Flight sample 2 (2F-A-00) had initially consisted of three (3) identical segments. After processing, the two segments nearest the heat sink (cold end) were found to be fused together (see Figure 3-91). Figure 3-92 is a sketch of the sample as obtained after sectioning. As seen, the cold end of the sample had extruded material over part of the sample end. This sample was labeled for analysis as follows:

Sample 2F-A-00-C - Sample segment nearest the heat sink (cold end)

Sample 2F-A-00-B - Sample segment second in line - Fused to 2F-A-00-C

Sample 2F-A-00-A - Sample segment furthest from the heat sink (hot end)

Also shown on the sketch in Figure 3-92 are the paths utilized in obtaining the directional displays and cross directional displays.

Figures 3-93 and 3-94 are representative photomicrographs at 100X of the Boron Carbide distribution for the directional display of sample 2F-A-00-C. Figures 3-95 and 3-96 are representative of 2F-A-00-B and Figures 3-97 and 3-98 are representative of the directional display for sample 2F-A-00-A.

Figure 3-99 is a plot of volume percent Boron Carbide (B_4C) versus position along the three flight segments compromising sample 2F-A-00. Also

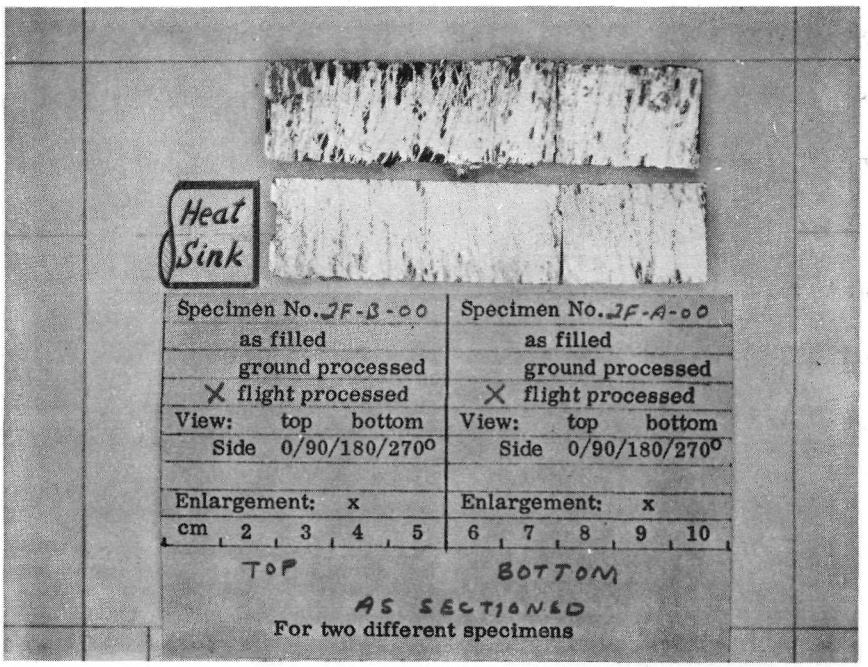

Figure 3-91 FLIGHT SAMPLE 2 (2F-A-00) AFTER SECTIONING

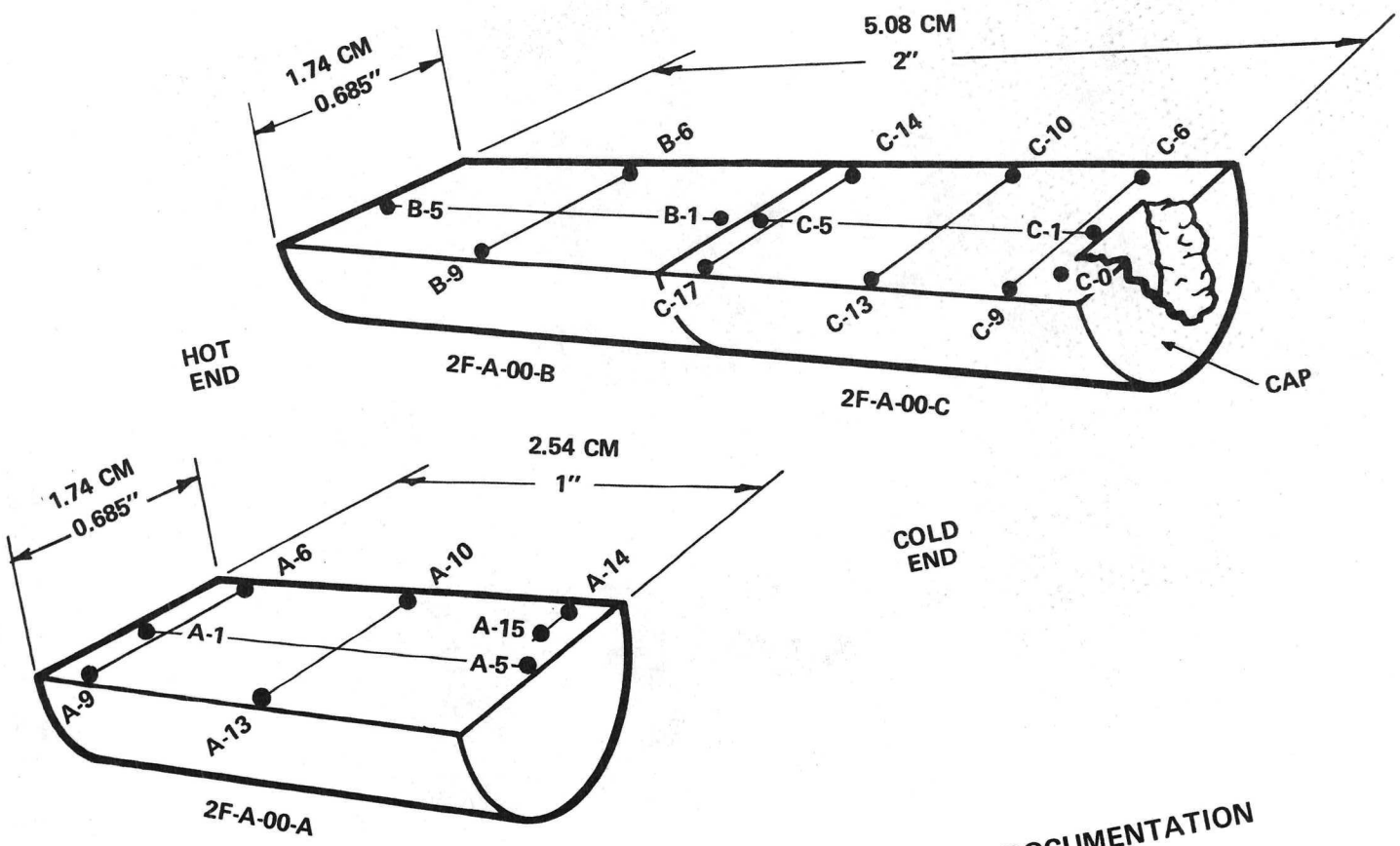

Figure 3-92 SCHEMATIC OF PHOTOGRAPHIC DOCUMENTATION

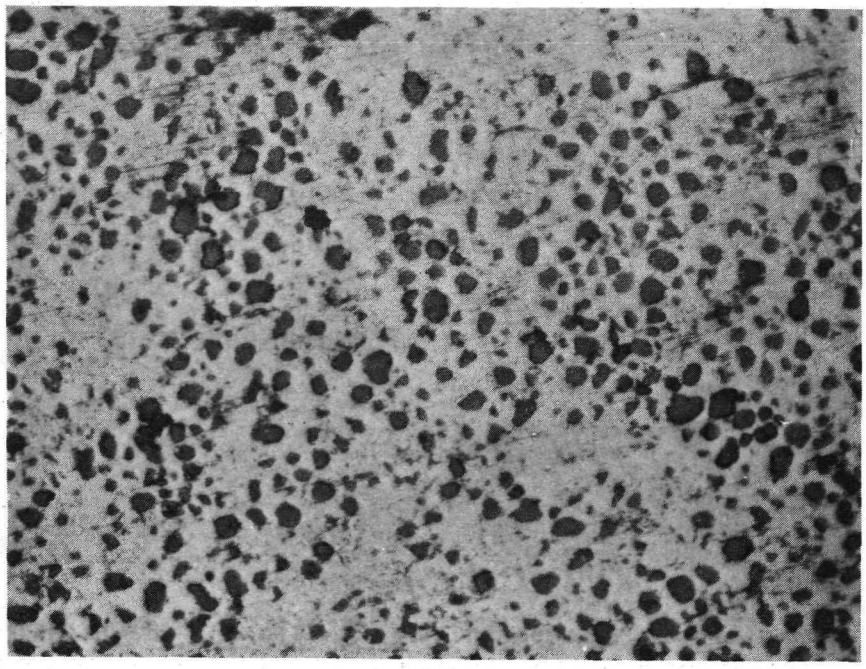

Figure 3-93

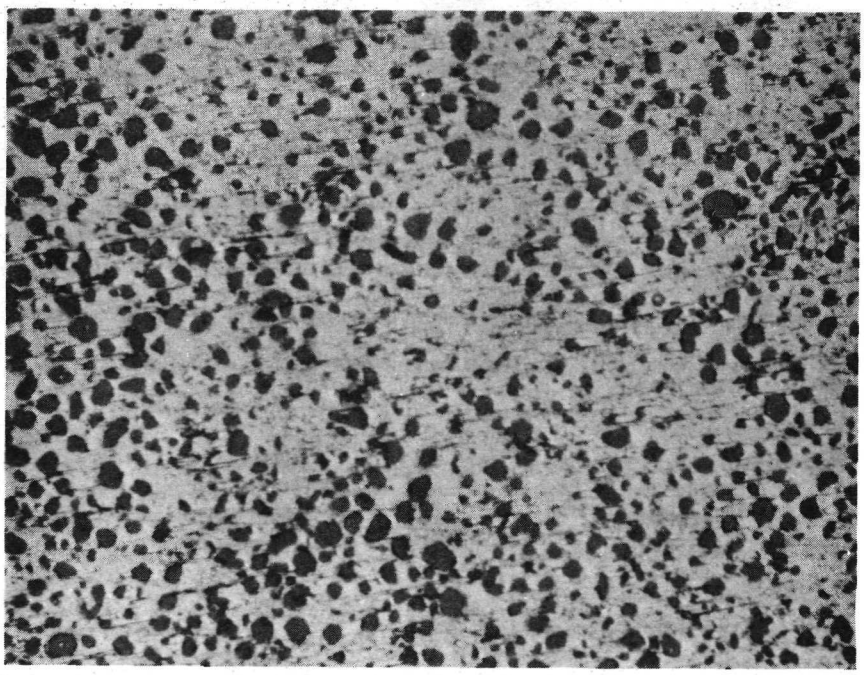

Figure 3-94 FLIGHT SAMPLE 2 (2F-A-00-C) DIRECTIONAL DISPLAY AT 100X

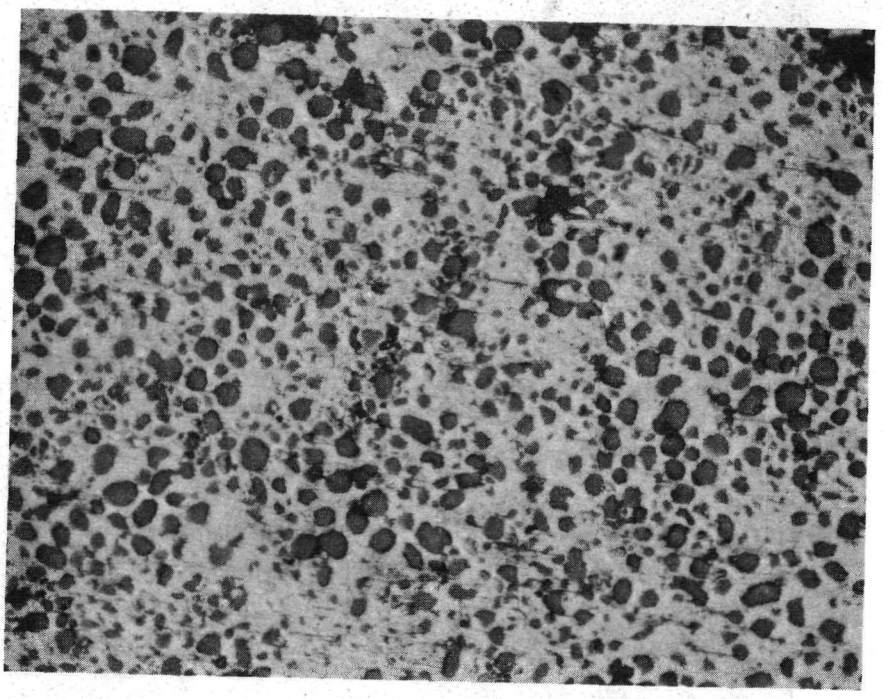

Figure 3-95

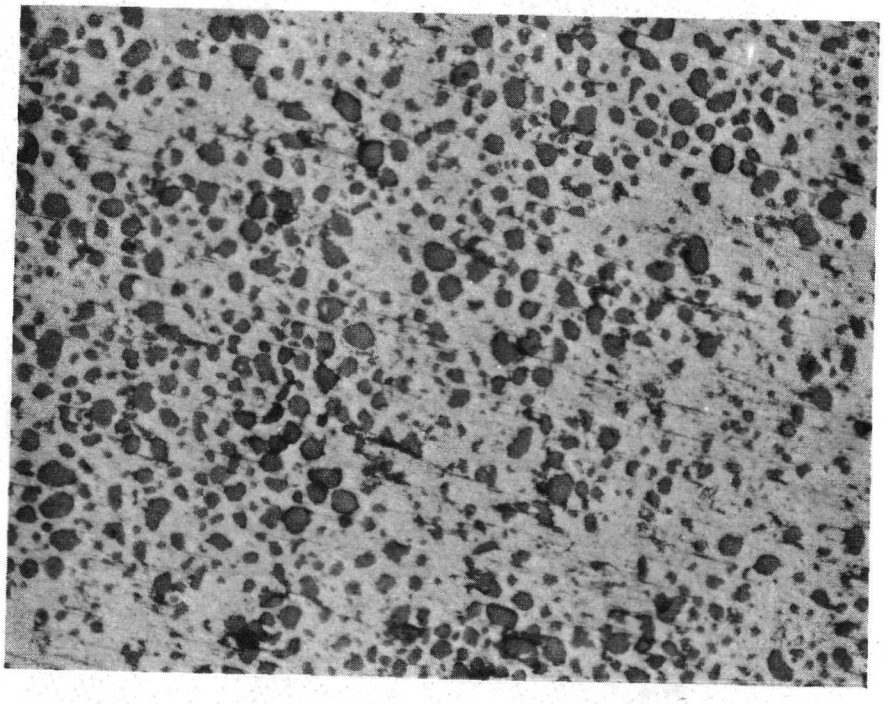

Figure 3-96 FLIGHT SAMPLE 2 (2F-A-00-B) DIRECTIONAL DISPLAY AT 100X

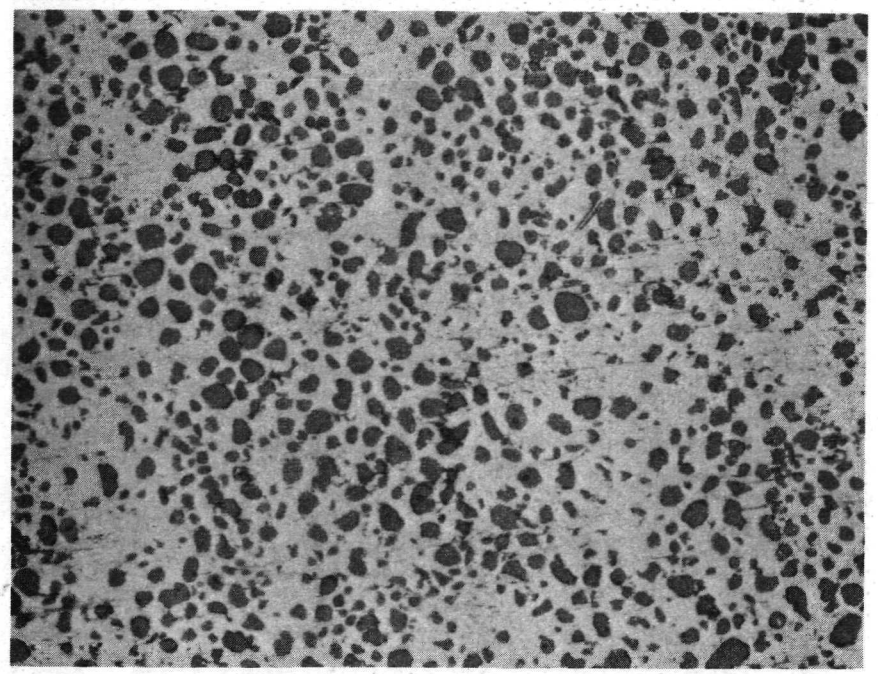

Figure 3-97

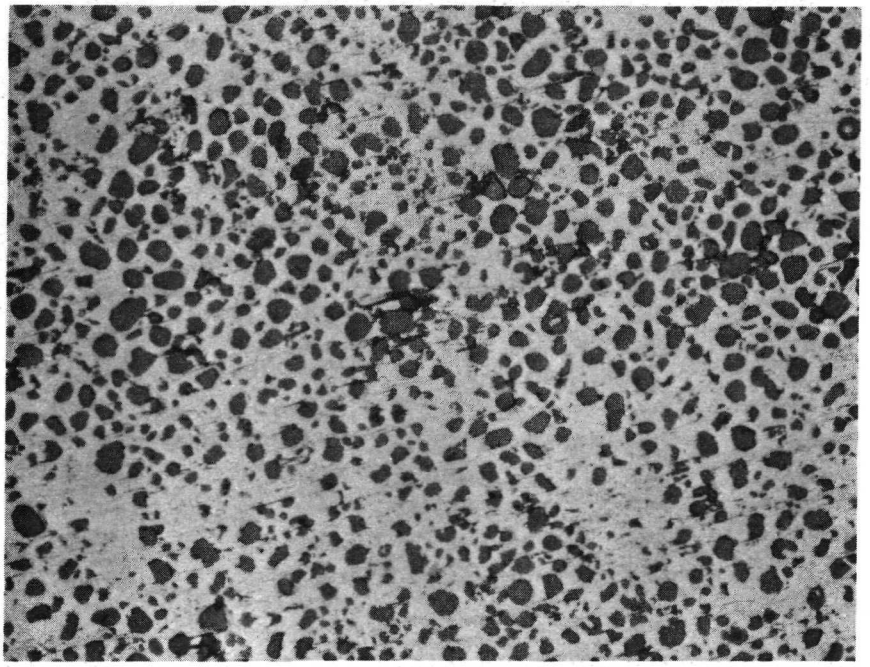

Figure 3-98 FLIGHT SAMPLE 2 (2F-A-00-A) DIRECTIONAL DISPLAY AT 100X

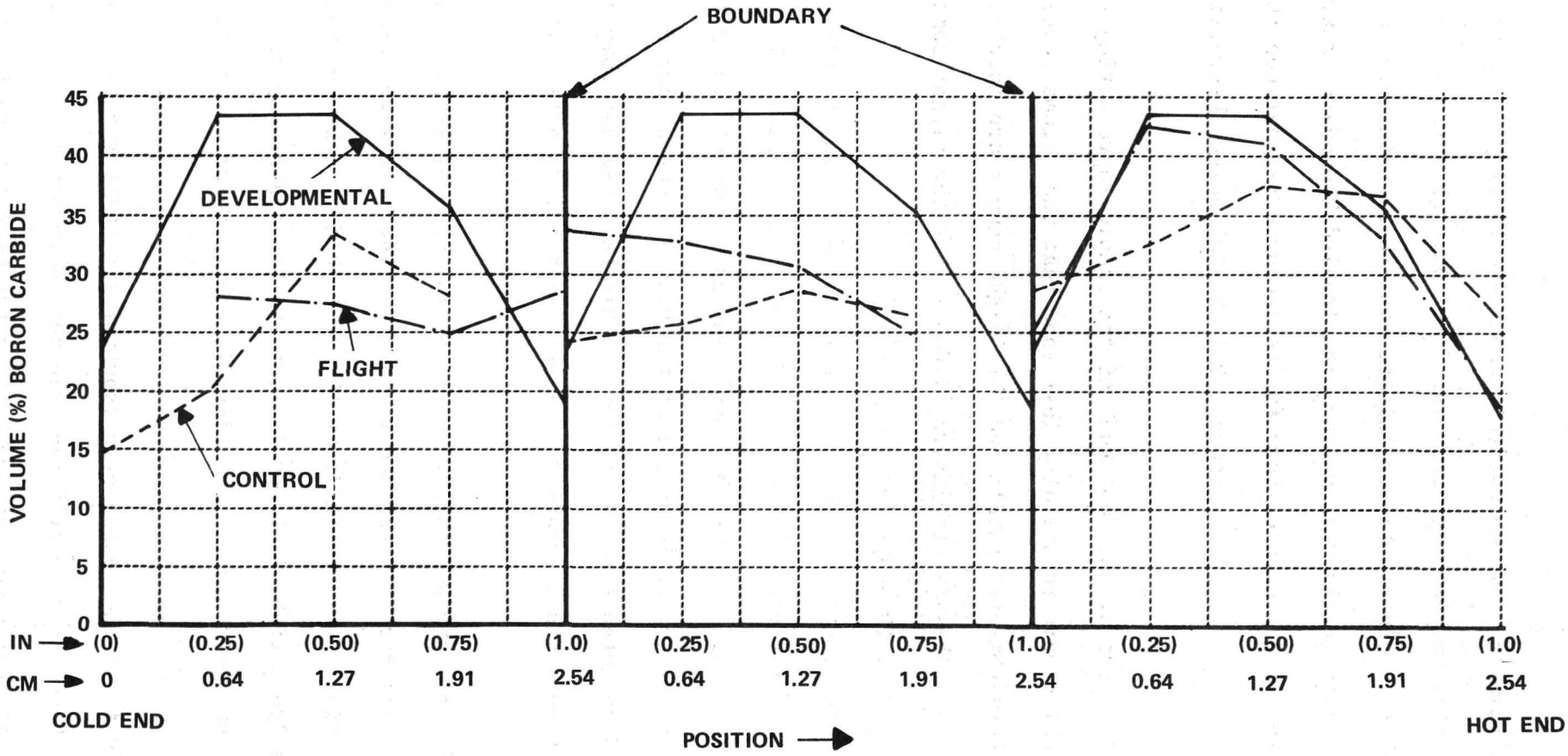

Figure 3-99 SAMPLE 2 – SPECIMEN POSITION IN CAPSULE

included are the results from the control sample and finally the plot obtained for the developmental sample is given. The developmental curve is plotted three times in that it represents the initial distribution in each case.

On the plots in Figure 3-99 the line labeled "Boundary" represents the position on the flight sample where fusion had occurred between the individual segments. From this plot (Figure 3-99) the following observations can be made:

(1) The plots at the "Hot End" of the sample representing those sample segments which were to solidify last show that the volume percent boron carbide for the developmental sample and the flight sample are identical within experimental limits. This is conclusive evidence that the flight sample did not melt at this end of the capsule.

(2) Redistribution of the boron carbide particles in the two flight sample segments near the heat sink end (cold end) of the capsule did occur. However, this redistribution must be considered as incomplete in that the value for B_4C volume percent is not identical at the boundary where some fusion did occur. It should be noted that the fusion in this case was not complete and that these samples segments did separate as a result of handling during mechanical polishing.

(3) The redistribution for the three (3) control samples is in no case identical. This must be regarded as evidence that complete sample melting did not occur. This is substantiated by the fact that for the control sample each segment was found to be individual after the heating procedure. It is obvious that although some surface melting did occur, complete sample melting did not occur.

(4) There is indication of a tendency for redistribution in the flight sample with position towards the cold end (heat sink) of the capsule. This would indicate that a non-uniform heating had been applied to the capsule.

3.3.5.4.2 Conclusions Sample 2

The highly reproducible curves for B_4C distribution in the developmental sample and the flight sample near the hot end of the capsule (Figure 3-99) must be regarded as evidence that melting did not occur here. Although it is apparent from the remaining distribution curves of flight sample 2 that some amount of melting did occur in these two sections it is not felt that a high degree of significance be applied to these results from a quantitative point of view. However, from a qualitative point of view, it can be concluded that in those sample segments which had undergone some degree of melting, the tendency for B_4C redistribution in the flight sample can be considered as positive, in that a trend to a more uniform distribution seems to have been initiated.

3.4 Experiment 10

The flight and control samples for this experiment were designed and produced by MSFC personnel. CAL involvement began after the flight and ground control samples were sectioned longitudinally and was concerned only with the post-flight analysis of sample halves identified as 10F-A-00 and 10C-A-00. For this reason the following report does not include an analysis of a developmental sample nor any detailed description of the sample preparation method.

3.4.1 Capsule Contents

70 percent Indium Bismuth - 30 percent Tungsten particles.

3.4.2 Sample Composition and Preparation

Approximately 105 grams (30 volume percent) of copper-coated spherical tungsten particles (approximately 100 microns in diameter) were placed into a preheated aluminum capsule, a tungsten mixing pellet added, and then approximately 100 grams of molten Indium Bismuth eutectic (70 volume percent) was poured into the capsule. After the alloy had solidified, the capsule was sealed.

3.4.3 Objectives and Expected Observations

The objective of this demonstration was to achieve a uniform dispersion of the dense particles in the metal matrix. Areas of dispersed particles were expected in the flight sample. Gravity-induced segregation was expected in the ground control sample.

3.4.4 Results

The following results include the observations made by CAL personnel during the initial sample removal and subsequent evaluation at CAL.

3.4.4.1 Control Sample 10 (10C-00)

When the capsule was opened, large quantities of the tungsten microspheres fell out of the container. Figure 3-100 shows the capsule in a partially opened condition. The figure shows that the sample material contained a large number and variety of holes from which the microspheres emerged. Figure 3-101 shows the sample after complete removal from the capsule. The tungsten mixing pellet is visible in the center portion of the sample. The sample itself had a dark red or burnt appearance very similar to what would be expected if the copper-coated tungsten spheres had oxidized. Figure 3-102 is the 180° view of Figure 3-101.

Several conclusions can be reached from the general appearance of this sample. Firstly, the copper-coated microspheres were not completely wetted by the molten In-Bi alloy as evidenced by the large quantity of microspheres that fell out of the sample. The quantity of microspheres was not weighed because it was not expected that they would fall out and no provision was made to retain them. Secondly, the microspheres did not predominantly go to the bottom of the specimen and since the tungsten pellet was found in the central region of the sample, it is apparent that the sample solidified during shaking. Thirdly, the

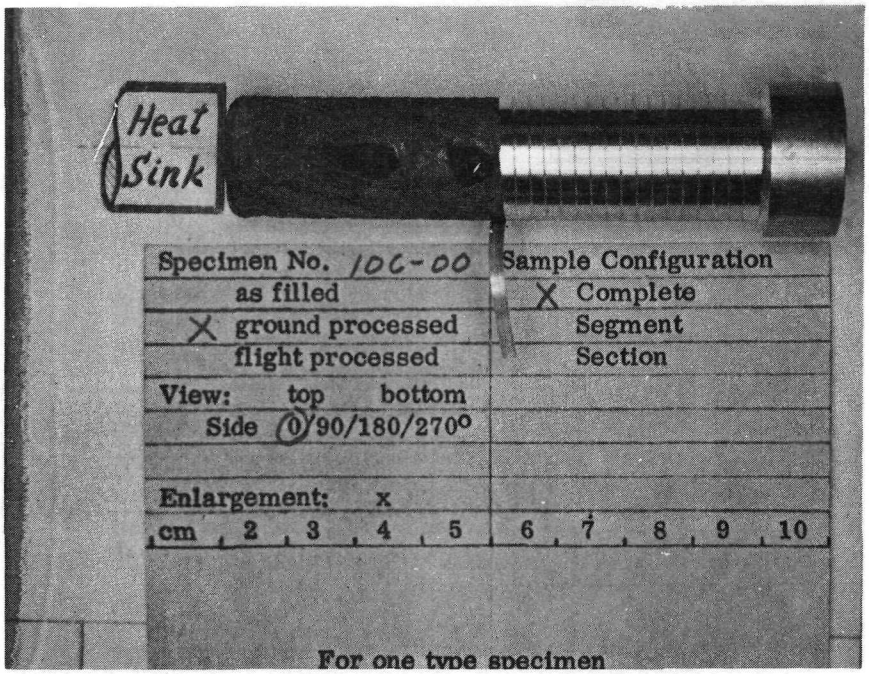

Figure 3-100 CONTROL SAMPLE 10 (10C-00) PARTIALLY REMOVED FROM CAPSULE, O° VIEW

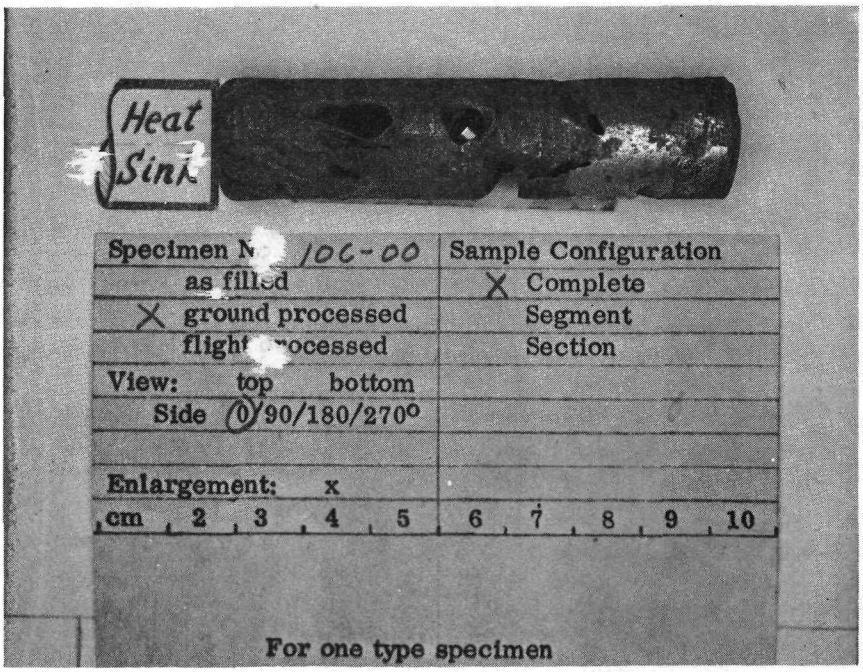

Figure 3-101 CONTROL SAMPLE 10 (10C-00) WITHOUT CAPSULE, O° VIEW

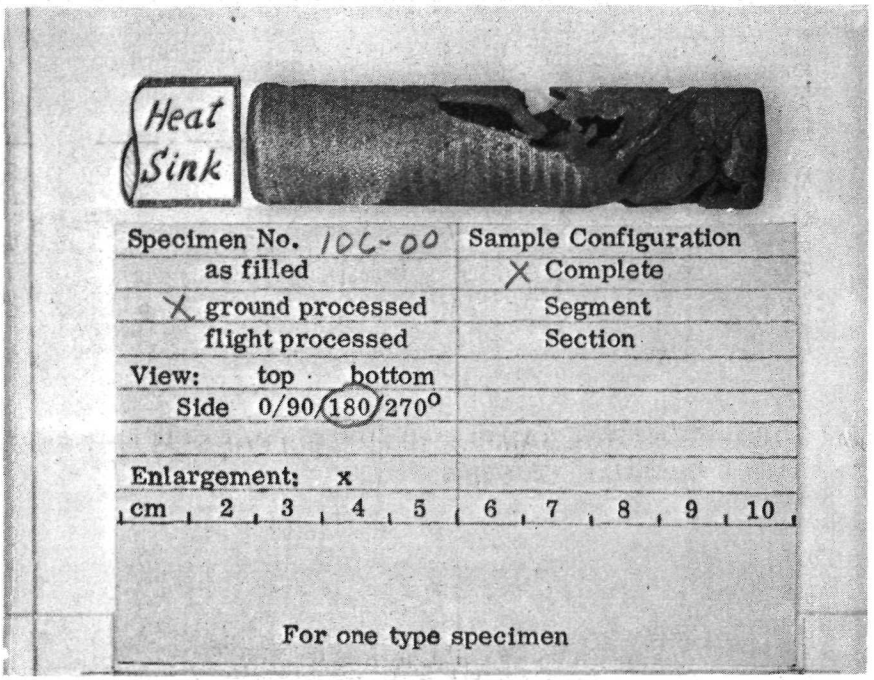

Figure 3-102 CONTROL SAMPLE 10 (10C-00) WITHOUT CAPSULE, 180° VIEW

dark-red color of the sample indicates that the surface must certainly be composed of the copper-coated (and oxidized) microspheres.

3.4.4.1.1 Surface Condition of Control Sample 10 (10C-00)

As was mentioned above the surface of this sample had a dark-red color. On examination with a stereomicroscope it is very clear that the complete surface is covered by microspheres. In addition, all of the hole or void surfaces in the sample are also covered with the microspheres. Figure 3-103 shows this condition on the surface and is also representative of the surface condition of holes or large voids in the sample. This surface condition is very representative of a non-wetting material combination - strongly suggesting that the copper-coated microspheres had oxidized prior to filling the capsule and were therefore not wetted by the molten In-Bi. This would then explain the release of large quantities of microspheres when the capsule was opened because the non-wetting particles were rejected by the molten alloy and did not disperse throughout the specimen.

3.4.4.1.2 Metallographic Description

After removal of the sample from the capsule the sample was sectioned longitudinally. Figure 3-104 represents the longitudinal planes in the as-sectioned condition and shows the large holes or pockets that contained the loose non-wetting spheres. The surfaces of these pockets are covered with microspheres similarly to the outside surface of the sample.

The longitudinal half section 10C-A-00 was subsequently sectioned in a transverse direction into five separate sections. The results of this sectioning procedure are shown in Figure 3-105 with the corresponding section identification scheme. Metallographic examination was limited to Section 005 inasmuch

Figure 3-103 TUNGSTEN MICROSPHERES ON SURFACE OF CONTROL SAMPLE 10 (10C-00) AFTER REMOVAL FROM CAPSULE

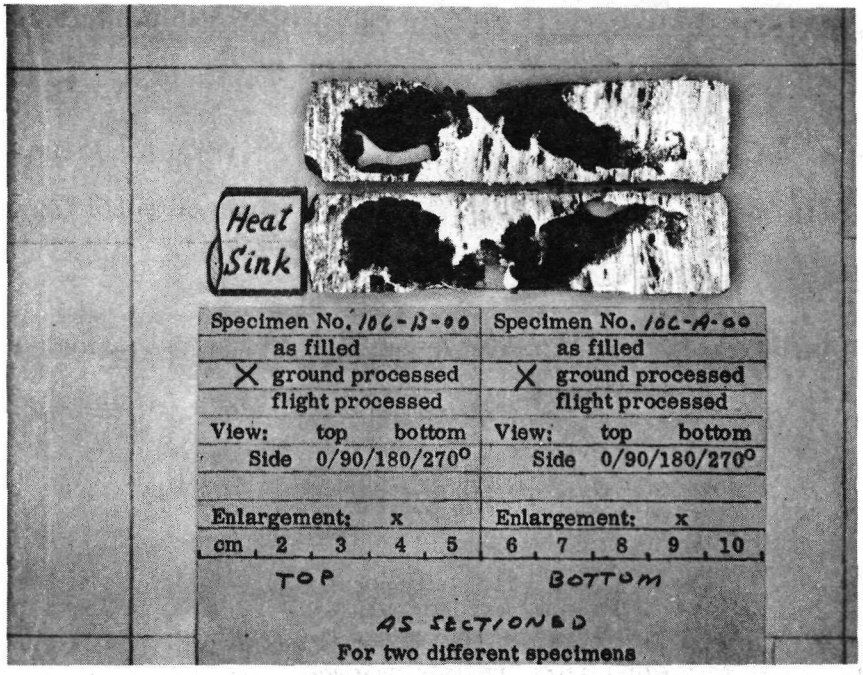

Figure 3-104 BISECTED CONTROL SAMPLE 10 (10C-A-00 AND 10C-B-00)

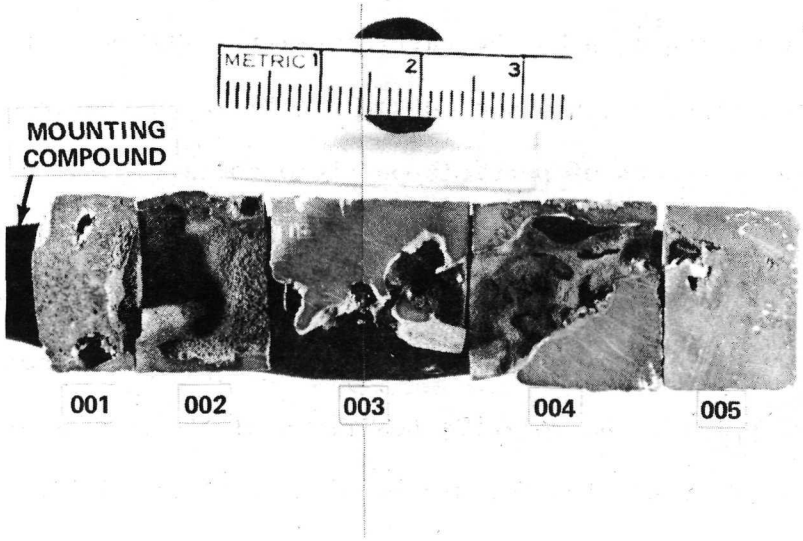

Figure 3-105 SECTIONING PROCEDURE FOR CONTROL SAMPLE 10 (10C-A-00)

as this section was the most intact and demonstrated the important features of the sample. Such features include (1) gross eutectic structure resulting from the absence of large concentrations of particles (Figure 3-106); (2) an area of "high" particle concentration (Figure 3-107); and (3) the cold end edge structure (Figure 3-108).

Figure 3-106 demonstrates a very characteristic feature of the material combination; i.e., that in those areas that are void of the tungsten microspheres the eutectic structure is well formed and massive. This same feature is shown in Figure 3-107 where on the left-hand edge, which is void of particles, the eutectic is well formed whereas in the central regions, where particles are present, the eutectic structure is not formed.

It was stated above that Figure 3-107 represents the highest concentration of particles formed in this section (005). The interesting feature of this concentration of particles is that they are well separated from each other. This is unexpected inasmuch as the particle-matrix system is thought to be non-wetting, and the expectation would be for highly agglomerated or bunched particles reflecting high instances of particle-particle contact. The explanation may reside in the shaking action which was accompanied with rapid cooling. If the shaking action was such as to separate those few microspheres that were incorporated into the matrix, then the condition that the sample solidified during shaking may account for the relative positions of the microspheres to each other. This same particle separation feature is seen in Figure 3-108 which represents the structure at the edge of the sample.

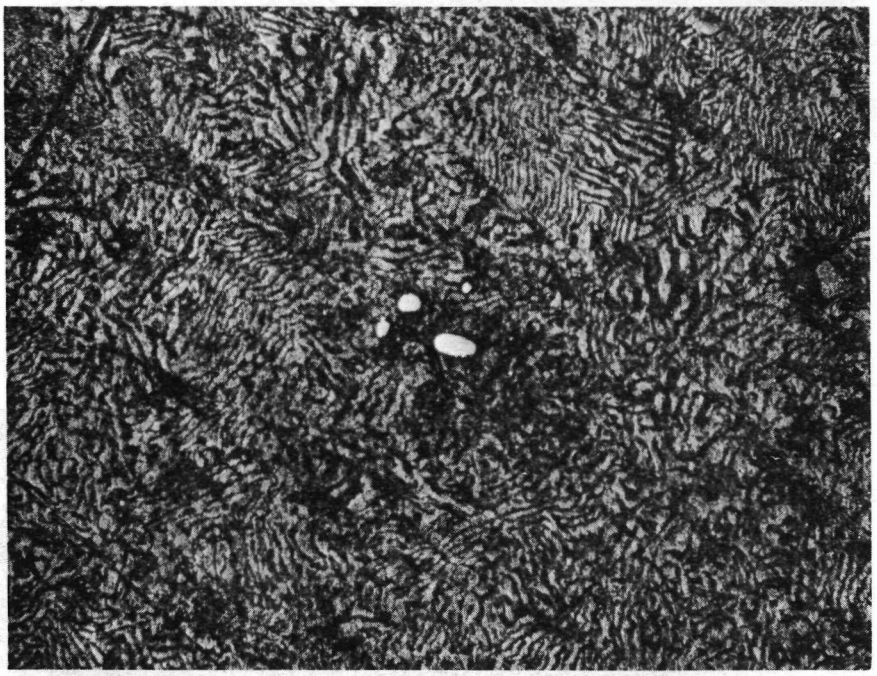

Figure 3-106 MASSIVE EUTECTIC STRUCTURE OBSERVED IN CONTROL SAMPLE 10 SECTION 10C-A-005

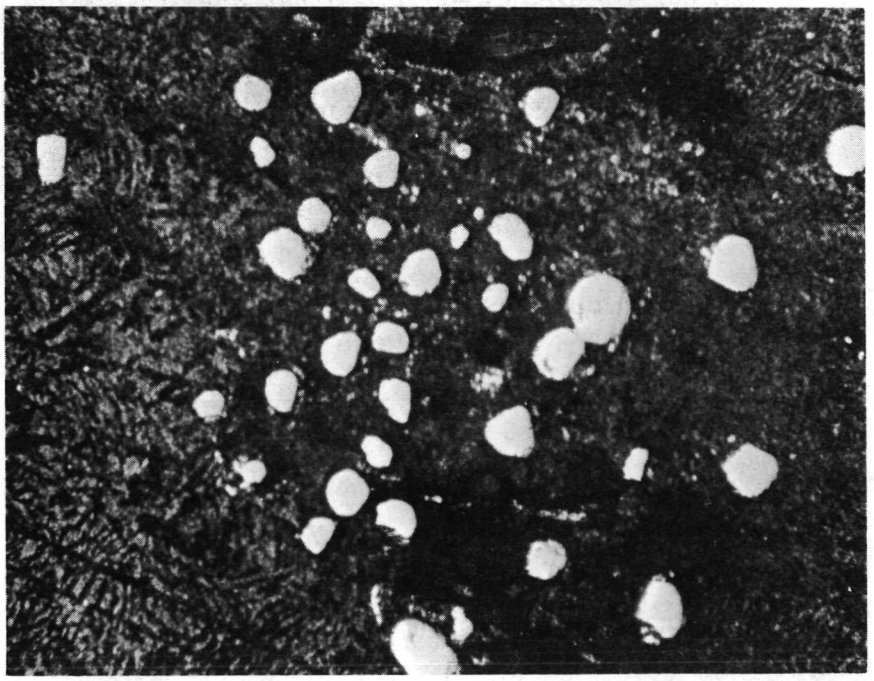

Figure 3-107 HIGHEST CONCENTRATION OF TUNGSTEN MICROSPHERES OBSERVED IN CONTROL SAMPLE 10 SECTION 10C-A-005

Figure 3-108 EDGE FEATURES OF CONTROL SAMPLE 10 SECTION 10C-A-005

3.4.4.2 Flight Sample 10 (10F-00)

This specimen was melted and shaken in space more than once because of RCS firings during the cooling cycle and for this reason the total time involved is not known. Similar to the control sample (10C-00), when the capsule was opened large quantities of the tungsten microspheres fell out and no accounting of these was made. Figure 3-109 is a photograph of the capsule in a partially opened condition and shows that the sample material contained a large area free of matrix alloy from which the microspheres emerged. The complete sample after removal from the capsule is shown in Figures 3-110 and 3-111. These figures show that the sample has an intact surface throughout the half opposite the heat sink or that all the apparent void space was associated with the heat sink end of the sample. The surface color of the sample was similar to that of the control sample, i.e., a dark red indicating that the surface was covered with oxidized copper-coated microspheres.

3.4.4.2.1 Surface Condition of Flight Sample 10 (10F-00)

All surfaces, both external and internal, exhibit a dark red color and are covered by microspheres. Figure 3-112 demonstrates the general appearance of the external surface and clearly shows its complete coverage with microspheres. The appearance of the surface-attached microspheres at the heat sink or cold end of the sample indicates a more severe degree of oxidation than to the surface microspheres in the central or hot end of the sample. No apparent explanation exists for this observation.

The general appearance of the surface-attached microspheres strongly indicate that the system was non-wetting. If the system was wetting, i.e., if the In-Bi liquid (matrix) wet the copper-coated tungsten spheres, there should

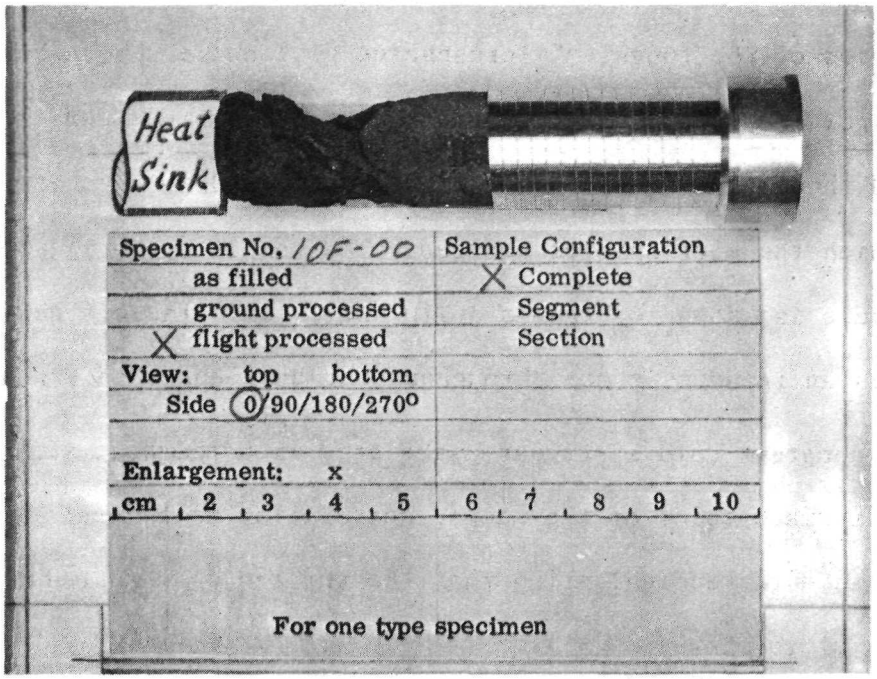

Figure 3-109 FLIGHT SAMPLE 10 (10F-00) PARTIALLY REMOVED FROM CAPSULE, 0° VIEW

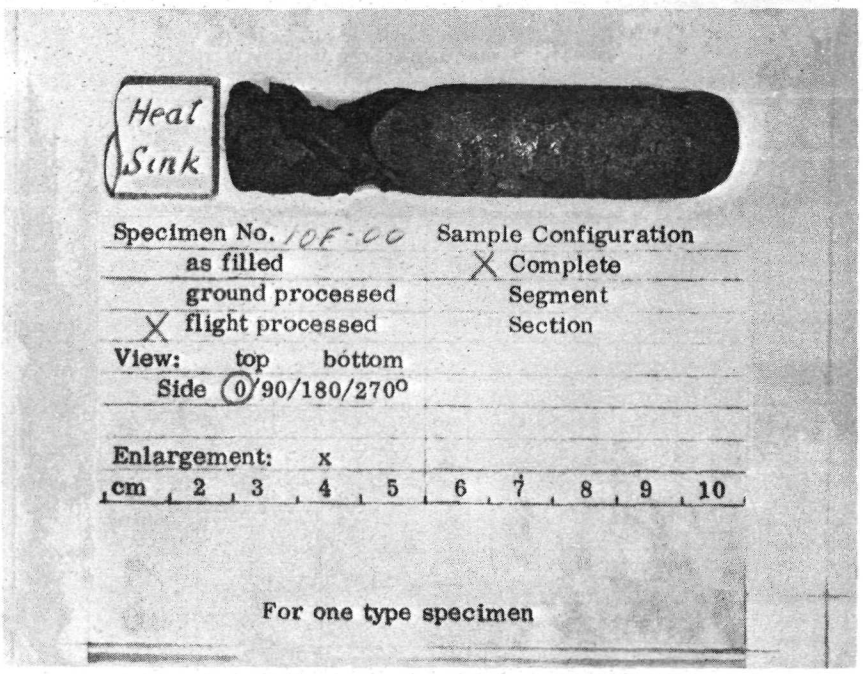

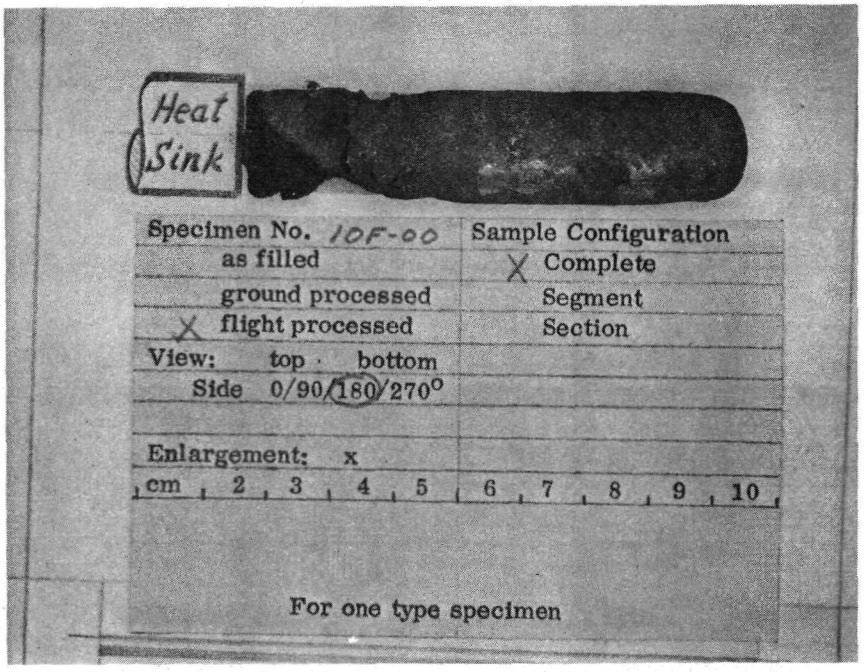

Figure 3-111 FLIGHT SAMPLE 10 (10F-00) WITHOUT CAPSULE, 180° VIEW

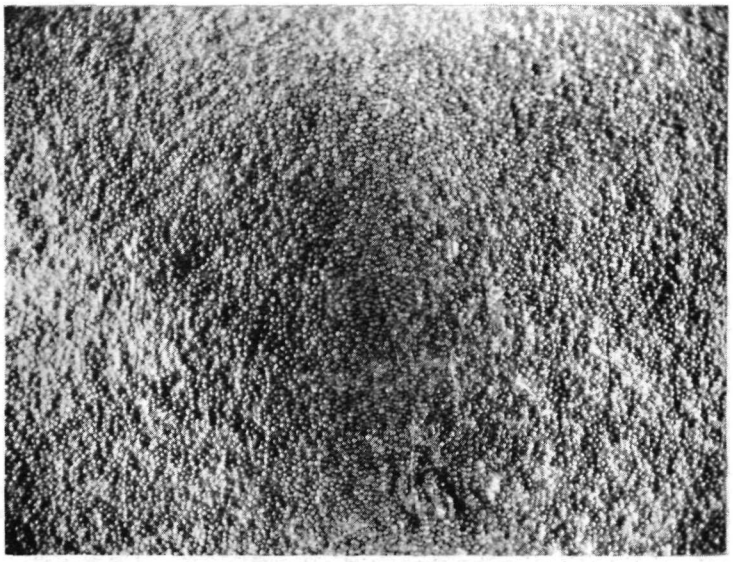

Figure 3-112 TUNGSTEN MICROSPHERES ON SURFACE OF FLIGHT SAMPLE 10 (10F-00) AFTER REMOVAL FROM CAPSULE

have been evidence of the matrix within interparticle spacings. There is no such evidence between the microspheres on this sample surface.

3.4.4.2.2 Metallographic Description

The sample was sectioned longitudinally after removal from the capsule. Figure 3-113 represents the longitudinal planes in the as-sectioned condition and shows the presence of large voids together with the tungsten mixing pellet. As for the control sample, the tungsten mixing pellet is found in the central portions of the sample indicating that the sample may have solidified during shaking. Also, in both instances the mixing pellet was found to be free of any In-Bi alloy demonstrating the non-wetting behavior of this material combination. The hole or pocket associated with the mixing pellet is completely lined with the tungsten microspheres and in addition has a shape tending towards a spherical appearance rather than one which could rigidly describe the cylindrical shape of the pellet. When Figures 3-104 and 3-113 are compared, it is evident that the flight samples external shape and void or pocket shapes show more spheroidicity. The surfaces of all these holes, pockets or voids are covered with microspheres.

The longitudinal half section 10F-A-00 was subsequently sectioned in a transverse direction into five sections as shown in Figure 3-114 with metallographic examination reported from section 002. The most immediate observation is that this flight sample contains significantly more microspheres in the In-Bi matrix material than does the control sample. Figure 3-115 shows the maximum concentration found in section 002. The striking increase between this concentration and that found in the control sample can be demonstrated by comparing Figures 3-107 and 3-115. Figure 3-116 shows the "average" concentration and distribution along the full length of the sample. The distribution of micro-

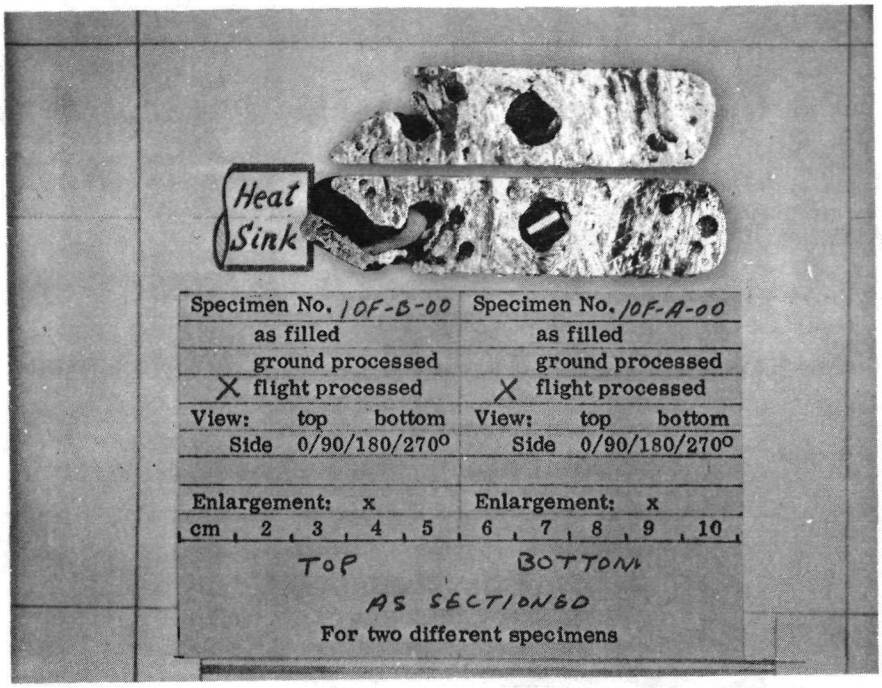

Figure 3-113 BISECTED FLIGHT SAMPLE 10 (10F-A-00 AND 10F-B-00)

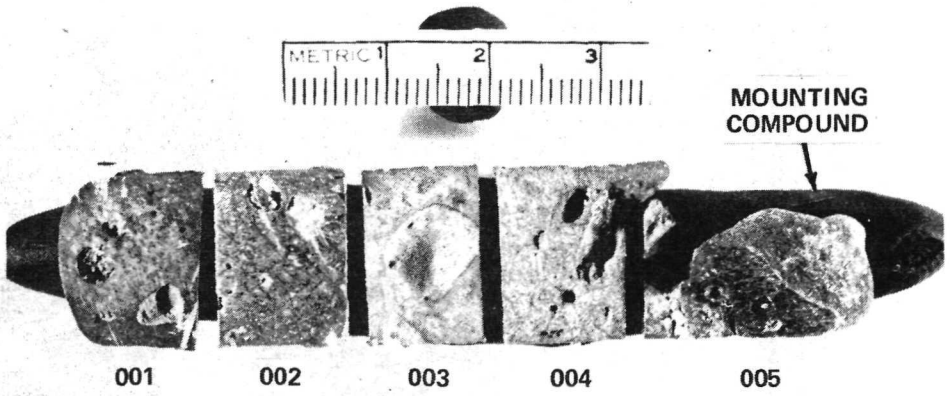

Figure 3-114 SECTIONING PROCEDURE FOR FLIGHT SAMPLE 10 (10F-A-00)

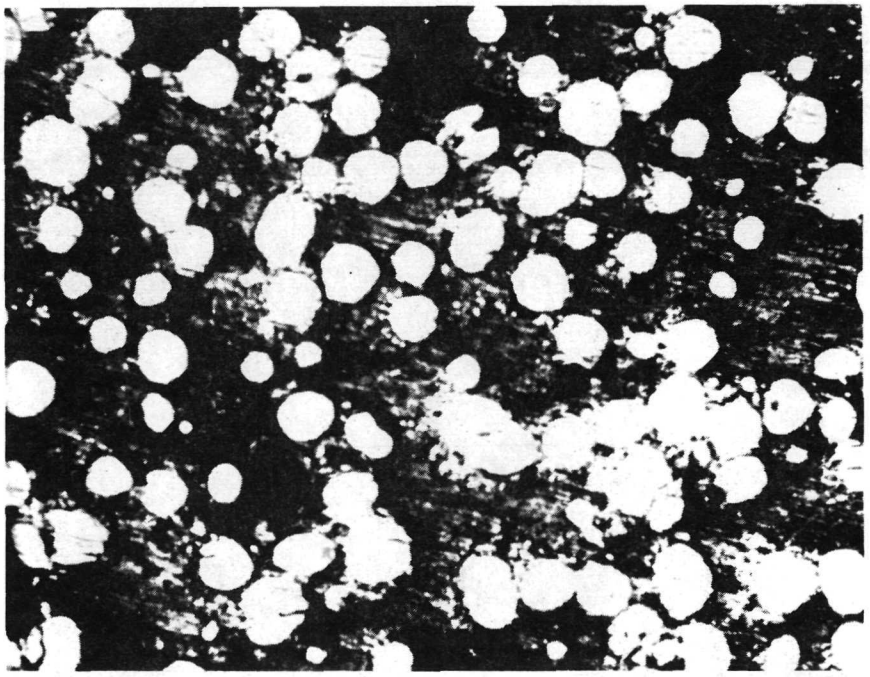

Figure 3-115 HIGHEST CONCENTRATION OF TUNGSTEN MICROSPHERES OBSERVED IN FLIGHT SAMPLE 10 SECTION 10F-A-002

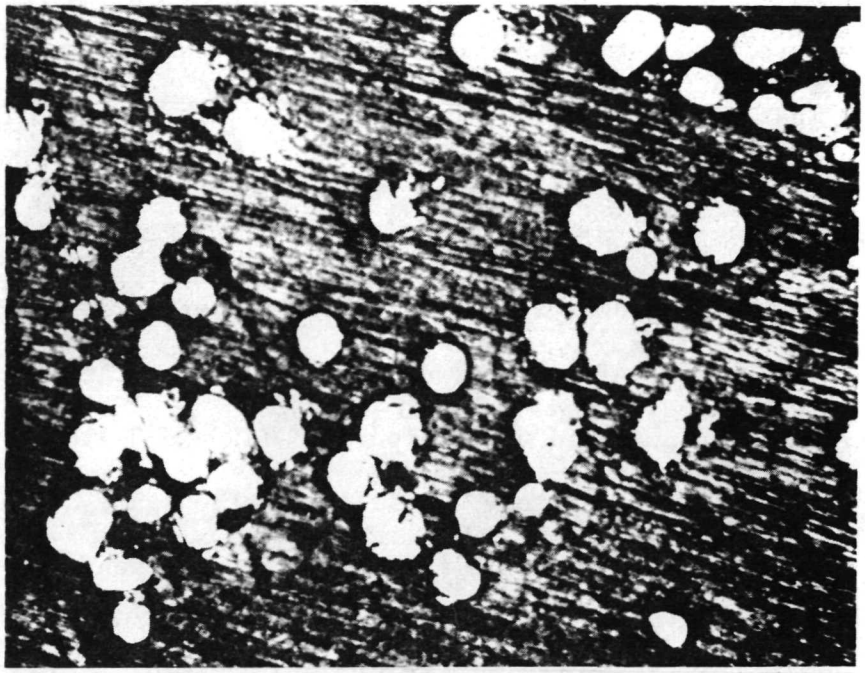

Figure 3-116 AVERAGE CONCENTRATION OF TUNGSTEN MICROSPHERES OBSERVED IN FLIGHT SAMPLE 10 SECTION 10F-A-002

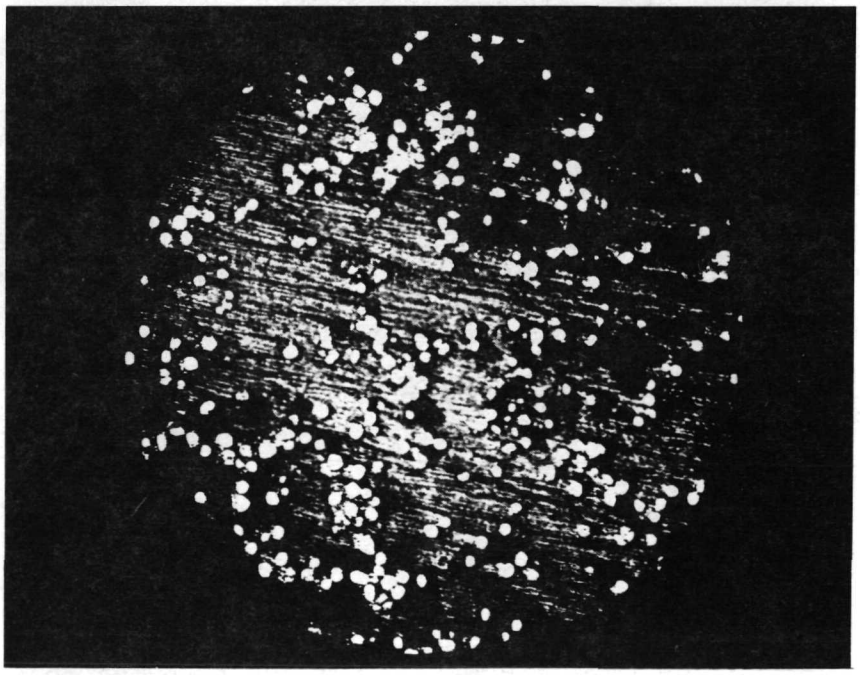

Figure 3-117 AREAS OF HIGH MICROSPHERE CONCENTRATIONS IN FLIGHT SAMPLE 10 SECTION 10F-A-002

spheres was seemingly unaffected by the presence of large or small voids. In addition, no massive dendrintic structure was observed which is consistent with the observation that such a structure is associated with particle free areas.

The microspheres in the flight sample are also observed to be concentrated in what may be referred to as agglomerates, i.e., they are concentrated in such a manner as to provide areas of very high and very low concentrations. This is very characteristic of non-wetting systems. Also, there is a great deal of particle-particle contact evident in Figures 3-115 and 3-116 further confirming the non-wetting nature of the system. These observations are demonstrated more clearly in Figure 3-117 which is a X25 magnification representation of the microsphere distribution.

3.4.5 Conclusions, Experiment 10

Because the copper-coated tungsten microspheres were not wetted by the liquid In-Bi alloy the original objectives of this experiment were not realized, i.e., a uniform dispersion of the dense tungsten particles in the metal matrix of the flight sample was not achieved. However, a comparison of the flight and control samples allows for the following observations.

(1) The liquid matrix of the flight sample accepted or incorporated more of the non-wetted microsphere than did the liquid matrix of the control sample. The precise reason for this occurrence is not clear inasmuch as the details of the flight specimen heating history are not known and thus cannot be compared to those of the control sample. However, the evidence strongly indicates that a potential zero gravity effect exists between non-wetting systems.

(2) The microscopic effect observed in item #1 above is not reflected on a microscopic scale. That is, even though the liquid matrix accepts larger quantities of the non-wetting spheres their behavior on a microscopic scale,

reflected by the occurrence of particle-particle contact, is that common to non-wetting systems.

(3) Adhesion of the microspheres to the metal matrix is apparent at all exposed surfaces. The precise details of the adhesion process cannot be determined from the experiment; however, optical observations indicate that the phenomena is common to both the flight and control specimens.

(4) Greater spheroidicity is associated with the flight sample both with regard to the external and internal surfaces. This is expected of liquid systems solidified in space.

ATTACHMENT I

The following series of four (4) memorandum is presented as a study by Mr. H. T. McAdams of CAL and forms the basis for the eventual use of "Point-Count-Analysis" in determining the distribution of and volume of fraction of dispersed particles in the Apollo 14 samples.

CORNELL AERONAUTICAL LABORATORY, INC.
Buffalo, New York, 14221

April 12, 1971
HTMcA:jjy
N56-001

To: R.C. and T.J. Fabiniak
From: H.T. McAdams
Subject: Apollo 14 Sample Analysis
cc: H. Leland/A.O'Connor, R. Klingaman, P. Schnizler

As a preliminary to formulating an approach to the analysis of sample dispersions, it is informative to consider the various ways that spheres can pack and to have a look at the relation between void fraction and mean distance between centers.

Case I. "Most Open" Packing

A cubic lattice arrangement of spheres places the center of a sphere at each corner of a cube. If the spheres have radius r, then the cube edge has length $2r = d$ and the cube has volume $8r^3 = d^3$. The cube contains one octant of a sphere with center at each of its vertices and hence contains a total of one sphere, with volume $4/3\ \pi r^3 = 1/6\ \pi d^3$. The ratio of the solid (sphere) volume to the volume of the cube is

$$\frac{\text{Sphere volume}}{\text{Unit cell volume}} = \frac{1/6\ \pi d^3}{d^3} = \pi/6 = 0.5236$$

The void fraction is therefore

$$1 - 0.5236 = 0.4764$$

Therefore, the most open arrangement which will still have all spheres in contact has 47.64% void space.

Let us now "expand" the lattice so that the distance between sphere centers is $d + \delta$ but the centers of spheres still form a cubic lattice array. Now the volume of the cubic unit cell is $(d + \delta)^3$, but the sphere volume remains the same.

Then:

$$\frac{\text{Sphere volume}}{\text{Unit cell volume}} = \frac{1/6\,\pi d^3}{(d+\delta)^3} = 1 - v$$

where v is defined as the void fraction.

On the left-hand side we divide both numerator and denominator by d^3 to obtain:

$$\frac{1/6\,\pi}{(1+\delta/d)^3} = 1 - v$$

Then

$$(1+\delta/d)^3 = \frac{1/6\,\pi}{1-v} = \frac{0.5236}{1-v}$$

$$1+\delta/d = \sqrt[3]{\frac{0.5236}{1-v}} = \frac{0.806}{\sqrt[3]{1-v}}$$

As an example, if v = 0.70, so that 1 - v = 0.30, we have

$$1+\delta/d = \frac{0.806}{\sqrt[3]{0.30}} = \frac{0.806}{0.669} \approx 1.20.$$

Thus in a mix which is 30% spheres by volume, the spheres would be 1.2 diameters from center to center.

Case II. "Most Dense" Packing

A rhombohedral arrangement of spheres constitutes the most dense arrangement. In this arrangement, the spheres contact each other in such a way that in a typical plane the spheres are centered at the vertices of an equilateral triangle. The volume of the unit cell is

$$V = d^3\sqrt{1 - 3\cos^2\alpha + 2\cos^3\alpha}$$

where $\alpha = 60^\circ$.* Then

$$V = d^3\sqrt{1 - 3(1/2)^2 + 2(1/2)^3} = d^3\sqrt{1/2}$$

$$= 0.707\,d^3$$

* See Appendix III, Crystal Geometry in C.S. Barrett, Structure of Metals, McGraw-Hill, N.Y. 1952, or other texts on crystallography.

Since the unit cell again contains one complete sphere,

$$\frac{\text{Sphere volume}}{\text{Unit cell volume}} = \frac{1/6\,\pi d^3}{0.707\,d^3} = \frac{0.5236}{0.707}$$

$$= 0.7406$$

$$= 1 - v$$

and the void fraction is 0.2594.

Again, let us expand the lattice so that the distance between sphere centers is $d + \delta$. Then the volume of the unit cell is

$$V = 0.707\ (d+\delta)^3$$

and

$$\frac{1/6\,\pi\, d^3}{0.707\,(d+\delta)^3} = 1 - v$$

or

$$\frac{\pi/6}{0.707(1+\delta/d)^3} = 1 - v$$

Upon rearrangement,

$$(1+\delta/d)^3 = \frac{\pi/6}{0.707(1-v)} = \frac{0.7406}{1-v}$$

or

$$1+\delta/d = \sqrt[3]{\frac{0.7406}{1-v}} = \frac{0.905}{\sqrt[3]{1-v}}$$

As in the previous example, if v = 0.70, 1 - v = 0.30 and

$$1 + \delta/d = \frac{0.905}{\sqrt[3]{0.30}} = \frac{0.905}{0.669} = 1.35$$

Thus in a mix which is 30% spheres by volume, the spheres would be 1.35 diameters from center to center if (1) the spheres are "uniformly" dispersed throughout the mix and (2) assume an orientation with respect to each other so that the distance of closest approach is realized.

Implications

Consider a sample with 30% spheres and 70% matrix, by volume. Since the rhombohedral arrangement represents the configuration of greatest symmetry, the distance from a sphere to its nearest neighbor would be 1.35 d, measured center to center, and this distance would be uniform for all spheres (variance of the nearest-neighbor distances would be zero.) If any segregation occurs, part of the specimen volume must register a decrease in δ (and a corresponding increase in 1-v), while the remainder of the specimen volume must register an increase in δ (and a corresponding decrease in 1-v). Complete segregation would consist of a "sediment" and a "supernatant", as shown in Figure 1.

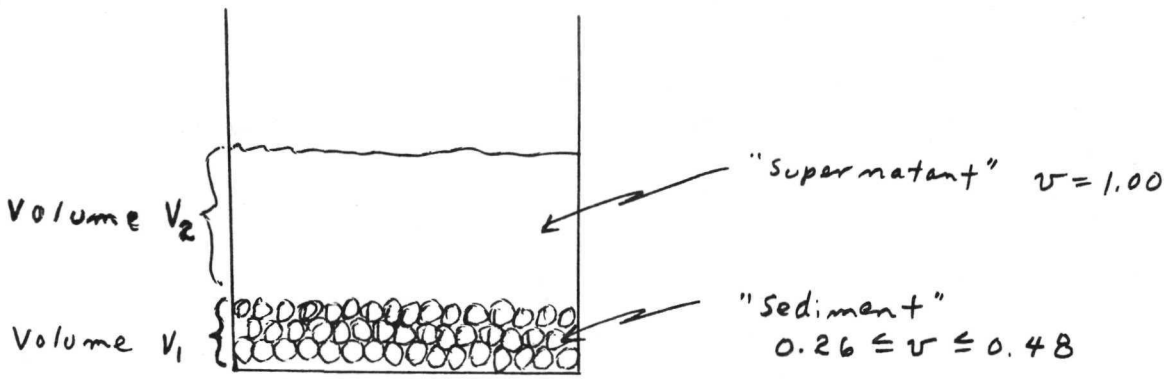

FIGURE 1
IDEALLY SEGREGATED SPECIMEN

For a nominal mix in which v = 0.70, we can compute the relative volumes V_1 and V_2 for the sediment and supernatant. If we assume maximum density for the sediment,

$$0.26\ V_1 + V_2 = 0.70$$

subject to the constraint

$$V_1 + V_2 = 1$$

(assuming unit volume total). Then

$$0.26\ V_1 + 1 - V_1 = 0.70$$

$$0.74\ V_1 = 0.30$$

$$V_1 = 0.405$$

$$V_2 = 0.595$$

In short, approximately 60% of the total volume could be devoid of spheres, if the remaining 40% contains all the spheres at maximum compaction. If we assume minimum density ("most open" packing),

$$0.48\ V_1 + 1 - V_1 = 0.70$$

$$0.52\ V_1 = 0.30$$

$$V_1 = 0.58$$

$$V_2 = 0.42$$

In short, <u>at least</u> 42% of the total volume could be devoid of spheres, if the remaining 58% contains all the spheres in most open packing.

What are the implications for variation in density?

Consider the compact in which 30% of the volume consists of tungsten spheres with density 19.3 and 70% of the volume consists of eutectic with density 8.2. If one assumes ideal geometry (so that no volume is contributed by other than the two phases), then the overall (ideal) density would be

$$(0.30)\ (19.3) + (0.70)\ (8.2) =$$

$$5.79 + 5.74 = 11.53$$

But it has been shown above that if complete segregation of the spheres occurred, part of the specimen might be pure eutectic. Therefore, part of the specimen (in fact as much as 60% of the volume) could be devoid of spheres and hence have a density as low as 8.2. The remaining 40% of the volume could be closely packed spheres with the interstices filled with eutectic. In this case, 74% of the "sediment" would consist of spheres of density 19.3 and 26% would consist of eutectic with density 8.2 (assuming "most dense" packing). The combined density would then be

$$(0.74)\ (19.3) + (0.26)\ (8.2) =$$
$$14.28 + 2.13 = 16.41$$

Thus part of the specimen (in fact as much as 40% of the volume) could have a density as high as 16.4 (exactly twice the density of the eutectic). Thus the specimen could vary in density over a range of two to one. Of course, if we consider the ultimate variation as the sample size decreases and approaches the size of the spheres, the variation could be locally as great as 19.3/8.2 =2.35 to one. This degree of variation represents the ultimate "granularity" of a density determination.

A Tentative Approach

A statistical approach to evaluating the distribution of spheres in the matrix is required. The above analysis has attempted to bound the statistical possibilities by postulating two extremes. In the first, the spheres are uniformly distributed, and, for any subsample having a volume greater than the unit cell, the nominal value of $v = 0.70$ would be realized and the variance in these samples would be zero. In the second case (assuming rhombohedral packing in the sediment), part of the subsamples could register $v = 0.26$ and the remainder $v = 1.00$. Then,

$$\sigma^2 = 0.4\ (0.70 - 0.26)^2 + 0.6\ (0.70 - 1.00)^2$$
$$= 0.13$$

or

$$\sigma = 0.36$$

Thus the standard deviation of void fraction could be as great as 0.36, if computed over the entire specimen. It is required to assess the spatial distribution of spheres and to place this distribution in its proper place between the allowable extremes.

It would be desirable to undertake a statistical model which would predict the variation to be expected if the particles are distributed randomly throughout the specimen. Here one can take various approaches, depending on assumptions.

Let us consider, as a possible approach, the assumption that the particles and matrix obey a binomial distribution.

Consider a cubic centimeter of material. If this consists of 30% by volume of spheres, then the volume of spheres = 0.3 cm^3. Suppose each sphere has a diameter of 40 microns ($d = 4 \times 10^{-3}$ cm). Then each sphere has volume

$$V = \tfrac{1}{6}\pi d^3 = (1/6)(3.1416)(64 \times 10^{-9})\ cm^3$$

$$= 33.5 \times 10^{-9}\ cm^3$$

and in each cubic centimeter the "expected" number of particles would be

$$n = \frac{3 \times 10^{-1}\ cm^3}{33.5 \times 10^{-9} cm^3} = 0.0896 \times 10^8 \text{ particles}$$

or roughly 1×10^7 particles.

The cubic centimeter of material can be viewed somewhat differently, however. Let us consider the cubic centimeter to be made up of N discrete "boxes", each of which might or might not contain a sphere. How many such boxes would the cubic centimeter contain? We find approximately

$$N = \frac{1\ cm^3}{33.5 \times 10^{-9}\ cm^3} = 3 \times 10^7$$

boxes per cubic centimeter.

Several considerations run counter to the assumption of Bernoulli trials, but we consider it possible to get a first approximation to variability in this way. In a binomial distribution, if p is the probability of "success" of an event, $q = 1-p$ is the probability of failure, and N is the number of trials, then

$$\mathcal{P}(s) = (q + p s)^N$$

is a probability generating function which, upon expansion, yields a series of terms in powers of the "operator" s. The coefficient of s^k is the probability that exactly k successes are realized. The expected number of successes is Np and the variance of the number of successes is $Np\,q$. If $p = 0.30$ is the probability that a "box" chosen at random contains a sphere and $N = 3 \times 10^7$ is the number of boxes in 1 cm^3 of material, then

$$Np = (3 \times 10^7)\ (0.3) \approx 1 \times 10^7$$

and

$$Npq = (3 \times 10^7)\ (0.3)\ (0.7) \approx 0.6 \times 10^7.$$

Then the standard deviation of the number of particles in a cubic centimeter sample is

$$\sqrt{Npq} = 2.45 \times 10^3$$

Alternatively, we can inquire concerning the sample value of p which we might compute from a count of all particles contained in one cubic centimeter of material. Let X be a random variable denoting the particle count. It can be shown that

$$E\left[\frac{X}{N}\right] = p$$

$$\mathrm{Var}\left[\frac{X}{N}\right] = \frac{pq}{N}$$

Thus, for the case cited above

$$E\left[\frac{X}{N}\right] = 0.3$$

-- that is, the volume fraction of spheres can be estimated unbiasedly from the ratio of the number of spheres counted to the total number of "boxes" which they might occupy.

The variance, then is

$$\mathrm{Var}\left[\frac{X}{N}\right] = \frac{(0.3)(0.7)}{3 \times 10^{7}}$$

$$= 0.7 \times 10^{-8}$$

and the standard deviation is

$$\sqrt{0.7 \times 10^{-8}} = 0.84 \times 10^{-4}$$

Thus it is seen that the variation in the estimate of p for a sample as large as a cubic centimeter would be substantially negligible.

It is instructive to see how the variance and standard deviation vary as a function of N (see table below)

N	V (cm^3)	$\frac{\text{Var}\,(X/N) \text{ for } p = 0.3}{pq/N}$	$\sqrt{pq/N}$
1	3.4×10^{-8}	0.21	0.46
4	1.3×10^{-7}	0.052	0.23
9	3.0×10^{-7}	0.023	0.15
100	3.4×10^{-6}	0.0021	0.046
10,000	3.4×10^{-4}	0.000021	0.005
30,000	1×10^{-3}	0.000007	0.0026

V = approximate sample volume

The last entry approximates a volume of 1 cubic millimeter. In short, when $V = 1\ mm^3$, the standard deviation of p, the volume fraction of spheres, might be expected to be of the order of 1% of its expected value.

How would this variation be reflected in terms of density variation?

As a first approximation, it can be reasonably argued that the binomial distribution would approach the normal distribution for the values of N and p under consideration. A band covering two standard deviations on either side of the mean would range approximately from 0.295 to 0.305. The corresponding

densities would be

$$(.295)\ (19.3) + (.705)\ (8.2) = 11.47$$

and

$$(.305)\ (19.3) + (.695)\ (8.2) = 11.59$$

Therefore, if only random effects are operative, one might expect the maximum range in density of cubic millimeter samples to be not more than two or three percent of the nominal value. The variation would, of course, be much less for cubic centimeter samples.

Summary

This memorandum has undertaken only a "quick and dirty" look at the variations which might be expected in the Apollo 14 samples. The approach is presently very tentative, and conclusions can not yet be made until further study. It appears, however, that random variations would be substantially reduced to negligible proportions for samples as large as a cubic millimeter or more.

H.T McAdams

H. T. McAdams
Ext. 540

CORNELL AERONAUTICAL LABORATORY, INC.
Buffalo, New York, 14221

April 14, 1971
HTMcA:jjy
N56-001

MEMO FOR THE RECORD

To: T.J. and R.C. Fabiniak

From: H. T. McAdams

Subject: Apollo 14 Sample Analysis (2)

cc: H.Leland/A.O'Connor, R. Klingaman, R. Schnizler

SUMMARY

A tentative look is taken at statistical problems involved in estimating the distribution of the particulate phase in the Apollo 14 samples. It is argued that a plane section provides an unbiased estimate of the volume ratio of the particulate phase: the estimate is obtained by computing the area ratio of the particles exposed in the section. An example is analyzed to show that the variance of such an estimate may be large, however, unless an adequate sample size is taken. A tentative "first cut" at the statistical requirements suggests that a one-square-millimeter area at 100X magnification might be a reasonable starting point. This area and magnification would be compatible with the size of image accommodated by the Flying Spot Scanner and would give a "least count" of the order of a square micron.

1. Area Ratio as an Estimator of Volume Fraction

A 1963 publication by Boeing Scientific Research Laboratories* provides a concise summary of methods of rapid determination of volume fraction of a dispersed phase. The summary includes a discussion of: (1) area fraction

* Regis M.N. Pelloux, Influence of Constituent Particles on Fatigue Crack Propagation in Aluminum Alloys, Boeing Scientific Research Laboratories D1-82-0297 (September 1963). Appendix - Rapid Determination of Volume Fraction, by B.C.Wonsiewicz.

technique, (2) linear intercept technique, and (3) point count technique. We consider here only the first.

The area fraction technique is based on an argument attributed to M. Delesse* who, it is said, in 1848 showed that the area fraction of a three-dimensional feature on a random plane provides an unbiased estimate of the volume fraction of that feature. Some statistical comparison of procedures for quantitative metallography are given by Hilliard and Cahn,** but we make an independent approach in this memorandum. Further, since the work by Delesse has not reached my hands, I provide my own arguments for his alleged findings.

Consider Figure 1, in which particles of irregular size and shape are randomly distributed in a solid matrix. The figure presents a random section of a cube s units on a side, and we assume the volume ratio of particles to be p. The combined area A of the exposed particle sections can be regarded as a random variable provided that a meaningful probability space can be defined.

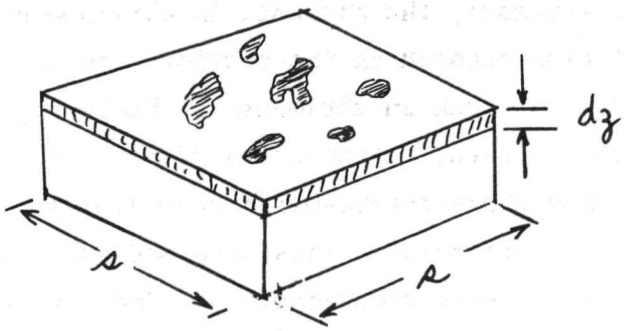

FIGURE 1
INTERCEPTED AREA

Special note is made of the fact that the random variable is created by a random sampling process and that it is important to define this random process clearly and unambiguously. Once this has been done, we can realistically talk about the intercepted area A of particles in the random plane as a random variable

* M. Delesse, Annales des Mines 13, (1848) p.379.

** J.E. Hilliard and J.W. Cahn, "An Evaluation of Procedures in Quantitative Metallography for Volume-Fraction Analysis", Trans. Metallurgical Society of AIME, Vol. 221 (April 1961), 344-352.

having cumulative distribution function $F(A)$ and probability density function $f(A) = F'(A)$, where the prime denotes differentiation.

To induce a statistical distribution of A we first consider a random variable Z, which denotes the height of the random section relative to the base plane. Let Z be uniformly distributed from 0 to s. The probability density function is

$$f(z) = 1/s \qquad 0 \le z \le s$$

For each value of Z there is defined an area ratio $A(z)/s^2$. The height Z, taken as a random variable as defined above, thus induces a random variable $A(z)/s^2$. It is not necessary to define explicitly the probability density function of this random variable in order to compute its expectation. Indeed, the expected value is just

$$E\left[\frac{A(z)}{s^2}\right] = \int_0^s \frac{A(z)}{s^2} \cdot \frac{1}{s}\, dz = \frac{1}{s^3}\int_0^s A(z)\, dz \qquad (1)$$

Now consider $A(z)$ as a <u>mathematical</u> function which expresses the particle intercept area as a <u>function</u> of the height or z coordinate. Then the volume of particles contained in a height increment dz is A(z) dz and the total volume of particles is

$$V = \int_0^s A(z)\, dz$$

The volume fraction is

$$\frac{V}{s^3} = \frac{1}{s^3}\int_0^s A(z)\, dz \qquad (2)$$

Note that this result is the same as that obtained in (1). That is,

$$E\left[\frac{A(z)}{s^2}\right] = \frac{V}{s^3}$$

and the area fraction is established as an unbiased estimator of the volume fraction. Note, however, that the equivalence depends on defining f(z) as a uniform or rectangular distribution. If A is taken as a random variable

induced by another random process, equivalence does not necessarily hold. This becomes evident, of course, if we consider the "degenerate" probability density function in which all probability density is assigned to a single value $Z = z$ (Dirac delta function).

2. An Example of Area Ratio Applied to Spheres

It is convenient that spheres are nonorientable in three-space. Therefore, to characterize a random sectioning plane, one needs only to specify the perpendicular distance R from the center of the sphere to the plane, as shown in Figure 2, and to postulate a statistical distribution for R as a random variable.

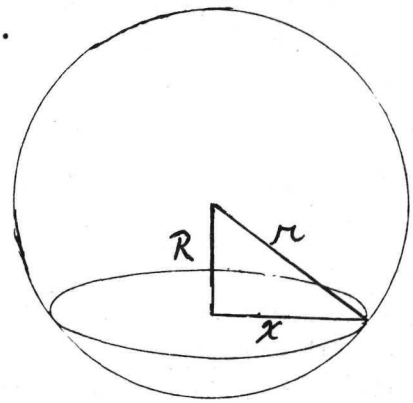

FIGURE 2
RANDOM PLANE THROUGH A SPHERE

A reasonable assumption is that R is uniformly distributed between $R = 0$ and $R = r$. Therefore, the probability density function is

$$f(R) = 1/r \qquad 0 \le R \le r$$

and the cumulative distribution function is

$$F(R) = \int_0^R \frac{1}{r}\, dy = \frac{R}{r} \qquad 0 \le R \le r$$

Now the area of the cross-section intercepted by the random plane is

$$A = \pi x^2$$

where $x^2 = r^2 - R^2$. Therefore,

$$A = \pi (r^2 - R^2) = \pi r^2 - \pi R^2$$

The probability that the random variable A takes on values not exceeding $\alpha = \pi R^2 - \pi \rho^2$ is exactly the probability that the random variable R takes on values greater than ρ.

$$P_r(A \leq \alpha) = P_r(R > \rho)$$
$$= 1 - F(\rho)$$
$$= 1 - \rho/R$$

Since $\alpha = \pi R^2 - \pi \rho^2$

$$\rho = \sqrt{R^2 - \alpha/\pi}$$

and we can write

$$P_r(A \leq \alpha) = P_r(R > \rho) = 1 - \rho/R$$

$$= 1 - \frac{\sqrt{R^2 - \alpha/\pi}}{R} = 1 - \sqrt{1 - \frac{\alpha}{\pi R^2}}$$

Therefore, the cumulative distribution function for the intercepted area can be written as

$$F(A) = 1 - \sqrt{1 - \frac{A}{\pi R^2}} \qquad 0 \leq A \leq \pi R^2$$

and, upon differentiating with respect to A, one obtains the probability density function

$$f(A) = -\tfrac{1}{2}\left(1 - \frac{A}{\pi R^2}\right)^{-1/2} \cdot \left(-\frac{1}{\pi R^2}\right)$$

$$= \frac{1}{2R\sqrt{\pi}\sqrt{\pi R^2 - A}} \qquad 0 \leq A \leq \pi R^2$$

We proceed now to compute the expected value of A and its variance.

$$E[A] = \int_0^{\pi R^2} \frac{A\,dA}{2R\sqrt{\pi}\sqrt{\pi R^2 - A}} = \frac{1}{2R\sqrt{\pi}} \int_0^{\pi R^2} \frac{A\,dA}{\sqrt{\pi R^2 - A}}$$

The integral $I_1 = \int_0^{\pi R^2} \frac{A\,dA}{\sqrt{\pi R^2 - A}}$

is of the form

$$\int \frac{x\,dx}{\sqrt{a+bx}} = \frac{-2(2a-bx)}{3b^2}\sqrt{a+bx}$$

where $a = \pi R^2$ and $b = -1$.

Therefore,

$$I_1 = \frac{-2(2\pi R^2 + A)}{3}\sqrt{\pi R^2 - A}\Bigg|_0^{\pi R^2}$$

$$= \frac{2(2\pi R^2)}{3}\sqrt{\pi R^2}$$

and

$$E[A] = \frac{1}{2R\sqrt{\pi}} I_1 = \frac{1}{2R\sqrt{\pi}} \cdot \frac{2(2\pi R^2)}{3}\sqrt{\pi R^2}$$

$$= 2/3\ \pi R^2$$

The expected value of A^2 can be computed in a similar way.

$$E[A^2] = \frac{1}{2R\sqrt{\pi}} \int_0^{\pi R^2} \frac{A^2\,dA}{\sqrt{\pi R^2 - A}}$$

The integral $I_2 = \int_0^{\pi R^2} \frac{A^2\,dA}{\sqrt{\pi R^2 - A}}$

is of the form

$$\int \frac{x^2\,dx}{\sqrt{a+bx}} = \frac{2(8a^2 - 4abx + 3b^2x^2)}{15b^3}\sqrt{a+bx}$$

where $a = \pi r^2$ and $b = -1$.

Therefore,

$$I_2 = -\frac{2(8\pi^2 r^4 + 4\pi r^2 A + 3A^2)}{15}\sqrt{\pi r^2 - A}\Bigg|_0^{\pi r^2}$$

$$= \frac{2(8\pi^2 r^4)}{15}\sqrt{\pi r^2}$$

and $$E[A^2] = \frac{1}{2r\sqrt{\pi}} I_2 = \frac{1}{2r\sqrt{\pi}} \frac{2(8\pi^2 r^4)}{15}\sqrt{\pi r^2}$$

$$= \frac{8}{15}\pi^2 r^4$$

The variance of A can then be computed as

$$Var[A] = E[A^2] - \left(E[A]\right)^2$$

$$= 8/15\,\pi^2 r^4 - (2/3\,\pi r^2)^2$$

$$= (8/15 - 4/9)\pi^2 r^4 = 4/45\,\pi^2 r^4$$

Then the standard deviation of A is

$$\sigma_A = \sqrt{\frac{4}{45}\pi^2 r^4} = \frac{2}{3\sqrt{5}}\pi r^2$$

$$= 0.298\,\pi r^2$$

and $$\frac{\sigma_A}{E[A]} = \frac{0.298\,\pi r^2}{0.667\,\pi r^2} = 0.447$$

Thus it is seen that the standard deviation of A is about 45% of its expected value.

How does the expected value of the area cross-section compare with the volume fraction constituted by the sphere when embedded in a matrix?

Assume the sphere to be circumscribed by a cube of edge 2 r. The volume of the sphere is

$$V_{sphere} = 4/3\ \pi r^3$$

and the volume of the cube is

$$V_{cube} = (2r)^3 = 8r^3$$

Then

$$\frac{V_{sphere}}{V_{cube}} = \frac{4/3\ \pi r^3}{8r^3} = 1/6\ \pi$$

and we note that this is exactly the ratio of the expected sphere cross-section to an orthogonal cross-section of the cube:

$$\frac{E[A]}{(2r)^2} = \frac{2/3\ \pi r^2}{4r^2} = 1/6\ \pi$$

Since the orthogonal cross-section is constant, the above quantity can be taken as the expected value of the area ratio and, for the specific case treated, we have shown that the areal ratio is an unbiased estimator of the volume ratio.

The standard deviation of the areal ratio, however, is

$$\frac{0.298\ \pi r^2}{4r^2} = 0.0745\ \pi = 0.234$$

or $\frac{0.0745}{0.1667}$ = 0.447 of the expected ratio.

Unless an appreciable cross-section is taken, therefore, the variance of the measurement would be excessive for discriminating significant differences.

Consider random cross-sections of a large specimen and isolate all those sections which contain exactly n circular sections of spheres. For example, for n = 4, three typical sections might be as shown in Figure 3.

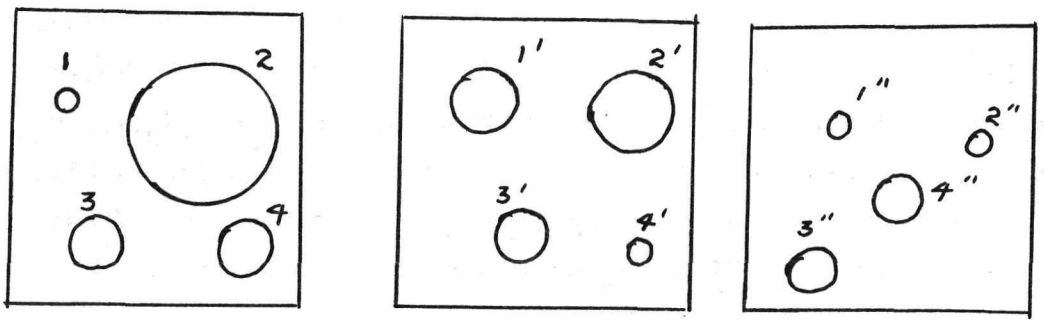

FIGURE 3
RANDOM SECTIONS OF FOUR SPHERES IN MATRIX

It is presumed that the distance of the plane from the center of a particular sphere in no way affects the distance for another sphere; in short, we assume that the random variables R_1, R_2, R_3, R_4 for the four spheres are statistically independent. Under this assumption, we total, for each random section, the areas intercepted for the four spheres and express this total as a fraction of the area of the slice. According to the statistics of independent random variables, the effect is that of averaging four measurements and the average would have one-fourth the variance associated with a single sphere.

For example, consider the case previously treated in which the expected area ratio is $1/6\pi$ = 0.5236 and the standard derivation is 0.234 (the relative standard deviation is 0.45). To reduce the standard deviation to one-tenth of its value would require n = 100 (the relative standard deviation would still be nearly 5%). If we had n = 2500, the relative standard deviation would be close to 1%. It appears, therefore, that a cross-section large enough to "capture" a few hundred to a few thousand spheres would be required to estimate volume ratios with the required degree of precision.

Before leaving this matter, however, two additional points should be noted. First, the above conclusions address only the conditional distribution given that n, the number of spheres captured, is fixed. In reality, this number itself is a random variable and the variation in the number captured must be taken into account. The effect of this variation can be examined later; for the moment, it suffices to bound the problem under consideration by a loose statement like "a few hundred to a few thousand". Second, it does not necessarily follow that the distances R_1, R_2,...,R_n are statistically independent. If the concentration of spheres is high, each sphere is under position constraint by neighboring spheres (in a dense-packed specimen the distances R_1, R_2,...,R_n would be highly correlated).

To obtain the desired number of spheres in a cross-section, how large would the area section need to be? In a previous memorandum*, it was shown that a cubic millimeter sample containing 30% by volume of 40-micron (diameter) spheres has approximately 30,000 spheres. Suppose we "slice" this cube into sections 40 microns thick. There would be $\frac{1000}{40} = 25$ such slices, and each slice would contain the equivalent of slightly over 1000 spheres. Therefore, one would expect at least 1000 circular sections to be evident if one square millimeter of area were examined, and this "ball-park" estimate of sample size would seem to be compatible with the preceding statistical argument. If replicate sections (at least duplicate) are made, the combined data should satisfy the required precision and provide much-needed information on reproducibility.

3. Implementation of an Area-Ratio Approach

The previously developed arguments have made assumptions regarding ideally spherical, monodisperse particles as a first cut at estimating information requirements. It was also shown that estimates of phase concentration can be based on areal ratios even if particles are of irregular shape and are

---

* H.T.McAdams to R.C. and T.J. Fabiniak, "Apollo 14 Sample Analysis," 12 April 1971

polydisperse. Further, it has been indicated that an area of approximately one square millimeter approaches the size which might be "lived with" from the standpoint of statistical variation.

For estimating the area occupied by the particulate phase, we should consider using the Flying Spot Scanner (FSS). At a magnification of 100X, a 1-mm. square object area becomes a 10 cm. square image, or a picture about 4 inches on a side. (This is about the size which can be accommodated by the FSS: normal operating conditions are a 1024 x 1024 raster on a 3-inch square image, giving a nominal spot size of approximately 0.003 inches.) If one assume an approximate resolution of 3 mils, this is equivalent to about 0.076 mm in image space or 0.76 microns in object space at 100X magnification. It appears, therefore, that 100X might be adequate and might be consistent with other constraints on the data-collection task. (Note that a 40-micron diameter particle, in equatorial section, would have an area of approximately 1250 square microns and would yield a count of over 1650 units.) As an initial approach, therefore, transparencies at 100X magnifications seem logical.

4. Statistical Approach

A combination of variance decay (as a function of scanning aperture size) and inference methods such as analysis of variance and contingency tables is considered. More on this point will be covered in a later memorandum.

H.T. McAdams

H.T. McAdams
Ext. 540

April 21, 1971
HTMcA:htm
N56-001

MEMO FOR THE RECORD

To: The Brothers Fabiniak
From: H. T. McAdams
Subject: Apollo 14 Sample Analysis (3)
cc: H. Leland/A.O'Connor, R.Klingaman, R. Schmizler, P. Reese, A. Keller

SUMMARY

Here is a look at point-count techniques of evaluating the Apollo specimens. The approach would be easy to implement and the question of aggregation of particles can be analyzed in a straightforward manner.

****

A previous memorandum* has discussed the prospect of an areal analysis as a means for finding an unbiased estimate of the volume fraction of a dispersed phase in a metallographic specimen. A random or "systematic" point count, as noted by Hilliard and Cahn**, has certain advantages.

First, a note of clarification is in order concerning the distinction between random and systematic. By random point count we mean that, in a polished section, we select points in the plane of the polish as if they satisfied a two-dimensional or bivariate uniform distribution. Refer to Figure 1. A point P can occur anywhere in the rectangle, and its

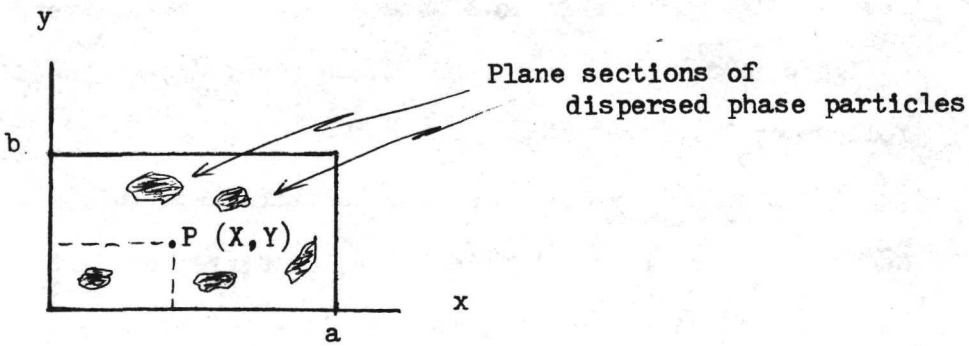

Figure 1
Bivariate Uniform Distribution

coordinates can be considered as a two-dimensional random variable

* H. T. McAdams to T.J. and R.C. Fabiniak, "Apollo 14 Sample Analysis (2), April 14, 1971

** J. E. Hilliard and J.W. Cahn, "An Evaluation of Procedures in Quantitative Metallography for Volume-Fraction Analysis," Trans. of the Metallurgical Society of AIME, Vol. 221, 344-352 (April, 1961)

or random vector (X,Y) satisfying the probability density function

$$f(x,y) = \begin{cases} 1/ab & \text{if } 0 \leq x \leq a,\ 0 \leq y \leq b \\ 0 & \text{otherwise} \end{cases}$$

For a given polish section, therefore, either P will fall in one of the shaded areas (dispersed phase) or it will not, and the probability of success (point falls in shaded area) is the ratio of the area of the aggregated shaded portion to the total area ab of the plane section. Therefore, the number of points <u>observed</u> in the shaded portion will be an (unbiased) estimate of the area fraction (it has earlier been shown that the area fraction is an unbiased estimate of the volume fraction).

To lay down a random pattern of points is troublesome at best and the randomization can always be questioned. Consequently, we dodge the issue by means of a ploy both expedient and practical. Let there be established over the area ab a regular grid or lattice of points. If it eases our conscience any, we can assume that the points were there <u>before</u> the sample ever existed, and the dispersed particles can be taken as the randomly distributed elements. Now we raise the question: does a random element or particle "cover" one of the grid points. Again the probability of coverage is just the ratio of shaded area to total area, and an unbiased estimate of area fraction (and volume fraction) of the dispersed phase follows as before.

In the Apollo experiment, we <u>want</u> to claim randomness--that is, we hope not to see any "pattern" in the dispersed particles, pattern such as clusters, lineal arrays, and the like. I propose to examine this hypothesis by means of a combination of Hilliard and Cahn's systematic point count and the notion of a granularity function, as employed, e.g., in the characterization of photographic emulsions.

Let the distance between grid points be such that a single particle will not "catch" more than one grid point. (This is what Hilliard and Cahn refer to as a "coarse" grid.) Then all one needs to do is to

count the number of grid points covered by particles and express this number as a ratio of the total number of grid points in the area. The result should be an unbiased estimate of the area (and volume) fraction of dispersed phase. Such a count could be made readily by eyeball or by Flying Spot Scanner.

Now suppose, however, that we wish to see if clustering or other patterning occurs. Since the probability of grid point coverage depends only on the aggregate area of all the particles, statistical outputs deriving from some systematic sampling procedure derived from the grid should behave according to a binomial distribution and independent Bernoulli trials.

In particular, suppose we consider not a single grid point but a set of n (n greater than 1) points. Regardless of how these grid points are taken to form sets, the assumed randomness of the particles should be capable of being relied on to produce a random sampling process. Departures from randomness should then be detectable by appropriate statistical procedures.

1. "Aperture" Size and Variance "Decay"

If we examine every point in the grid for occupancy by a particle, we have, in effect, sampled a binomial distribution in which the probability of "success", p, is the area fraction of the dispersed phase. Let N be the total number of grid points and let k be the number occupied. Then, $E[k/N] = p$ and $Var[k/N] = pq/N$, where $q = 1-p$. Now suppose that we let $n = 4$ and let these four grid points form the corners of a square, as shown in Figure 2.

Figure 2

Grid-Point Occupancy
in a Multiple-Point Aperture

Let the sample "aperture" run over the plane section. At each way station or stop in the scanning process, the 4-point sampling aperture can assume one of five possible states: 0, 1, 2, 3, 4 points occupied. (Note: in the case for n = 1, there were only two states, 0 and 1.) The generating function

$$\mathcal{P}(s) = (q + ps)^4$$

$$= q^4 + 4q^3ps + 6q^2p^2s^2 + 4qp^3s^3 + p^4s^4$$

gives the probability that 0,1,2,3,4 points in the sampling aperture will be occupied. These probabilities can be estimated from observed counts of the number of corners of the square which are actually covered by a particle of the dispersed phase.

For example, suppose $p = 0.1$. Then the probabilities of Table 1, which follows, apply.

Table 1

Probabilities for $n = 4$, $p = 0.1$

Number of Points Occupied	Probability of Occurrence
0	0.6561
1	0.2916
2	0.0486
3	0.0036
4	0.0001

The expected number of points occupied would be $np = 0.4$ and $\sigma^2 = npq = 0.36$. Then $\sigma = 0.6$. Significant departures from the tabulated probabilities or from the variance figure could be taken as evidence of "clustering." For example, if 10% of the apertures had all points occupied and 90% had no points occupied, the variance would be 1.44 rather than 0.36. Similar analysis for pattern could be performed by taking --say-- n points in a straight line. Other sizes of apertures can be chosen to show where (if anywhere) departures from randomness occur and in what size "domains"

or clusters this patterning takes place. A study of the expected number of clusters of various sizes has been made by Mack.*

To show how the above argument works in practice, consider a random number table, a portion of which is shown in Figure 3**. We would not expect "pattern" to be present here. An experiment was run on the area marked off (as if this were the polished section). A zero can then be taken as denoting "coverage" of the grid point by a particle of the dispersed phase (this would be equivalent to a case in which the dispersed phase constituted 10% by volume). A 2 x 2 point "aperture" was run over the boxed-off area, making 96 stops in the process. At each stop, note was made of how many of the four aperture points were occupied by a zero. The results of Table 2 were obtained.

Table 2

Occupancy for 2 x 2 Aperture (96 Cases)

Number of Grid Points Occupied	Number of Cases	Fraction Favorable
0	58	0.604
1	28	0.292
2	9	0.094
3	1	0.010
4	0	0.000

We note "reasonable" agreement with Table 1, but may well ask, "Why is it not better?" The answer resides in the fact that the region of the random number table is finite in size and contains, in fact, only 125 points. There is, therefore, a sampling error attending the fact that there will not be exactly 10% of the 125 numbers which are zeros. In reality, there were exactly 15 zeros in the 125 digits taken as the basis for study, giving a probability of 15/125 = 0.12 instead of the theoretical 0.10.

*C. Mack, "The Expected Number of Aggregates in a Random Distribution of n Points," Proc. Cambridge Philosophical Soc., 46, 285-292 (1950)

** See last page of this memo.

Table 1 is recomputed for $p = 0.12$ as Table 3, which follows.

Table 3

Probabilities for $n = 4$, $p = 0.12$

Number of Points Occupied	Probability of Occurrence
0	0.600
1	0.326
2	0.067
3	0.006
4	0.000

The fact that Table 2 (the observations) agree better with Table 3 than with Table 1 emphasizes an important point, and one made admirably by Hilliard and Cahn in their analysis: there are two sources of variability to be reckoned with in analyzing the Apollo dispersions. First, there is variability arising from the fact that no two plane sections will be quantitatively the same. Second, given a particular plane polish section, there will be variation within that plane as one moves from one coordinate position to another. Hilliard and Cahn's treatment of this "between-plane" and "within-plane" variance is straightforward and the expressions they derive for the variance components are directly applicable to our problem.

2. Implementation

The type of analysis described above would be extremely easy to implement via Flying Spot Scanner. Once the scanned data were recorded (and appropriately thresholded into an array of zeros and ones), it would be necessary only to interrogate the data at preselected grid points (or aperture configurations of grid points) to obtain the necessary counts of occupancy states. Statistical analysis would

be effected by straightforward procedures such as chi-square goodness-of-fit tests, contingency table analysis, analysis of variance (possibly factorial chi square), and so on. Though chi square and other goodness-of-fit tests have (to me) certain philosophical objections as commonly employed, I believe that possibly here is an application where the legitimate use of such tests come to the fore. There will be more on this point in a later memo.

3. Acknowledgment

H. T. M'Adams

TABLE 3
TEN THOUSAND RANDOMLY ASSORTED DIGITS

	00-04	05-09	10-14	15-19	20-24	25-29	30-34	35-39	40-44	45-49
00	54463	22662	65905	70639	79365	67382	29085	69831	47058	08186
01	15389	85205	18850	39226	42249	90669	96325	23248	60933	26927
02	85941	40756	82414	02015	13858	78030	16269	65978	01385	15345
03	61149	69440	11286	88218	58925	03638	52862	62733	33451	77455
04	05219	81619	10651	67079	92511	59888	84502	72095	83463	75577
05	41417	98326	87719	92294	46614	50948	64886	20002	97365	30976
06	28357	94070	20652	35774	16249	75019	21145	05217	47286	76305
07	17783	00015	10806	83091	91530	36466	39981	62481	49177	75779
08	40950	84820	29881	85966	62800	70326	84740	62660	77379	90279
09	82995	64157	66164	41180	10089	41757	78258	96488	88629	37231
10	96754	17676	55659	44105	47361	34833	86679	23930	53249	27083
11	34357	88040	53364	71726	45690	66334	60332	22554	90600	71113
12	06318	37403	49927	57715	50423	67372	63116	48888	21505	80182
13	62111	52820	07243	79931	89292	84767	85693	73947	22278	11551
14	47534	09243	67879	00544	23410	12740	02540	54440	32949	13491
15	98614	75993	84460	62846	59844	14922	48730	73443	48167	34770
16	24856	03648	44898	09351	98795	18644	39765	71058	90368	44104
17	96887	12479	80621	66223	86085	78285	02432	53342	42846	94771
18	90801	21472	42815	77408	37390	76766	52615	32141	30268	18106
19	55165	77312	83666	36028	28420	70219	81369	41943	47366	41067
20	75884	12952	84318	95108	72305	64620	91318	89872	45375	85436
21	16777	37116	58550	42958	21460	43910	01175	87894	81378	10620
22	46230	43877	80207	88877	89380	32992	91380	03164	98656	69337
23	42902	66892	46134	01432	94710	23474	20423	60137	60609	13119
24	81007	00333	39693	28039	10154	95425	39220	19774	31782	49037
25	68089	01122	51111	72373	06902	74373	96199	97017	41273	21546
26	20411	67081	89950	16944	93054	87687	96693	87236	77054	33848
27	58212	13160	06468	15718	82627	76999	05999	58680	96739	63700
28	70577	42866	24969	61210	76046	67699	42054	12696	93758	03283
29	94522	74358	71659	62038	79643	79169	44741	05437	39038	13163
30	42626	86819	85651	88678	17401	03252	99547	32404	17918	62880
31	16051	33763	57194	16752	54450	19031	[illegible]	[illegible]	[illegible]132	60631
32	08244	27647	33851	44705	[illegible]	[illegible]	[illegible]	[illegible]	[illegible]74	72655
33	59497	04392	09419	[illegible]	[illegible]	[illegible]	[illegible]	[illegible]	[illegible]06	83864
34	97155	13428	[illegible]	[illegible]	[illegible]	[illegible]	[illegible]	[illegible]	058	82859
35	[illegible]	[illegible]	[illegible]	[illegible]	[illegible]	[illegible]	[illegible]	39435	11859	41567
36	[illegible]	[illegible]	[illegible]	[illegible]	[illegible]	[illegible]	[illegible]06	61203	53634	22557
37	[illegible]	[illegible]	[illegible]	[illegible]	[illegible]	[illegible]	05400	66669	48708	03887
38	[illegible]	[illegible]	[illegible]	[illegible]28	12275	24816	68091	71710	33258	
39	[illegible]	[illegible]	[illegible]9042	98364	02306	24617	09609	83942	22716	
40	79152	53829	77250	20190	56535	18760	69942	77448	33278	48805
41	44560	38750	83635	56540	64900	42912	13953	79149	18710	68618
42	68328	83378	63369	71381	39564	05615	42451	64559	97501	65747
43	46939	38689	58625	08342	30459	85863	20781	09284	26333	91777
44	83544	86141	15707	96256	23068	13782	08467	89469	93842	55349

From G.W. Snedecor, Statistical Methods, 5th ed., Iowa State College Press, Ames, Iowa, c1956.

PROCEDURE FOR POINT-COUNT ANALYSIS
OF APOLLO SPECIMENS
(Tentative)

A typical polish cross-section of the Apollo specimens, at 100X, represents approximately one square millimeter of area (see memo 2, H. T. McAdams). From examination of a representative picture, one sees that the maximum cross-section of a particle is about 0.15 inches, or, in object space, about 38 microns. The "typical" size of a particle cross section is about 2/3 of this value (see memo 2, H. T. McAdams) or about 25 microns. This estimate is, in general, consistent with available particle size distribution information.

The optimum size of grid for point counting is just larger than the largest observed particle cross section. It would appear, therefore, that a grid approximately 4 mm square would be satisfactory. If the image were enlarged 2 1/2 times (total magnification 250X), this would make the final grid to be considered 1 cm square. It is believed that such a grid would be relatively easy to read and "score".

Consider also the following matters of convenience

- The 100X photograph is 3 1/2" x 4 1/2" multiplied by 2 1/2, this comes to 8 3/4" x 11 1/4", or approximately 9" x 12", and would easily fit on standard-sized photographic paper.

- Note that 8 3/4" $\approx$ 22 cm and 11 1/4" $\approx$ 28 cm. By rejecting a bit of area near the boundary, we could use a grid 20 x 25 = 500 points.

- Key punching of data could use a format-of-say - 25 entries per card for 20 cards, using single digits to record a 0 or a 1. Alternatively, we could put 2 rows per card and still have 30 columns left to record identification information and comment.

For a polish section having actually p = 30 (30%) particles, the ratio of grid points covered to grid points counted is an estimate of p with a standard deviation.

$$\sigma = \sqrt{\frac{pq}{m}} = \sqrt{\frac{(0.3)\ (0.7)}{500}}$$

$$= \sqrt{0.00042} \approx 0.02$$

A 2-sigma band provides an approximate 95% "confidence interval" for p. This band would be p $\pm$ 0.04; therefore, if p is in the vicinity of 30%, the counting of a single picture should give an estimate within 4% of that value. This variance, of course, does not consider the fact that the specimen sample itself is variable; a replicate sample would not give the same value, even if no error in counting occurred. The extent of this variance has been previously considered (see memo 2, H. T. McAdams) and is the basis for the selection of the 1 square millimeter sample area. The area should be replicated at least once (that is, duplicate areas). To gain further precision, the number of replicates could be increased.

The following procedure is therefore suggested as a "first cut". It should be held open for iteration, because several modifications may become evident when the procedure is put into practice.

1. Photograph at 100X.
   It is proposed to make this original photograph a positive transparency (for reasons noted in step 3).

2. Using the 100X positive transparency, make a 2 1/2 X negative print.

3. Using a thin sheet of paper with 1 cm ruled grid as overlay, check with a pencil mark each grid point occupied by a particle. A light table would be used here. It is presumed that if the print is a negative, the particles would be light-transmitted and the grid points would show up readily against them. (If difficulty

is encountered or the system does not work as proposed, we might wish to reverse the role of positive and negative images). Also, it might be practical to use projection.

4. Record on each record sheet the identifying information -- that is, specimen number, section, location, etc. (Exact details must be decided upon).

5. Pass the record sheet on to a keypunch operator, who would prepare the input cards in an accepted format.

6. Develop a computer routine to "score" the counts on a total-specimen basis (single-point aperture) and on a variable - aperture basis to develop patterning information.

H. T. McAdams

Comments, please?

☆U. S. GOVERNMENT PRINTING OFFICE: 1971—745-380/4035-Region 4